



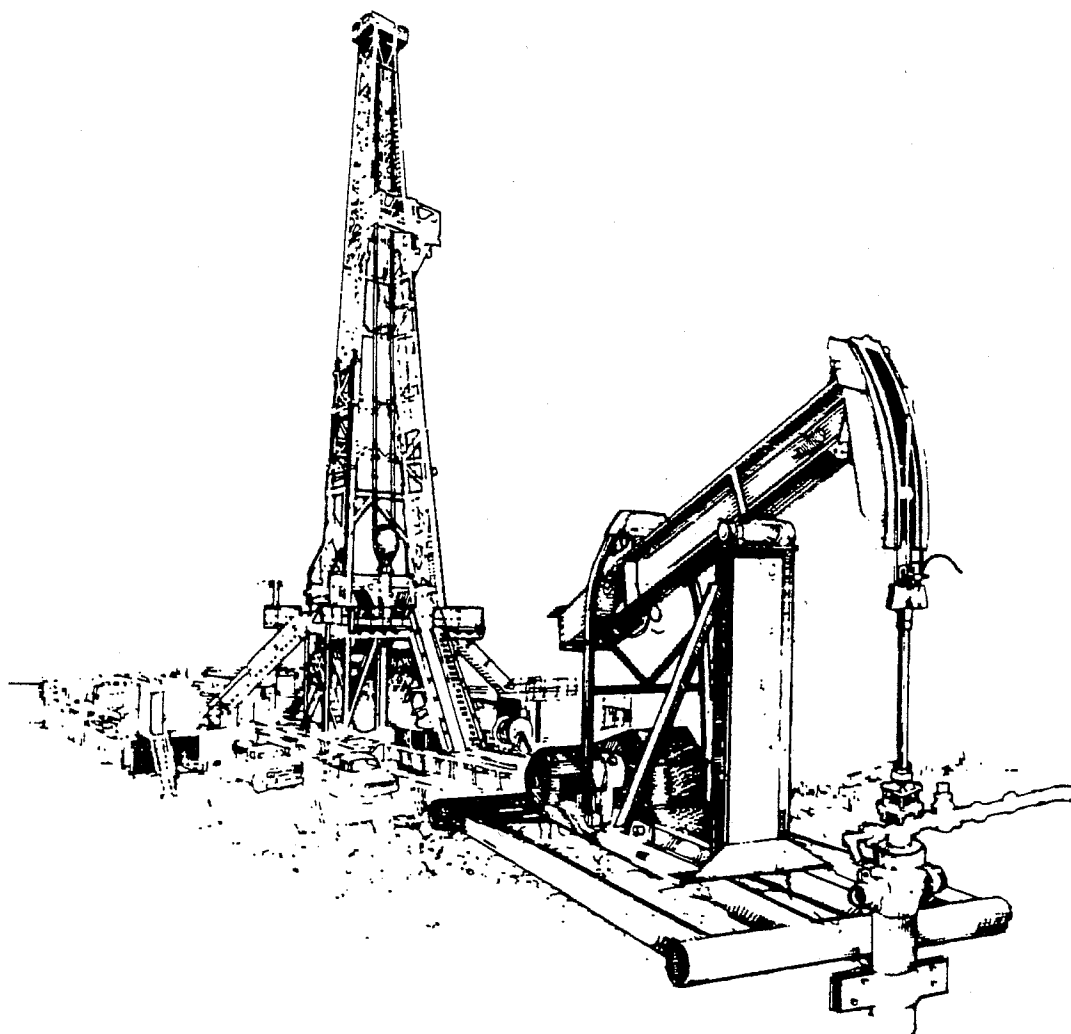
Contracts for field projects
and supporting research on . . .

73

Enhanced Oil Recovery

Reporting Period October–December 1992

DOE/BC--93/1
(DE93000136)
PROGRESS REVIEW
Quarter Ending December 31, 1992



United States Department of Energy
Office of Gas and Petroleum Technology
and Bartlesville Project Office

DISCLAIMER

This report was prepared as an account of work sponsored by an agency of the United States Government. Neither the United States Government nor any agency thereof, nor any of their employees, makes any warranty, express or implied, or assumes any legal liability or responsibility for the accuracy, completeness, or usefulness of any information, apparatus, product, or process disclosed, or represents that its use would not infringe privately owned rights. Reference herein to any specific commercial product, process, or service by trade name, trademark, manufacturer, or otherwise does not necessarily constitute or imply its endorsement, recommendation, or favoring by the United States Government or any agency thereof. The views and opinions of authors expressed herein do not necessarily state or reflect those of the United States Government or any agency thereof.

Available to DOE and DOE contractors from the Office of Scientific and Technical Information, P.O. Box 62, Oak Ridge, Tennessee 37831; prices available from (615) 576-8401.

Available to the public from the National Technical Information Service, U.S. Department of Commerce, 5285 Port Royal Rd., Springfield, Virginia 22161; prices available from (703) 487-4650.

U.S. Department of Energy
Washington, D.C. 20545

DOE/BC--93/1
(DE93000136)
Distribution Category UC-122

JACK SIEGEL
Acting Assistant Secretary
for Fossil Energy
Room 4G-084 Forrestal Building
Telephone Number 202-586-4695

DONALD JUCKETT
Acting Deputy Assistant Secretary for Gas
and Petroleum Technology

DONALD JUCKETT
Director for Oil and Gas Exploration
and Production

Bartlesville Project Office
P.O. Box 1398
Bartlesville, Oklahoma 74005
Telephone No. 918-337-4401

THOMAS C. WESSON
Director

R. M. RAY
Deputy Director

EDITH ALLISON
Acting Program Coordinator,
Enhanced Oil Recovery

HERBERT A. TIEDEMANN
Project Manager for
Technology Transfer

PROGRESS REVIEW NO. 73

CONTRACTS FOR FIELD PROJECTS AND SUPPORTING RESEARCH ON ENHANCED OIL RECOVERY

Date Published - December 1993

UNITED STATES DEPARTMENT OF ENERGY



PUBLICATIONS LIST

Bartlesville Project Office

Thomas C. Wesson, Director

AVAILABILITY OF PUBLICATIONS

The Department of Energy makes the results of all DOE-funded research and development efforts available to DOE and DOE contractors from the Office of Scientific and Technical Information, P.O. Box 62, Oak Ridge, TN 37831; prices available from (615) 576-8401, FTS 626-8401.

Available to the public from the National Technical Information Service, U.S. Department of Commerce, 5285 Port Royal Road, Springfield, VA 22161; prices available from (703) 487-4650.

Give the full title of the report and the report number.

Sometimes there are slight delays between the time reports are shipped to NTIS and the time it takes for NTIS to process the reports and make them available. Accordingly, we will provide one copy of any individual report as long as our limited supply lasts. Please help us in our effort to eliminate wasteful spending on government publications by requesting only those publications needed. Order by the report number listed at the beginning of each citation and enclose a self-addressed mailing label. Available from DOE Bartlesville Project Office, ATTN: Herbert A. Tiedemann, P.O. Box 1398, Bartlesville, OK 74005; (918) 337-4293.

Quarterly Reports

DOE/BC-92/1 **Contracts for Field Projects and Supporting Research on Enhanced Oil Recovery. Progress Review No. 69. Quarter ending December 31, 1991. February 1993. Order No. DE92001069.** Status reports are given for various enhanced oil recovery and gas recovery projects sponsored by the Department of Energy. The field tests and supporting research on enhanced oil recovery include chemical flooding, gas displacement, thermal/heavy oil, resource assessment, geoscience technology, microbial technology, novel technology, and environmental technology.

Chemical

NIPER-631 **Evaluation of Mixed Surfactants for Improved Chemical Flooding. Topical Report. National Institute for Petroleum and Energy Research. February 1993. 112 pp. Order No. DE93000117.** Phase behavior studies were conducted using combinations of a primary surfactant component and several ethoxylated surfactants. The objective of the study is to evaluate combinations of surfactants, anionic-nonionic and anionic-anionic mixtures, that would yield favorable phase behavior and solubilization capacity. The dependence of the solution behavior on the additive surfactant structure, surfactant type, oil, surfactant proportion, salinity, HLB, and temperature was observed. The results showed that the ethoxylated surfactants can improve the solution behavior of the overall system. The increase in optimum salinity range of these solutions corresponded to an increase in the degree of ethoxylation of additive surfactant, up to a certain limit. The nonionic surfactant additives yielded much higher salinities compared to the results from the ethoxylated anionics tested. The proportion of surfactant component in solution was critical in achieving a balance between the solubilization capacity and the enhancement in the system's salinity tolerance. Some combinations of these types of surfactants showed improved solution behavior with favorable solubilization capacity.

NIPER-635 **The Effect of Polymer-Surfactant Interaction on the Rheological Properties of Surfactant-Enhanced Alkaline Flooding Formulations. Topical Report. National Institute for Petroleum and Energy Research.**

February 1993. 28 pp. Order No. DE93000118. Surfactant-enhanced, lower pH (weak) alkaline chemicals are effective for mobilizing residual oil. Polymer is used for mobility control because if mobility control is lost, oil recovery is reduced. The ability to maintain mobility control during surfactant-alkaline flooding can be adversely affected by chemical interaction. In this work, interaction between polymers and surfactants was shown to be affected by pH, ionic strength, crude oil, and the properties of the polymers and surfactants. Polymer-surfactant interaction (phase separation, precipitation, and viscosity loss) occurred between most of the polymers and surfactants that were tested. Polymer-surfactant interaction is difficult to eliminate, and no method was found for completely eliminating interaction. Polymer-surfactant occurred at optimal salinity and below optimal salinity. Polymer-surfactant interaction had an adverse effect on polymer rheology; however, the adverse effect of interaction on polymer rheology was lessened when oil was present. Increasing the pH of chemical systems further reduced the adverse effect of interaction on polymer rheology.

Thermal Recovery

DOE/BC/14600-38 **Ultrasonic Rate Measurement of Multiphase Flow. SUPRI TR 89. Stanford University. January 1993. 40 pp. Order No. DE93000112.** One of the most important tools in production logging and well testing is the downhole flowmeter. Unfortunately, existing tools are inaccurate outside of an idealized single-phase flow regime. Spinner tools are inaccurate at extremely high or low flow rates and when the flow rate is variable. Radioactive tracer tools have similar inaccuracies and are extremely sensitive to the flow regime. Both tools completely fail in the presence of multiphase flow, whether gas/oil, gas/water or fluid/solid. The goal of this project is the investigation of accurate downhole flowmetering techniques for all single-phase flow regimes and multiphase flows. The measurement method investigated in this report is the use of ultrasound. There are two ways to use ultrasound for fluid velocity measurement. The first method, examined in Chapter 2, is the contrapropagation, or transit-time, method which compares travel times with and against fluid flow. Chapter 3 details the second method which measures the Doppler frequency shift of a reflected sound wave in the moving fluid. Chapter 4 describes the proposed downhole multiphase flowmeter. It will have many advantages and will be discussed in full in that chapter.

DOE/BC/14600-41 **Aspects of Non-Newtonian Flow and Displacement in Porous Media. Topical Report. University of Southern California. February 1993. 76 pp. Order No. DE93000128.** The flow of fluids through a variety of porous media is common in many petroleum engineering applications. A partial list includes filtration, ground water flow, production of oil and gas from underground reservoirs, ion exchange and adsorption. Most of these involve either single- or multi-phase flow of fluids in order to achieve desired objectives. In some of these applications, non-Newtonian fluids are extensively involved. Particular examples include heavy oils and enhanced oil recovery (EOR). The rheology of many heavy oils has been shown to be non-Newtonian, Bingham plastics being one manifestation of heavy oil flow. In EOR applications, non-Newtonian fluids such as low-concentration polymer solutions, emulsions, gels, etc. are simultaneously injected to increase the viscosity of driving agents that displace oil. Such rheologically complex fluids are used to improve sweep efficiencies, divert displacing fluids and block swept zones. The present study has been undertaken to understand the flow of non-Newtonian fluids through porous media. The work considered involves the numerical (pore network) modeling of both single- and multi-phase flow of power-law and Bingham plastic fluids in network-like porous media.

DOE/BC/14721-4 **Cleanup/Stimulation of a Horizontal Wellbore Using Propellants. Final Re-**

port. Rougeot Oil and Gas Corporation. January 1993. 60 pp. Order No. DE93000113. This report documents the stimulation/cleanup of a horizontal wellbore (Wilson 25) using propellants. The Wilson 25 is a Bartlesville Sand well located in Flatrock Field, Osage County, Oklahoma. The final report covers the cleanup/stimulation of that well, includes the rationale, planning, results, and recommendations for using propellants as a means to cleanup/stimulate a horizontal wellbore. The data from the Wilson 25 will allow independent producers to estimate the cost, and to plan and perform a propellant shot cleanup/stimulation of a horizontal wellbore. The Wilson 25 results indicated that a propellant shot treatment is an economically viable means to cleanup/stimulate a horizontal wellbore.

DOE/BC/93000111 The Influence of Disjoining Pressure on Foam Stability and Flow in Porous Media. Topical Report. Lawrence Berkeley Laboratory. January 1993. 40 pp. Order No. DE93000111. Foam flowing in porous media can exhibit large flow resistances that make it an attractive fluid for improving underground oil recovery. To be an effective displacement fluid, however, the lamella, which discretize the gas into foam bubbles, must remain stable. This work studies how the stability of single foam films, as gauged by the magnitude of their disjoining pressures, influences the flow resistance of foam in porous media. When gas and a dilute surfactant solution flow simultaneously through a porous medium to form a foam, measured pressure drops can be orders of magnitude larger than when there is no surfactant in the aqueous phase. The large flow resistance of foam in porous media makes it a desirable mobility-control agent for improving underground oil recovery.

DOE/BC-93/3/SP Seventh Amendment and Extension to Venezuela/DOE Annex IV-8 U.S. Department of Energy and The Ministry of Energy and Mines of the Republic of Venezuela. February 1993. 344 pp. Order No. DE93000115. This report contains the results of efforts under the six tasks of the Seventh amendment and Extension of Annex IV, Enhanced Oil Recovery Thermal Processes of the Venezuela/USA Agreement. The report is presented in sections (for each of the six tasks) and each section contains one or more reports prepared by various individuals or groups describing the results of efforts under each of the tasks. A statement of each task, taken from the agreement, is presented on the first page of each section. The tasks are numbered 50 through 55. The first, second, third, fourth, fifth, sixth and seventh reports on Annex IV, Venezuela MEM/USA-DOE Fossil Energy Report IV-1, IV-2, IV-3, IV-4, IV-5 and IV-6 (DOE/BETC/SP-83-15, DOE/BC-84/6/SP, DOE/BC-86/2/SP, DOE/BC-89/1/SP, DOE/BC-90/1/SP, and DOE/BC-92/1/SP) contain the results for the first 49 tasks. These reports are dated April 1983, August 1984, March 1986, July 1987, November 1988, December 1989, and October 1991, respectively.

Geoscience

DOE/BC/14656-8 Minor and Trace Authigenic Components as Indicators of Pore Fluid Chemistry During Maturation and Migration of Hydrocarbons. Final Report. Texas A&M University. February 1993. 124 pp. Order No. DE93000125. Variations in mineralogy and composition of late authigenic sulfur-bearing minerals in upper Smackover limestones recorded diagenetic events associated with hydrocarbon migration. This suite of minerals was examined in samples taken from 18 subsurface cores of the upper Smackover from northern Louisiana and southern Arkansas. Spatial variations in cadmium concentration of sphalerite, Ba concentration of celestite, and the $\delta^{34}\text{S}$ values of galena and sphalerite suggest that fluids associated with the hydrocarbons in the lower Smackover migrated into the upper Smackover along faults at the Louisiana-Arkansas border. A second generation of sulfide mineralization and heavy sulfur isotopic ratios of some sulfides suggest that thermochemical sulfate reduction occurred after hydrocarbon migration, resulting in the formation of the "sour gas belt". Study of these minerals in the upper Smackover limestones has provided the first concrete evidence of migration of late-stage pore fluids into these rocks along faults and has shown that this flow was focused in specific areas. This knowledge allows a clearer and more specific interpretation of previous authors observations and data.

NIPER-615 Data Requirements and Acquisition for Reservoir Characterization. Topical Re-

port. National Institute for Petroleum and Energy Research. March 1993. 32 pp. Order No. DE93000121. This report outlines the types of data, data sources and measurement tools required for effective reservoir characterization, the data required for specific enhanced oil recovery (EOR) processes, and a discussion of the determination of the optimum data density for reservoir characterization and reservoir modeling. The value of data can be assessed as the corresponding loss resulting from poor or incomplete data; however, determining the optimum data density for reservoir characterization is difficult because the value of the data may not be known until it is acquired and analyzed. Effective simulation studies are needed to evaluate the magnitude and direction of errors that can be expected in oil recovery prediction with varying amount of data. A quantitative approach using the variogram is proposed, where the correlation length is used as a guide to the minimum sampling distance for data collection.

NIPER-634

Integration of the Geological/Engineering Model with Production Performance for Patrick Draw Field, Wyoming. Topical Report. National Institute for Petroleum and Energy Research. March 1993. 132 pp. Order No. DE93000130. This report covers work conducted in FY92 and includes the following topics: (1) the application of hydrogeochemical techniques to reservoir characterization; (2) the effect of salinity variations in the determination of oil saturation by wireline logs; (3) structural and sedimentological features that control fluid distribution and movement; and (4) analysis of lateral variations in production performance. The major findings of the research include: (1) hydrogeochemical analytical techniques were demonstrated to be an inexpensive reservoir characterization tool that provides information on reservoir architecture and compartmentalization; (2) the formation water salinity in Patrick Draw Field varies widely across the field; and (3) an analysis of the enhanced oil recovery (EOR) potential of Patrick Draw Field indicates the CO_2 flooding in the Monell Unit and horizontal drilling in the Arch Unit are potential methods to recover additional oil from the field.

NIPER-648

Special Core Analyses and Relative Permeability Measurement on Almond Formation Reservoir Rocks. Topical Report. National Institute for Petroleum and Energy Research. February 1993. 36 pp. Order No. DE93000119. This report describes the results from special core analyses and relative permeability measurements conducted on samples of rock from the Almond Formation in Greater Green River Basin of southwestern Wyoming. The core was from Arch Unit well 121 of Patrick Draw field. Thin section evaluation, X-ray diffraction, routine permeability and porosity, capillary pressure and wettability tests were performed to characterize the samples. Fluid flow capacity characteristics were measured during two-phase unsteady- and steady-state and three-phase steady-state relative permeability tests. Relative permeability results are compared with those of a 260-mD, fired Berea sandstone sample which was previously subjected to similar tests. Brine relative permeabilities were similar for the two samples, whereas oil and gas permeabilities for the Almond Formation rock were higher at equivalent saturation conditions compared to Berea results. Most of the tests described in this report were conducted at 74° F laboratory temperature. Additional tests are planned at 150° F temperature. Equipment and procedural modification to perform the elevated temperature tests are described.

Gas

DOE/MC/26031-8

Field Verification of CO_2 -Foam. Third Annual Report. October 1, 1991 - September 30, 1992. New Mexico Institute of Mining and Technology. February 1993. 80 pp. Order No. DE93000127. The East Vacuum Grayburg/San Andres Unit (EVGSAU), operated by Phillips Petroleum Company, is the site selected for a comprehensive evaluation of the use of foam for improving the effectiveness of a CO_2 flood. This third annual report details various aspects of the CO_2 -Foam Field Verification Pilot test at EVGSAU. The report presents: 1) an overview of the operating plan for the project, 2) details of the foam injection schedule and design criteria, 3) a discussion of the data collection program and performance criteria to be used in evaluating successful application of foam for mobility control in the EVGSAU CO_2 project, and (4) preliminary results from the field injection test. Specific items discussed in the foam injection design include the

determination of surfactant volume and concentration, selection of the surfactant-alternating-gas (SAG) injection sequence for foam generation, field facilities, operations during foam injection, and contingency plans. An extensive data collection program for the project is discussed including production testing, injection well pressure and rate monitoring, injection profiles, production well logging, observation well logging program, and both gas and water phase tracer programs.

DOE/MC/26253-9 Scale-up of Miscible Flood Process. Final Report. Stanford University. February 1993. 308 pp. Order No. DE93000126.

Results of a wide-ranging investigation of the scaling of the physical mechanisms of miscible floods are reported. Advanced techniques for analysis of crude oils are considered in Chapter 2. Application of supercritical fluid chromatography is demonstrated for characterization of crude oils for equation-of-state calculations of phase equilibrium. The theory of development of miscibility is considered in detail in Chapter 3. The theory is extended to four components, and sample solutions for a variety of gas injection systems are presented. In Chapter 4, the interactions of viscous fingering and permeability heterogeneity are examined. Results of flow visualizations are reported for unstable displacements in synthetic heterogeneous porous media. In Chapter 5, the combined efforts of capillary and gravity-driven crossflow are considered. The experimental results presented show that very high recovery can be achieved by gravity segregation when interfacial tensions are moderately low. In addition, results of flow visualization experiments are presented that illustrate the interplay of crossflow driven by gravity with that driven by viscous forces.

Resource Assessment Technology

DOE/ID/12842-1 Pilot Oil Atlas for Louisiana. Final Report. Louisiana State University. January 1993. 96 pp. Order No. DE93000114.

In recent years, it has become increasingly difficult for major oil companies to economically produce many of the older domestic reservoirs because of declining well productivity and more stringent environmental regulations. Smaller independent operators are playing an increasing important role in producing the remaining oil and gas, and it is anticipated that this trend will continue in the future. The small independent producers do not maintain research and development laboratories, nor do they have the large technical-support staffs found in the major oil companies. In mature fields with declining productivity, they seek to maintain profitability primarily through reduced overhead and hence rely, to a great extent, on technology and information available in the public domain. Thus it is becoming increasingly important to maintain strong university components capable of supporting the domestic oil and gas producing industry. The database format suggested in this report would allow production information to be easily displayed by reservoir as well as by lease, unit, or well. Enlargement of the information base maintained by using other public input data sources is also recommended. The data collected as part of the bypassed-oil study was used to illustrate the proposed new format. This pilot database, or atlas, contains information available for 15 reservoirs.

DOE/BC/14425-7 Reservoir Characterization of the Smackover Formation in Southwest Alabama. Final Report. Geological Survey of Alabama. February 1993. 136 pp. Order No. DE93000122.

The Upper Jurassic Smackover Formation is found in an arcuate belt in the subsurface from south Texas to panhandle Florida. The Smackover is the most prolific hydrocarbon-producing formation in Alabama and is an important hydrocarbon reservoir from Florida to Texas. Most Smackover reservoirs originated as nearshore-marine carbonate sediments with minor admixtures of noncarbonate material. The most common Smackover reservoir rocks are nonskeletal grainstone, dominated by pellets, ooids, and oncoids, in order of decreasing abundance. Mixed-particle grainstone/packstone is the second most common reservoir type in the Smackover of southwest Alabama. Quartzose sandstone, commonly dolomitic, forms permeable reservoirs with interparticle pore systems locally in southern Monroe County (e.g., North Waller Creek field). The most common kinds of pores in the Smackover are particle molds, secondary intraparticle (partial moldic) pores, and interparticle pores. The various pore types lend different petrophysical characteristics to pore systems, and combinations of different kinds of pores in varying proportions create further effects. In this study, Smackover reservoir rocks are classified using capillary-pressure curve shape. Pore systems in reservoir rocks of the Smackover Formation in southwest Alabama are dominated either by moldic plus secondary intraparticle pores or by intercrystalline pores. Intermediate pore systems are less common. Therefore, two pore facies, rock units characterized by certain pore types or combinations of pore types, and by certain consequent pore-throat-size distribution, are defined.

Fundamental Petroleum Chemistry

NIPER-536 Vanadium and Nickel Complexes in Petroleum Resid Acid, Base, and Neutral Fractions. Topical Report. National Institute for Petroleum and Energy Research. January 1993. 32 pp. Order No. DE93000101.

Acid and base fractions from petroleum vacuum resid with no detectable (by visible spectrophotometry) quantities of porphyrinic Ni or V complexes were hydrotreated under various conditions to determine if significant amounts of porphyrinic metals were released, via disassociation or other means, upon hydrotreating. No significant quantities were observed, thereby indicating that nonporphyrinic metals were not simply associated, complexed or otherwise masked (in terms of visible spectrophotometric response) porphyrinic metal complexes. However, it is possible that hydrotreating was simply not effective in breaking up these associates and/or that some porphyrinic forms of metal were in fact released but were rapidly destroyed by hydrotreating.

NIPER-659 The Thermodynamic Properties of Thianthrene and Phenoxathiin. Topical Report. National Institute for Petroleum and Energy Research. March 1993. 60 pp. Order No. DE93000124.

Measurements leading to the calculation of the ideal-gas thermodynamic properties are reported for thianthrene and phenoxathiin. Experimental methods included combustion calorimetry, adiabatic heat-capacity calorimetry, vibrating-tube densitometry, comparative ebulliometry, inclined-piston gauge manometry, and differential-scanning calorimetry (d.s.c.). Critical properties were estimated for both materials based on the measurements results. Entropies, enthalpies, and Gibbs energies of formation were derived for the ideal gas for both compounds for selected temperatures between 298.15K and 700K. The property-measurement results reported here for thianthrene and phenoxathiin provide the first experimental gas-phase Gibbs energies of formation for tricyclic diheteroatom-containing molecules.

INDEX

COMPANIES AND INSTITUTIONS

	Page		Page
Brookhaven National Laboratory		Development of Improved Alkaline Flooding Methods	24
Effects of Selected Thermophilic Microorganisms on Crude Oils at Elevated Temperatures	111	Development of Improved Microbial Flooding Methods	114
Columbia University		Feasibility Study of Heavy Oil Recovery in the Midcontinent Region (Oklahoma, Kansas, and Missouri)	52
Surfactant Loss Control in Chemical Flooding: Spectroscopic and Calorimetric Study of Adsorption and Precipitation on Reservoir Minerals	10	Field Application of Foams for Oil Production Symposium	56
Idaho National Engineering Laboratory		Gas Flood Performance Prediction Improvement	33
Microbial Enhanced Oil Recovery and Wettability Research Program	105	Imaging Techniques Applied to the Study of Fluids in Porous Media	81
Illinois Department of Energy and Natural Resources		Microbial Enhanced Waterflooding Field Project	116
Research on Improved and Enhanced Oil Recovery in Illinois Through Reservoir Characterization	66	Mobility Control and Sweep Improvement in Chemical Flooding	25
Illinois Institute of Technology		Profile Modifications, Mobility Control, and Sweep Improvement in Gas Flooding	35
Surfactant-Enhanced Alkaline Flooding for Light Oil Recovery	1	Reservoir Assessment and Characterization	93
Injectech, Inc.		Simulation Analysis of Steam-Foam Projects	55
New Microorganisms and Processes for Microbial Enhanced Oil Recovery	107	Surfactant-Enhanced Alkaline Flooding Field Project	27
Lawrence Berkeley Laboratory		Surfactant Flooding Methods	20
Electrical and Electromagnetic Methods for Reservoir Description and Process Monitoring	67	Thermal Processes for Heavy Oil Recovery	50
Lawrence Berkeley Laboratory/Industry Heterogeneous Reservoir Performance Definition Project	75	Thermal Processes for Light Oil Recovery	48
Lawrence Livermore National Laboratory		Third International Reservoir Characterization Technical Conference	99
Oil Field Characterization and Process Monitoring Using Electromagnetic Methods	45	Three-Phase Relative Permeability Research	79
Lomax Exploration Company		TORIS Research Support	98
Green River Formation Waterflood Demonstration Project, Uinta Basin, Utah	117	Upgrade of the Bartlesville Project Office Crude Oil Analysis Database	100
Los Alamos National Laboratory		New Mexico Institute of Mining and Technology	
Advanced Seismic Geodiagnosics—Borehole Acoustic Source	78	Field Verification of CO ₂ -Foam	13
Morgantown Energy Technology Center		Improved Techniques for Fluid Diversion in Oil Recovery	3
Quantification of Mobility Control in Enhanced Recovery of Light Oil by Carbon Dioxide	37	Research & Engineering Consultants, Inc.	
National Institute for Petroleum and Energy Research		Advanced Secondary Recovery Demonstration for the Sooner List	120
Compilation and Analysis of Outcrop Data from the Muddy and Almond Formations	103	Sandia National Laboratories	
		Geodiagnosics for Reservoir Heterogeneities and Process Mapping	77
		Stanford University	
		Scaleup of Miscible Flood Processes	31
		Stanford University Petroleum Research Institute	
		Research on Oil Recovery Mechanisms in Heavy Oil Reservoirs	57

Surtek, Inc.

Investigation of Oil Recovery Improvement by Coupling an Interfacial Tension Agent and a Mobility Agent and a Mobility Control Agent in Light Oil Reservoirs	4
---	---

University of California, Berkeley

Geophysical and Transport Properties of Reservoir Rocks	68
--	----

University of Kansas

Improving Reservoir Conformance Using Gelled Polymer Systems	8
---	---

University of Michigan

Characterization and Modification of Fluid Conductivity in Heterogeneous Reservoirs To Improve Sweep Efficiency	85
---	----

University of Oklahoma

Dispersion Measurement as a Method of Quantifying Geologic Characterization and Defining Reservoir Heterogeneity	89
Quantification of Microbial Products and Their Effectiveness in Enhanced Oil Recovery	108

University of Southern California

Modification of Reservoir Chemical and Physical Factors in Steamfloods To Increase Heavy Oil Recovery	41
---	----

University of Southern Mississippi

Responsive Copolymers for Enhanced Petroleum Recovery	16
--	----

University of Texas at Austin

A Novel Approach to Modeling Unstable Enhanced Oil Recovery Displacements	129
Development of Cost-Effective Surfactant Flooding Technology	16
Oil Recovery from Naturally Fractured Reservoirs by Steam Injection Methods	88
Revitalizing a Mature Oil Play: Strategies for Finding and Producing Unrecovered Oil in Frio Fluvial-Deltaic Reservoirs of South Texas	126

University of Tulsa

Reservoir Characterization of Pennsylvanian Sandstone Reservoirs	73
---	----

West Virginia University

Measuring and Predicting Reservoir Heterogeneity in Complex Depositional Systems	59
---	----

CONTENTS BY EOR PROCESS

Chemical Flooding—Supporting Research	1
Gas Displacement—Supporting Research	31
Thermal Recovery—Supporting Research	41
Geoscience Technology	59
Resource Assessment Technology	93
Microbial Technology	105
Reservoir Classes	117
Novel Technology	129

**DOE Technical Project Officers for
Enhanced Oil Recovery**

DIRECTORY

Name	Phone number	Name of contractor
U. S. Department of Energy Gas and Petroleum Technology Oil and Gas Exploration and Production 3E-028/FORS Washington, D.C. 20585		
Bartlesville Project Office P. O. Box 1398 Bartlesville, Oklahoma 74005		
Edith Allison	918-337-4390	Lomax Exploration Company National Institute for Petroleum and Energy Research Research & Engineering Consultants, Inc. University of Texas West Virginia University
Jerry Casteel	918-337-4412	Columbia University Illinois Institute of Technology National Institute for Petroleum and Energy Research New Mexico Institute of Mining and Technology Stanford University Surtek, Inc. University of Kansas University of Southern Mississippi University of Texas at Austin
Robert Lemmon	918-337-4405	Lawrence Berkeley Laboratory Los Alamos National Laboratory National Institute for Petroleum and Energy Research Sandia National Laboratories University of California, Berkeley University of Michigan
Rhonda Lindsey	918-337-4455	Brookhaven National Laboratory Idaho National Engineering Laboratory Injectech, Inc. National Institute for Petroleum and Energy Research University of Tulsa
Chandra Nautiyal	918-337-4409	National Institute for Petroleum and Energy Research
R. Michael Ray	918-337-4403	Illinois Department of Energy and Natural Resources
Thomas Reid	918-337-4233	Lawrence Livermore National Laboratory National Institute for Petroleum and Energy Research Stanford University Petroleum Research Institute University of Southern California
Metairie Site Office 900 Commerce Road, East New Orleans, Louisiana 70123		
Jerry Ham	504-734-4906	University of Texas at Austin
E. B. Nuckols	504-734-4806	University of Oklahoma
Gene Pauling	504-734-4131	University of Oklahoma
Morgantown Energy Technology Center P. O. Box 880 Morgantown, West Virginia 26505		
Royal Watts	304-291-4218	Morgantown Energy Technology Center New Mexico Institute of Mining and Technology

CHEMICAL FLOODING— SUPPORTING RESEARCH

SURFACTANT-ENHANCED ALKALINE FLOODING FOR LIGHT OIL RECOVERY

Contract No. DE-AC22-92BC14883

**Illinois Institute of Technology
Chicago, Ill.**

**Contract Date: Sept. 21, 1992
Anticipated Completion: Sept. 20, 1995
Government Award: \$150,000
(Current year)**

**Principal Investigator:
Darsh T. Wasan**

**Project Manager:
Jerry Casteel
Bartlesville Project Office**

Reporting Period: Oct. 1–Dec. 31, 1992

Objective

The overall objective of this project is to develop a very cost-effective method for formulating a successful surfactant-enhanced alkaline flood by appropriately choosing mixed alkalis that form inexpensive buffers to obtain the desired pH (between 8.5 and 12.0) for ultimate spontaneous emulsifica-

tion and ultralow interfacial tension. In addition, the novel concept of pH gradient design to optimize floodwater conditions will be tested.

Summary of Technical Progress

In the recent past, a model for the interfacial activity of alkaline/acidic oil systems which accounted for adsorption of un-ionized acid on the interface was developed.¹ The model explained why interfacial tension reaches ultralow values; however, the mechanistic picture was not complete. It did not adequately explain why interfacial tension decreased when the system is above the critical micelle concentration (CMC) of ionized acid.

This quarter the interfacial activity model was extended to account for a mixed interfacial layer and mixed micelle formation by ionized and un-ionized acid. The ultralow value of interfacial tension is shown to result from the simultaneous adsorption of ionized and un-ionized acid upon the interface, and the lowering results from the formation of mixed micelles of ionized and un-ionized acid.

Results and Discussion

The mathematical model that has been developed relates the chemistry of an alkaline/acidic oil system to the interfacial tension through adsorption isotherms. It accounts for mixed adsorption and mixed micelle formation of the ionized as well as the un-ionized acid species. A brief description of the theoretical model follows.

The chemistry is represented as reversible reactions for (1) dimerization of un-ionized acid in the oil, (2) distribution of un-ionized acid between oil and water, (3) dissociation of the un-ionized acid into hydronium ion and ionized acid, (4) salt formation of the ionized acid in the water, (5) distribution of an acid salt to the oil phase (not used for oleic acid system), (6) mixed micelle formation of ionized and un-ionized acid in the water phase (phase separation theory), and (7) dissociation of water. The NaOH and NaCl were assumed to be completely dissociated. A molal balance for ionized acid and sodium ion and a charge balance yield a system of three equations and four unknowns which are the concentration of ionized acid in the aqueous and micellar phases and sodium ion and hydroxide ion in the aqueous phase. To solve for the unknowns and completely describe the system chemistry, another equation needs to be specified. This relationship between these unknowns comes from the formation of micelles. The semi-empirical micellar relationship used is that developed by Shinoda,^{2,3} which is applied to mixed micelles with the phase separation assumption. These equations are combined to form a set of three nonlinear algebraic equations that are solved by a Newton-Raphson numerical scheme.

An adsorption equation was used to calculate the interfacial concentration of ionized acid as well as un-ionized acid with the double layer being described by the Gouy-Chapman theory. The equation-of-state approach yields a relationship between the surface pressure and concentration of adsorbed species. Surface pressure has a kinetic contribution, obtained by considering a hypothetical uncharged film and a contribution from the electrical double layer. Finally, interfacial tension is obtained from the difference in surface pressure of a clean interface and one that contains surface-active material.

Figure 1 shows a comparison between the theoretically used hydroxide ion values and the experimentally measured value, represented as the equilibrium pH. The pH values for 13.0 mol/m³ initial acid were used to obtain exactly the experimentally measured interfacial tension values shown in Fig. 2. Then, the initial acid concentration in the oil was changed to 5.0 and 40.0 mol/m³, and the model yielded the results shown without any modification to the constants. It can be seen that there exists a linear relationship between the equilibrium pH, initial pH, and the logarithm of the initial acid concentration at the minimum in interfacial tension. Figure 2 shows that more hydroxide is needed to reach the minimum in interfacial tension as the initial acid concentration is increased. The minimum in interfacial tension corresponds to half-ionization of the acid.

Figure 3 shows the normalized ionized acid concentration as a function of the un-ionized acid concentration in the alkaline solution. Since most of these theoretical results form a straight line, the semi-empirical micellar relationship is satisfactory. This relationship is good for NaOH concentrations at and after the point where the minimum in interfacial tension just starts. The deviation before the start of the minimum is believed to result because either the phase

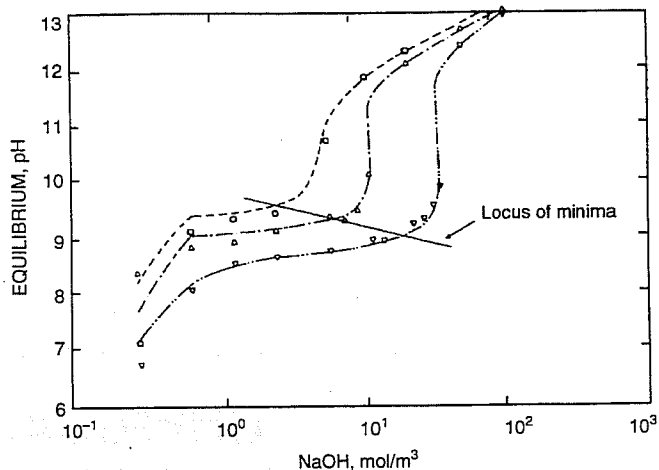


Fig. 1 Comparison of theory with experiments for the effect of alkali on the equilibrium pH at different initial acid concentrations. Decane/oleic acid $\text{Na}^+ = 171 \text{ mol/m}^3$. \circ , --- 5.0 mol/m³ initial acid. Δ , --- 13.0 mol/m³ initial acid. ∇ , --- 40.0 mol/m³ initial acid.

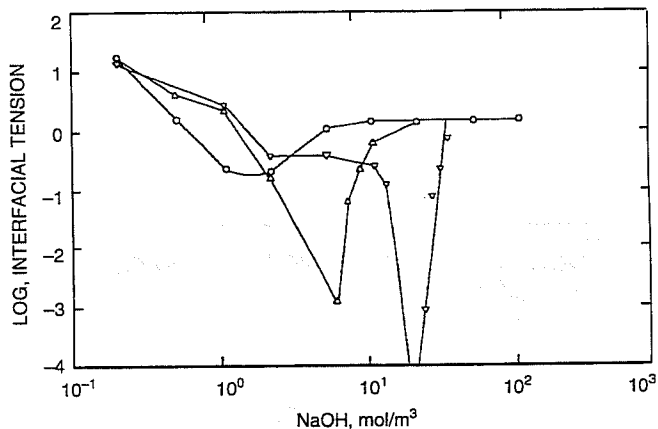


Fig. 2 Effect of alkali on interfacial tension for different initial acid concentrations. Decane/oleic acid $\text{Na}^+ = 171 \text{ mol/m}^3$. \circ , 5.0 mol/m³ initial acid. Δ , 13.0 mol/m³ initial acid. ∇ , 40.0 mol/m³ initial acid.

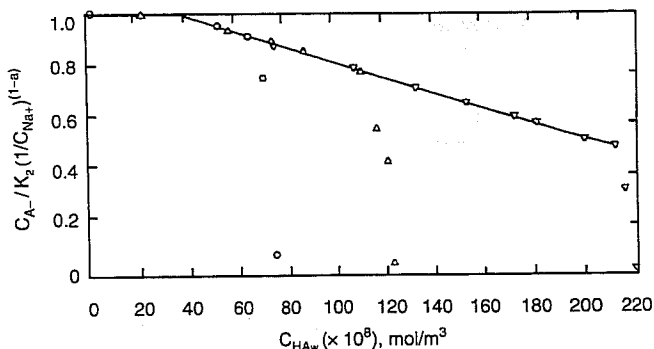


Fig. 3 Normalized ionized acid monomer concentration as a function of un-ionized acid concentration in the alkaline solution. Decane/oleic acid $\text{Na}^+ = 171 \text{ mol/m}^3$. \circ , 5.0 mol/m³ initial acid. Δ , 13.0 mol/m³ initial acid. ∇ , 40.0 mol/m³ initial acid. $R^2 = 0.999$. $K_0 = 2.88 \times 10^5 \text{ m}^3/\text{mol}$. Intercept = 1.1.

separation assumption becomes invalid or the distribution coefficient of un-ionized acid between the aqueous phase and micelle is no longer constant with increase in concentration.

Even at low alkali concentrations, enough acid is extracted for the ionized acid to be above its CMC. Why then does interfacial tension go through a minimum? The interfacial tension goes through a minimum with pH (see Fig. 4) because, at low pH, the high concentration of un-ionized acid reduces the CMC of the ionized acid, resulting in lower interfacial coverage and higher interfacial tension. As pH increases, the un-ionized acid concentration decreases and the CMC of the ionized acid increases, resulting in increased interfacial coverage and a reduction in interfacial tension. With further increase in pH, the acid is completely ionized, and interfacial tension rises because the loss of un-ionized acid is contributing to interfacial tension. Thereafter, interfacial tension is constant and results from only adsorption of ionized acid.

These results show that the un-ionized acid should be present in the alkali/crude oil system to obtain ultralow interfacial tensions. As a result, a proper intermediate alkaline pH (8.5 to 12.0) should be operative during the reservoir flood. This situation may be realized by using a "pH gradient" designed flood. This pH gradient concept is currently under investigation at this laboratory.

Next quarter the mechanisms responsible for producing the spontaneous emulsification observed in surfactant-enhanced alkali/acidic oil systems will be investigated.

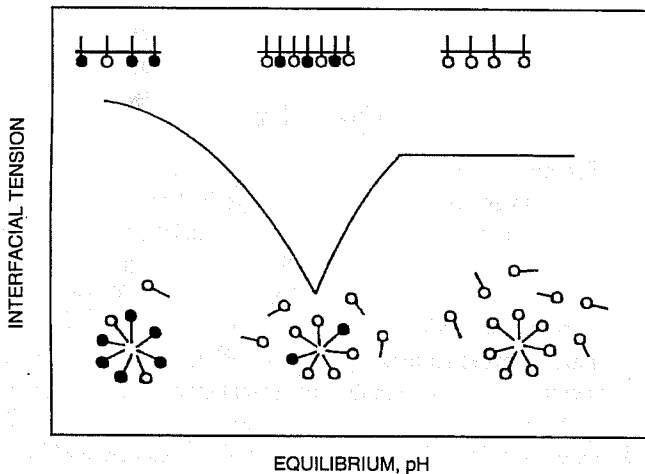


Fig. 4 Illustration of the synergistic effect.

References

1. D. T. Wasan, *Enhanced Oil Recovery Through In Situ-Generated Surfactants Augmented by Chemical Injection*, Progress Report submitted to DOE for the period April 1–June 30, 1989, DOE/BC–89/3, May 1990.
2. K. Shinoda, The Effect of Alcohols on the Critical Micelle Concentrations of Fatty Acid Soaps and the Critical Micelle Concentration of Soap Mixtures, *J. Phys. Chem.*, 58: 1136 (1954).
3. K. Shinoda, The Effect of Chain Length of Salts and Alcohols on the Critical Micelle Concentration, *Bull. Chem. Soc. Jpn.*, 26: 101 (1953).

IMPROVED TECHNIQUES FOR FLUID DIVERSION IN OIL RECOVERY

Contract No. DE-AC22-92BC14880

New Mexico Institute of Mining and Technology
Petroleum Recovery Research Center
Socorro, N. Mex.

Contract Date: Sept. 17, 1992

Anticipated Completion: Sept. 30, 1995

Government Award: \$192,590

Principal Investigators:

Randall S. Seright

F. David Martin

Project Manager:

Jerry Casteel

Bartlesville Project Office

Reporting Period: Oct. 1–Dec. 31, 1992

Objectives

This three-year project has two general objectives. The first objective is to compare the effectiveness of gels in fluid diversion with those of other types of processes. Several different types of fluid-diversion processes will be compared, including those using gels, foams, emulsions, and particulates. The ultimate goals of those comparisons are to (1) establish which of these processes are most effective in a given application and (2) determine whether aspects of one process can be combined with those of other processes to improve performance. Analyses will be performed to assess where the various diverting agents will be most effective (e.g., in fractured vs. unfractured wells, in deep vs. near-wellbore applications, in reservoirs with vs. without crossflow, or in injection wells vs. production wells). Experiments will be performed to verify which materials are the most effective in entering and blocking high-permeability zones. Another objective of the project is to identify the mechanisms by which materials (particularly gels) selectively reduce permeability to water more than to oil. In addition to establishing why this occurs, research will attempt to identify materials and conditions that maximize this phenomenon.

Summary of Technical Progress

Work in the first quarter focused on two areas: (1) comparing the effectiveness of emulsions in fluid diversion with that of gels and (2) examining why gels selectively reduce permeability to water more than to oil. This property is critical to the success of gel treatments in production wells if zones cannot be isolated during gelant placement.^{1,2}

Several different mechanisms that could conceptually allow gels to reduce permeability to water more than to oil have

been identified. Experiments are under way to test the validity of each of these ideas. Some of the mechanisms (expressed in question form) include

1. Do gels shrink when contact is switched from water to oil and swell when contact is switched from oil to water? This explanation was first proposed by Sparlin.³ Two sets of experiments are under way to test this mechanism. First, gels are being observed macroscopically to find whether volume changes occur when switching contact from water to oil and back. These experiments are being performed both at 1 atm and 102 atm. Second, corefloods are being performed to determine oil and water residual resistance factors as a function of pressure between 1 atm and 102 atm. If volume changes are important, the residual resistance factors should vary with pressure.

2. Is the disproportionate permeability reduction caused by a lubrication effect? This mechanism was proposed by Zaitoun and Kohler.⁴ If this explanation is valid, then the ratio of water to oil residual resistance factors in strongly water-wet cores should vary significantly with oil viscosity. Therefore experiments with oils of different viscosity are being performed.

3. Do gels make cores more water wet and is wettability strongly linked to the disproportionate permeability reduc-

tion? To test this idea, oil and water residual resistance factors are being determined in cores with different wettabilities.

4. Does gravity influence the location of gel particles in pores? Residual resistance factors should depend on where gel particles lodge in a pore; that is, particles trapped in pore throats could reduce permeability more than those in other locations. Pore orientation, fluid velocity, and fluid densities could affect the probability that gel particles will locate in pore throats. To test this possibility, corefloods are being performed using different core orientations, different fluid velocities, and oils with different densities.

References

1. J. Liang, R. L. Lee, and R. S. Seright, *Placement of Gels in Production Wells*, paper SPE/DOE 20211 presented at the 1990 SPE/DOE Enhanced Oil Recovery Symposium, Tulsa, Okla., Apr. 22-25, 1990.
2. J. Liang, H. Sun, and R. S. Seright, *Reduction of Oil and Water Permeabilities Using Gels*, paper SPE/DOE 24195 presented at the 1992 SPE/DOE Enhanced Oil Recovery Symposium, Tulsa, Okla., Apr. 21-24, 1992.
3. D. D. Sparlin, An Evaluation of Polyacrylamides for Reducing Water Production, *J. Pet. Technol.*, 906-914 (August 1976).
4. A. Zaitoun and N. Kohler, *Two-Phase Flow Through Porous Media: Effect of an Adsorbed Polymer Layer*, paper SPE 18085 presented at the 1988 Annual Technical Conference and Exhibition, Houston, Tex., Oct. 2-5, 1988.

Objectives

The study will investigate two major areas concerning co-injecting an interfacial tension (IFT) reduction agent(s) and a mobility control agent. The first will consist of defining the mechanisms of interaction of an alkaline agent, a surfactant, and a polymer on a fluid-fluid and a fluid-rock basis. The second is the improvement of the economics of the combined technology.

This report examines the effect of different alkaline agents, surfactants, and combinations of surfactant and alkaline agents on the reduction of IFT between a fluvial deltaic crude oil and the aqueous solution. The preliminary evaluations of the effect of pH, surfactant structure, and alkali type will be discussed.

Summary of Technical Progress

Crude Oil

A fluvial deltaic crude oil from the Adena field in Morgan County, Colo., was selected for the study. The Adena crude oil is a 42 °API gravity crude oil with a dead oil viscosity of 3.8 cP at 72 °F and 1.3 cP at the 180 °F reservoir temperature.

Water

All solutions are dissolved in 1000 mg/L NaCl.

INVESTIGATION OF OIL RECOVERY IMPROVEMENT BY COUPLING AN INTERFACIAL AGENT AND A MOBILITY CONTROL AGENT IN LIGHT OIL RESERVOIRS

Contract No. DE-AC22-92BC14886

**Surtek, Inc.
Golden, Colo.**

**Contract Date: Sept. 28, 1992
Anticipated Completion: Sept. 30, 1995
Government Award: \$219,925
(Current year)**

**Principal Investigator:
Malcolm J. Pitts**

**Project Manager:
Jerry Casteel
Bartlesville Project Office**

Reporting Period: Oct. 1-Dec. 31, 1992

Interfacial Tension with Alkali

The IFT was determined at 72 °F with aqueous sodium carbonate (Na_2CO_3)–sodium bicarbonate (NaHCO_3), sodium hydroxide (NaOH), and sodium dibasic phosphate (Na_2HPO_4)–sodium tribasic phosphate (Na_3PO_4). For the multi basic alkaline agents, the two components were tested with each component individually as well as a 2:1 and a 1:2 mixture. Alkaline agent concentrations between 0.0 and 2.0 wt % were tested. A 2.0 wt % limit was imposed because of economic restraints on an injected chemical solution in a field application. The minimum IFT values were measured at 2.0 wt % for all of the alkaline agent combinations and the values are shown in Table 1. Interfacial tension determinations were either DuNouy ring tensiometer¹ or spinning drop tensiometer² measurements.

A plot of pH vs. the minimum IFT values at a constant alkali concentration is shown in Fig. 1. The IFT reduction is independent of pH and appears to be dependent on the alkaline agent.

Interfacial Tension with Surfactants

The IFT between the Adena crude oil and the surfactants listed in Table 2 was determined at 72 °F. Surfactants were selected based on commercial availability and on structure variation. Surfactant concentrations of 0.1 and 0.2 active wt % were selected for study, again considering field economic restraints on injected solutions.

The preliminary results listed in Table 2 suggest that within each structure group, the IFT increased with molecular weight. Branched side-chain structures generally had lower IFT values than linear side-chain structures. An aromatic ring in the structure resulted in lower IFT values. Sterically hindering side-chain movement did not affect IFT reduction effectiveness.

Interfacial Tension with Surfactant Plus Alkaline Agents

The IFT between the Adena crude oil and the various surfactants combined with the three alkaline agents was

TABLE 1
Minimum Interfacial Tension
Values of Alkaline Agents

Alkaline agent	Interfacial tension, mN/m
Water	19.6
NaOH	4.2
NaHCO_3	17.7
2:1 NaHCO_3 : Na_2CO_3	17.2
1:2 NaHCO_3 : Na_2CO_3	5.8
Na_2CO_3	12.6
Na_2HPO_4	13.8
2:1 Na_2HPO_4 : Na_3PO_4	0.397
1:2 Na_2HPO_4 : Na_3PO_4	0.014
Na_3PO_4	0.006

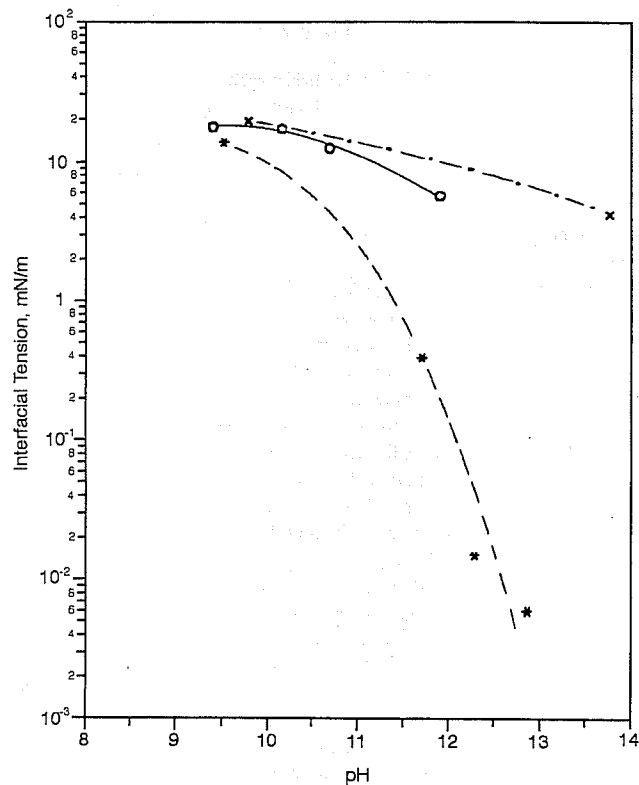


Fig. 1 Interfacial tension reduction of Adena crude oil with 2.0 wt % alkali as a function of pH. x, NaOH. o, Na_2CO_3 – NaHCO_3 . *, Na_3PO_4 – NaH_2PO_4 .

determined. A 0.1 and 0.2 active wt % surfactant was blended with seven concentrations of alkali between 0.5 to 2.0 wt %. A typical IFT vs. alkaline agent curve is shown in Fig. 2. The minimum IFT values for the various surfactant–alkaline agent combinations are listed in Table 3.

Combining the various surfactants with the different alkaline agents reduced the IFT values significantly, which suggests a synergism between the two IFT agents. Other investigators have observed the same phenomenon.^{3–6} Comparison of the Na_3PO_4 IFT data with Na_3PO_4 plus IOS 1517 or LXS 395 or LTS-18 data suggests that the surfactant is the dominant IFT agent. However, each alkaline agent obviously interacts differently with each surfactant. Lowering the pH of the alkaline agent–surfactant solution resulted in an increase in IFT. Depending on the surfactant, ultralow IFT was still observed with lower pH alkalis even though the absolute value has increased relative to the higher pH system. The presence of an aromatic ring appears to be beneficial. With the alkyl aryl surfactants, increasing the alkyl carbon chain beyond 18 carbons appears to increase the IFT. Lower IFT values were observed with branched alkyl side chains than with linear. Sterically hindering the rotation of the branched chain by adding a methyl group to the aryl ring increased the IFT values.

Current investigations are to expand the surfactant structures within each class and to expand the classes of surfactant studied. As a result, some of the surfactant structure conclusions may be altered.

TABLE 2
Interfacial Tension Between Adena Crude Oil and Surfactants

Surfactant	Structure	Interfacial tension, mN/m	
		0.1 wt %	0.2 wt %
LXS-370	Linear xylene sulfonate (molecular weight 370, 11 to 12 carbon side chain)	0.437	0.253
LXS-395	Linear xylene sulfonate (molecular weight 395, 13 to 14 carbon side chain)	8.2	0.900
LTS-18	Linear toluene sulfonate (molecular weight 446, 18 carbon side chain)	13.2	12.0
Petrostep B-105	Linear aryl alkyl sulfonate (molecular weight 465, 20 to 21 carbon side chain)	4.5	5.1
Petrostep B-100	Branched aryl alkyl sulfonate (molecular weight 410, 16 to 17 carbon side chain)	0.086	0.851
Chaser XP-100	Branched toluene sulfonate (molecular weight 430, 16 to 17 carbon side chain)	0.032	0.016
Neodol IOS 1517	Internal olefin sulfonate (molecular weight 348, 15 to 17 carbon chain)	0.9	1.5
Neodol IOS 1720	Internal olefin sulfonate (molecular weight 380, 17 to 20 carbon chain)	2.0	1.8
Neodol 25-3S	Sulfated ethoxylated alcohol (molecular weight 399, 12 to 15 carbon chain)	1.595	1.473

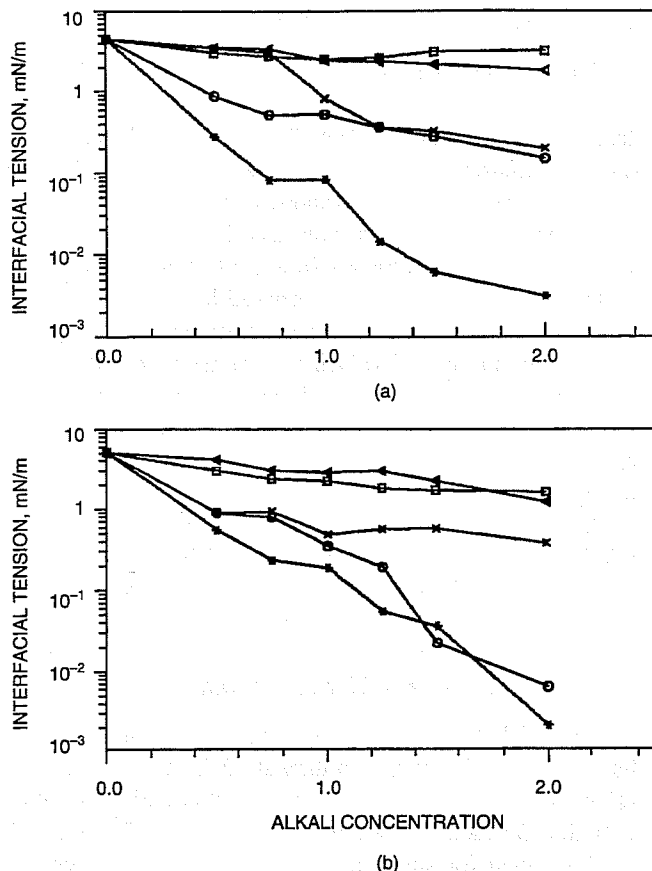


Fig. 2 Interfacial tension between Adena crude oil at 72 °F and aqueous alkali-surfactant vs. alkali concentration. (a) 0.1 wt % Petrostep B-105 plus alkali. (b) 0.2 wt % Petrostep B-105 plus alkali. ○, NaOH. ×, Na₂CO₃. *, Na₃PO₄. □, NaHCO₃. Δ, NaHPO₄.

TABLE 3
Minimum Interfacial Tension Values for Surfactant-Alkaline Agent Combinations

Surfactant	Alkali	Interfacial tension, mN/m		Alkali concentration, wt %		pH	
		0.1 wt %*	0.2 wt %*	0.1 wt %*	0.2 wt %*	0.1 wt %*	0.2 wt %*
LXS 370	NaOH	0.009	0.017	1.00	0.75	12.44	12.89
	Na ₂ CO ₃	0.011	0.001	0.75	1.50	11.08	11.13
	NaHCO ₃	0.015	0.002	2.00	2.00	9.83	9.63
	Na ₃ PO ₄	<0.001	0.018	0.50	2.00	12.13	12.29
	Na ₂ HPO ₄	0.369	0.001	1.00	1.00	8.92	8.60
LXS 395	NaOH	0.031	<0.001	0.50	1.00	12.68	12.84
	Na ₂ CO ₃	0.011	0.011	1.00	0.75	11.58	11.22
	NaHCO ₃	0.015	0.018	1.00	1.00	9.86	9.79
	Na ₃ PO ₄	0.017	0.018	0.75	2.00	12.12	12.27
	Na ₂ HPO ₄	0.069	0.022	0.50	1.00	8.59	8.73
LTS-18	NaOH	0.004	0.019	2.00	0.50	13.03	12.69
	Na ₂ CO ₃	0.093	0.109	1.25	0.50	11.21	11.13
	NaHCO ₃	0.114	0.260	2.00	0.75	8.43	8.50
	Na ₃ PO ₄	0.047	0.036	2.00	2.00	12.12	12.12
	Na ₂ HPO ₄	0.120	0.056	2.00	0.50	8.86	8.65

(Table continues on next page.)

TABLE 3 (Continued)

Surfactant	Alkali	Interfacial tension, mN/m		Alkali concentration, wt %		pH	
		0.1 wt %*	0.2 wt %*	0.1 wt %*	0.2 wt %*	0.1 wt %*	0.2 wt %*
Petrostep B-105	NaOH	0.143	0.006	2.00	2.00	13.01	13.23
	Na ₂ CO ₃	0.188	0.352	2.00	2.00	11.28	11.53
	NaHCO ₃	2.5	1.5	1.00	2.00	9.16	8.97
	Na ₃ PO ₄	0.003	0.002	2.00	2.00	12.48	12.38
	Na ₂ HPO ₄	1.7	1.144	2.00	2.00	9.05	8.81
Petrostep B-100	NaOH	0.001	0.001	0.50	0.50	12.82	12.76
	Na ₂ CO ₃	<0.001	<0.001	0.50	0.50	11.74	11.66
	NaHCO ₃	0.034	0.007	1.25	1.25	9.64	9.65
	Na ₃ PO ₄	0.007	0.005	0.50	0.50	12.22	12.30
	Na ₂ HPO ₄	1.7	1.144	2.00	2.00	8.90	8.65
Chaser XP-100	NaOH	0.007	0.004	1.25	1.25	12.90	12.87
	Na ₂ CO ₃	0.002	0.004	0.75	2.00	11.35	11.69
	NaHCO ₃	0.001	<0.001	1.25	1.00	8.97	8.97
	Na ₃ PO ₄	0.003	0.002	0.75	1.25	12.10	12.43
	Na ₂ HPO ₄	<0.001	<0.001	0.75	1.00	8.79	8.74
Neodol IOS 1517	NaOH	0.348	0.282	1.50	2.00	12.89	13.23
	Na ₂ CO ₃	0.324	0.222	2.00	2.00	11.43	11.22
	NaHCO ₃	0.680	0.645	2.00	2.00	9.88	9.83
	Na ₃ PO ₄	0.292	0.186	0.75	0.75	12.13	11.98
	Na ₂ HPO ₄	0.700	0.701	2.00	2.00	9.18	9.14
Neodol IOS 1720	NaOH	0.061	0.018	2.00	2.00	13.84	13.94
	Na ₂ CO ₃	0.040	0.026	1.50	2.00	11.78	11.72
	NaHCO ₃	0.066	0.124	2.00	1.50	9.83	9.85
	Na ₃ PO ₄	0.006	0.012	1.25	2.00	12.71	12.87
	Na ₂ HPO ₄	0.280	0.281	2.00	2.00	8.90	9.02
Neodol 25-3S	NaOH	0.131	0.087	2.00	2.00	13.00	13.15
	Na ₂ CO ₃	0.131	0.188	2.00	2.00	11.62	11.60
	NaHCO ₃	—	—	—	—	—	—
	Na ₃ PO ₄	0.141	0.194	1.25	2.00	12.11	12.59
	Na ₂ HPO ₄	—	—	—	—	—	—

*Surfactant concentration.

References

1. J. L. Cayias, R. S. Schechter, and W. H. Wade, The Measurement of Low Interfacial Tension via the Spinning Drop Technique, *Adsorption at Interfaces*, ACS Symposium Series, No. 8, pp. 234-247, 1975.
2. American Standards Testing Method ASTM D791, *Annual Book of ASTM Standards*, Petroleum Products and Lubricants, Vol. 05.01, pp. 435-437.
3. R. C. Nelson, J. B. Lawson, D. R. Thigpen, and S. D. Stegemeier, *Cosurfactant Enhanced Alkaline Flooding*, paper SPE/DOE 12672 presented at the SPE/DOE Fourth Symposium on Enhanced Oil Recovery April 15-18, 1984, Tulsa, Okla.
4. F. F. J. Lin, G. J. Besserer, and M. J. Pitts, Laboratory Evaluation of Crosslinked Polymer and Alkaline-Polymer-Surfactant Flood, *J. Can. Pet. Technol.*, 26: 54-65 (1987).
5. S. R. Clark, M. J. Pitts, and S. M. Smith, *Design and Application of an Alkaline-Surfactant-Polymer Recovery System to the West Kiehl Field*, paper SPE 17538 presented at the Rocky Mountain Regional Meeting, May 11-13, 1988, Casper, Wyo.; *SPE Advanced Technology Series*, Vol. 1, pp. 172-179.
6. T. R. French, C. B. Josephson, and D. B. Evans, *The Effect of Alkaline Additives on the Performance of Surfactant Systems Designed to Recover Light Oils*, Department of Energy Report, Niper-506, February 1991.

IMPROVING RESERVOIR CONFORMANCE USING GELLED POLYMER SYSTEMS

Contract No. DE-AC22-92BC14881

University of Kansas
Center for Research
Lawrence, Kans.

Contract Date: Sept. 25, 1992
Anticipated Completion: Sept. 24, 1995
Government Award: \$707,123

Principal Investigators:

Don W. Green
G. Paul Willhite

Project Manager:

Jerry Casteel
Bartlesville Project Office

Reporting Period: Oct. 1–Dec. 31, 1992

Objectives

The general objectives are to (1) identify and develop gelled polymer systems that have potential to improve reservoir conformance of fluid displacement processes, (2) determine the performance of these systems in bulk and in porous media, and (3) develop methods to predict the capability of these systems to recover oil from petroleum reservoirs.

This work focuses on three types of gel systems—an aqueous polysaccharide (KUSP1) system that gels as a function of pH, the chromium-based system where polyacrylamide and xanthan are cross-linked by Cr(III), and an organic cross-linked system. Development of the KUSP1 system and evaluation and identification of the organic cross-linked system will be conducted.

The laboratory research is directed at the fundamental understanding of the physics and chemistry of the gelation process in bulk form and in porous media. This knowledge will be used to develop conceptual and mathematical models of the gelation process. Mathematical models will then be extended to predict the performance of gelled polymer treatments in oil reservoirs.

Summary of Technical Progress

Development and Selection of Gelled Polymer Systems

One of the goals is to examine the effects of chemical modification of KUSP1. There is indirect evidence that suggests that the alkali-extracted KUSP1 polymer may differ chemically from its in situ form. The in situ form is considered to be the form in which KUSP1 exists, in the intact capsule of the cell, prior to alkaline extraction. If esters exist in the in situ form they will be hydrolyzed during the alkaline extraction of

the polysaccharide. To circumvent that possibility a comparison of properties of alkali-extracted polymer and polymer extracted with dimethylsulfoxide (DMSO) has been initiated. DMSO extraction is not expected to result in ester hydrolysis, and KUSP1 extracted with this solvent is expected to be representative of the in situ form. Thus far it is clear that the hydrogel formed by purified DMSO-extracted KUSP1 holds significantly less water than the alkali-extracted form. The chemical basis for that difference has not yet been established.

Progress has been made in the scaleup of polymer production. The known properties of KUSP1 have been established with polymer prepared from small shake flask cultures. Scaleup of the production process by use of 16-L airlift fermentor initially resulted in poor yields of the polymer, and the gels formed by the produced KUSP1 were not as rigid as those from KUSP1 from smaller cultures. This difference apparently was a consequence of the difficulty in providing adequate aeration. Inadequate aeration caused an increase in accumulation of acid in the *Cellulomonas flavigena* cultures and a concomitant decrease in yield of KUSP1. A method for adequate control of culture pH has been developed.

Selection of Organic Cross-Linking System to be Investigated

A search of the literature was conducted to identify gelled polymer systems that have been investigated. Oil field service companies were contacted and requested to provide literature on gelled polymer systems that are currently in use. Compilation and organization of the information and the definition of criteria for the selection of an organic gel system were started.

Screening experiments were initiated to provide data for the selection of an organic gel system. The gelation behavior of a resorcinol and formaldehyde system over ranges of key variables were determined at 41 °C. Gel time and gel structure (appearance) were sensitive to initial pH, salinity, and hardness. Gel times for three series of samples as a function of salt concentration are shown in Fig. 1. Gel times on the order of

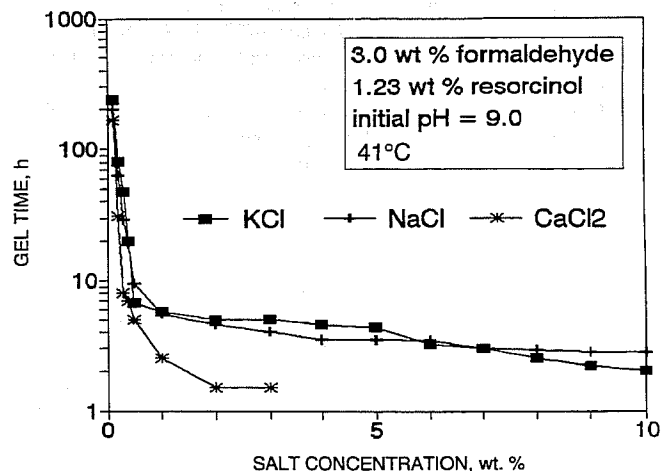


Fig. 1 Gel times for a formaldehyde-resorcinol gel system as a function of salt type and concentration.

days were obtained only at concentrations of salt below 0.5% where the gel time was very sensitive to salinity. Divalent ions accelerated the gelation rate as shown in Fig. 1 for the calcium salt. Additional experiments also showed that gelation times were also sensitive to initial pH values.

Ionic groups introduced on the resorcinol ring should achieve higher salinity tolerance for the gel system. Sulfomethylation was performed to add a sulfonate group to the resorcinol ring. Gelation behavior studies of the sulfonated resorcinol-formaldehyde system were initiated.

Physical and Chemical Characterization of Gel Systems

Setup of the Bohlin CS rheometer and the R-19 Weissenberg Rheogoniometer and familiarization with their operations have been completed. Rheological data have been obtained for selected polyacrylamide solutions and the KUSP1 system.

Viscosity data on KUSP1 solutions were obtained as a function of shear rate, polymer concentration, initial pH values, and time. The data showed that viscosity was a weak function of shear rate at pH values of 14, 13.5, and 13. For solutions at successively lower pH values, the viscosity was higher and exhibited shear-thinning behavior. KUSP1 was a rigid gel at pH values lower than 10.8.

Properties of the KUSP1 solutions were a function of the age of the sample. Viscosity decreased with time for samples prepared at initial pH values between 12.5 and 14. Viscosity increased for samples prepared at an initial pH of 12. Largest changes in viscosity occurred at lower shear rates. The pH of the solutions decreased with time for all samples. The pH values dropped approximately 0.5 unit over 10 d. Color changes over time were also observed in the KUSP1 solutions at initial pH values of 13 and above. For samples at polymer concentrations of 1.0%, a yellow color developed over a 10-d time period. For samples at 2.0% concentration, the yellow color developed within 2 d and darkened to a brown color at 10 d. The cause of the color change was not determined. Viscosity, pH, and color changes did not appear to alter the gelation of the alkali solutions when the pH was reduced to values below 10.

Mathematical Modeling of Gel Systems

Laboratory-scale experiments involving the flooding of sandpacks with high pH brine solutions were simulated using the UTCHEM chemical flooding simulator that was devel-

oped at the University of Texas. The purpose for these simulations was to study fluid-rock interactions and their effect on pH for a relatively simple system. A pure silica matrix was considered that exhibited silica dissolution and zero cation exchange capacity. Equilibrium reactions for the hydrolysis of the silica anions to four complex silicate anions in the fluid phase were modeled. Injection of brine with a pH of 11.9 into a sandpack containing brine at an equilibrium pH of 6.5 was simulated.

Results from the simulations show the significant role of numerical and physical dispersion on the pH profiles in the sandpack. This role is shown in Fig. 2 where pH is plotted as a function of sandpack length after 0.25 PV of brine injection for three cases of selected numerical dispersion control and physical dispersion. Comparison of curves 1 and 2 shows the effect of numerical dispersion with no physical dispersion. Numerical dispersion advanced the pH front considerably deeper in the sandpack. The position of curve 2 shows that the third order total variation diminishing method of numerical control sufficiently diminished the numerical dispersion. Curve 3 is the pH profile for a case that incorporated physical dispersion with the numerical dispersion control. This profile shows the significant role of dispersion on the propagation of the pH front. The logarithmic nature of the pH function caused the importance of dispersion in that relatively small changes in the hydrogen ion concentration lead to large changes in pH. An accurate description of dispersion will be a key to the modeling processes dependent on pH values.

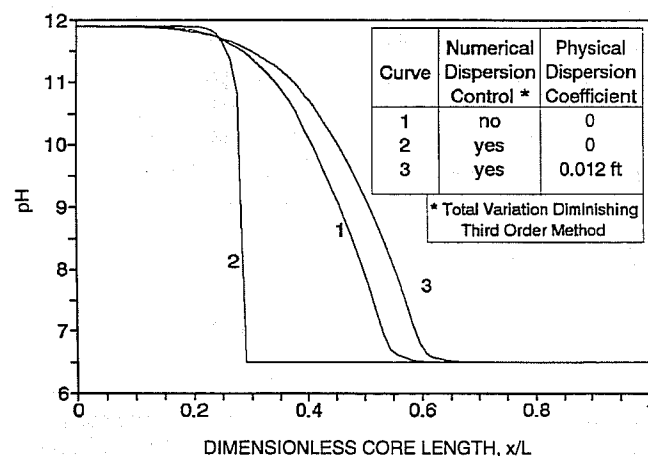


Fig. 2 Profiles of pH in sandpack for three cases of dispersion modeling.

**SURFACTANT LOSS CONTROL
IN CHEMICAL FLOODING:
SPECTROSCOPIC AND CALORIMETRIC
STUDY OF ADSORPTION AND
PRECIPITATION ON RESERVOIR
MINERALS**

Contract No. DE-AC22-92BC14884

Columbia University
New York, N.Y.

Contract Date: Sept. 30, 1992
Anticipated Completion: Sept. 29, 1995
Government Award: \$602,232

Principal Investigator:
P. Somasundaran

Project Manager:
Jerry Casteel
Bartlesville Project Office

Reporting Period: Oct. 1–Dec. 31, 1992

Objective

The objective of this project is to elucidate the mechanisms of adsorption and surface precipitation of flooding surfactants on reservoir minerals. The effect of surfactant structure, surfactant combinations, and other inorganic and polymeric species will also be determined with the use of solids of relevant mineralogy. A multipronged approach consisting of micro and nano spectroscopy, microcalorimetry, electrokinetics, surface tension, and wettability will be used to achieve the goals. The results of this study should help in controlling surfactant loss in chemical flooding and also in developing optimum structures and conditions for efficient chemical flooding processes.

Summary of Technical Progress

Adsorption of selected individual surfactants on oxide minerals was determined. The goal was to characterize the microstructure of the adsorbed layers. Work was begun with alkyl phenoxy polyethoxy type nonionic surfactants and anionic *meta*-xylene sulfonates.

Adsorption of Nonionic Surfactants

Earlier results had shown that ethoxylated surfactants adsorb strongly on silica, and, depending upon the number of ethylene oxide groups, the adsorption density as well as the wettability of the substrate is drastically altered. The adsorption of nonyl phenoxy polyethoxy ether with 10 and 40 ethyleneoxide (EO) groups on silica was studied, and results suggested that the surfactant with the shorter EO chain adsorbed

to a greater extent, possibly because of the formation of surfactant aggregates at the solid–liquid interface. Fluorescence spectroscopy was used to determine the nature of the adsorbed layer in terms of micropolarity.

Pyrene monomer fluorescence is used to determine the polarity of unknown environments. The ratio of intensities of the third to the first peaks on the pyrene emission spectrum is sensitive to the polarity of the medium in which the pyrene resides. In polar solvents, such as water, the value of this ratio (I_3/I_1) is ~ 0.6 , but in nonpolar solvents and hydrocarbons, it varies from 1 to 1.7; in sodium dodecylsulfate micelles, I_3/I_1 is ~ 1.0 . Because this ratio characterizes the polarity it is termed here the *polarity parameter*.

The solution behavior of nonylphenoxy polyoxyether with 40 ethylene oxide groups (EO40) was determined by surface tension and fluorescence spectroscopy. It is seen in Fig. 1 that the critical micelle concentration (CMC) of EO40 surfactant is $\sim 6 \times 10^{-4}$ kmol/m³, and the value obtained by surface tension measurements compares well with that obtained by fluorescence spectroscopy. However, the surfactant used was of commercial grade and not very pure as evidenced by the minima in the surface tension measurements.

The adsorption of EO40 on silica was determined in the presence of low concentrations of pyrene, and emission spectra were obtained from both the slurry and the supernatant. There was no effect of the pyrene on the amount of surfactant adsorbed. Fluorescence emission spectra were recorded from the suspension as well as the supernatant to determine the presence of hydrophobic aggregates. The results are shown in Fig. 2. At low values of adsorption density (low residual concentration) the value of the I_3/I_1 ratio is ~ 0.6 , indicating an aqueous environment. Only above 10^{-3} kmol/m³ surfactant, the value of the I_3/I_1 ratio increases to ~ 0.8 . At this concentration there are micelles in the supernatant that are detected by pyrene. Because the emissions from the

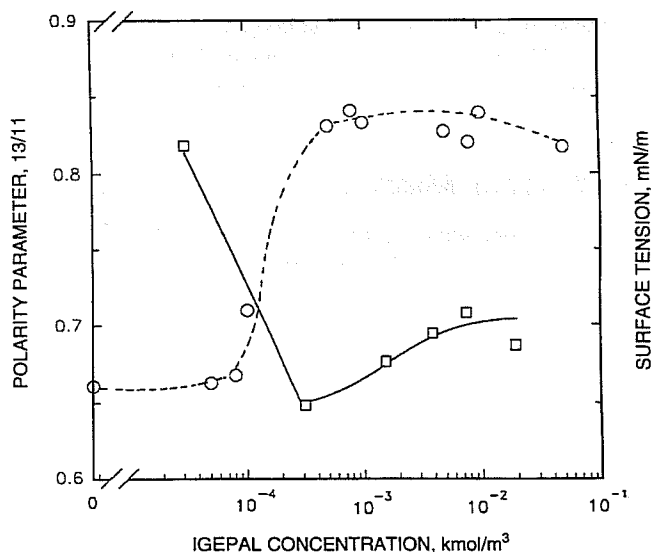


Fig. 1 Solution behavior of EO40 surfactant as determined by surface tension (□) and fluorescence measurements (○).

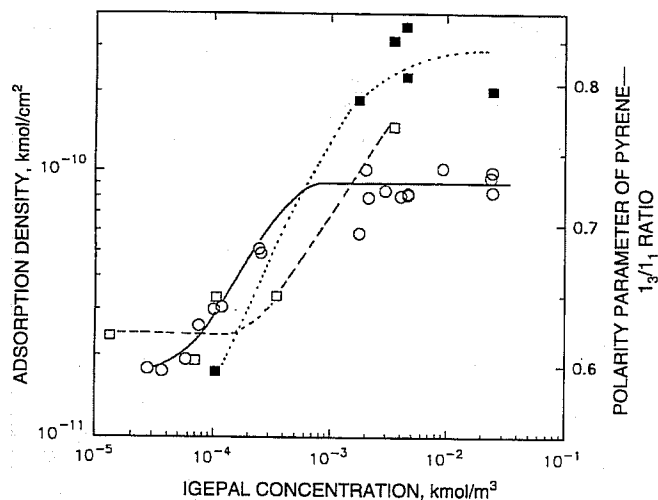


Fig. 2 Adsorption of EO40 surfactant on silica and characterization of adsorbed layer using fluorescence spectroscopy. Polarity parameters: □, suspension; ■, supernatant. ○, adsorption density.

suspension and the supernatant are similar, it is proposed that there are no hydrophobic aggregates at the solid-liquid interface in this case. The long ethylene oxide chain prevents aggregation between the hydrocarbon chains. Similar experiments are being conducted with EO5 and EO10 surfactants to determine the microstructure of the adsorbed layer.

Effect of Surfactant Structure on Adsorption of Xylene Sulfonates

In the case of alkyl xylene sulfonates, preliminary results showed a marked effect of the position of the functional groups on adsorption. When the sulfonate was in the *meta* position with respect to the methyl groups (124 MXS), surfactant adsorption on alumina was less than when the sulfonate was in the *para* position (135 PXS—*Para*1). The molecular structure of these surfactants is shown in Fig. 3.

Adsorption of another *para*-xylene sulfonate, 125 *para*-xylene sulfonate (*para*2), on alumina was studied to further examine the role of position of sulfonate and methyl groups on adsorption. The results in Fig. 4 indicate that both *para*1 and *para*2 adsorb to the same extent. This suggests that the position of the methyl groups does not play as important a role as the position of the sulfonate. Also, it is proposed that the higher steric hindrance to the packing of molecules in surfactant aggregates at solid-liquid interface in the *meta*-xylene sulfonate is the result of the alkyl chain being closer to the sulfonate.

Electrokinetic Measurements

It was proposed that at low concentrations adsorption of the *meta*-xylene sulfonate was low presumably because of lower electrostatic interaction between the mineral and the sulfonate. It is known that the electron density is different for different positions on the benzene group depending upon the

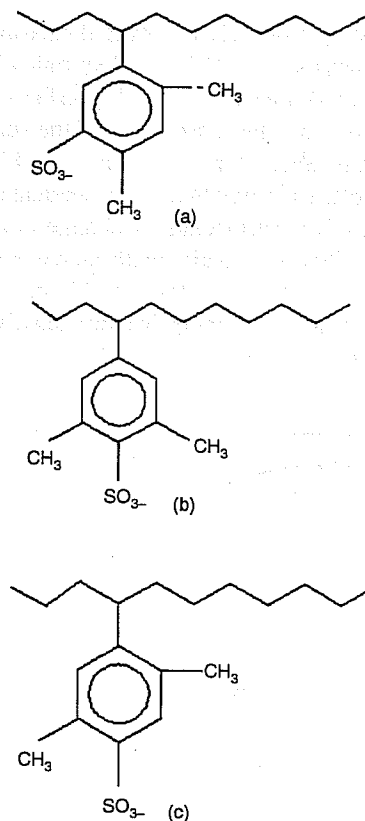


Fig. 3 The molecular structure of surfactants (a) 4C11, 2,4 *Meta*-xylene sulfonate (*meta*), (b) 4C11 3,5 *para*-xylene sulfonate (*para*1), and (c) 4C11 2,5 *para*-xylene sulfonate (*para*2).

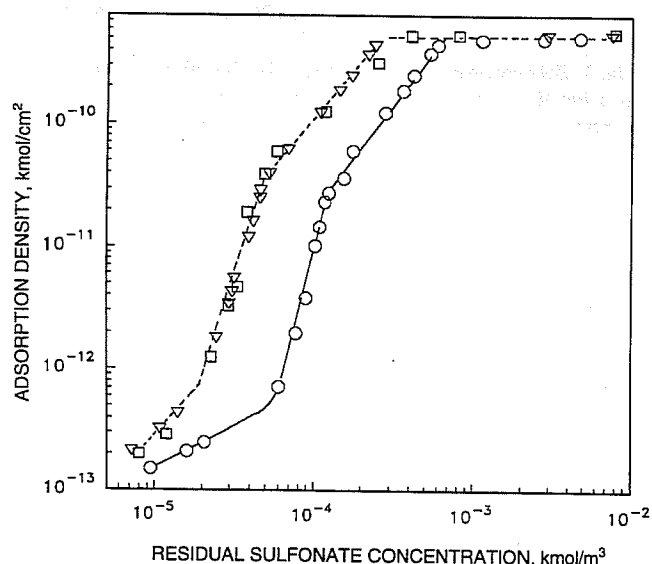


Fig. 4 Adsorption of alkyl xylene sulfonates with varying position of the sulfonate group on the benzene ring. ○, *meta*. ▽, *para*1. □, *para*2

functional groups attached and the point of attachment. The sulfonate of *para*-xylene sulfonates should have a higher electronic charge than that of the *meta*-xylene sulfonate because of its proximity to the methyl groups, which are

electron-donating groups. Zeta potential measurements were made to test whether the different electronic charges led to different charge characteristics of the surfactants. The zeta potential of alumina after adsorption of the surfactants was measured and is reported in Figs. 5 and 6. In Fig. 5, the zeta potential is plotted as a function of the residual (equilibrium) concentration of the surfactants. A change in zeta potential value from positive to negative with increase in adsorption correlates well with the adsorption isotherm.

The zeta potential of alumina is more negative with *para*-xylene sulfonates adsorbed than with the *meta*-xylene sulfon-

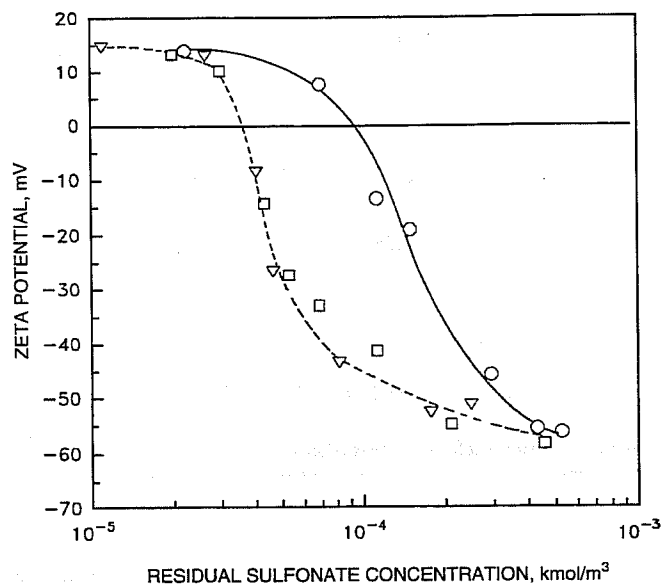


Fig. 5 Zeta potential of alumina with adsorbed alkyl xylene sulfonates as a function of residual sulfonate concentration. \circ , *meta*. ∇ , *para1*. \square , *para2*.

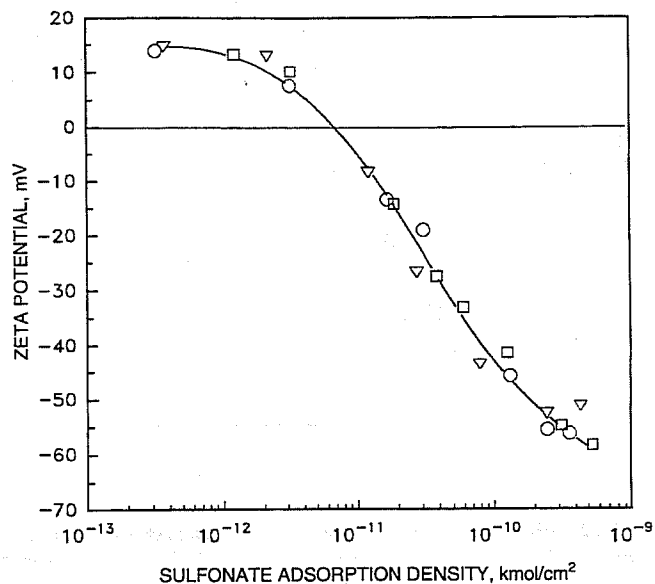


Fig. 6 Zeta potential of alumina with adsorbed alkyl xylene sulfonates as a function of adsorbed surfactant density. \circ , *meta*. ∇ , *para1*. \square , *para2*.

ate. However, when the zeta potential is plotted as a function of adsorption density (Fig. 6), there is no difference in the behavior of the three surfactants. Thus there seems to be no measurable difference in the charge characteristics of the surfactants at least in the adsorbed layer.

Future Work

- Microstructure of adsorbed layers for ethoxylated surfactants.
- Effect of temperature on the adsorption of xylene sulfonates.

FIELD VERIFICATION OF CO₂-FOAM

Contract No. DE-FG21-89MC26031

**New Mexico Institute of Mining and Technology
Petroleum Research Center
Socorro, N. Mex.**

Contract Date: Sept. 17, 1992

Anticipated Completion: Sept. 16, 1995

Total Project Cost:

DOE	\$2,000,000
Contractor	2,035,000
Total	\$4,035,000

Principal Investigators:

**F. David Martin
John P. Heller
William W. Weiss**

Project Manager:

**Royal Watts
Morgantown Energy Technology Center**

Reporting Period: Oct. 1–Dec. 31, 1992

Objectives

This project is a cooperative effort of industry, university, and government to transfer laboratory research technology to a field demonstration test. The primary objective of the project is to evaluate the use of foam for mobility control and fluid diversion in a field-scale CO₂ flood.

Summary of Technical Progress

The East Vacuum Grayburg/San Andres Unit (EVGSAU), operated by Phillips Petroleum Company, was the site selected for a comprehensive evaluation of the use of foam for improving the effectiveness of a CO₂ flood. The Petroleum Recovery Research Center (PRRC), a division of the New Mexico Institute of Mining and Technology (NMIMT), is providing laboratory and research support for the project. The four-year project is jointly funded by the EVGSAU Working Interest Owners (WIO), the U.S. Department of Energy (DOE), and the state of New Mexico. A Joint Project Advisory Team (JPAT) composed of WIO technical representatives from several major oil companies provides input, review, and guidance for the project. The project began in late 1989 and is now in the fourth and final year.

During this quarter, the third annual report was assembled and submitted, the field test of the foam injection was completed, and results from the project continued to be collected for evaluating the effectiveness of CO₂-foam. This quarterly report provides the status of the project through the end of December 1992.

Project Design

The design for the EVGSAU field test includes the injection of a pre-foam surfactant pad for 3 months, followed by the injection of an 80% quality CO₂-foam during approximately 3 months of a rapid surfactant-alternating-gas (SAG) cycle. In both the pre-foam pad and the surfactant solution for the SAG cycle, the design called for 2500-ppm Chevron Chaser CD-1045[®]. The surfactant pad both satisfies the adsorption and compensates for the adsorption-induced retardation of the surfactant band. This should result in effective utilization of surfactant for foam generation. Although the laboratory results indicated that simultaneous injection of surfactant solution and CO₂ was desirable, operational problems were anticipated with co-injection in that the line pressure varies considerably between water and CO₂. Thus, a rapid SAG injection mode was selected that is expected to closely approach the benefits achieved by simultaneous injection. This rapid SAG process involves alternate injections of a 3-d cycle of water [3000 Reservoir Barrels (RB)] followed by a 12-d cycle of CO₂ (12,000 RB) to give an approximate 80% quality foam. The 3- and 12-d cycles were selected over a more rapid cycle because this schedule can be maintained throughout the project. The design approved by the JPAT includes five alternate SAG cycles. Because the mechanical characteristics of a SAG may cause changes in injection pressure, a baseline period of a rapid water-alternating-gas (WAG) cycle was performed prior to surfactant injection.

Foam Injection Test and Project Monitoring

The pre-foam surfactant pad injection was started in Well 3332-001 on April 14, 1992, and was completed on July 14, 1992. Following the 3 months of pre-foam surfactant pad, water was injected for 3 d to displace the surfactant solution from the immediate vicinity of the wellbore. On July 17, 1992, the rapid SAG cycle began. The fifth cycle of foam generation, which completed the rapid SAG injection test, ended on October 9, 1992. The 3-month CO₂ injection cycle then began and continued through the end of the year.

The injection pressure and rate data during and after the rapid SAG test are shown in Fig. 1. At the nominal injection rate of 1000 RB/d, the injection pressures stabilized at higher than pre-SAG levels. A comparison of the SAG rate and pressures and the baseline rapid WAG is shown in Fig. 2; the lower injectivity during the SAG cycle is apparent.

The pattern producing well (3332-032) that has experienced the most severe CO₂ breakthrough in this pattern started flowing during the Thanksgiving weekend. The oil response following the rapid SAG is much higher than recent production levels, including the rates that occurred after the baseline rapid WAG (see Fig. 3). After reaching a peak in early December, the oil production rate decreased as the CO₂ production increased, but a definite incremental oil response is occurring. During this time, Well 3332-032 was flowing at about 250 psi tubing pressure, which was considerably lower than the 600 to 800 psi tubing pressure after the rapid WAG.

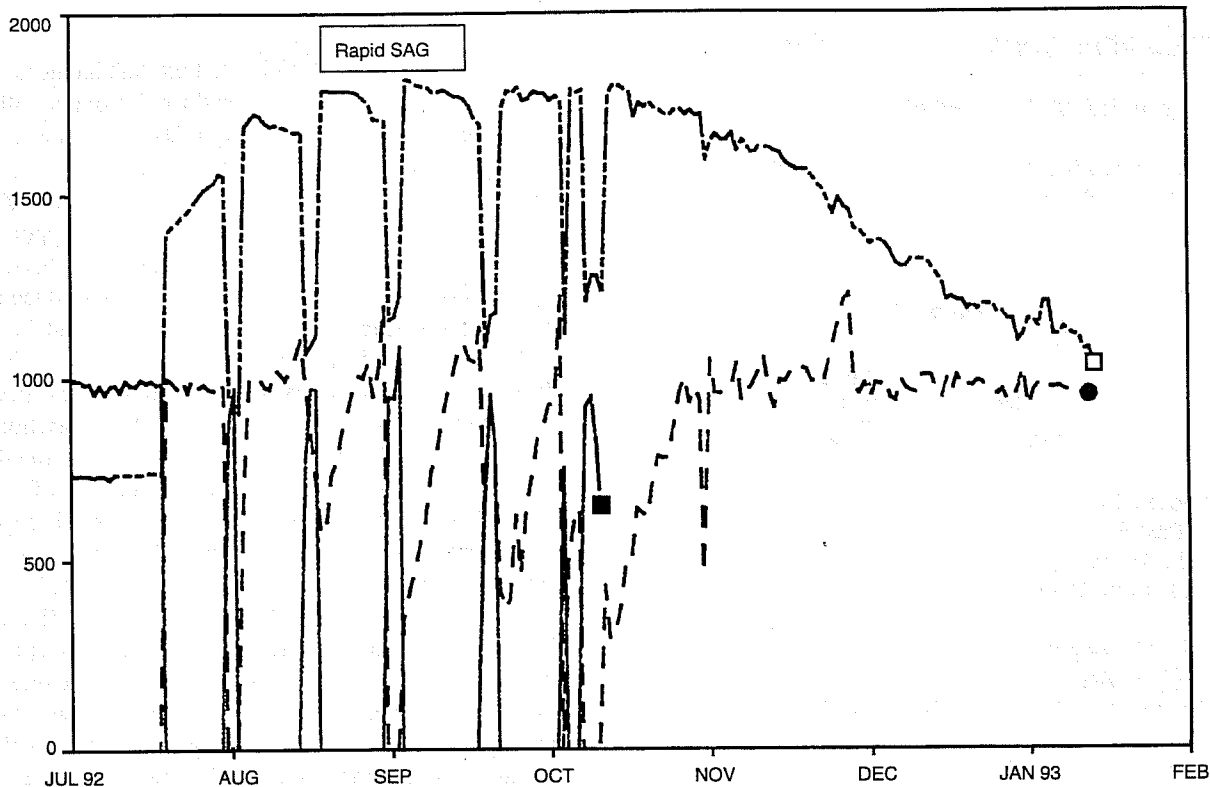


Fig. 1 Injection pressure and rate during foam generation of Well 3332-001. ■, injection rate, barrels of water per day. □, injection pressure, psi. ●, injection rate, barrels of CO₂ per day.

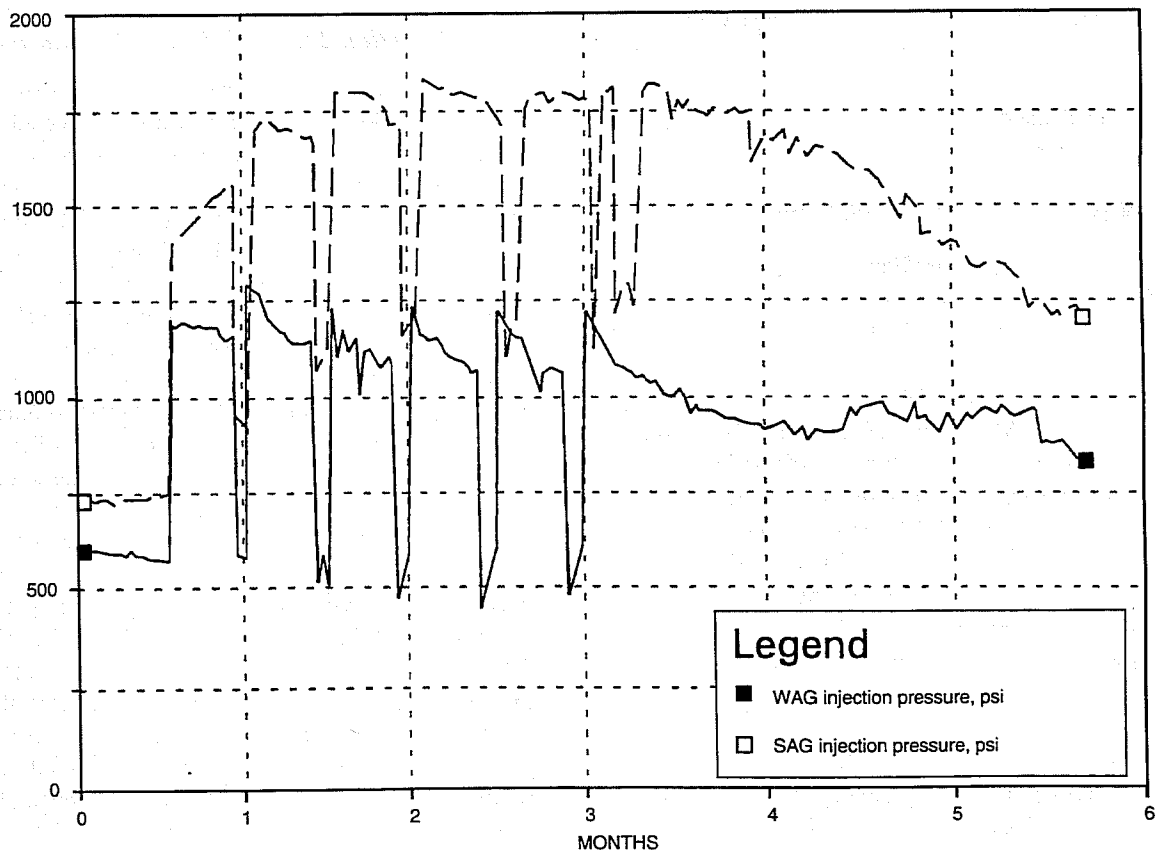


Fig. 2 Injection pressure and rate of Well 3332-001. Comparison of water alternating gas (WAG) vs. surfactant alternating gas (SAG).

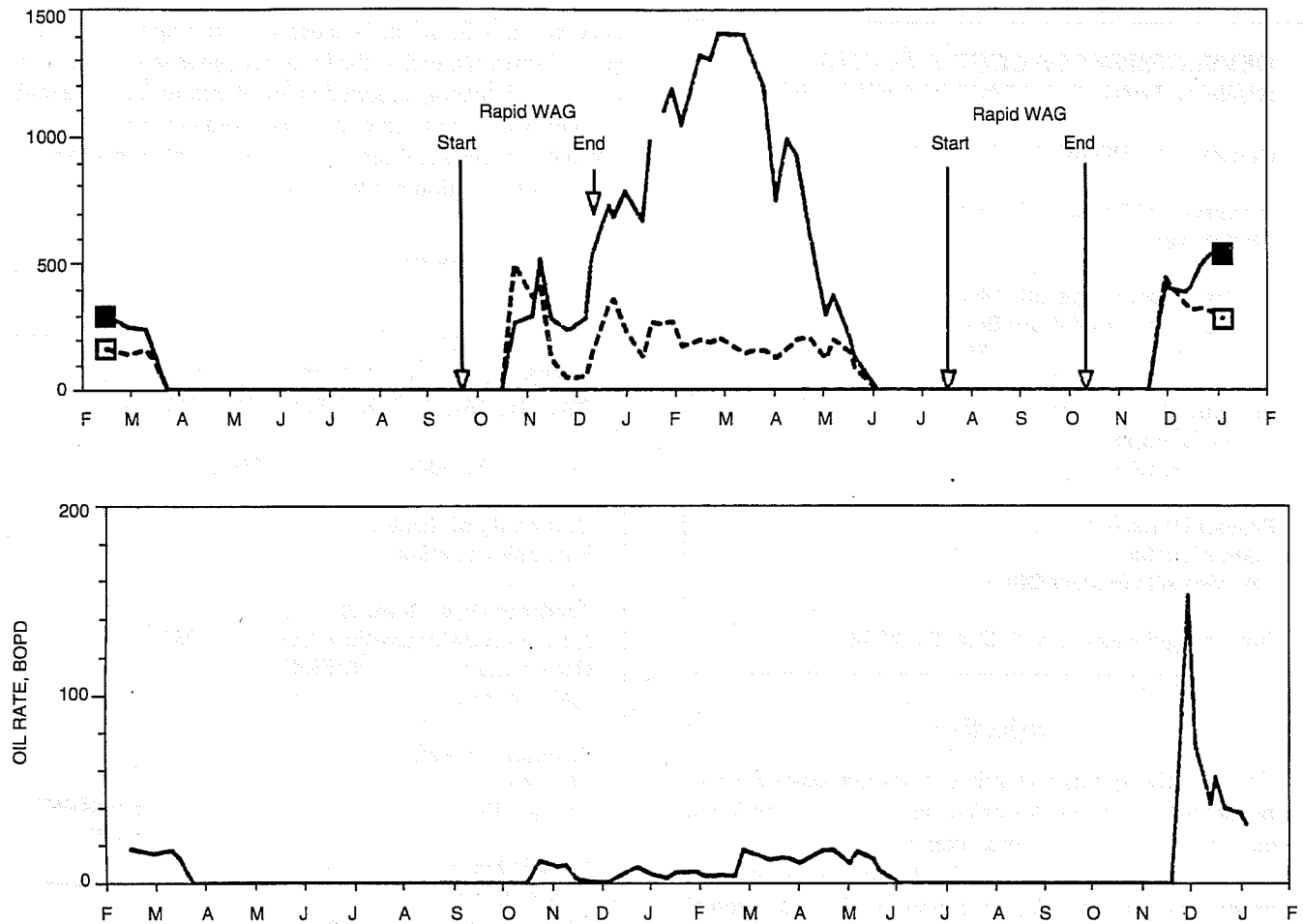


Fig. 3 East Vacuum Grayburg/San Andres Unit (EVGSAU) Well 3332-032 weekly well tests for February 1991-January 1993. ■, gas rate, million cubic feet per day. □, water rate, barrels of water per day. WAG, water alternating gas. SAG, surfactant alternating gas.

Monitoring throughout the CO₂ injection cycle will continue, and the incremental oil production and decreased CO₂ production will be quantified.

A comprehensive evaluation of the logging program in the observation well is currently under way. Results of this evaluation will be available during the next quarter of the project.

Project Plans

A JPAT meeting was held on November 9, 1992, in Plano, Tex., to discuss results from the project as well as the desirability of a second foam injection test. At that meeting, the JPAT agreed to delay making a decision regarding a future course of action until additional results from the field monitoring become available. At the current schedule, the CO₂

injection cycle will be completed by mid-January. After an 11-d pressure falloff test is performed, the original plan calls for a 4-month water injection period, unless the plan is modified to include a second foam test.

Synopsis

Two favorable conclusions may be drawn from the results: (1) as indicated by the higher well pressures required to inject CO₂ during the SAG cycles, the injectivity into the formation was indeed reduced; and (2) even at this early date, two improvements in production are apparent. These are a decrease in the rate of CO₂ flow and an increase in oil rate from producing well 3332-032. More quantitative evaluations of the improvements and the extent of mobility reduction are expected after additional time passes and data accumulate.

DEVELOPMENT OF COST-EFFECTIVE SURFACTANT FLOODING TECHNOLOGY

Contract No. DE-AC22-92BC14885

**University of Texas at Austin
Austin, Tex.**

**Contract Date: Sept. 30, 1992
Anticipated Completion: Sept. 29, 1995
Government Award: \$765,557**

**Principal Investigators:
Gary A. Pope
Kamy Sepehrnoori**

**Project Manager:
Jerry Casteel
Bartlesville Project Office**

Reporting Period: Oct. 1–Dec. 31, 1992

Objective

The objective of this research is to develop cost-effective surfactant flooding technology by using surfactant simulation studies to evaluate and optimize alternative design strategies and taking into account reservoir characteristics, process chemistry, and process design options such as horizontal wells. Task 1 is the development of an improved numerical method for the simulator so that a wider class of these difficult simulation problems can be solved accurately and affordably. Task 2 is the application of this simulator to the optimization of surfactant flooding to reduce its risk and cost.

Summary of Technical Progress

A fully implicit algorithm has been developed that is second-order correct in time and that uses a third-order finite-difference method to discretize the first-order space derivatives and a new total variation diminishing flux limiter to constrain the gradients of the fluxes to obtain accurate, oscillation-free numerical solutions. This algorithm combines the best features of several recent numerical schemes since it is both stable and accurate. Unlike many numerical schemes in the literature, there are no problems with generalizations of this scheme to multidimensional, multicomponent, multiphase flow problems, such as arise in the simulation of compositional chemical flow problems that are the specific focus of this project. The coding and testing of this algorithm for chemical flooding simulation is in progress. Initial results for simple test problems, such as the convection–diffusion problem and the Buckley–Leverett problem, look very good compared with the explicit schemes that have been used to date. Much larger time steps can be taken with this new implicit scheme than with the explicit schemes used previously, yet the

accuracy is still good, because the time approximation is second-order rather than the first-order approximation used in reservoir simulators reported in the literature. This is a major advance in reservoir simulation technology with applications not only to chemical simulations but to all other types of reservoir simulation as well.

RESPONSIVE COPOLYMERS FOR ENHANCED PETROLEUM RECOVERY

Contract No. DE-AC22-92BC14882

**University of Southern Mississippi
Hattiesburg, Miss.**

**Contract Date: Sept. 22, 1992
Anticipated Completion: Sept. 21, 1995
Government Award: \$273,400
(Current year)**

**Principal Investigators:
Charles McCormick
Roger Hester**

**Project Manager:
Jerry Casteel
Bartlesville Project Office**

Reporting Period: Oct. 1–Dec. 31, 1992

Objective

The overall objective of this research is the development of advanced water-soluble copolymers for use in enhanced oil recovery (EOR) that rely on reversible microheterogeneous associations for mobility control and reservoir conformance.

Summary of Technical Progress

Advanced Copolymer Synthesis

A synthesis work force has been organized and reagents have been collected to begin production of both associative and ampholytic copolymers. Initial work has centered on synthesis of PAM/NaA/AM and PAM/NaAMPS/AM associative polymers. Also, techniques to produce AMPDAPS/AM and AMPDAC/NaAMPS copolymers are being developed.

Characterization of Macromolecular Structure and Properties

A preparative scale-size exclusion chromatographic (SEC) system is being placed into operation. The system is similar to

that constructed previously for hydrodynamic size analysis of large water-soluble polymers.¹ The system is being interfaced with a personal computer for automatic data collection and analysis. SEC calibration is being performed with polydispersed polyacrylamide using an eluent viscosity detector that measures polymer hydrodynamic size.²

Two other techniques, dynamic and static light scattering, are being used to measure both polymer-solution interaction properties, molecular weights, and hydrodynamic coil size as a function of solvent composition. These analytical systems have been made functional for water-soluble macromolecules.

Solution Rheology in a Porous Media

Considerable efforts have been undertaken to define the flow properties of polymer solutions through porous media. Both the shear and elongational viscosity properties of a high-molecular-weight polymer solution in a porous medium must be characterized as a function of macromolecular structure and solvent-polymer interactions so that mobility performance for a polymer reservoir injection can be optimized.

Dimensional analysis has been used to define the major parameters controlling the flow resistance or mobility of a polymer solution through beds of uniform spherical particles. Dimensionless groups have been used to show correlation between parameters. The bed Reynolds number, N_{Re} , and fluid friction factor, f , are defined as

$$N_{Re} \equiv \frac{vd\rho}{\eta_s(1-\phi)} \quad (1)$$

$$f \equiv \frac{d\phi^3}{v^2(1-\phi)\rho} \frac{\Delta P}{\Delta \ell} \quad (2)$$

$$\Lambda = N_{Re}f \quad (3)$$

Within these two dimensionless groups the nature of the porous media is given by the diameter of the spherical particles, d , forming a bed having porosity, ϕ . The driving force for fluid flow through the bed is given by the pressure drop per unit length of bed, $\Delta P/\Delta \ell$. Flow conditions through the bed are defined by the average fluid velocity, v . This velocity is based on the cross-section area of an empty bed. The fluid velocity within the pore channels comprising the bed would be the empty bed velocity divided by the bed porosity. Solution fluid properties of shear viscosity, η_s , and density ρ , are also used in the dimensionless groups.

The N_{Re} establishes flow conditions, and the friction factor is a measure of fluid resistance at the given flow conditions. For Newtonian fluids, such as water, experimentation has found that³

$$\Lambda = 175 + 1.75 N_{Re} \quad (4)$$

When the Newtonian fluid contains large water-soluble polymers, the relationship described by Eq. 4 may not be valid. At a critical flow condition the polymer coils within the solvent passing through the porous medium begin to elongate and produce additional resistance to flow. This resistance, which is caused by polymer coil elongation, is called the solution elongational viscosity, η_e . At certain flow conditions the resistance caused by the solution's elongational viscosity can be two or three orders of magnitude greater than that caused by the shear viscosity.

Usually a polymer coil starts to elongate when the product of its response time, τ , and the elongation rate, Γ , equal 0.1. This dimensionless product is called the Deborah number, N_{De}

$$N_{De} = \Gamma\tau \quad (5)$$

The fluid elongation rate is the change in fluid velocity with respect to direction of flow. For a porous media of spheres, the elongation rate is dependent on the fluid velocity and bed porosity.

$$\Gamma = \frac{(2)^{1/2} v}{\phi d} \quad (6)$$

The coil response time, τ , can be estimated from the intrinsic viscosity of the polymer, $[\eta]$, and the polymer's molecular weight, M .

$$\tau = \frac{\eta_s[\eta]M}{RT} \quad (7)$$

In Eq. 7, R and T are the gas law constant and temperature, respectively.

The magnitude of the Deborah number is a measure of a polymer coil's ability to react by extension (its response time) to a given flow condition (the fluid elongation rate). The degree of coil extension depends upon the Deborah number. When the Deborah number is much less than one, minimum coil extension is experienced. However, when the Deborah number is greater than one, the coil is fully extended. This extension followed by a relaxation to a random coil state converts kinetic energy to heat and thereby increases resistance to fluid flow through a porous medium.

Durst⁴ reported a maximum flow resistance at Deborah numbers greater than one. The maximum friction factor observed by Durst, f_m , when compared with the solvent friction factor, f_s , is defined by Eq. 8 for a solution containing polymer coils at concentration, C , which have N number of macromolecular sub-elements in the coil that are capable of contributing to the elongation of the coil.

$$\frac{f_m - f_s}{f_s} = \left[\frac{N[\eta]C}{50} \right]^{2/3} \quad (8)$$

The number of macromolecular sub-elements can be determined if the polymer's repeat unit (monomer) molecular weight, M_0 , and the length of the repeat unit, ℓ_0 , are known.

$$N = \left(\frac{\ell_0}{M_0} \right)^2 \left(\frac{\Phi}{[\eta]} \right)^{3/2} M^{1/2} \quad (9)$$

In Eq. 9, Φ is the Fox-Flory constant.⁵

A combination of Eqs. 8 and 9 shows how macromolecular structure (coil size, capacity to elongate, monomer influence, concentration, and polymer interaction with solvent) should affect the maximum fluid flow resistance experienced when a polymer solution is forced through a porous medium. Note that the maximum mobility change per volume fraction of polymer coils in the solution, $(f_m - f_s)/(f_s[\eta]C) \equiv \psi_{\max}$, predicted by Eq. 10 is a product of a constant, $(\Phi^4/[50^6 A^6])^{1/2}$, the contour length of the macromolecule, $(\ell_0 M/M_0)^{1/2}$, the hydrodynamic size of the coil, $(M/[\eta])^{1/2}$, and the number of polymer coils per unit volume of solution $[AC/M]^{1/2}$.

$$\psi_{\max} \equiv \frac{f_m - f_s}{f_s[\eta]C} = \left(\frac{\Phi^4}{50^6 A^6} \right)^{1/2} \left(\frac{\ell_0 M}{M_0} \right)^{1/2} \frac{(M/[\eta])^{1/2}}{[\eta]C} \left[\frac{AC}{M} \right]^{1/2} \quad (10)$$

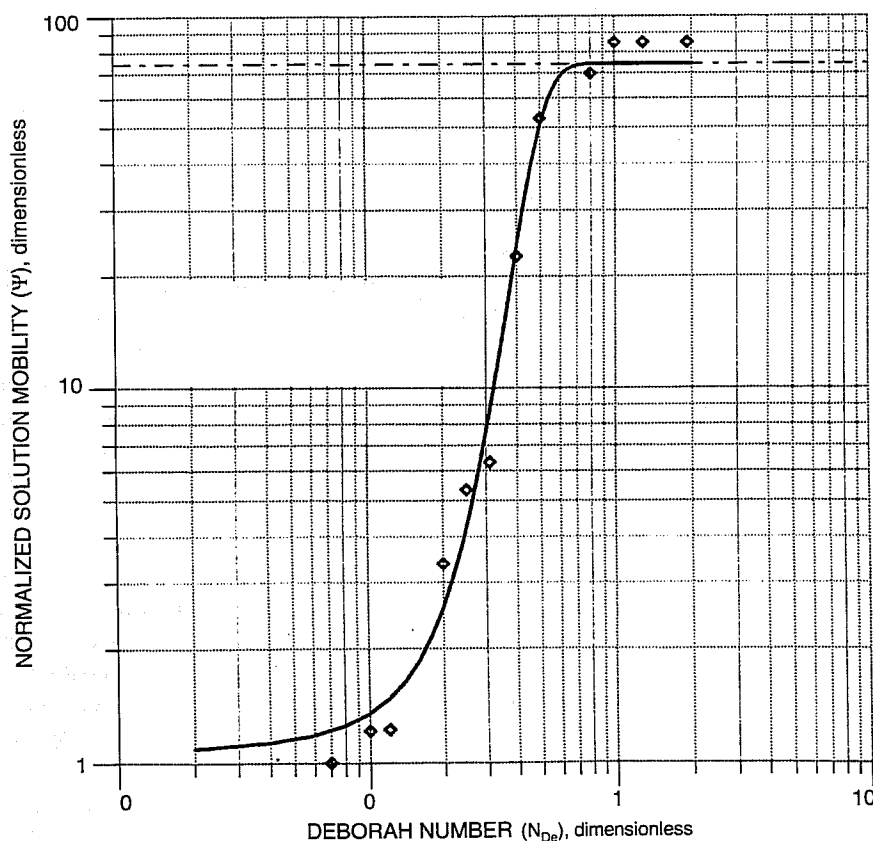
In Eq. 10, A is Avogadro's number. This equation was developed for dilute solutions of linear, nonassociation polymer coils that elongate as finitely extensible nonlinear elastic springs.⁶ A dilute solution exists when the volume fraction of polymer in solution, $[\eta]C$, is less than $1/10$.

Equation 10 gives the maximum expected normalized mobility decrease, $(f_m - f_s)/(f_s[\eta]C) \equiv \psi_{\max}$, for a polymer solution in which the macromolecular coils are fully expanded. As previously discussed, the amount of coil expansion depends upon the Deborah number developed within the porous media by the polymer solution. Data published by Durst⁴ using high-molecular-weight polyacrylamide in aqueous solutions suggest that the dependence of solution mobility on the Deborah number can be given by

$$\psi = \psi_{\max} \frac{1 + \operatorname{erf} \left(\frac{N_{De} - \mu}{\sigma} \right)}{2} \quad (11)$$

where $\psi \equiv (f_p - f_s)/(f_s[\eta]C)$ and f_p is the friction factor of the polymer solution. When all polymer coils in the solution experience full extension ($N_{De} > 1$), then $f_p = f_m$ and $\psi = \psi_{\max}$.

Equation 11 contains adjustable parameters μ and σ . Values for these parameters probably depend upon the variation of the porous media structure and/or the distribution of polymer coil sizes found in the solution. Figure 1 shows the good



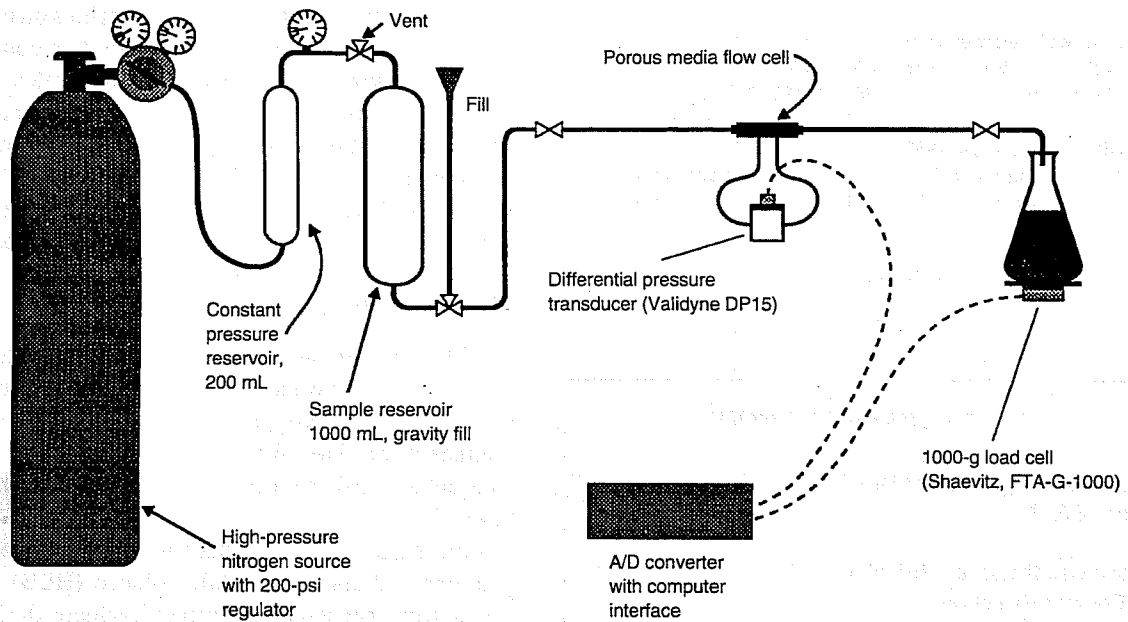
Parameter Values		
Symbol	Description	
M	Polymer molecular weight, g/mol	10.71×10^6
ℓ_0	Monomer length, cm	2.51×10^{-8}
M_0	Monomer molecular weight, g	71
Φ	Fox-Flory constant, 1/mol	2.8×10^{23}
C	Polymer concentration, ppm	25
$[\eta]$	Intrinsic viscosity, cm ³ /g	2200
μ	Error function fit parameter	0.31
σ	Error function fit parameter	0.20

Fig. 1 Mobility plot for PAM in 0.5M NaCl. \diamond , Durst data. —, Fit generated from Eqs. 10 and 11. - - -, ψ_{\max} .

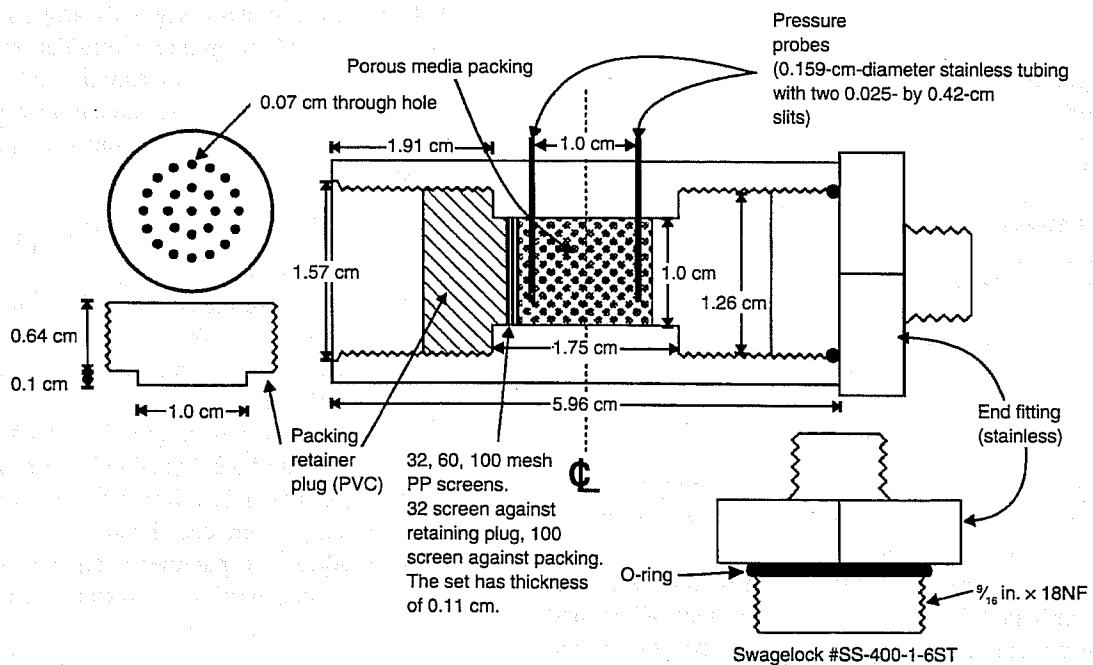
agreement between the Durst experimental ψ values and the ψ function given by Eq. 11.

Equations 10 and 11 are extremely powerful relationships that show how polymer solution mobility is dependent upon macromolecular properties, fluid flow conditions, and porous media structure. These relationships should apply to EOR and may be used as a guide for synthesizing superior polymer solutions for reservoir flooding.

A porous media elongational rheometer is being constructed to confirm the expectations predicted from Eqs. 10 and 11. As shown in Fig. 2, polymer solutions will be forced through a cell packed with small uniform spherical particles. The fluid flow rate through the cell will be controlled by adjusting the nitrogen pressure used to force movement of the solution. For a given polymer solution, the pressure drop per unit length of porous media will be recorded for several flow



(a)



(b)

Fig. 2 Porous media elongational flow rheometer system (a) and porous media flow cell details (b).

rate conditions. The data thus collected will be used to test the validity of Eqs. 10 and 11.

References

1. A. M. Safieddine and R. D. Hester, Size Exclusion Chromatography of High Molecular Weight Water-Soluble Polymers, Chap. 7 in *Polymers for Mobility Control in Enhanced Oil Recovery, Final Report*, DOE/BC/10844-20, 1990.
2. A. M. Safieddine and R. D. Hester, *J. Appl. Polym. Sci.*, 43: 1987-1990 (1991).
3. R. B. Bird, W. E. Stewart, and E. N. Lightfoot, *Transport Phenomena*, pp. 196-200, John Wiley & Sons, N.Y., 1960.
4. F. Durst and R. Haas, *Rheol. Acta*, 20: 179-192 (1981).
5. P. J. Flory, *Principles of Polymer Chemistry*, pp. 602-612, Cornell University Press, London, 1953.
6. R. B. Bird, C. F. Curtiss, R. C. Armstrong, and O. Hassager, *Dynamics of Polymeric Liquids*, Vol. 2, Kinetic Theory, pp. 85-88, John Wiley & Sons, N.Y., 1987.

SURFACTANT FLOODING METHODS

Cooperative Agreement DE-FC22-83FE60149,
Project BE4A

National Institute for Petroleum
and Energy Research
Bartlesville, Okla.

Contract Date: Oct. 1, 1983
Anticipated Completion: Sept. 30, 1993
Funding for FY 1993: \$640,000

Principal Investigators:
Bonnie L. Gall
Feliciano M. Llave
Leo A. Noll

Project Manager:
Jerry Casteel
Bartlesville Project Office

Reporting Period: Oct. 1-Dec. 31, 1992

Objectives

The objectives of this year's work are to (1) apply advanced enhanced oil recovery (EOR) technology based on mixed surfactant systems to improve oil recovery from Class 1 and other reservoirs targeted by the Department of Energy (DOE); (2) adapt surfactant EOR technology to different salinity and temperature ranges by developing surfactant systems that are tolerant to changes in chemical composition in selected reservoirs; and (3) develop cost-effective systems for selected applications using low-concentration surfactants with alkaline additives or other sacrificial agents. Studies will concen-

trate on problem areas that have adverse effects on performance and economics of chemical EOR in order to achieve a balance between cost and oil recovery effectiveness.

Summary of Technical Progress

Environmental, Health, and Safety

Admiral Watkins' 10-point plan and other DOE orders emphasize the need to place high priorities on environmental, safety, and health issues for all activities conducted by the National Institute for Petroleum and Energy Research (NIPER). During the first part of this quarter, the experimental program for Project BE4A was reviewed to evaluate the procedures, equipment, and working conditions to ensure that environmental, safety, and health considerations are satisfied. Results of this review were submitted to DOE in a report.¹

Mixed Surfactant Systems

Phase inversion temperature (PIT) experiments were conducted using selected combinations of nonionic surfactants with different alkanes (i.e., heptane, dodecane, and tetradecane). The difference in behavior of the nonionic surfactants, particularly the linear alkyl alcohol ethoxylate type (i.e., the Neodol® and Genapol® series) were compared to the dialkyl phenol surfactants (i.e., the Igepal series) at similar hydrophile-lipophile balance (HLB) levels. These tests were necessary to further evaluate the trends in the observed behavior of these types of surfactants. These studies supplement the results presented in last fiscal year's work on these systems with *n*-decane and *n*-octane.²

Salager and coworkers originally proposed general correlations to determine the optimum formulations of both anionic and nonionic surfactants. For anionic surfactant (i.e., alkyl aryl sulfonates, ester sulfates, and carboxylates) it was suggested that the following correlation was applicable at optimum conditions:³

$$\ln(S) - K(\text{EACN}) - f(A) + \sigma - a_T(T - 25) = 0 \quad (1)$$

where S = salinity of the aqueous phase in wt % NaCl

EACN = Equivalent Alkaline Carbon Number (which corresponds to the number of carbon atoms of the oil molecule)

$f(A)$ = parameter function of both the type and concentration of alcohol added to the mixture

σ = parameter descriptive of the type of the surfactant

a_T = temperature coefficient

K = adjustable parameter dependent on the hydrophilic part of the surfactant group and the type of electrolyte used

The correlation for ethoxylated nonionic surfactants at optimum conditions was suggested to be of the form:⁴

$$a - \text{EON} - k(\text{EACN}) + m_1 C_{ai} + bS + C_T(T - 28) = 0 \quad (2)$$

where a = parameter dependent on the lipophilic tendency of the surfactant

EON = average number of ethylene oxide in the surfactant molecule

k = parameter constant

m_i = coefficient dependent on the type of alcohol added

C_{ai} = concentration of the alcohol

b = coefficient based on the type of electrolyte in solution

C_T = temperature coefficient

For the types of nonionic surfactants used in this study, ethoxylated nonionics, the HLB is related to the EON parameter in Eq. 2 by the original expression proposed by Griffin:⁵

$$HLB = \frac{\text{wt \% EO}}{5} \quad (3)$$

Equation 2 should be the correlation that aptly describes the behavior of the systems containing combinations of the nonionic surfactants used in this study. For mixtures of both anionic–nonionic systems, some combination of the two equations should be descriptive of the behavior of these systems at optimum conditions.

Figures 1 and 2 show plots of the optimum salinity (S^*) of these mixtures vs. the HLB of the nonionic surfactant components tested with the different alkanes. As shown in these figures, the data presented did not seem to correspond well to a linear relationship of S^* similar to Eq. 2, particularly in the

case of the linear alkyl alcohol ethoxylates. An alternative form of Eq. 1 was used to represent the data presented in these figures. Figures 3 and 4 show plots of the log of optimum salinity, $\ln(S^*)$, vs. the HLB of the nonionic surfactant components of the systems tested at 50 °C. The mixtures of dialkyl phenols exhibited a more significant dependence on the HLB value than the linear ethoxylates. The contrast in the behavior of these two types of surfactants was more pronounced at lower HLB values and decreased at higher HLB values. As previously reported, the two types of surfactants indicated a difference in dependence of optimal salinity with the HLB of the nonionic components in the system. The results presented in Figs. 3 and 4 also show that the $\ln(S^*)$ appears to be a better parameter for correlation than the S^* form originally suggested in Eq. 2. This was true for nonionic mixtures as well as anionic–nonionic mixtures.² Efforts to correlate the behavior of these nonionic mixtures as well as combinations of the primary anionic surfactant with the nonionic components are continuing.

Alpha olefin sulfonates (AOS) have also been studied by earlier researchers as potential candidates for application in chemical flooding. These systems have relatively good salt tolerance and yield favorable oil/water solubilization parameters and interfacial tension (IFT) with selected oils. However, substantial amounts of alcohol and elevated temperatures were found to be necessary to maintain favorable solubility in high-salinity brines. Preliminary phase behavior studies as well as IFT measurements are being conducted on selected samples of these anionic surfactants. Current efforts include

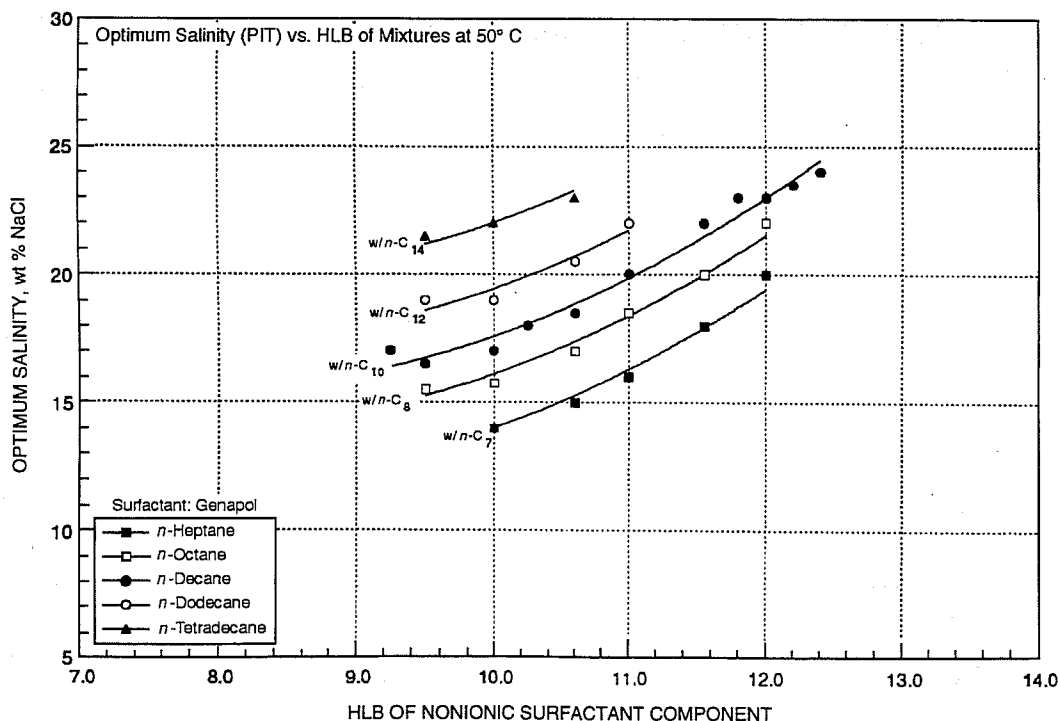


Fig. 1 Optimum salinity vs. hydrophile-lipophile balance (HLB) using Genapol mixtures with different alkanes at 50 °C.

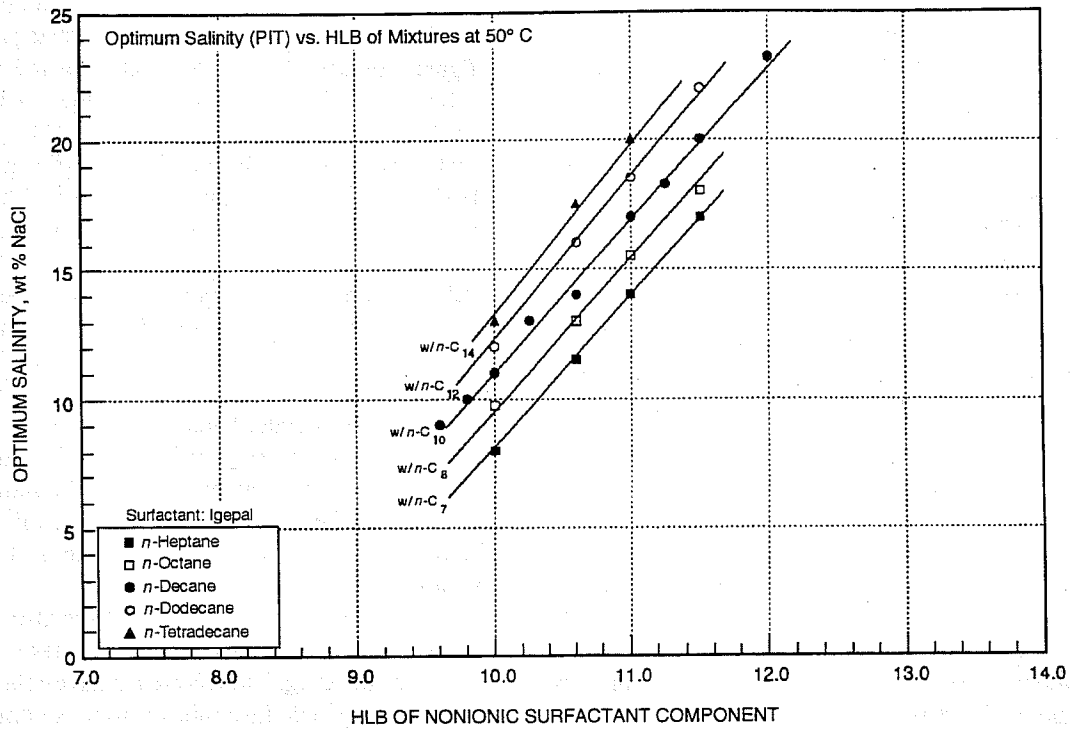


Fig. 2 Optimum salinity vs. hydrophile-lipophile balance (HLB) using Igepal mixtures with different alkanes at 50° C.

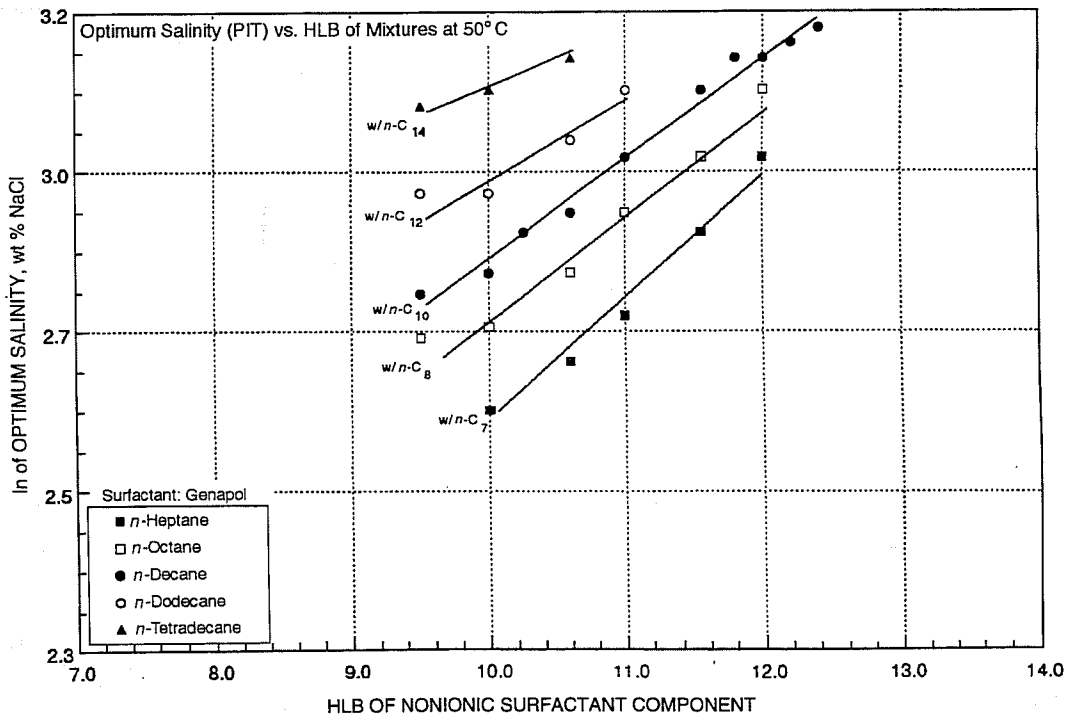


Fig. 3 Log (ln) of optimum salinity vs. hydrophile-lipophile balance (HLB) using Genapol mixtures with different alkanes at 50° C.

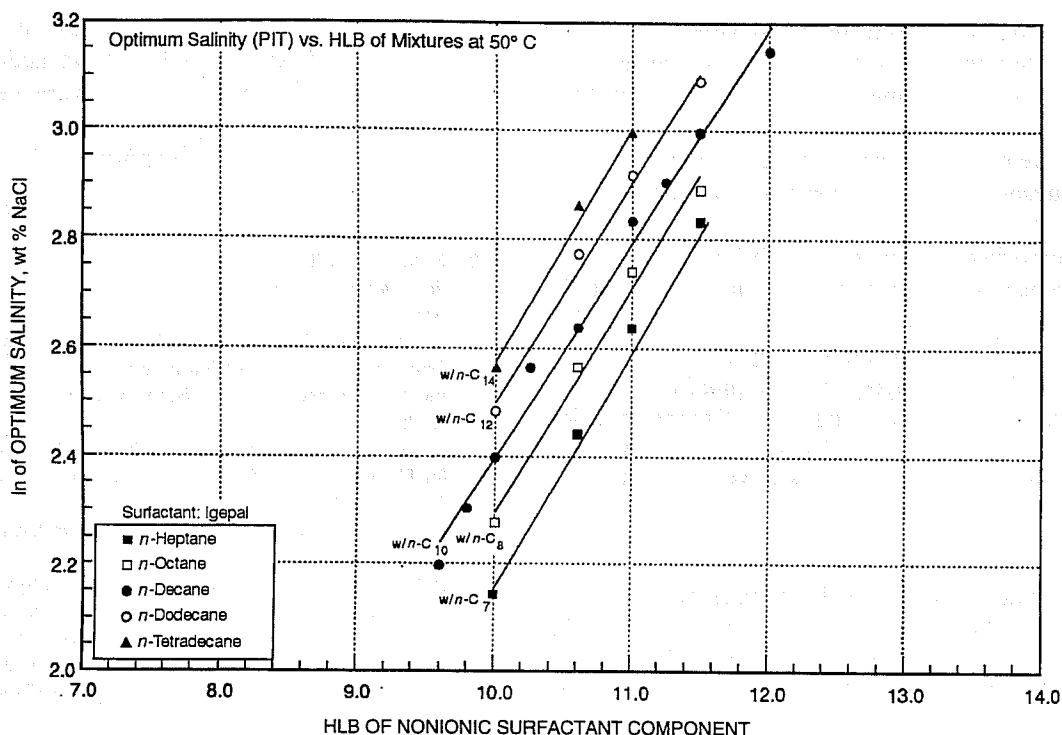


Fig. 4 Log (ln) of optimum salinity vs. hydrophile-lipophile balance (HLB) using Igepal mixtures with different alkanes at 50° C.

establishing base information on the degree of oil/water solubilization, IFT, and S^* values for several commercial surfactants (i.e., C_{14-16} AOS and C_{16-18} AOS). Results of the preliminary screening indicates relatively good agreement with results presented in the literature for a similar class of surfactants with different alkane chain structure. Tests of combinations of these anionic surfactants with the nonionic surfactants will be initiated shortly.

Surfactant Loss—Mixed Surfactants

A mixed surfactant system that contains the surfactants TRS 10-410, an anionic surfactant, and Igepal DM 530, a nonionic ethoxylated dialkyl phenol, at a total concentration of 2.0% by weight, was selected for evaluation. It will be determined if surfactant adsorption from the mixed surfactant system is different from adsorption of the individual surfactants. Analysis for the nonionic surfactant (cobalt thiocyanate method) has been complicated by the formation of emulsions. Experiments that use lower surfactant concentrations are being performed. It is expected that with use of lower surfactant concentrations there will be fewer analytical problems from emulsion formation.

Computerized Tomography Imaging of Oil Recovery in Class 1 Reservoir Rock

An oil recovery experiment was conducted using core from North Burbank Unit (NBU), Osage County, Okla. This reservoir is a Class 1 reservoir that is oil-wet because of a coating

of chamosite, an iron-rich mineral, on the pore surfaces.⁶ The coreflood was conducted at reservoir temperature (50° C) using simulated reservoir water (6.65% NaCl, 1.54% $CaCl_2$, and 0.24% $MgCl_2$) and NBU oil that was tagged with 18% iododecane to provide greater computerized tomography (CT) density contrast between the aqueous and hydrocarbon fluids in the core. The chemical system used for the oil recovery experiment was a mixed surfactant system that has been used previously with NBU oil at this temperature and salinity for oil recovery experiments in water-wet cores.⁷ The surfactants were Stepan B-105, a mixed anionic surfactant (alkyl aryl sulfonate and ethoxylated sulfate), and Stepan B-110 (alkyl aryl sulfonate) in a 7 to 1 ratio. Total surfactant injected was 0.3 PV of a 1% active weight solution. Mobility control was provided by 1500 ppm Xanthan polymer solution. All injected chemicals were prepared in simulated NBU water.

Volumetric measurements of oil recovery indicated that approximately 80% of the residual oil after waterflood (S_{owf}) was produced by this chemical system. This compares with approximately 40% of S_{owf} produced from a water-wet core (all other conditions remaining the same). This may represent optimistic recovery conditions, however, because the initial oil saturation was lower for the oil-wet core than for the water-wet core. Injection of oil under higher pressure conditions may be required to increase the initial oil saturation in the oil-wet core. If higher saturations could be achieved, the incremental oil may or may not be produced as easily by the chemical system. Experimental procedures will be modified to provide higher oil injection pressures.

Additional problems were observed when average oil saturations determined by volumetric measurements were compared with those determined using CT density measurements. Significantly higher oil saturations were indicated by the CT measurements at all stages of the oil recovery experiment. This suggested that adsorption of iododecane on the oil-wet surface could cause errors in the calculated saturations. Systematic experiments to investigate this problem are now under way. Since the salinity of NBU is fairly high, it may be possible to avoid this problem by tagging the brine instead of the oil for experiments using this oil-wet rock.

A paper entitled *CT-Imaging of Surfactant/Polymer EOR Corefloods* has been reviewed and submitted for presentation at the 205th National American Chemical Society Meeting Symposium on Enhanced Oil Recovery, March 1993.

Surfactant Database

A surfactant literature database has been assembled. There are now about 1800 references in the master list. From the master list, papers will be selected for in-depth review. Surfactant information, properties, and experimental data from the

literature and from studies performed at NIPER will be entered in the database to aid in the prediction of conditions and application for chemical oil recovery methods.

References

1. B. Gall, *Environmental, Safety, and Health Review of Project BE4A*, DOE Report NIPER-638, December 1992.
2. F. M. Llave, T. R. French, and P. B. Lorenz, *Evaluation of Mixed Surfactants for Improved Chemical Flooding*, DOE Report NIPER-631, November 1992.
3. J. L. Salager, J. Morgan, R. S. Schechter, W. H. Wade, and E. Vasquez, Optimum Formulation of Surfactant/Water/Oil Systems for Minimum Interfacial Tension or Phase Behavior, *Soc. Pet. Eng. J.*, 19: 107-115 (1978).
4. M. Bourrel, J. L. Salager, R. S. Schechter, and W. H. Wade, A Correlation for Phase Behavior of Nonionic Surfactants, *J. Colloid Interface Sci.*, 75(2) (June 1980).
5. W. C. Griffin, Classification of Surface-Active Agents by "HLB," *J. Soc. Cosmet. Chem.*, 1: 311-326 (1949).
6. D. F. Boneau and R. L. Campitt, A Surfactant System for the Oil-Wet Sandstone of the North Burbank Unit, *J. Pet. Technol.* (May 1977).
7. F. M. Llave, B. L. Gall, T. R. French, L. A. Noll, and S. A. Munden, *Phase Behavior and Oil Recovery Investigations Using Mixed and Alkaline-Enhanced Surfactant Systems*, DOE Report NIPER-567, December 1991.

Summary of Technical Progress

Interactions that occur between enhanced oil recovery (EOR) chemicals during surfactant-enhanced alkaline flooding were investigated during FY92. The effects of interactions between polymers and surfactants on rheology were shown to be significant, and so far no satisfactory way has been found to mitigate these effects.¹ During FY93, experiments are being conducted that should contribute to a better understanding of chemical interactions that have detrimental effects on the rheological properties of surfactant-enhanced alkaline flooding chemical formulations.

Before FY93 experimental work was begun, an Environment, Safety and Health (ES&H) review was completed for project BE4B.² The review showed that the project is being conducted in a safe manner compatible with maintenance of a clean environment. The review also showed that personnel are properly trained in the use of several hazardous chemicals and that appropriate monitoring demonstrates that personnel are not exposed to dangerous levels of hazardous chemicals.

After completion of the ES&H review, experiments were begun with instruments that have not previously been used for project BE4B. A C. N. Woods Model 6000 light-scattering instrument is being used for the conclusion of the study on dispersions/interactions associated with surfactant-enhanced alkaline flooding. The mathematics associated with the interpretation of light-scattering measurements is associated with the accurate determination of the differences between the refractive indexes of the liquid mixtures being studied. A C. N. Woods Model RF-600 differential refractometer is in use for measuring differential refractive index (Δn). Figure 1

DEVELOPMENT OF IMPROVED ALKALINE FLOODING METHODS

Cooperative Agreement DE-FC22-83FE60149,
Project BE4B

National Institute for Petroleum
and Energy Research
Bartlesville, Okla.

Contract Date: Oct. 1, 1983
Anticipated Completion: Sept. 30, 1993
Funding for FY 1993: \$200,000

Principal Investigator:
Troy R. French

Project Manager:
Thomas Reid
Bartlesville Project Office

Reporting Period: Oct. 1-Dec. 31, 1992

Objectives

The major objective is to develop cost-effective and efficient chemical flooding formulations using surfactant-enhanced, weakly alkaline systems. Specific objectives for FY93 are to (1) determine the effect of variables on surfactant and polymer propagation and retention during alkaline flooding and (2) perform studies designed to support a field test.

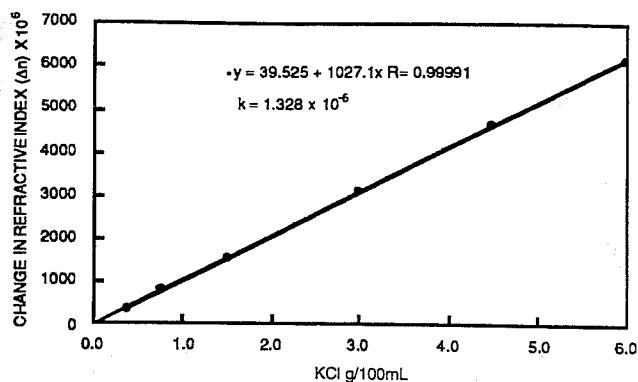


Fig. 1 Differential refractive index, 436 nm.

shows the results of calibrating the instrument at a wavelength of 436 nm with several KCl solutions. It was shown that Δn can be measured quite accurately until the differences measured become very small. An accurate measurement of Δn can be made down to about 300 or 400×10^{-6} .

Light-scattering measurements were commenced on solutions of Chevron CF-100 surfactant. This surfactant is of particular interest because it is being used for a field project being conducted under the Supplemental Government Program. The planned procedure was light-scattering measurements with surfactant, polymer, and surfactant-polymer mixtures. The results of the measurements conducted with surfactant are shown in Table 1. Notice in Table 1 that Δn is less than 300 in all the measurements. The uncertainty of this

TABLE 1
Light-Scattering Measurements with CF-100
Surfactant, 436 nm, 23 °C

Surfactant concentration, g/mL × 10 ⁴	$\Delta n \times 10^6$	$Hc/\tau \times 10^8$
1.00	13	1.47
3.00	68	0.76
5.00	100	0.70

measurement leads to inaccuracy in calculating Hc/τ . It was not possible, therefore, to determine the apparent molecular weight of the surfactant. The only information generated is that the critical micelle concentration (CMC) of this surfactant is apparently between 1 and 3×10^{-4} g/mL.

It is apparent that light-scattering measurements conducted with solutions of the surfactant are not useful for this work. The approach now will be to conduct light-scattering measurements with polymer solutions that contain variable amounts of surfactant. These experiments are in progress.

References

1. T. R. French and C. B. Josephson, *The Effect of Polymer-Surfactant Interaction on the Rheological Properties of Surfactant-Enhanced Alkaline Flooding Formulations*, DOE Report NIPER-635, October 1992.
2. T. R. French, *Analysis of Planned Tasks and Evaluation of the Procedures and Equipment for Environmental, Safety and Health Requirements—Project BE4B*, DOE Report NIPER-642.

Objectives

The objectives of this project are to develop improved methods for maintaining effective mobility control throughout the reservoir in chemical flooding and to use the permeability modification simulator to design a cost-effective gel treatment using polymer gel systems.

Summary of Technical Progress

An Environmental, Safety, and Health (ES&H) review¹ was completed and submitted to the Bartlesville Project Office.

For the investigation of the effect of lamination angle on polymer retention in unfired Berea sandstone cores, the first of a series of corefloods was conducted with a rectangular Berea sandstone core that had laminations parallel to the longest axis of the core. After injection of the first slug (3.5 PV) of a 1000-ppm biopolymer solution in 2% KCl into the core, it was found that the maximum amount of polymer retention during polymer flow was 1200 kg/acre/m. This amount was 20% higher than that in a similar but fired Berea core (1007 kg/acre/m). Firing was done at 1000 °F for 24 h to stabilize the clays. Before polymer injection, tracer tests were

MOBILITY CONTROL AND SWEEP IMPROVEMENT IN CHEMICAL FLOODING

Cooperative Agreement DE-FC22-83FE60149,
Project BE4C

National Institute for Petroleum
and Energy Research
Bartlesville, Okla.

Contract Date: Oct. 1, 1983
Anticipated Completion: Sept. 30, 1993
Funding for FY 1993: \$240,000

Principal Investigator:
Hong W. Gao

Project Manager:
Jerry Casteel
Bartlesville Project Office

Reporting Period: Oct. 1–Dec. 31, 1992

conducted by injection of a slug (0.278 PV) of tagged brine (7% KI) into the core to determine the flow path of the injection fluid.

Polymer Retention in an Unfired Rectangular Berea Sandstone Core

The first of a series of corefloods designed to investigate the effect of lamination angle on polymer retention in unfired rectangular Berea sandstone cores was initiated. The core being used was cut along the direction of laminations. Its dimensions were 4.00 cm × 3.94 cm × 24.02 cm. Brine permeability was 180 mD. The porosity determined from a computerized tomography (CT) scanner was 18.9%, compared with 19% from a brine saturation method. The brine used to saturate the core and in the coreflood experiment was 2% KCl. The purpose of using 2% KCl was to stabilize clays present in the sandstone. The salt concentration was selected after several coreflood tests with 1, 1.5, 2, and 3% KCl in another similar unfired rectangular Berea core were conducted. With this concentration (2%), clays were found to be stabilized as indicated by the steady pressure drop across the core during corefloods. After the brine concentration was selected, a calibration curve for the viscosity of biopolymer solution in 2% KCl as a function of polymer concentration was constructed as shown in Fig. 1. This calibration curve was used to determine the effluent biopolymer concentration. The biopolymer solution used in the coreflood was prepared from Pfizer's FLOCON 4800C. The concentration of biopolymer solution used was 1000 ppm. Both biopolymer solution and brine contained 500 ppm of 37.3% formaldehyde as a biocide.

Before polymer injection, tracer tests were conducted at 1.4 ft/d (5.34 mL/h) by injecting a slug (0.278 PV) of tagged brine (7% KI) into the core followed by 2% KCl brine. The flow behavior of the tagged brine was monitored throughout its advance through the core by conventional CT and topogram scanning. The resulting images will be compared with those after the polymer flow to determine how the retained polymer affects the stability of the fluid front in core.

The coreflood was conducted at room temperature (22 °C). The injection sequence was brine, polymer, and brine. Total volume of the first slug of polymer injected was 3.5 PV (252 mL). Total active biopolymer injected was 0.252 g. The flow rate used was 4.3 mL/h (apparent shear rate inside the core was 10 sec⁻¹).

The effluent biopolymer concentration was determined by viscosity measurements at a shear rate of 20.4 sec⁻¹ using a Contraves Low Shear 30 viscometer. Figure 2 shows the normalized effluent biopolymer concentration as a function of pore volumes injected. The effluent biopolymer concentration had not reached that of the injected biopolymer solution, indicating that equilibrium retention had not been reached.

Figure 3 shows the polymer retained as a function of PV. The maximum amount of polymer retained inside the core during polymer flow was 1200 kg/(acre-m), compared with 1007 kg/(acre-m) in a similar but fired Berea core.² Higher

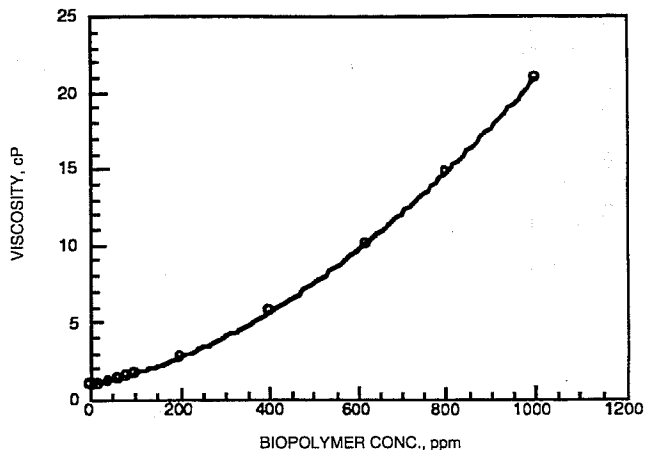


Fig. 1 Viscosity as a function of biopolymer concentration in 2% KCl with a shear rate of 20.4 sec⁻¹.

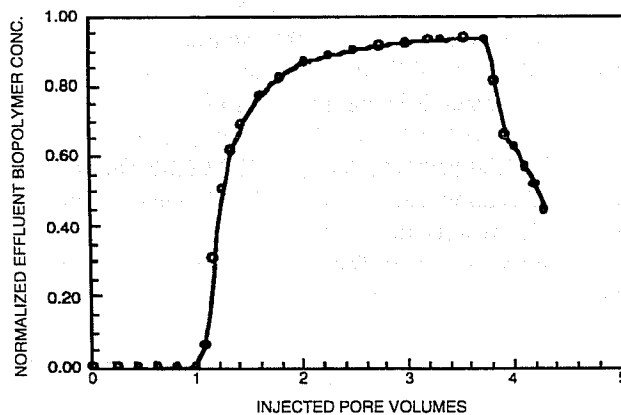


Fig. 2 Normalized effluent concentration profile for a biopolymer from an unfired Berea sandstone core. Lamination angle, 0°. Porosity, 19%. 1 pore volume, 71.9 mL. Brine permeability, 180 mD. Polymer injection, 0 to 3.5 PV. Flow rate, 4.3 mL/h. Apparent shear rate, 10 sec⁻¹.

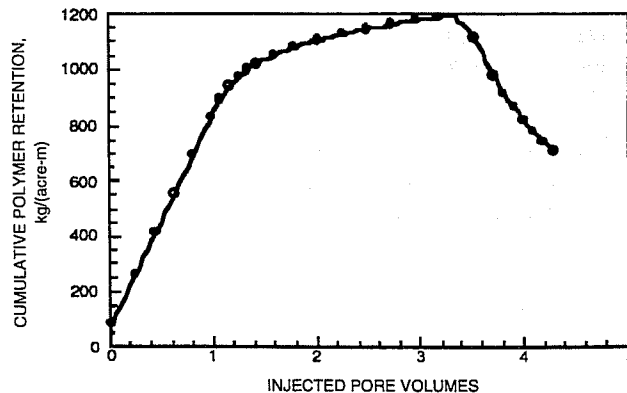


Fig. 3 Retention of a biopolymer in an unfired Berea sandstone core during polymer flow. Lamination angle, 0°. Porosity, 19%. 1 pore volume, 71.9 mL. Brine permeability, 180 mD. Polymer injection, 0 to 3.5 PV. Flow rate, 4.3 mL/h. Apparent shear rate, 10 sec⁻¹.

polymer retention in an unfired core than in a fired core is expected. These results will be compared with those of future corefloods with cores that have crossbed laminae.

A paper, entitled *The Effects of Layer Permeability Contrast and Crossflow on the Effectiveness of Polymer Gel Treatments in Polymer Floods and Waterfloods*, was submitted for presentation at the 1993 Society of Petroleum Engineers Production Operations Symposium to be held in Oklahoma City, Mar. 21–23, 1993.

References

1. H. W. Gao, *Environmental, Safety, and Health Review of Project BE4C*, DOE Report NIPER-643, December 1992.
2. H. W. Gao, *The Effect of Lamination Angle on Polymer Retention*, DOE Report NIPER-630, September 1992.

SURFACTANT-ENHANCED ALKALINE FLOODING FIELD PROJECT

**Cooperative Agreement DE-FC22-83FE60149,
Project SGP41**

**National Institute for Petroleum
and Energy Research
Bartlesville, Okla.**

**Contract Date: July 18, 1990
Anticipated Completion: Sept. 30, 1993
Funding for FY 1993: \$318,000**

**Principal Investigator:
Troy R. French**

**Project Manager:
Thomas Reid
Bartlesville Project Office**

Reporting Period: Oct. 1–Dec. 31, 1992

Objectives

The objectives of this pilot project are to (1) obtain information and data that will help to demonstrate the applicability of surfactant-enhanced alkaline flooding as a cost-effective enhanced oil recovery (EOR) method, (2) transfer the surfactant-enhanced alkaline flooding technology that has been developed under the sponsorship of the Department of Energy (DOE) to the petroleum industry, and (3) obtain information regarding procedures for designing and applying

this technology that will assist independent producers in sustaining production from mature producing oil fields rather than abandoning marginal wells.

Summary of Technical Progress

The site selected for conducting a field pilot test using surfactant-enhanced alkaline flooding methods is Hepler (Kansas) oil field. Hepler field is located in Crawford and Bourbon counties. This near-term application of a promising EOR technology in a fluvial-dominated deltaic type reservoir is consistent with U.S. Department of Energy oil research strategy.¹

In September, field cores were obtained from three locations on the lease site. The results of chemical flooding of several of the cores are given in Table 1. The initial oil saturations of core plugs RP-26, RP-29, and RP-30 were, respectively, 39.2, 39, and 42% PV. These saturations were somewhat lower than was expected. The initial oil saturation of core plug RP-27 was 59% PV.

Core plugs RP-26 and RP-27 were oilflooded and then waterflooded before chemical injection was begun. Chemical injection was commenced in core plugs RP-29 and RP-30 without a prior waterflood. In each case, the chemical formulation contained Chevron CF-100 or XP-100 surfactant, Tronacarb (sodium bicarbonate), and STPP (sodium triphosphosphate). Alcoflood 1135 polymer, a polyacrylamide, was used for mobility control. All formulations were mixed in water from a water supply well located on the lease.

Examination of Table 1 reveals that oil recovery efficiency from chemical flooding was low, except when the polymer concentration was very high. The amount of oil recovered from core RP-27 was high, but only after repeated chemical floods with increasing polymer concentrations. One of the results that all of the corefloods had in common was the nearly immediate breakthrough of chemicals after chemical injection was commenced. Figure 1 shows the analysis of effluent fractions for a chemical flood conducted with core plug RP-26. The early chemical breakthrough shown in Fig. 1 is typical of the floods that were conducted with the other core plugs.

A series of experiments that help to explain the coreflood results was conducted. Figure 2 shows the results from minipermeameter measurements across core plug RP-26. [The measurements were taken such that the cross section measured represents a 1.5-in. (3.81-cm) vertical slice of the reservoir core from well J-4]. Permeability across the core plug varied as much as 400 mD over a distance of 1.6 cm. The existence of a channel through the center of the core plug was confirmed with computerized tomography (CT) scanning. Similar minipermeameter results are shown in Fig. 3 for core plug RP-29.

Further confirmation of the suspected channeling of injected fluid is shown in Fig. 4. Figure 4 shows CT scans of the flow of tracer (an aqueous solution of sodium iodide) through core plug RP-30. After 0.25 cm³ of injection, flow through a

TABLE 1
Corefloods with Field Core

Coreflood	K, mD	ϕ , %	PV, mL	Original S_{oi} , % PV	S_{oi} before WF, % PV	S_{owf} , % PV	S_{ocf} , % PV
RP-26	154.2	21.1	14.60	39	82	43.0	39.1
RP-27	211	22.6	15.06	59	81	26.8	25.3
RP-27A	-	-	-	-	-	25.3*	25.1
RP-27B	-	-	-	-	-	25.1*	24.6
RP-27C	-	-	-	-	-	24.6*	22.3
RP-27D	-	-	-	-	-	22.3*	17.4
Total RP-27	-	-	-	59	81	26.8	17.4
RP-29	28.2	17.81	12.14	39	39	27.3	22.9
RP-30	175.7	21.87	14.74	-	-	-	41.0

*Oil saturation after waterflooding and prior to chemical floods.

Coreflood	Oil produced, % PV		Recovery efficiency, %			Coreflood notes
	WF	CF	WF	CF	Overall	
RP-26	39	4.20	47.6	9.10	52.30	High permeability variation 0.5% XP-100, 1.2% NaHCO ₃ , 0.45% STPP, 1200 ppm Alcoflood 1135
RP-27	54.4	1.55	68.4	5.80	68.84	0.5% XP-100, 1.2% NaHCO ₃ , 0.45% STPP, 1200 ppm Alcoflood 1135
RP-27A	-	0.20	-	0.80	69.10	0.5% XP-100, 1.2% NaHCO ₃ , 0.45% STPP, 2000 ppm Alcoflood 1135
RP-27B	-	0.52	-	2.07	69.73	0.5% XP-100, 1.2% NaHCO ₃ , 0.45% STPP, 2500 ppm Alcoflood 1135
RP-27C	-	2.21	-	9.00	72.45	0.5% XP-100, 1.2% NaHCO ₃ , 0.45% STPP, 3500 ppm Alcoflood 1135
RP-27D	-	4.97	-	15.70	78.57	0.5% XP-100, 1.2% NaHCO ₃ , 0.45% STPP, 5000 ppm Alcoflood 1135
Total RP-27	-	9.45	-	35.93	78.57	
RP-29	11.7	4.40	30	16.00	41.20	Highly laminated 0.5% CF-100, 2.2% NaHCO ₃ , 0.45% STPP, 1200 ppm Alcoflood 1135
RP-30	-	0.78	-	1.87	1.87	CT tracer test indicates channeling 0.5% XP-100, 1.2% NaHCO ₃ , 0.45% STPP, 1200 ppm Alcoflood 1135

Note: ϕ , porosity. S_{oi} , initial oil saturation. S_{owf} , original waterflood. S_{ocf} , original coreflood. WF, waterflood. CF, coreflood. STPP, sodium tripolyphosphate.

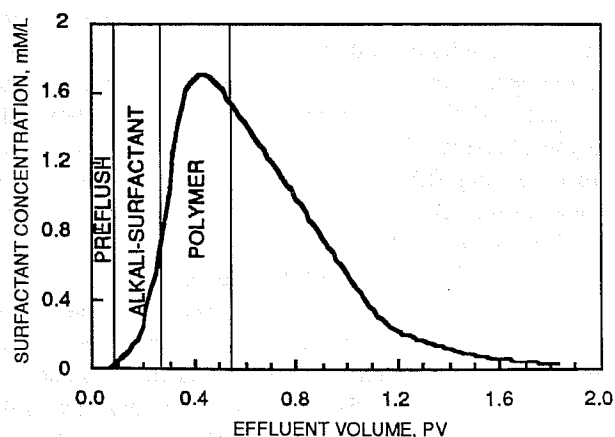


Fig. 1 Analysis of effluent fractions from coreflood RP-26.

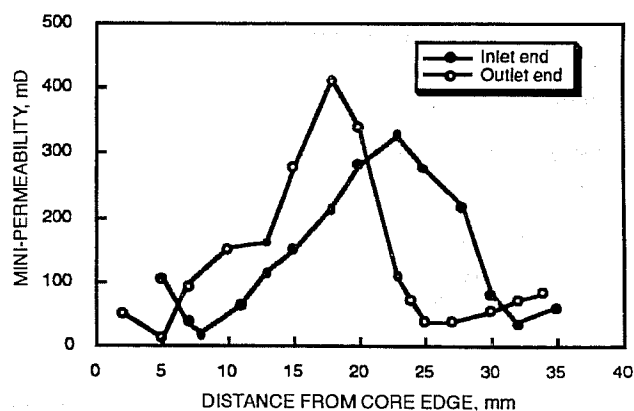


Fig. 2 Minipermeameter measurements across core plug RP-26.

channel can be seen in the lower portion of the core. After 1.25 cm³ (8% PV) of injection, the channel was more visible and tracer had already exited the core. This was confirmed by the presence of tracer in the outlet end-piece of the core holder after 1.25 cm³ of injection. Eventually, after many pore volumes had been injected, the tracer was detected throughout

most of the core plug. Unfortunately, good sweep cannot be expected with small amounts of injected chemicals.

Oil recovery was lower with field cores than with Berea sandstone. This was apparently the result of heterogeneity in the field core. The prior experiments with Berea sandstone demonstrated that the oil could be mobilized with the

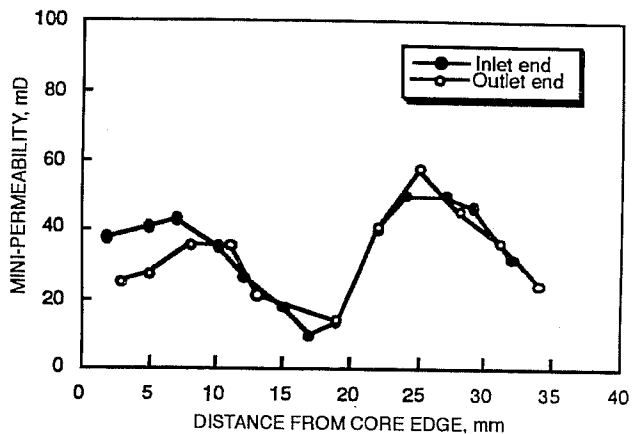


Fig. 3 Minipermeameter measurements across core plug RP-29.

chemical formulation that is being used.^{2,3} There is reason to believe that channeling is more of a problem in short core plugs than it will be in the reservoir. The reason that channeling may be magnified in the core plugs is because reservoir compartments are severed at each end of the short core plugs, thereby creating direct channels. It appears difficult to extrapolate or scale the results obtained in short core plugs to the reservoir. On reservoir scale, the compartments have boundaries that may reduce channeling in the reservoir. Another reason to believe that channeling may be less in the reservoir is that a successful polymer flood was conducted north of the Elmer lease.

A report, *Environmental Investigation of Hepler Field for an Alkali-Surfactant-Polymer Enhanced Oil Recovery Field-Pilot Demonstration Project*, by W. I. Johnson and T. R. French was submitted for peer review.

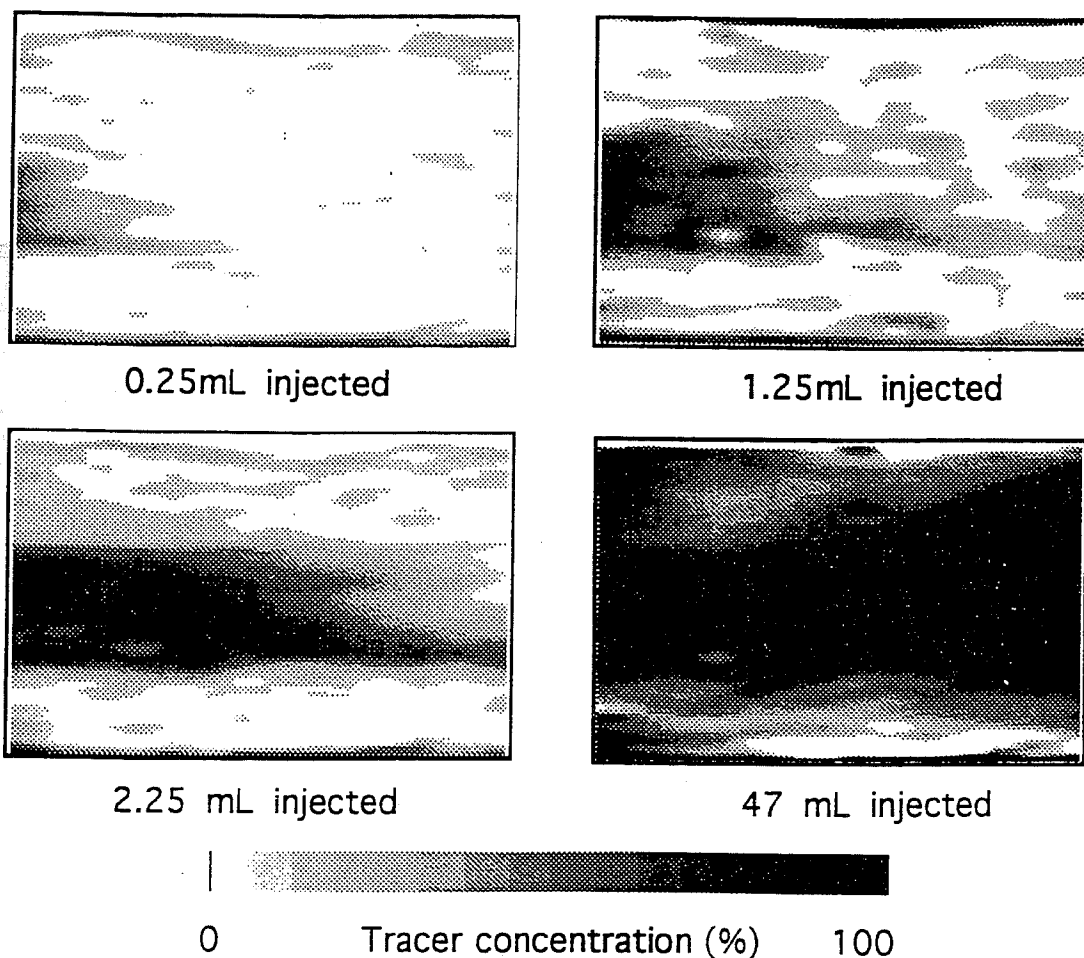


Fig. 4 Computerized tomography (CT) scan of tracer propagation through core plug RP-30.

References

1. U.S. Department of Energy, *Oil Research Program Implementation Plan*, DOE Report DOE/FE-0188P, April 1990.

2. T. R. French and C. B. Josephson, *Alkaline Flooding Injection Strategy*, DOE Report NIPER-563, September 1991.

3. T. R. French, *Surfactant-Enhanced Alkaline Flooding Field Project*, DOE Report NIPER-569, October 1991.

GAS DISPLACEMENT— SUPPORTING RESEARCH

SCALEUP OF MISCIBLE FLOOD PROCESSES

Contract No. DE-FG22-92BC14852

**Stanford University
Stanford, Calif.**

**Contract Date: Sept. 30, 1992
Anticipated Completion: Sept. 30, 1995
Government Award: \$349,985**

**Principal Investigator:
Franklin M. Orr, Jr.**

**Project Manager:
Jerry Casteel
Bartlesville Project Office**

Reporting Period: Oct. 1–Dec. 31, 1992

Objective

The objective of this project is to make more accurate quantitative predictions of the impact of nonuniform flow, crossflow, and phase behavior in flows in heterogeneous reservoir rocks. In the past the instabilities arising from unfavorable mobility ratios that occur during injection of a

solvent such as CO₂ have been reported. Experiments performed in this lab indicate that the spatial variability in permeability tends to control the displacement process in near miscible injections. This report focuses on the flow regimes that result from heterogeneities within the reservoir and the dimensionless scaling parameters that control a given situation. The transition from a capillary-dominated flow to a gravity-controlled system with experimental results obtained during low interfacial tension (IFT) drainage from vertically oriented cores will be demonstrated.

Summary of Technical Progress

Dimensionless Scaling Parameters

Viscous, gravity, and capillary forces interact to determine the performance of any fluid displacement in heterogeneous porous media, whether the flow setting involves gas injection for enhanced oil recovery or the transport of hydrocarbon contaminants in an aquifer. As the scales of the flow and of the heterogeneities change, the relative importance of the individual viscous, gravity, and capillary contributions also changes. In this report, the flow regimes that arise as the relative magnitudes of the three contributions vary are investigated.

At the start the dimensionless groups that control the transition from one flow regime to another are derived by scaling the material balance equations for two-phase flow in

a two-dimensional, heterogeneous porous medium. The resulting dimensionless groups are (1) a mobility-weighted capillary number (ratio of capillary to viscous forces),

$$N_c = \frac{p_c^* k_{ah}}{Lq\mu_o} \frac{M}{1+M} \quad (1)$$

where p_c^* = characteristic capillary pressure

k_{ah} = characteristic horizontal permeability

L = length of the system

q = flow rate

μ_o = oil viscosity

M = mobility ratio defined as $M = \lambda_w / \lambda_o$

(2) a mobility-weighted gravity number (ratio of gravity to viscous forces),

$$N_g = \frac{\Delta\rho g H k_{av}}{Lq\mu_o} \frac{M}{1+M} \quad (2)$$

where $\Delta\rho$ is the density difference and H is the flow thickness, and (3) a shape factor defined as

$$R_1 = \frac{L}{H} \left(\frac{k_{av}}{k_{ah}} \right)^{1/2} \quad (3)$$

where k_{ah} is a characteristic vertical permeability.

The regimes considered so far are gravity-dominated crossflow, capillary-dominated crossflow, capillary-gravity equilibrium, and viscous-dominated crossflow. The conditions required for flow in each of the regimes are identified as limiting cases of the full-flow equations. This work and a recent publication⁴ provides a systematic analysis of the scaling conditions under which a simplified limiting case flow equation is appropriate.

Transitions from one flow regime to another occur as the dimensionless groups are changed. Experimental and simulation data from the literature have been compiled in terms of the dimensionless structure derived to establish the ranges of values of each group over which the transitions occur. Figure 1 shows a schematic of the transitions and the various flow regimes.

Capillary to Gravity Transition

In the preceding section three dimensionless groups were defined which, depending on the magnitude of each, will determine the prevalent force and the required scaling parameter. Several "free-fall" drainage experiments have been performed at various values of capillary to gravity ratio (CGR or inverse Bond number, N_B^{-1}) in vertically oriented cores. When the IFT between the wetting fluid initially in the core and the nonwetting fluid surrounding the core at the beginning of each experiment is altered, the final recovery at the end of drainage can be plotted against the CGR.

Initially, a core is saturated with the wetting phase. The core is transferred to a Plexiglas cell and rapidly surrounded

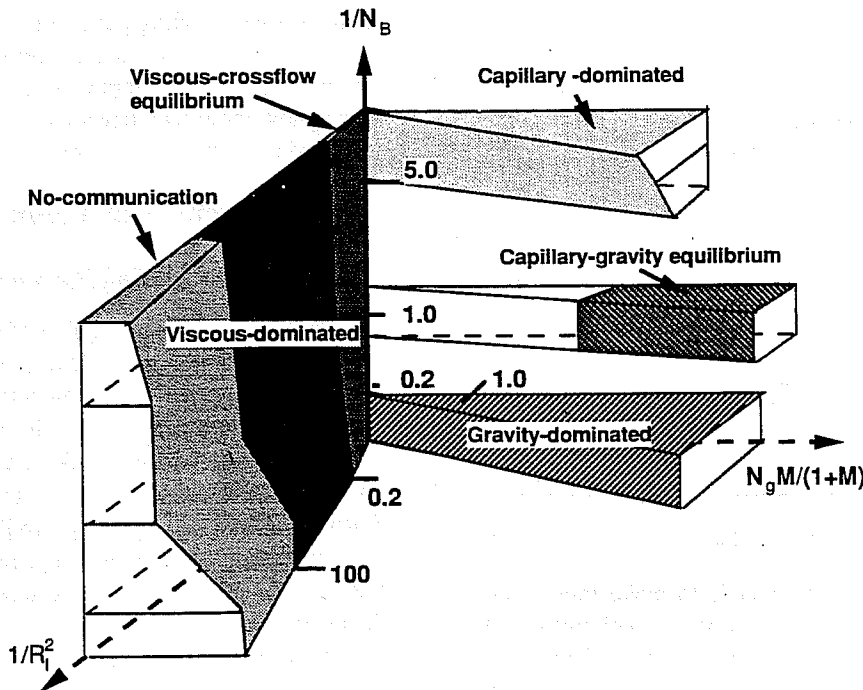


Fig. 1 Schematic diagram of the flow regions in heterogeneous porous media.

with the nonwetting phase. Gravity drainage causes the wetting phase to flow from the bottom of the core. Recovery vs. time is recorded. More details regarding the cores and procedures may be found elsewhere.^{2,3}

Figure 2 is a plot of remaining saturation at the end of a drainage experiment vs. the CGR for experiments performed in this lab and all other free-fall drainage experiments found in the literature.^{2,4,5,6} At a CGR of 5, there is no recovery of the wetting phase. As the CGR is reduced to near unity, the wetting phase begins to flow. At a value near 0.3, more than 60% of the wetting phase is recovered. Further reductions in the CGR result in modest decreases in the residual saturation. This observation is consistent with classic drainage capillary pressure measurements. To reduce the saturation to less than 20%, the disjoining pressure that holds the film immobile on the surface must be overcome, which requires extremely large capillary pressures. As demonstrated in Fig. 2, there is a strong correlation between final recovery and the CGR.

Thus the experiments described demonstrate the transition from a capillary-dominated situation to gravity-dominated flow. As shown in Fig. 1, for inverse Bond numbers (shown on the y-axis) greater than 5, the system is controlled by capillary forces. The transition zone is shown as the CGR is reduced below 5. Further reductions in the CGR below 1 result in gravity-dominated flow. Work is currently being done on delineating the boundaries between the flow regimes described.

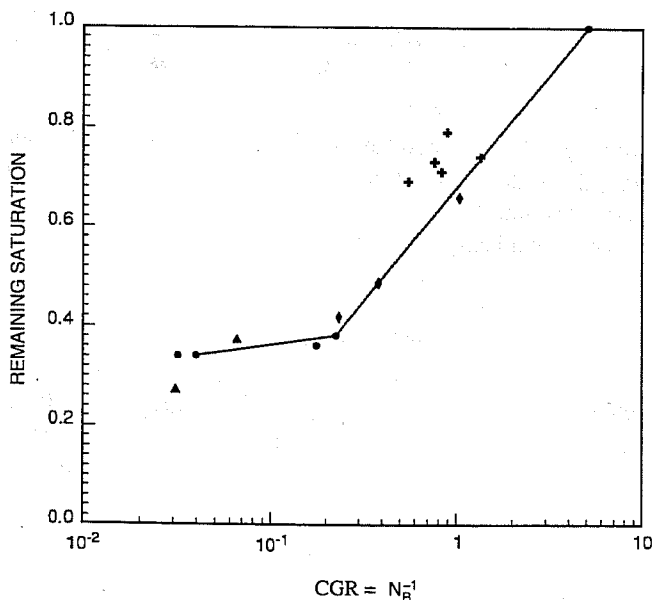


Fig. 2 Remaining saturation vs. capillary to gravity ratio (CGR) for free-fall drainage experiments. ●, Schechter et al.³ ▲, Pavone et al.⁴ +, Stensen et al.⁵ ◆, Suffridge and Renner.⁶

References

1. M. Shook, D. Li, and L. W. Lake, Scaling Immiscible Flow Through Permeable Media by Inspectional Analysis, *In Situ*, 16: 311-349 (1992).

2. D. S. Schechter, Capillary Imbibition and Gravity Drainage at Low IFT, Ch. 5.1 in *Scale-Up of Miscible Flood Processes*, Final Report to U.S. DOE Grant No. DE-FG21-89MC26253, October 1992.
3. D. Schechter, D. Zhou, and F. M. Orr, Jr., Capillary Imbibition and Gravity Segregation in Low IFT Systems, paper SPE 22594 presented at 66th Annual Technical Conference and Exhibition, Dallas, Tex., Oct. 6-9, 1991.
4. D. Pavone, P. Bruzzi, and R. Verre, Gravity Drainage at Low IFT, 5th European Symposium on Enhanced Oil Recovery, October 1989, Budapest, Hungary, pp. 165-174.
5. J. Stensen, A. Skauge, P. Monstad, and A. Graue, *The Effect of Interfacial Tension on Gas Gravity Drainage*, presented at 2nd North Sea Chalk Symposium, Copenhagen, Denmark, June 11-12, 1990.
6. F. E. Suffridge and T. A. Renner, *Diffusion and Gravity Drainage Tests to Support the Development of a Dual Porosity Simulator*, presented at 6th European IOR Symposium, Stavanger, Norway, May 21-23, 1991.

GAS FLOOD PERFORMANCE PREDICTION IMPROVEMENT

Cooperative Agreement DE-FC22-83FE60149,
Project BE5A

National Institute for Petroleum
and Energy Research
Bartlesville, Okla.

Contract Date: Oct. 1, 1983
Anticipated Completion: Sept. 30, 1993
Funding for FY 1993: \$250,000

Principal Investigator:
Ting-Horng Chung

Project Manager:
Jerry Casteel
Bartlesville Project Office

Reporting Period: Oct. 1-Dec. 31, 1992

Objective

The objective of this research project is to improve prediction techniques for gas miscible displacement through fundamental research in displacement mechanisms. The effects of carbon dioxide on interfacial tension (IFT) and relative permeability for reservoir fluids are the research subjects of this project.

Summary of Technical Progress

Environment, Safety and Health Assessment

The planned tasks have been analyzed to determine if the equipment and experimental procedures meet safety and environmental requirements and if the health of operators will be affected by any of these tasks. Experimental procedures

have been established and equipment has been reviewed by IIT Research Institute's Environment, Safety and Health Manager. A status report on the results of these analyses has been submitted to the Bartlesville Project Office (BPO).¹

Construction and Testing of the High-Pressure Interfacial Tension Measurement Apparatus

The effects of IFT between crude oil and displacing fluids on crude oil displacement efficiency are revealed from the change of relative permeability curves with IFT.² With lower IFT, the displacing fluids can reach higher saturation or, in other words, more oil can be displaced. In gas miscible displacement, the ideal situation is to let the injected gas make direct contact with reservoir oil and reach low IFT with the oil. In most cases, under reservoir conditions, the residual oil phase is encompassed by the water phase after waterflooding. The injected gas may have to pass through the water phase before dissolving into the residual oil phase. Therefore, the IFT between water and crude oil phases can still be the controlling factor for the displacement of oil. Carbon dioxide has higher solubilities in both water and oil phases than nitrogen and hydrocarbon gases have. The objective of this research is to study the effects of the dissolution of CO₂ on the IFT of water-oil systems.

A literature survey has been conducted, and IFT data for hydrocarbon-water systems and for CO₂-hydrocarbon systems have been collected. However, no IFT measurement for hydrocarbon-water systems with CO₂ dissolved at reservoir pressure and temperature ranges has been found in the literature. Methods including pendant drop, sessile drop, and spinning drop methods have been used for IFT measurements. Current developments in personal computers with the ability to capture and digitize video images provide an improved process to determine the IFT. A simple and fast system for measuring IFT using the pendant drop method coupled with an image analysis technique has been developed in this work. A schematic diagram of the apparatus for pendant drop IFT measurements is shown in Fig. 1. The major parts are high-pressure IFT cell (Temco, Co.), optical system, and computer image processing system. Pendant drops are generated inside the IFT cell, which can be operated at temperatures to 177 °C (350 °F) and pressures to 69 MPa (10,000 psi). The small liquid drop is magnified by a high-resolution stereo-microscope (Nikon Inc.), and the image is captured and converted to electrical signals by a color CCTV camera (JAVELIN JE3462 RGB). The red, green, and blue (RGB) signals from the camera are fed to a frame grabber (Truevision TARGA-Plus) inside the personal computer. The frame grabber card is connected with the computer monitor and an additional S-VHS video monitor. The drop image is viewed from the video monitor. The captured drop images are stored in the computer as digital information and can be printed in color or in black and white. An image analysis software (Image-Pro Plus) is used to digitize the edge of the drop image,

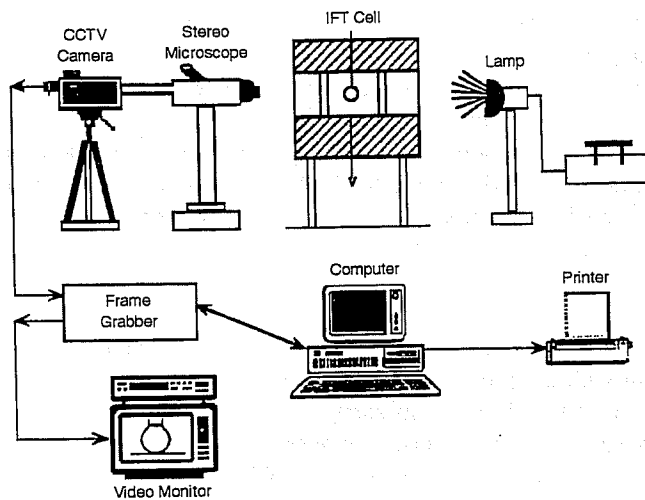


Fig. 1 Schematic setup of the interfacial tension (IFT)-measuring apparatus.

which gives the X- and Z-coordinates of the points at the boundary of the drop profile.

Method for IFT Determination

The drop profile is described by the classical Young-Laplace equation:

$$\gamma \left(\frac{1}{R_1} + \frac{1}{R_2} \right) = \Delta P \quad (1)$$

where γ is the interfacial tension, R_1 and R_2 represent the two principal radii of curvature, and ΔP is the pressure difference across the interface.

Mathematically, the curve of the drop profile (shown in Fig. 2) can be described in a parametric form

$$X = X(S) \text{ and } Z = Z(S) \quad (2)$$

where S is the arc length measured from the origin, o . Following previous development,³ the equation of Young and Laplace can be expressed as a set of three differential equations:

$$\frac{dx}{ds} = \cos \phi \quad (3)$$

$$\frac{dz}{ds} = \sin \phi \quad (4)$$

$$\frac{d\phi}{ds} = 2 - \beta z - \frac{\sin \phi}{x} \quad (5)$$

with the initial condition

$$x(0) = z(0) = s(0) = \phi(0) = 0 \quad (6)$$

The dimensional coordinates, x , z , and s are defined as

$$x = X/R_o, z = Z/R_o, s = S/R_o \quad (7)$$

and

$$\beta = \frac{(\Delta\rho) \cdot g \cdot R_o^2}{\gamma} \quad (8)$$

For given R_o and β [$(\Delta\rho)g/\gamma$], the complete shape of the curve may be obtained by integrating simultaneously the Eqs. 3 to 5. Equations 3 to 5 with the initial condition 6 can be solved using a fourth-order Runge-Kutta numerical method. The optimal values of R_o and β are determined by minimizing the objective function⁴

$$E = \sum_{i=1}^N \left\{ [X_i - X(z_i, \beta, R_o)] \sin \phi \right\}^2 \quad (9)$$

where X_i , $i = 1, N$ are the X -coordinates of the selected points at the edge of the drop image, and X is the calculated value of the corresponding point (at the same Z -coordinate). At any step in the regression, values of R_o and β are updated from the previous step. Good initial estimates of R_o and β are obtained from the ratio $\sigma = D_s/D_e$ and the following correlations.⁵

$$\beta = 0.12836 - 0.7577\sigma + 1.7713\sigma^2 - 0.5426\sigma^3 \quad (10)$$

$$\frac{D_e}{2R_o} = 0.9987 + 0.1971\beta - 0.0734\beta^2 + 0.34708\beta^3 \quad (11)$$

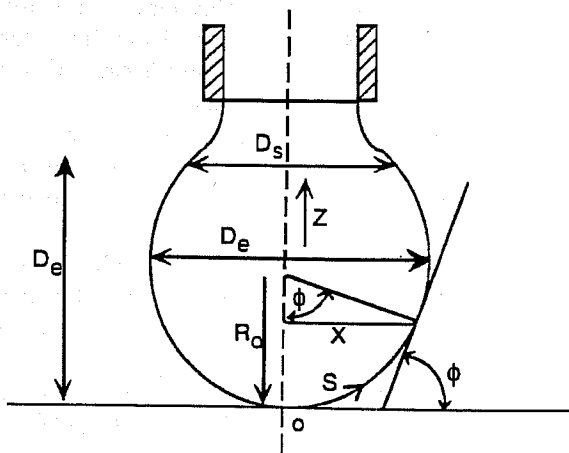


Fig. 2 Geometry of pendant drop with variables.

A regression package to match the captured drop profile with the Young-Laplace equation (Eqs. 3-5) and determine the IFT, γ , has been developed. The equipment as well as the IFT-measuring method is being tested with literature-reported IFT data for hydrocarbon-water systems. Results will be presented in the next report.

References

1. T. H. Chung, *Environment, Safety and Health Review of Project BE4A*, DOE Report NIPER-641, December, 1992.
2. H. Asar and L. L. Handy, Influence of Interfacial Tension on Gas/Oil Relative Permeability in a Gas-Condensate System, *SPE Reserv. Eng.*, 257-264 (February 1988).
3. Y. Rotenberg, L. Boruvka, and A. W. Neumann, Determination of Surface Tension and Contact Angle from the Shapes of Axisymmetric Fluid Interfaces, *J. Colloid Interface Sci.*, 93(1): 169-183 (May 1983).
4. C. Huh and R. L. Reed, A Method for Estimating Interfacial Tensions and Contact Angles from Sessile and Pendant Drop Shapes, *J. Colloid Interface Sci.*, 91(2): 472-484 (1983).
5. F. K. Hansen and G. Rodsrud, Surface Tension by Pendant Drop: 1. A Fast Standard Instrument Using Computer Image Analysis, *J. Colloid Interface Sci.*, 141(1): 1-9 (January 1991).

PROFILE MODIFICATIONS, MOBILITY CONTROL, AND SWEEP IMPROVEMENT IN GAS FLOODING

Cooperative Agreement DE-FC22-83FE60149,
Project BE5B

National Institute for Petroleum
and Energy Research
Bartlesville, Okla.

Contract Date: Oct. 1, 1983
Anticipated Completion: Sept. 30, 1993
Funding for FY 1993: \$375,000

Principal Investigator:
Clarence Raible

Project Manager:
Jerry Casteel
Bartlesville Project Office

Reporting Period: Oct. 1-Dec. 31, 1992

Objectives

The objectives of this project are to (1) conduct phase behavior experiments and evaluate feasibility for alcohol-induced salt precipitation as a method for profile modification, (2) conduct experiments to change permeability of porous media using salt precipitation, and (3) conduct profile modification studies using polymer gels or alcohol-induced salt precipitation as methods to modify flow profiles.

Summary of Technical Progress

Introduction

In FY93, a new method¹ will be studied for plugging high-permeability zones. This method is based on salt precipitation resulting from the injection of concentrated brine and alcohol slugs. Mixing of the alcohol and concentrated brine will cause a reduction in the salt solubility and precipitation of solid salt in the larger pores and more permeable flow channels. The method potentially could result in the selective plugging of the more permeable flow paths and divert subsequent fluid flow to less permeable areas to improve the sweep efficiency of CO₂ floods.

There are several potential advantages for the "salting out" method over other profile modification techniques. The injected fluids of brine and alcohol both have low viscosities. Fluids with low viscosities will reduce viscous crossflow during fluid injection. Polymer solutions used for profile modification typically have relatively high viscosities. Various authors^{2,3} have shown that viscous fluid injection can result in crossflow into less permeable strata where polymer invasion can impede and block subsequent flooding processes such as CO₂ floods. Also, processes that form polymer gels are subject to the same problems of viscous crossflow during injection. In addition, polymer gelation processes often require a suitable pH range to prevent cross-linker precipitation and to initiate cross-linking to form a gel, a condition that is difficult to control in the reservoir. The pH of the reservoir and injected solutions will have little or no effect on the salt precipitation method.

Phase Behavior Studies

For mobility control of gasflooding, a feasibility study using salt precipitation was conducted. Phase equilibrium experiments were performed to determine the quantity of salt precipitation with different alcohols. Screening tests were performed with several candidate alcohols at room temperature.

Ethyl alcohol used in these studies was supplied by Quantum Chemical Corp. According to the manufacturer, the alcohol was 200 proof anhydrous ethanol containing less than 0.5 ppm benzene. The other alcohols (methanol, isopropanol, and *n*-butanol) were reagent grade with a purity greater than 99.9%.

Methanol and ethanol were completely miscible with NaCl-saturated brines. Precipitation experiments were conducted by mixing ethanol and brine saturated with NaCl. Solutions were agitated for over 1 week to allow for complete phase equilibration. The solutions were then filtered through a 5- μ m filter, and the filtrate was evaporated to measure the quantity of dissolved salt. The quantity of salt precipitation was calculated as the difference between the salt in the initial brine and salt remaining in solution. As shown in Table 1, NaCl was virtually insoluble in the pure ethanol. Figure 1 shows the results of salt precipitation at 23.9 °C. The amount of NaCl dissolved per gram of water in the solvent (water and ethanol) was a linear function of the fractional water concentration of the solute. This linear relationship allowed for the calculation

TABLE 1

Solubility of NaCl in Various Alcohols at 23.5 °C

	Weight of NaCl*
Methanol	1.47
Ethanol	0.07
Isopropanol	0.013
<i>n</i> -Butanol	<0.008

*In grams per 100 grams of alcohol.

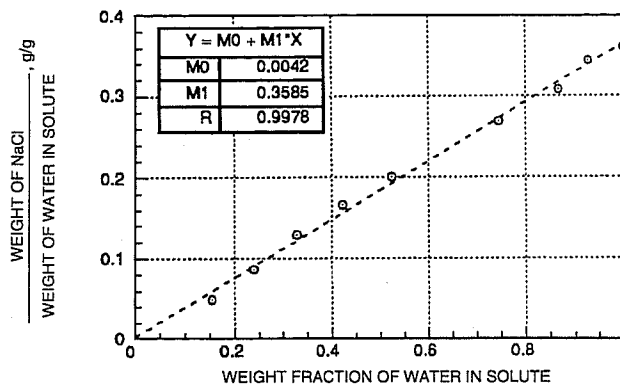


Fig. 1 Weight of NaCl dissolved in water-ethanol solutions after salt precipitation at 23.9 °C.

of the saturated salt concentration for any water-ethanol mixture at this temperature.

Additional experiments were performed for the dissolution of NaCl in various concentrations of water and ethanol containing an excess of salt. One of the objectives of the dissolution experiments was to develop a simplified experimental procedure for other phase studies. After the solutions were allowed to equilibrate, the NaCl concentration was measured by evaporation of the filtered solution. These results at 22.5 °C, shown in Fig. 2, had the same relationship as the salt precipitation experiments.

Other tests were performed at higher temperatures. Results at 49 °C (Fig. 3) show the same linear relationship, although the regression slope was slightly larger because of greater NaCl solubility at higher temperatures.

The regression intercept for these plots became meaningless at zero water concentration. Rather, the intercept was dependent upon the NaCl solubility of the alcohol. Since NaCl was virtually insoluble in ethanol (Table 1), the regression intercept was nearly zero. Therefore the NaCl solubility in ethanol mixtures can be closely approximated as a product of the water concentration by weight and the saturated NaCl solubility in water at a specific temperature.

Additional dissolution tests were performed with methanol. As shown in Table 1, NaCl was more soluble in pure methanol than in ethanol. Therefore the regression intercept for pure methanol, as shown in Fig. 4, was higher than a

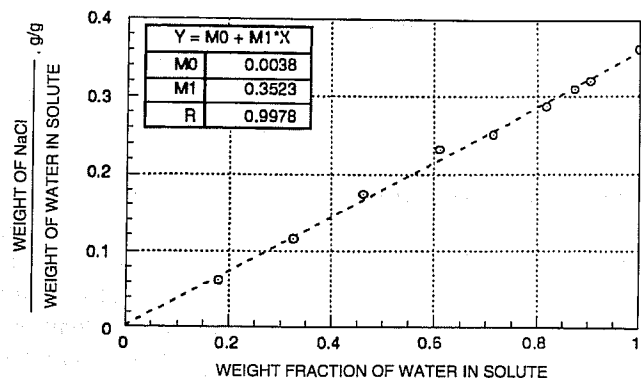


Fig. 2 Weight of NaCl dissolved in water-ethanol solutions by salt dissolution at 22.5 °C.

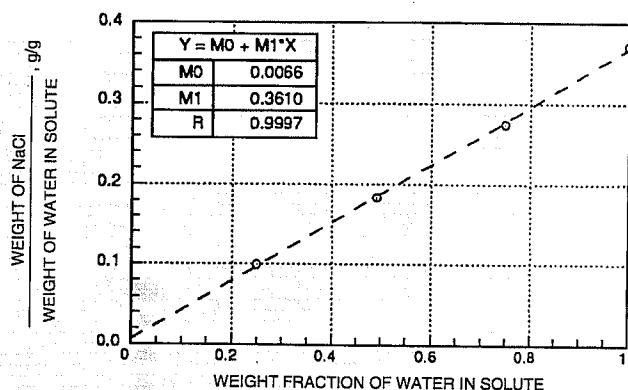


Fig. 3 Weight of NaCl dissolved in water-ethanol solutions by salt dissolution at 49 °C.

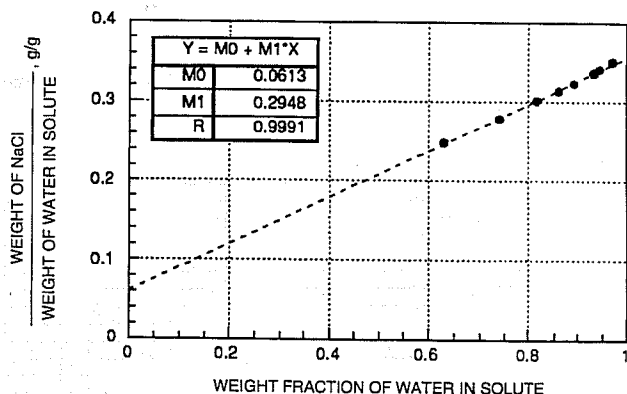


Fig. 4 Weight of NaCl dissolved in water-ethanol solutions by salt dissolution at 23 °C.

corresponding regression intercept for ethanol. Although the salt solubility in methanol was low, methanol would be slightly less effective on a weight basis for initiating NaCl precipitation than ethanol-brine mixtures.

Isopropanol and butanol were miscible with water. However, these alcohols separated into two phases when mixed with brines. Limited miscibility of isopropanol and butanol would limit the alcohol concentration in the brine. This also

would limit the quantity of salt precipitation. On the basis of these phase studies, isopropanol and butanol would be less effective for salt precipitation from brines.

These results indicated that on a weight basis ethanol produced the largest quantity of salt precipitation. Methanol also could be used for salt precipitation, although methanol would produce slightly less precipitation. For field applications of the salt precipitation process, the relative cost of methanol and ethanol would be important in determining which alcohol is the most cost-effective.

References

1. Tao Zhu and Diebbar Tiab, *Improved Sweep Efficiency by Selective Plugging of Highly Watered Out Zones by Alcohol Induced Precipitation*, CIM Paper No. 92-74 presented at the 1992 CIM Annual Technical Meeting, Calgary, June 7-10, 1992.
2. K. S. Sorbie and R. S. Seright, *Gel Placement in Heterogeneous Systems with Crossflow*, SPE/DOE paper 24192 presented at the 1992 SPE/DOE Symposium on Enhanced Oil Recovery, Tulsa, Okla, Apr. 22-24, 1992.
3. C. J. Raible and Tao Zhu, *Application of Polymer Gels for Profile Modification and Sweep Improvement of Gas Flooding*, DOE Report NIPER-632, October 1992.

QUANTIFICATION OF MOBILITY CONTROL IN ENHANCED RECOVERY OF LIGHT OIL BY CARBON DIOXIDE

Morgantown Energy Technology Center
Morgantown, W. Va.

Funding for FY 1993: \$347,000

Principal Investigator:
Duane H. Smith

Principal Manager:
Royal Watts
Morgantown Energy Technology Center

Reporting Period: Oct. 1-Dec. 31, 1992

Objectives

The objectives of this work are to develop the in-depth knowledge needed to improve miscible and near-miscible CO₂ flooding and related processes and to assist industry and others in the commercialization of new technologies based on this knowledge. Primary emphasis is on (1) scaling thermodynamics, (2) models of fluid flow and miscible fingering that also conform to current scaling theory, and (3) experiments and modeling for the development of surfactant-based mobility control on the basis of either leave-behind lamellae or fluid dispersions (two- and three-phase emulsions and foams).

Summary of Technical Progress

Liquid-liquid equilibria (LLE) and vapor-liquid equilibria (VLE) play a central role in enhanced oil recovery. Traditionally, the equilibria are treated by measurement of the compositions of the conjugate phases, followed by the fitting of a "classical" (e.g., cubic) equation of state to the data.

A combination of "new" experimental and theoretical methods are being developed in place of these traditional methods.¹ Experimentally, heats of mixing (excess enthalpies) are measured rather than conjugate phase compositions directly, and the phase compositions are obtained from the excess enthalpy data. Theoretically, critical scaling theory is developed and used to fit the excess enthalpies and these fits are used to obtain the phase compositions. These scaling theory equations also are consistent with the scaling-theory equations of state used for the phase compositions (in place of classical equations of state).

Figure 1 shows a typical set of enthalpy data obtained at 55 °C for the mixing of 2-butoxyethanol (i.e., C₄E₁) and water. The two curved lines and the straight line segment that connects them are fits of the theory to the data. The two compositions at which the straight line meets the curves are the compositions of the two conjugate phases at that temperature. Thus, mathematically, the phase compositions are obtained by (1) fitting a scaling-theory equation to the two single-phase regions (on either side of the conjugate phase compositions), (2) fitting a straight line to the data in the two-phase region (i.e., between the conjugate phase compositions), and (3) finding the points of intersection between the two equations.

By the lever rule, in the two-phase region the excess enthalpies are simply a linear function of the composition. For the measured single-phase excess enthalpies, H_w^E, starting from the hypothesis of Widom¹ and Kadanoff,² that scaling theory predicts

$$\begin{aligned} & \pm [(H_w^E - h_{ow} - h_{lw}w)/(1 + fw - w)]^{1/2} \\ & = (H_2)^{1/2} (OP - OP_{\pm}) \end{aligned} \quad (1)$$

where

- H_w^E = measured enthalpy per unit mass
- h_{ow} = intercept of the two-phase (straight line) fit
- h_{lw} = slope of the two-phase (straight line) fit
- w = weight fraction of one of the components
- f, OP_±, and H₂ = four fitting parameters in the nonlinear regression

Although it is convenient to write Eq. 1 in a way that explicitly contains the weight fraction, it is still an open question what composition units are most appropriate for scaling theory. In place of "ordinary" concentration units, such as w, it is preferable to use a fractional concentration (or,

in traditional scaling-theory terminology, "order parameter," OP) of the form

$$OP = fw/(1 + fw - w) \quad (2)$$

where f is a system-dependent parameter, whose value is found in the nonlinear regression of Eq. 1 to the data. (The value of f should be only very weakly dependent on temperature. For the butoxyethanol/water system f = 3.2 over the temperature range studied, namely, from the critical temperature to about 20 °C higher.) Hence, the OP_± data pairs are the values of OP in the pairs of conjugate phases.

Figure 2 illustrates a plot of the data of Fig. 1 in a form suggested by Eq. 1 and illustrates the ability of Eq. 1 to fit the

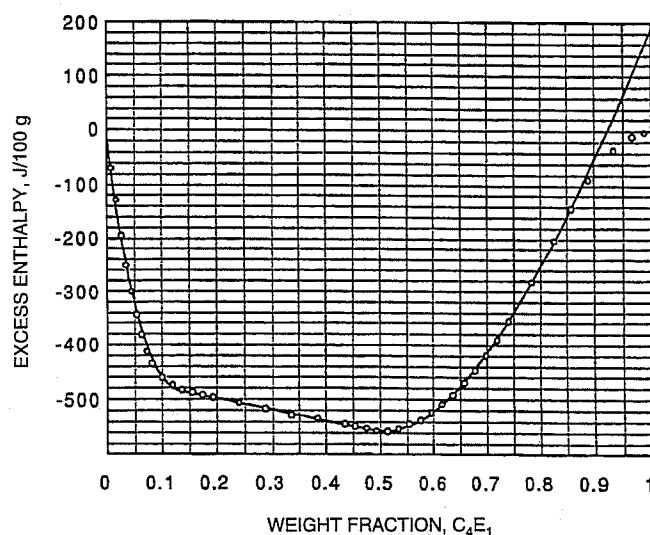


Fig. 1 Excess enthalpies measured at 55 °C for 2-butoxyethanol and water and fit of scaling-theory to the data.

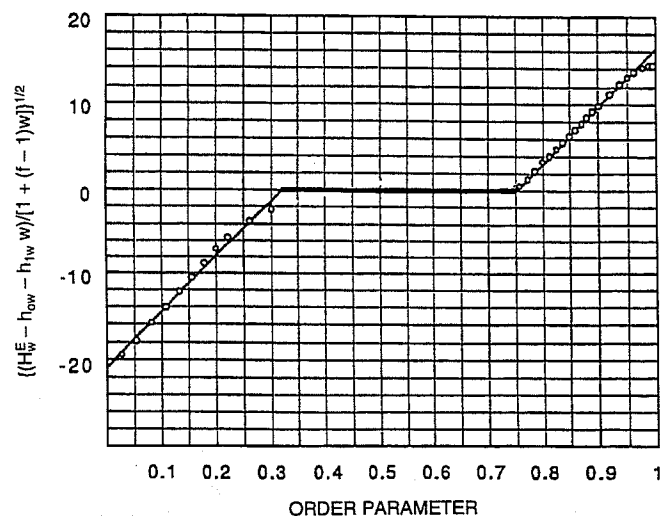


Fig. 2 Experimental data of Fig. 1, illustrating the nonlinear regression of Eq. 1 to the data, the symmetry properties of Eq. 1 and determination of the conjugate phase compositions from the enthalpy data.

data. As predicted by the theory, when plotted in the form suggested by Eq. 1 the single-phase enthalpies on either side of the two-phase region each fall on a straight line and the slopes of the two lines are equal.

In Fig. 2 the phase compositions are the respective x-axis intercepts of the two straight lines. Values of the conjugate phase compositions obtained by the new method described

here compared with phase compositions found by more conventional methods showed excellent agreement between the different methods.

References

1. B. Widom, *J. Chem. Phys.*, 43: 2898 (1965).
2. L. P. Kadanoff, *Physics*, 2: 263 (1966).



1000
900
800
700
600
500
400
300
200
100
0
-100
-200
-300
-400
-500
-600
-700
-800
-900
-1000

THERMAL RECOVERY— SUPPORTING RESEARCH

**MODIFICATION OF RESERVOIR
CHEMICAL AND PHYSICAL FACTORS
IN STEAMFLOODS TO INCREASE
HEAVY OIL RECOVERY**

Contract No. DE-FG22-90BC14600

**University of Southern California
Los Angeles, Calif.**

**Contract Date: Feb. 22, 1990
Anticipated Completion: Feb. 21, 1993
Government Award: \$150,000**

**Principal Investigator:
Yanis C. Yortsos**

**Project Manager:
Thomas Reid
Bartlesville Project Office**

Reporting Period: Oct. 1–Dec. 31, 1992

Objectives

Thermal methods, and particularly steam injection, are currently recognized as the most promising for the efficient recovery of heavy oil. Despite significant progress, however,

important technical issues remain open. Still lacking is the knowledge of the complex interaction between porous media and the various fluids of thermal recovery (steam, water, heavy oil, gases, and chemicals). The interplay of heat transfer and fluid flow with pore- and macro-scale heterogeneity is largely unexplored.

The objectives of this contract are to continue previous work and to carry out new fundamental studies in the following areas of interest to thermal recovery: displacement and flow properties of fluids involving phase change (condensation–evaporation) in porous media, flow properties of mobility control fluids (such as foam), and the effect of reservoir heterogeneity on thermal recovery. The specific projects are motivated by and address the need to improve heavy oil recovery from typical reservoirs as well as from less conventional fractured reservoirs producing from vertical or horizontal wells.

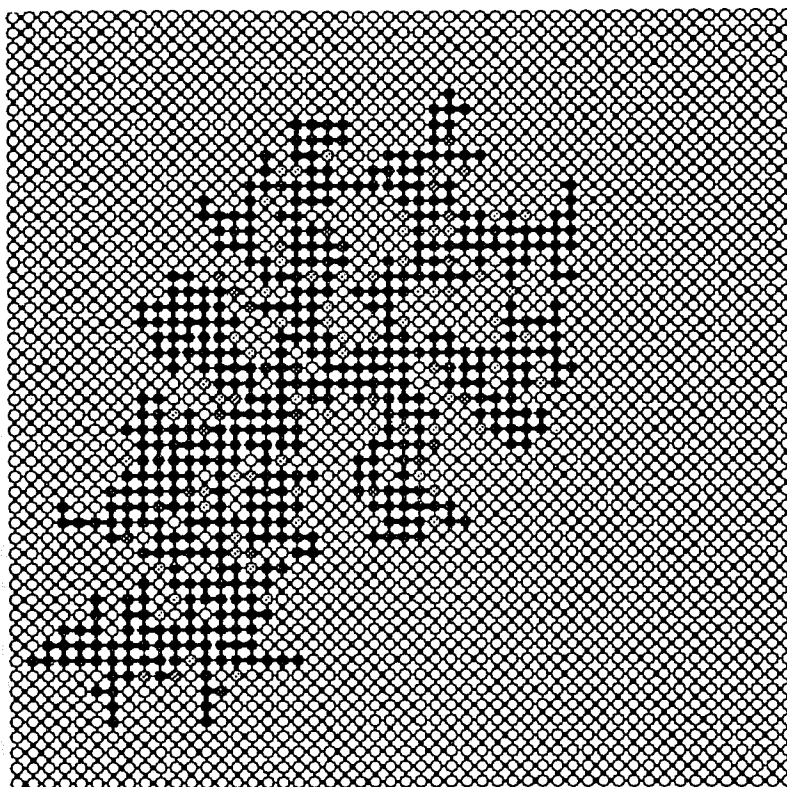
Summary of Technical Progress

Vapor–Liquid Flow

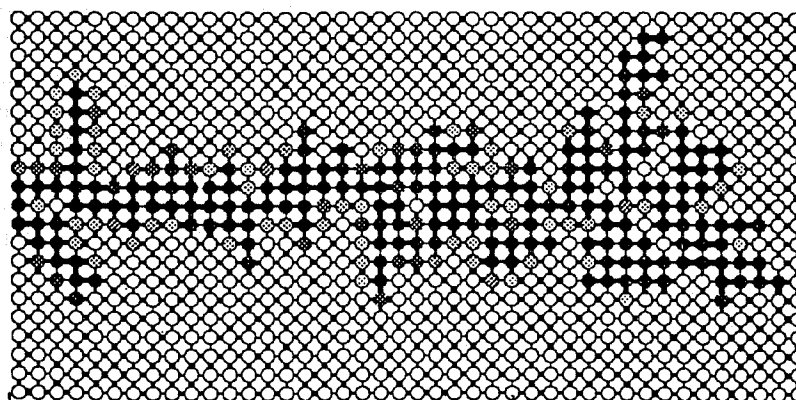
Work continued during this quarter in three areas related to vapor–liquid flow in porous media: experiments in Hele–Shaw cells, glass bead-packed cells and glass micromodels, pore network simulation, and a macroscopic analysis of such flows. Experiments involved steam displacement of various model oils to examine the physical mechanisms involved,

particularly spreading during film flow, and should be particularly pertinent to steam displacement in naturally fractured systems. The latter are modeled by appropriate glass micromodels designed to probe the interaction between matrix and fractures. This work, still in progress, complements the recent study of Hele-Shaw cells.¹ Displacement experiments involving only a single species were also conducted to study the mechanisms of steam condensation in the absence of oil. Various effects have been identified and are summarized in a forthcoming Annual Report.²

Theoretical work included further studies of the steam zone growth driven by a specified heat flux or a specified superheat in a pore network. Typical examples of the patterns obtained are shown in Fig. 1 for these two cases. In conjunction with the pore network simulation, a theory was developed that delineates the regimes obtained in terms of the size of the "bubble," the degree of superheat, and the effective capillary number. This approach parallels that of Lenormand³ and leads to conditions under which percolation regimes exist. The findings are summarized by Satik and Yortsos.⁴ When the



(a)



(b)

Fig. 1 Numerical simulation of steam bubble growth in a pore network from (a) applied superheat at boundaries and (b) applied heat flux on the left side.

percolation boundary is exceeded, the growth pattern is affected by additional factors and can be fingered. A stability analysis of radial growth in an effective pores medium was conducted to examine this behavior. It was found that in the absence of capillarity such processes are unstable, despite the effect of heat conduction. These results are to be contrasted with the results under steam injection where heat conduction and heat losses, in general, stabilize the growth pattern.⁵ Pore network simulation of steam injection also continued. Work is under way to solve some computational problems that arise as a result of phase change.

Heterogeneity

In the area of heterogeneity the research involves fractured systems and effects of heterogeneity on displacement processes. In the area of fractured systems a study of mechanism of drainage was completed that includes visualization experiments and pore network simulation.⁶ Drainage of a matrix block-fracture element can be represented as an invasion process, where both viscous and capillary forces compete, where a curve equivalent to a capillary pressure curve for homogeneous systems can be constructed, except that it is the capillary number rather than the capillary pressure that is related to saturation (Fig. 2) and that this curve also depends on the viscosity ratio M . Steady-state relative permeabilities for drainage in a fractured system were constructed based on the analogy with homogeneous systems.⁶ Similar work is about to be completed for the case of imbibition. In parallel, an investigation was completed on the use of fractal geometry for the representation of fractured systems and the use of pressure transients for its identification.⁷

Complementing previous works on capillary heterogeneity,^{8,9} a comprehensive study was completed that involved theory, experiments, and pore network simulations for drainage in media of variable heterogeneity.¹⁰ The pore network simulations, in particular, lend validity to many of the predictions of the continuum theory in processes involving heterogeneous media. The analogous study of imbibition is currently in progress. These works are done in collaboration with researchers at the Université Pierre et Marie Curie. Finally, progress was made with the development of a theory based on Vertical Flow Equilibrium (VFE) for steam injection processes. The VFE predictions for miscible displacement were simulated numerically and were found to be in excellent agreement with expectations (Fig. 3). This work continues with the use of correlated permeability fields.

Chemical Additives

Work continued in the area of non-Newtonian flow in porous media. A technical report was prepared describing aspects of displacement involving power-law fluids and Bingham plastics.¹¹ Experiments using glass micromodels and Hele-Shaw cells are under way. In parallel, investigation continued using pore networks to model foam formation and mobilization. A particular objective of this study is to test recent theories on critical pressure gradient for the onset of foam flow. Numerical results do not fully support the previous theories, either qualitatively or quantitatively. The disagreement is the result of differences in pore network structure (Bethe lattice vs. regular network) and also differences in the mechanisms used to represent the onset of mobilization. This work continues.

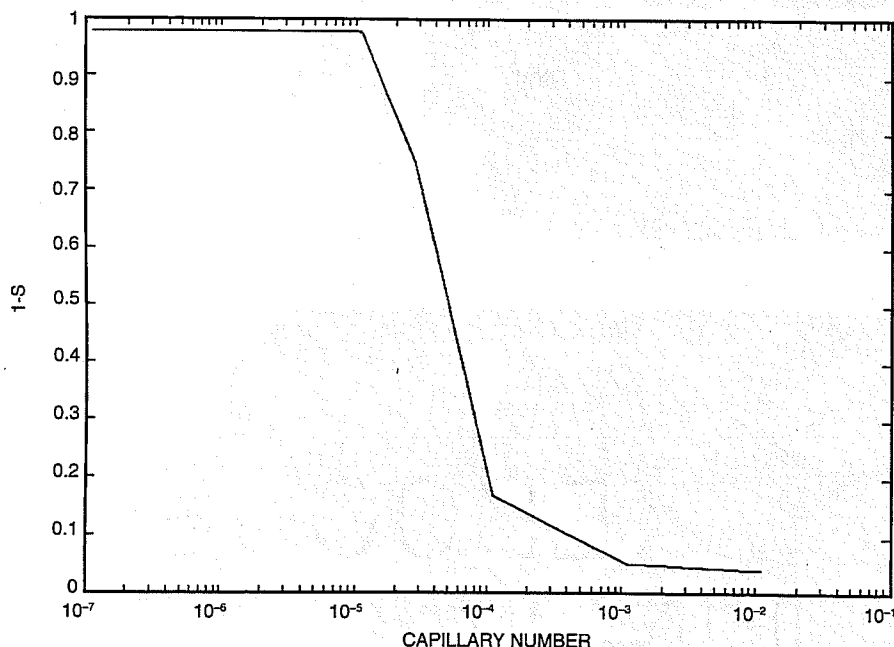


Fig. 2 Numerical simulation of wetting saturation vs. capillary number at steady state during drainage in a fractured system.

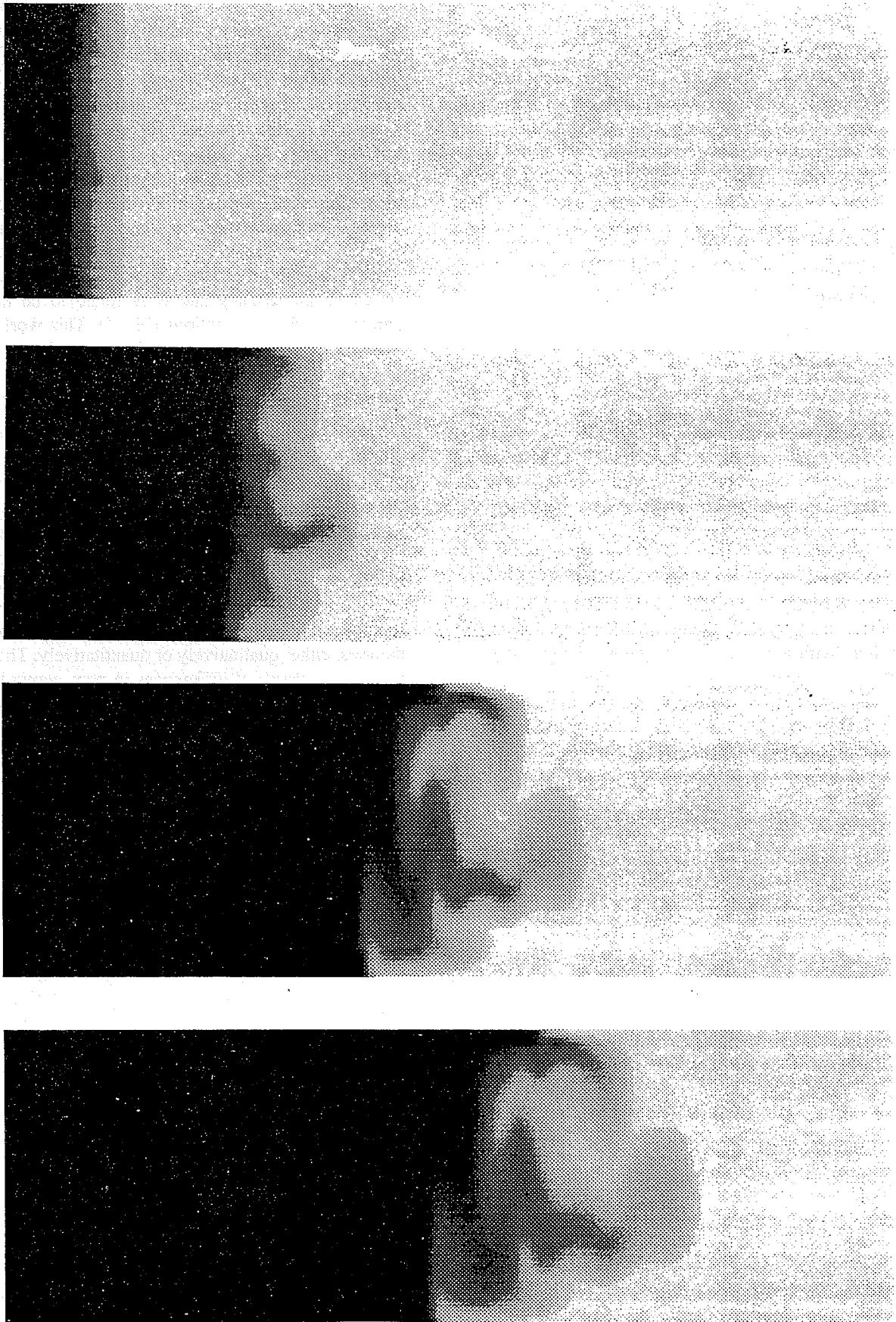


Fig. 3 Simulation of viscous fingering at conditions of Vertical Flow Equilibrium.

References

1. X. Kong, M. Haghghi, and Y. C. Yortsos, *Visualization of Steam Displacement of Heavy Oils in a Hele-Shaw Cell Fuel*, 71: 1465-1471 (1992).
2. Y. C. Yortsos, *DOE Annual Report*, in preparation, 1993.
3. R. Lenormand, Flow Through Porous Media: Limits of Fractal Patterns, *Proc. R. Soc. (London) Ser. A*, 423: 159-168 (1989).
4. C. Satik and Y. C. Yortsos, in preparation (1993).
5. Y. C. Yortsos, Effects of Lateral Heat Losses on the Stability of Thermal Displacement Fronts in Porous Media, *A.I.Ch.E. J.*, 28: 480-486 (1982).
6. M. Haghghi, B. Xu, and Y. C. Yortsos, *Visualization and Simulation of Immiscible Displacement in Fractured Systems Using Micromodels: I. Drainage*, submitted, 1993.
7. J. Acuna and Y. C. Yortsos, *Application of Fractal Geometry to the Study of Networks of Fractures and Their Pressure Transient*, submitted, 1993.
8. M. Chauuche, N. Rakatomalala, D. Salin, and Y. C. Yortsos, Capillary Effects in Immiscible Flows in Heterogeneous Porous Media, *Europhy. Lett.*, 21: 19-24 (1993).
9. M. Chauuche, N. Rakatomalala, D. Salin, B. Xu, and Y. C. Yortsos, Invasion Percolation in Hydrostatic or Permeability Gradient: Experiments and Simulations, *Phys. Rev. Lett.*, submitted (1992).
10. C. Shah and Y. C. Yortsos, *Aspects of Non-Newtonian Flow and Displacement in Porous Media*, DOE Topical Report, in press, 1993.
11. C. Shah and Y. C. Yortsos, *Aspects of Non-Newtonian Flow and Displacement in Porous Media*, DOE Topical Report, DOE/BC/14600-41, February 1993.

OIL FIELD CHARACTERIZATION AND PROCESS MONITORING USING ELECTROMAGNETIC METHODS

**Lawrence Livermore National Laboratory
Livermore, Calif.**

**Contract Date: Oct. 1, 1984
Anticipated Completion: Oct. 1, 1993
Government Award: \$350,000**

**Principal Investigator:
Mike Wilt**

**Project Manager:
Thomas Reid
Bartlesville Project Office**

Reporting Period: Oct. 1-Dec. 31, 1992

Objective

The objective of this project is to apply surface and borehole electromagnetic (EM) methods for oil field characterization and monitoring of in situ changes in the electrical conductivity during enhanced oil recovery (EOR) operations. The goal of this project is to develop practical tools for geophysical characterization of oil strata and monitoring of EOR processes in a developed field. Crosshole and surface-to-borehole EM are being applied to map discontinuous oil sands and to provide an image of electrical conductivity changes associated with EOR operations.

Summary of Technical Progress

In the final quarter of 1992 work began on a three-year program in reservoir characterization. This program applies EM methods to the problem of tracing oil-bearing strata and controlling structure in a developed field. It involves constructing hardware, developing software for interpretation, and doing field surveys in developed oil fields. Field hardware and companion software are being developed for this program jointly with Schlumberger-Doll Research (SDR). This is to share developmental costs and to ensure the commercial use of technology developed at Lawrence Livermore National Laboratory (LLNL). A three-year cooperative research and development agreement (CRADA) to support this activity was recently signed by LLNL and SDR.

The initial LLNL segment of the CRADA involves the development of a single-frequency prototype transmitter; the progress on the design and construction of this tool is described later in this report. In addition, some new field acquisition methods that use the surface-to-borehole configuration (STB) for underground imaging are being developed. These methods are well suited in areas where boreholes are widely spaced and the depth to the targets of interest is 1 km or less.

The new STB technology and the newly developed borehole transmitter will be initially applied in a field test at the Lost Hills No. 3 site. The goal for this field test is to map the controlling structure and bed continuity in the shallower strata of the oil field. The field survey will also serve as a new baseline data set for upcoming EOR activities in this producing field.

Cooperative Research Agreement with Schlumberger-Doll Research

A multifrequency multicomponent crosshole EM system for application to oil field characterization and process monitoring is being developed. The new system will offer improved data quality over the existing crosshole system and with companion software will provide dramatically improved subsurface imaging capabilities.

The system is being developed under a three-year CRADA signed by both LLNL and SDR in December 1992. This agreement calls for the joint development of the above crosshole EM system: LLNL will develop the multifrequency transmitter and SDR will develop the multicomponent receiver. The two systems will be linked either by synchronous pulses or clocks. The agreement also features the joint development of companion software and two field trials during the three-year project.

Construction of a New Borehole Transmitter

The initial step in LLNL's portion of the cooperative research plan is to develop a single-frequency d-c activated transmitter. This transmitter is preferred over the existing source because only direct current is supplied and the coil

self-resonates at a frequency controlled by the inductance of the coil and the series capacitance (Fig. 1). With the present tool a high-level a-c signal is sent down the wireline cable to be transmitted by the borehole tool; this invariably results in some signal leakage through the surface to the receiver station, thereby contaminating the measurements. The new tool lessens any chance of signal leakage and also makes it possible to develop an automatic switching system using computer-controlled relays to control the transmission frequency; it is designed to work at frequencies from 5 to 160 kHz.

During this quarter the ferrite core was wound, capacitor boards were built, and the circuit boards that control the self-resonating transmitter were tested. The new coil will have a maximum source moment of more than 700, which is five times more powerful than the present source. The new tool should also be considerably less noisy than the present transmitter. During the next quarter this tool will be packaged in a leak-proof fiberglass tube and tested locally before an initial field trial at the Lost Hills oil field.

The development of a multifrequency transmitter, as directed by the CRADA, is simply an extension of the new single-frequency tool. The multifrequency tool will have an array of capacitors and several separate windings on its core. To change the frequencies all that will be required is to switch

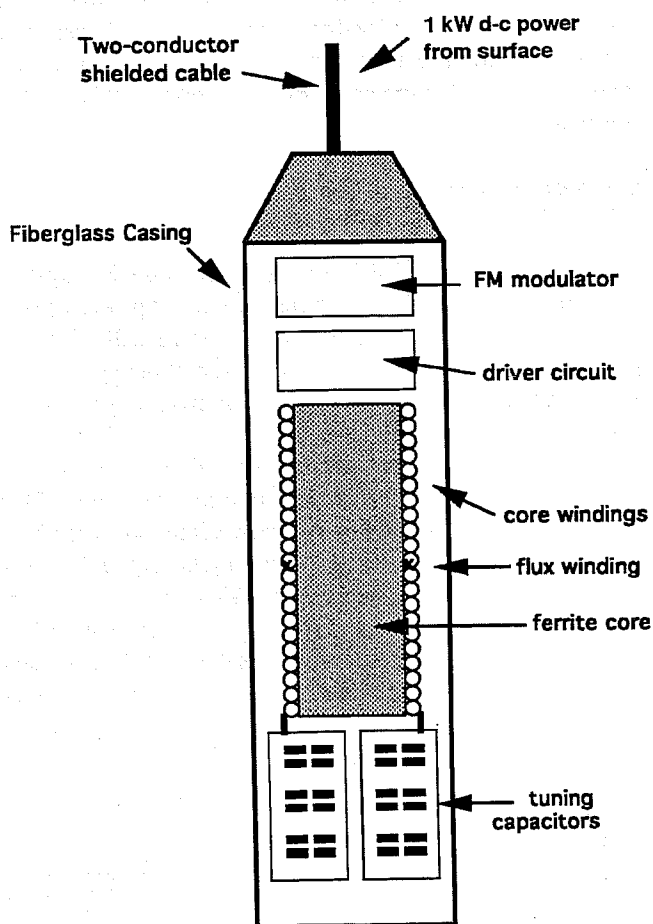


Fig. 1 Schematic diagram of the new-generation borehole transmitter.

between coil windings and capacitance values and the tool will self-resonate at a new frequency governed by this combination. The switching will be done with computer-controlled high-voltage relays located within the tool housing.

Surface-to-Borehole System Development

In fields where wells are spaced too far apart for the crosshole technique, the borehole access will still be used by applying the surface-to-borehole configuration. With this method the transmitter is situated at various surface locations along a profile and the receiver is placed at various depths within the borehole. The method is designed to extend the borehole induction log outward from the borehole into the formation along a particular profile. This technique has been used sparingly in the past because no software was available to interpret the data and because it is a lower resolution method than crosshole EM. A further advantage of this method is that it may be used in steel-cased boreholes.^{1,2}

As part of the three-year reservoir characterization plan, the data collection scheme is currently being updated to include multifrequency data. The large single-turn transmitter loop is being replaced with a smaller multi-turn loop for easier portability. Imaging codes for the STB configuration are also being developed. The new programs are an adaptation of "Born" approximation codes presently used for crosshole EM data.

Field Survey at Lost Hills No. 3

A field survey is being scheduled for reservoir characterization and steamflood monitoring at the Lost Hills No. 3 site in the coming months. The site was selected for its availability, access to fiberglass-cased boreholes, and suitability of geological targets. A new steamflood is scheduled to begin at Lost Hills in the spring of 1993 and the data will be used as a set of baseline measurements.

Figure 2 shows two electrical induction logs at the Lost Hills site from wells separated by 55 m. Outwardly the logs are quite similar, both showing the oil sands as high-resistivity horizons and the confining clays as low-resistivity units. A closer inspection, however, reveals that the upper sand dips about 15° from west to east and one of the deeper oil sands (4) is present in the western well but not in the eastern well.³

The objective of the upcoming survey is to trace the upper and lower resistive bodies between the boreholes. The STB method will be applied in the eastern well along a profile that connects the eastern and western wells. The crosshole technique will also be applied in these wells using higher frequencies than were previously applied, which should allow for improved definition.

This latest field survey at Lost Hills will also serve as a second set of baseline data for EOR monitoring. Earlier steam injection efforts by the operator (Mobil) in 1991 were not successful because of completion problems in the wells and sufficient time has passed so that the original baseline data set

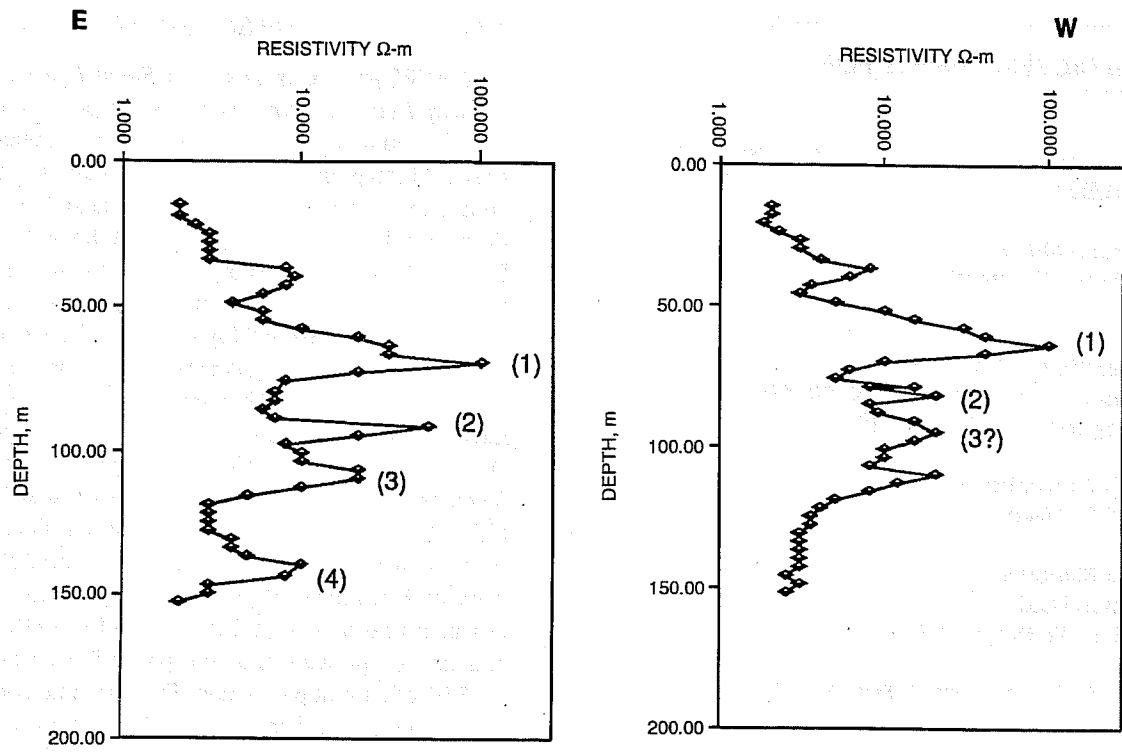


Fig. 2 Electrical induction logs from wells DRL-35N and DRL-35S at Lost Hills No. 3. Numbers in parentheses denote oil sands.

(August 1991) is unsuitable for monitoring. The operator is presently resuming well stimulation activities in this field and should be injecting steam in the spring of 1993.

References

1. M. Wilt and R. P. Ranganayaki, Surface-to-Borehole Electromagnetic Logging for Enhanced Oil Recovery Applications, Submitted to

the Society of Geophysicists Annual Meeting, San Francisco, Calif., 1990.

2. T. Uchida, K. H. Lee, and M. Wilt, Effect of Steel Casing on Crosshole EM Measurement, paper presented at the Society of Exploration Geophysicists Annual Meeting, Houston, Tex., 1991.

3. M. Wilt, Quarterly Progress Report for Project FEW6038, in *Activities of the Oil Implementation Task Force*, DOE Report DOE/BC-92/2, 1992.

THERMAL PROCESSES FOR LIGHT OIL RECOVERY

**Cooperative Agreement DE-FC22-83FE60149,
Project BE11A**

**National Institute for Petroleum
and Energy Research
Bartlesville, Okla.**

**Contract Date: Oct. 1, 1983
Anticipated Completion: Sept. 30, 1993
Funding for FY 1993: \$300,000**

**Principal Investigator:
David K. Olsen**

**Project Manager:
Thomas Reid
Bartlesville Project Office**

Reporting Period: Oct. 1–Dec. 31, 1992

Objectives

The FY93 objectives of this project are to (1) analyze planned tasks in this project to ensure they meet environment, safety and health (ES&H) requirements; (2) assess the thermal research performed at the National Institute for Petroleum and Energy Research (NIPER) over the past 10 years; (3) develop procedure and apparatus for measuring dynamic saturation changes in steamfloods at field conditions using X-ray and computerized tomography (CT) scanning that incorporate temperature and pressure measurements to calibrate a numerical simulator for predictive purposes; (4) conduct laboratory research in support of Naval Petroleum Reserve No. 3 (NPR-3), Teapot Dome (Wyoming) field light oil steamflood; and (5) participate in the Annex IV meetings conducted by the Department of Energy (DOE) and the Venezuelan Ministry of Energy and Mines.

Summary of Technical Progress

The ES&H requirements for this project were reviewed, and recommendations were made.¹ The task involving laboratory experiments posed a significant problem. Plans for relocation of the steamflood laboratory have been approved by the ES&H Manager; however, location and laboratory specifications have not been approved. The light oil steamflood operations at the NPR-3, Teapot Dome (Wyoming) field, were reviewed, and a paper was written.² An Annex IV meeting was held at DOE headquarters in Washington, D.C., on Oct. 1–2, 1993, to review research on thermal methods of oil recovery with DOE and the Venezuelan Ministry of Energy and Mines representative from INTEVEP.

NPR No. 3 Light Oil Steamflood

The SPE paper *Case History of Steam Injection Operations at Naval Petroleum Reserve No. 3, Teapot Dome Field, Wyoming*² documents the use of steam to produce a 32 °API gravity (0.86 g/cm³) light oil from a shallow, very heterogeneous, low-permeability reservoir that defies conventional thermal enhanced oil recovery (TEOR) screening criteria. Field geology, project history, pattern design, spacing, completions, operational problems, performance, and economics are detailed in the paper and highlights are included here.

The overall objective of the Shannon steamflood is to extend the economic life of NPR-3, thus allowing for future development of other producing formations. NPR-3, Teapot Dome field (Wyoming), is a federally owned oil field, located about 35 miles north of Casper, Wyoming. More than 24 million bbl (3.8 × 10⁶ m³) of oil has been produced since initiation of production in 1922; more than 15 million bbl (2.5 × 10⁶ m³) has been produced since full production began in 1976 (Ref. 3). The Shannon sandstone is the shallowest, 300 to 500 ft (90 to 150 m), and the most productive of nine producing zones and accounts for 55% of current production. The Shannon, composed of the Upper and Lower Shannon sandstones, was deposited as an offshore bar where bar margin, interbar, and bioturbated shelf sandstones are the reservoir.⁴ The reservoir is faulted and extensively fractured, with the two sandstone intervals separated by shaley nonproductive siltstone. Maximum gross sand thickness is 100 ft (30 m) with an average porosity of 18% and 63 mD air permeability.

Since only 5% of the Shannon's 144 million bbl (2.3 × 40⁷ m³) of original oil in place (OOIP) was estimated to be recoverable by primary means, a study of recovery technologies was conducted in 1980 resulting in implementation of a polymer-improved waterflood pilot and an in situ combustion pilot in 1981. Steam drive did not pass this initial screening because of estimated poor economics.⁵ Pilot projects were implemented to test in situ combustion and polymer-improved waterflooding in early 1982. The polymer flood experienced rapid channeling through the fracture network, and the pilot test was terminated. Injection of steam was used to preheat the formation before the start of an oxygen-enriched in situ combustion pilot. Although the pilot experienced ignition problems, steam injection produced significant oil. The in situ combustion pilot was a technical and marginally economic success and was terminated in 1986 because of low oil prices. Favorable response from steam in the in situ combustion pilot led to the implementation of a steam drive pilot in October 1985. The steamflood pilot results were encouraging enough to initiate other patterns and continued expansion. Currently 150 acres (60 ha) are being flooded using five 50-MMBtu/h steam generators. During FY92, the total oil production from the field was 2345 BOPD (373 m³/d). Steamflood oil production was 934 BOPD (148 m³/d) or 39.8% of total oil production, and primary production from the Shannon was 417 BOPD (66 m³/d) or 17.8% of total oil production.

A staged, 21-yr, commercial-scale development program has been designed that will use five 50-MMBtu/h gas-fired steam generators and one centrally located water treatment facility. Full implementation of the plan will require 330 new producing wells and 252 new injection wells (126 pairs). Current plans call for implementation of line drive steamfloods with 30 acres (12 ha) per generator, 6 acres (2.4 ha) per pair of injectors, with 150 acres (60 ha) being flooded at a time. Additional infill drilling, as required, will be implemented to achieve oil capture. Steam injection into a pattern is anticipated for 3 yr followed by a 7-yr waterflood. A water-alternating-steam process (WASP)⁶ is being tested as part of a tailout. The program is anticipated to recover 12.6 million bbl ($1.5 \times 10^6 \text{ m}^3$) of incremental oil.

The lack of a thermal simulator that permits incorporation of the complex reservoir geology led to design of the steamflood using a "pragmatic" approach. In other words, engineering effort focused on learning as much as possible from the pilot project and integrating actual pattern performance, field geology, and reservoir engineering. Emphasis has been on obtaining an understanding of the geologic influences (faults, fractures, and facies), pattern configuration (9-spot, 5-spot, and line drive), steam movement (areal and vertical; heat transfer and losses), production response, and trends as they relate to the distinct facies in the Upper and Lower Shannon.

Major mechanisms of oil recovery in this light oil steamflood are believed to be repressurization, steam distillation, thermal expansion of the oil, imbibition, oil viscosity reduction and alteration in oil/water relative permeability, and dry heat distillation.^{2,7}

The most important lesson learned from this project is that published screening guides should not be used as the criteria for selection of a reservoir for steamflood. The Shannon light oil steamflood does not meet published screening criteria but has produced over a million barrels of oil from the 150 acres (60 ha) currently being steamed. The steamflood recovers light oil from a tight, highly faulted and fractured, heterogeneous reservoir. Although the operation is economically marginal, the success of the steamflood is the result of the combination of multiple disciplines working together to de-

sign an oil recovery system that accommodates the reservoir characteristics. Modifications to patterns and operation have been undertaken to incorporate what has been learned from the response of previous patterns.

Heat management (steam rate and tailout), injector and producer well design, completion practices, and mode of operation are constantly being reviewed because they directly impact profitability. Because of the higher oil price for the light oil, the acceptable economic oil/steam ratio in light oil reservoirs can be much lower than that in heavy oil reservoirs. Because there are numerous tight, shallow, pressure-depleted, light oil reservoirs in the United States that are similar to the Shannon, lessons learned from this steamflood may help in evaluating the potential of thermal (steam) recovery in other reservoirs.

References

1. D. K. Olsen and P. S. Sarathi, *Environmental, Safety, and Health Assessment of FY93 Tasks in Project BE11A, Thermal Processes for Light Oil Recovery*, DOE Report NIPER-652, November 1992.
2. D. K. Olsen, P. S. Sarathi, M. L. Hendricks, R. K. Schulte, and L. A. Giangiacomo, *Case History of Steam Injection Operations at Naval Petroleum Reserve No. 3, Teapot Dome Field, Wyoming: A Shallow Heterogeneous Light Oil Reservoir*, paper SPE 25786 presented at the SPE 1993 International Thermal Operations Symposium, Feb. 8-10, 1993, Bakersfield, Calif.
3. Department of Energy, Naval Petroleum and Oil Shale Reserves, *Annual Report of Operations Fiscal Year 1991*, DOE Report DOE/FE-0254P.
4. R. S. Martinsen and R. W. Tilliman, *The Shannon Shelf-Ridge Complex, Salt Creek Anticline Area, Powder River Basin, Wyoming*, SEPM Special Publication No. 34, Tulsa, Okla., pp. 85-142, May 1984.
5. H. H. Chappelle, G. P. Emsurak, Jr., and S. L. Obernyer, *Screening and Evaluation of Enhanced Oil Recovery at Teapot Dome in the Shannon Sandstone: A Shallow, Heterogeneous Light-Oil Reservoir*, paper SPE/DOE 14918 presented at the 1986 SPE/DOE Fifth Symposium on Enhanced Oil Recovery, Tulsa, Okla., April 20-23, 1986.
6. K. C. Hong and C. E. Stevens, *Water-Alternating-Steam Process Improves Project Economics at West Coalinga Field*, presented at International Technical Meeting of Petroleum Society of CIM and the Society of Petroleum Engineers, Calgary, Canada, June 10-13, 1990, CIM/SPE 90-84.
7. P. S. Sarathi and D. K. Olsen, *Practical Aspects of Steam Injection Processes—A Handbook for Independent Operators*, DOE Report NIPER-580, October 1992.

THERMAL PROCESSES FOR HEAVY OIL RECOVERY

**Cooperative Agreement DE-FC22-83FE60149,
Project BE11B**

**National Institute for Petroleum
and Energy Research
Bartlesville, Okla.**

**Contract Date: Oct. 1, 1983
Anticipated Completion: Sept. 30, 1993
Funding for FY 1993: \$200,000**

**Principal Investigator:
Partha Sarathi**

**Project Manager:
Thomas Reid
Bartlesville Project Office**

Reporting Period: Oct. 1–Dec. 31, 1992

Objectives

The FY93 objectives are to (1) analyze the National Institute for Petroleum and Energy Research (NIPER) heavy oil database to screen Texas Gulf Coast reservoirs for priority ranking, (2) collect reservoir data for the most promising reservoirs, and (3) conduct simulation studies to determine the applicability of thermal enhanced oil recovery (EOR) techniques in the most promising heavy oil reservoirs in the Texas Gulf Coast area.

Summary of Technical Progress

Environment, Safety and Health Assessment

The objective of this task was to analyze planned tasks for FY93 to determine whether the proposed research activities pose any safety and health risks to researchers. A status report detailing the Environment, Safety and Health (ES&H) assessment was written and delivered to the Bartlesville Project Office (BPO).¹

Assessment of the Past NIPER Thermal EOR Research Program

The objective of this task was to review objectively the thermal EOR research performed at NIPER over the past 9 yr and recommend future direction for the program. This task was jointly undertaken with researchers of BE11A (thermal processes for light oil recovery), and a report detailing the assessment is currently being written.

Evaluation of Steamflood Potential in Texas Gulf Coast Heavy Oil Reservoirs

On the basis of the information available in the NIPER heavy oil database, a total of 73 heavy oil reservoirs, contain-

ing more than 1.2×10^9 bbl (0.2×10^9 m³), were found to exist in Districts 1 through 4 in the Texas Gulf Coast area. Data on density and viscosity of oil, depth, thickness, porosity, permeability, and cumulative oil production (until 1990) were available, but data on oil saturation were not available. A value of 65% was arbitrarily assumed to be the initial oil saturation for all the reservoirs. From the basic data of thickness (h), permeability (k), porosity (ϕ), oil saturation (S_o) and viscosity of oil (μ) ϕS_o , kh/ μ , oil recovery (until 1990) and oil in place (OIP) were calculated. The cumulative oil steam ratios (COSR) were calculated following an equation by Butler.² A value of 0.2 or more for COSR, the most commonly used criterion, is considered to be good.³

Screening guides proposed by several authors (Chu, Geffen, Ali, Lewin, and Iyoho) are given elsewhere (Table 4.1 in Butler, 1991).² Chu's guide³ with some modifications has been used in this work. Reservoirs were first sorted in descending order according to thicknesses and then screened for minimum thickness of 10 ft (3 m), maximum depth of 4000 ft (1200 m) according to Geffen's guide, minimum depth of 300 ft (91 m), minimum oil saturation of 0.40, minimum porosity of 0.20, minimum ϕS_o of 0.08, and minimum permeability of 100 mD (99×10^{-3} μ m²). The criterion of minimum depth was relaxed from 400 ft (122 m) to avoid elimination of a big field with a depth of 350 ft (107 m). In Chu's guide there are no criteria for maximum depth and minimum permeability. Although a minimum permeability of 1000 mD (987×10^{-3} μ m²) is suggested in Ali's guide, it was relaxed in view of the potential for application of horizontal wells.

Out of a total of 73 reservoirs, 16 reservoirs meet all the screening criteria mentioned previously (Table 1). However, 7 of these reservoirs have moderate oil viscosities (at reservoir temperature) in the range from 41 to 73 cP (41 to 73 PaS). Oil recoveries in these reservoirs by primary and secondary means are likely to exceed 25% making these reservoirs less economically attractive for steam injection processes because of low oil saturation. The remaining 9 reservoirs have a total OIP of 346 MMbbl (55×10^6 m³). These 9 reservoirs can be organized into two groups. Group 1 contains 5 reservoirs—Colemena, Comitas, Cedro Hill, Government Wells North, and Lundell—which are in the secondary stage of oil production. These reservoirs are currently being waterflooded. Oil recovery from waterflood in heavy oil fields is limited. These fields are most likely to be matured in the near future, and the feasibility of thermal EOR techniques should be considered. Group 2 contains 4 reservoirs—Los Olmos, Foss, Taylor-Ina, and Charco Redendo—which are in the primary stage of oil production. In addition to production, a waterflood operation provides important information regarding areal and vertical continuities of a reservoir which is very important for any displacement process to succeed.

These reservoirs have average net thicknesses ranging from 12 to 25 ft (3.6 to 7.6 m). The low average net thicknesses of the reservoirs is an indication that cyclic-steam stimulation alone probably will not recover a significant amount of oil.⁴ Cyclic-steam stimulation, however, is a

TABLE 1
Reservoir Data and Results of Screening Studies

No.	Field	County	Depth, ft	Den., API	Visc., cP	Area, acres	Net thick., ft	Perm., mD	Por., %	S _o , %	σ (S _o), frac.	kb/μ, mD ft/cP	COSR	Rec., %	Cum. prod., Mbbbl	OIP, Mbbbl	Annual prod., bbl
1	Colemena	Duval	1,500	19	109	950	25	1,958	30	53	0.159	449.08	0.12	12	3,901	29,266	33,167
2	Comitas	Zapata	800	20	193	1,020	14	500	24	48	0.115	36.269	0.07	17	2,641	13,312	0
3	Cedro Hill	Duval	1,440	19	116	1,800	12	600	35	46	0.161	62.069	0.11	19	6,577	28,616	7,355
4	Govt. Wells, North	Duval	918	20	166	100	12	1,068	33	48	0.158	77.205	0.1	17	316	1,527	1,019
5	Lundell	Duval	1,528	19	106	5,000	12	2,630	32	53	0.17	297.74	0.12	12	10,425	78,952	67,222
6	Los Olmos	Starr	700	20	221	590	25	900	30	60	0.18	101.81	0.11	5	987	19,612	2,147
7	Foss	McMullen	490	20	299	90	20	1,000	33	63	0.208	66.89	0.11	2	59	2,706	3,143
8	Taylor-Ina	Medina	350	16	1,258	7,710	16	240	28	62	0.174	3.0525	0.1	3	4,810	155,979	119,968
9	Charco Redondo	Zapata	339	17	927	680	15	2,800	34	61	0.207	45.307	0.11	4	659	15,485	5
10	Lost Lake	Chambers	2,382	20	42	240	30	500	30	42	0.126	357.14	0.13	23	2,336	7,719	54,830
11	Arnim, East	Fayette	2,151	20	50	160	17	300	33	55	0.182	102	0.15	10	437	3,742	2,627
12	Orlee	Duval	1,697	20	73	50	16	600	31	45	0.14	131.51	0.11	20	267	1,080	1,044
13	Hoffman, East	Duval	2,038	20	54	370	15	600	33	49	0.162	166.67	0.13	16	1,390	7,136	2,497
14	Petrox	Duval	2,024	20	55	590	15	400	30	44	0.132	109.09	0.12	21	2,632	9,727	55,474
15	Dinsmoor	Atascosa	2,060	19	65	225	12	500	24	42	0.101	92.308	0.1	23	853	2,913	5,933
16	Burmil	Burleson	2,659	19	41	120	11	500	24	53	0.127	134.15	0.13	12	211	1,510	3,614

necessary precursor to steamflood operations. The estimated COSR for all these reservoirs is about 0.1, which is low and indicates that steamfloods using conventional techniques will likely have poor performances. Low thicknesses seem to be the main reason for poor performances. The COSR is estimated using Chu's correlation. (See Eq. A-6 in Ref. 4). Application of horizontal wells for improving the steamflood performance in thin reservoirs is discussed by Sarkar and Sarathi (1992).⁴

Screening guides cannot be used for further prioritizing of reservoirs. Moreover, it should be noted that oil saturation values are assumed ones. Additional criteria, such as amount of target oil, availability of reservoir data, and uniqueness of a reservoir, should be used to select one of two reservoirs for simulation studies. Among the Group 1 reservoirs, Colemena has the greatest steamflood potential because it has the second highest OIP of 29 MMbbl ($4.6 \times 10^6 \text{ m}^3$) and the maximum thickness of 25 ft (7.6 m). Lundell field has the maximum OIP

of $79 \times 10^6 \text{ bbl}$ ($12.6 \times 10^6 \text{ m}^3$), but the average net thickness is only 12 ft (3.6 m). Collection of data for Colemena field, through the operator, is in progress. Among the Group 2 reservoirs, Taylor-Ina is an attractive one because it has the highest OIP of 155 MMbbl ($24.6 \times 10^6 \text{ m}^3$). It has a low depth of 350 ft (107 m), a low net thickness of 16 ft (4.9 m), and a low permeability of 240 mD ($237 \times 10^{-3} \mu\text{m}^2$). An operator in this field has provided some data.

References

1. P. Sarathi, *Environment, Safety and Health Assessment of Project BE11B*, DOE Report NIPER-640, December 1992.
2. R. M. Butler, *Thermal Recovery of Oil and Bitumen*, Prentice-Hall, Englewood Cliffs, New Jersey, October 1991.
3. C. Chu, State-of-the-Art Review of Steamflood Field Projects, *J. Pet. Technol.*, 1887 (October 1985).
4. A. K. Sarkar and P. S. Sarathi, *Feasibility of Steam Injection Processes in a Thin, Low Permeability Heavy Oil Reservoir of Arkansas—A Numerical Simulation Study*, DOE Report NIPER-661, December 1992.

**FEASIBILITY STUDY OF HEAVY OIL
RECOVERY IN THE MIDCONTINENT REGION
(OKLAHOMA, KANSAS, AND MISSOURI)**

Cooperative Agreement DE-FC22-83FE60149,
Project SGP37

National Institute for Petroleum
and Energy Research
Bartlesville, Okla.

Contract Date: Apr. 1, 1990
Anticipated Completion: June 1, 1993
Funding for FY 1993: \$293,000

Principal Investigator:
David K. Olsen

Project Manager:
Thomas Reid
Bartlesville Project Office

Reporting Period: Oct. 1–Dec. 31, 1992

Summary of Technical Progress

Heavy Oil in Alaska

A report on the feasibility of heavy oil recovery—Production, Marketing, Transportation, and Refining—constraints to increasing heavy oil production in Alaska was completed.¹ The term “heavy oil” as used in this study is oil of 10 to 20 °API (943 to 1000 kg/m³) inclusive at 60 °F (15.6 °C) with a gas-free viscosity of 100 to 10,000 cP (MPas) inclusive at original reservoir temperature.² This portion of the study was undertaken because previous studies have indicated the existence of a significant heavy oil resource in Alaska of 5 to 35 billion bbl (7.9×10^8 to 5.6×10^9 m³). There is a growing concern with the decline (Fig. 1) in Alaskan North Slope (ANS) crude oil production. As of October 1992, the production was 1.705 million BOPD (2.7×10^5 m³/d) of 27 °API gravity (890 kg/m³) crude. ANS contributes 24% of the total U.S. production³ and has a significant impact on the U.S. energy supply. Prudhoe Bay (Fig. 2) oil field has been in decline since May of 1989. Production is now restricted primarily by the amount of gas reinjection capability that currently exists at the North Slope and not by the capacity of the TransAlaskan pipeline (TAP) or State offtake restrictions, as was the case previously.⁴

Questions continue to be asked, including: Can Alaska continue to be the major U.S. oil producer if heavy oil is developed? Can thermal enhanced oil recovery (TEOR) (cyclic steam, steamflooding, and in situ combustion) technology be as successful in Alaska as it is in California? California is a model of TEOR success in recovering nearly 0.5 million BOPD (7.9×10^4 m³/d) (Ref. 5). Most of the data on Alaska are still confidential, and publicly known information comes

Objectives

The objectives of this nationwide heavy oil feasibility study are to (1) investigate from publicly available data the known heavy oil resources, (2) screen this resource for potential thermal or other enhanced oil recovery (EOR) techniques, and (3) evaluate various economic facets that may have an impact on the expansion of heavy oil production (refining, transportation, environmental, etc.).

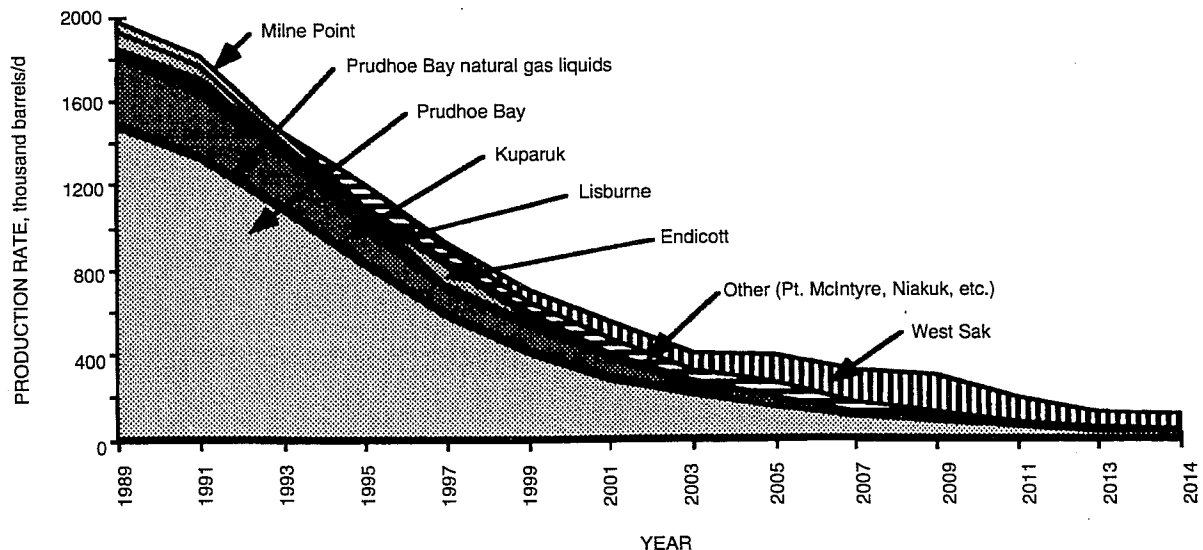


Fig. 1 Recent and projected production from North Slope of Alaska.¹⁰

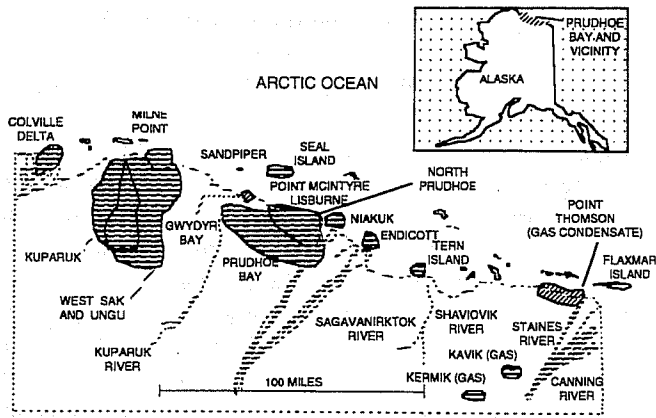


Fig. 2 Location of Alaskan oil and gas accumulations, highlighting North Slope fields.

from news releases and briefings that contain little technical data. The University of Alaska, the Alaska Oil & Gas Conservation Commission, and, more recently, the Department of Energy (DOE) (through EG&G Idaho, Inc.) have been the major sources of public information about these resources. The major objective of this study is to briefly summarize, compile, analyze, and present the relevant public-domain information in a simple and concise manner. A background listing of some of the technical, economic, and environmental constraints to the production of Alaska's heavy oil (AHO) has been reported.¹

Alaska produces heavy oil from Milne Point field, but the volume is small (<0.1% of total ANS daily oil production during the spring of 1992).⁶ However, this primary production is anticipated to increase based on the projected number of wells to be drilled in the field. Alaska is believed to have huge heavy oil deposits (Fig. 3), which at one time were thought to be as much as 35 billion bbl ($5.6 \times 10^9 \text{ m}^3$) (Refs. 7 and 8), of which 15 to 25 billion bbl (2.3×10^9 to $3.9 \times 10^9 \text{ m}^3$) was speculated to exist in the West Sak and 11 to 19 billion bbl (1.7×10^9 to $3.0 \times 10^9 \text{ m}^3$) in Ugnu. ARCO's initial target was 25 to 30% recovery of the estimated 5 to 11 billion bbl (7.9×10^8 to $1.7 \times 10^9 \text{ m}^3$) of oil in place in the West Sak sands using thermal methods.⁹ The heavy oil overlying Ugnu reservoir was estimated by ARCO to be 6 to 11 billion bbl (9.5×10^8 to $1.7 \times 10^9 \text{ m}^3$). On the basis of further exploration and drilling in the last few years, these estimates have been reduced to 5 billion bbl ($7.9 \times 10^8 \text{ m}^3$) (Ref. 6). Because of the expected low recovery factor, the recoverable oil is currently estimated to be only 423 million bbl ($6.7 \times 10^7 \text{ m}^3$) in the West Sak, the most viable large heavy oil reservoir.¹⁰ The factors critical to the development of these resources are world oil prices, governmental policies, environmental constraints, availability of a transportation system to deliver the produced heavy oil to a suitable refinery, availability of capital, and rate of return on investment.

Significant heavy oil exists in Alaska and is being produced in limited volumes, but technical, environmental, transportation, and refining constraints make near-term increased

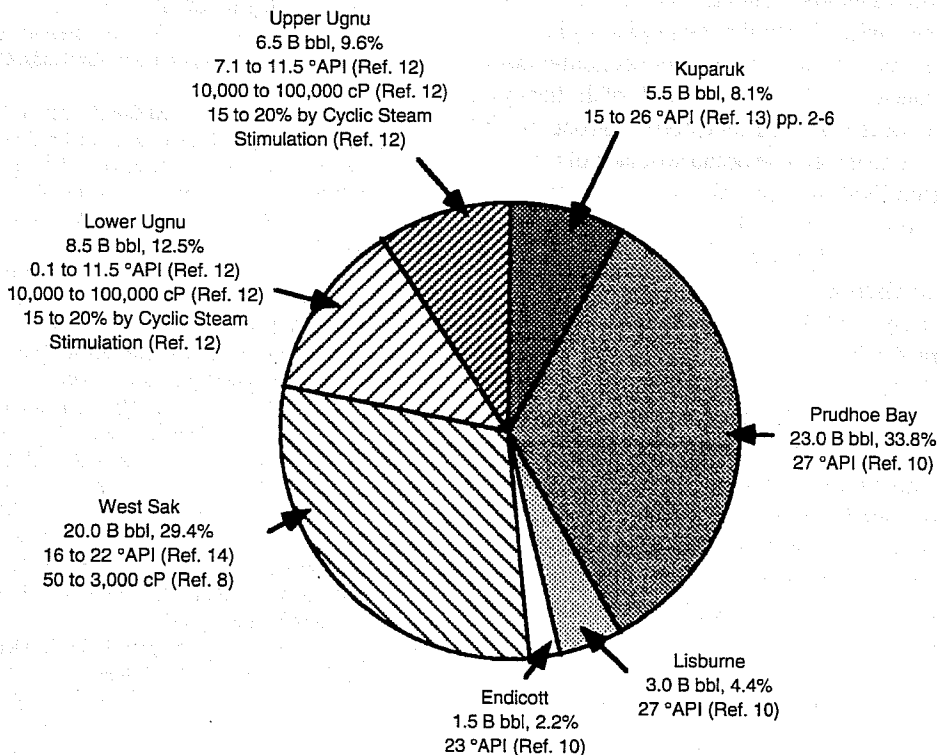


Fig. 3 The total estimated oil in place in the North Slope of Alaska¹¹ with API gravity and proposed recovery factors.^{10,12}

production unlikely because of unfavorable economics. The harsh climate for thermal (steam) recovery of AHO and the high cost of transport of a more viscous oil (through TAP to Valdez, Alaska, and then by tanker to the U.S. west coast refineries) significantly add to the production and delivery cost of a low-priced heavier oil. Economic recoverability of this oil is highly sensitive to the availability of existing facilities on a cost-sharing basis. For example, the limited capacity of the existing branch pipeline from Kuparuk River field to TAP is a likely cause for the delay of development of even the most promising heavy oil reservoir.

With the legislative constraint of having to sell ANS crude to the United States, AHO would have to compete not only with world oil but also with heavy oil produced in California, which refines most of Alaska's current production. This has an adverse effect on production and exploitation of Alaskan, and perhaps also Californian, heavy oil resources. The major heavy oil refining capacity is in California refining Californian, heavy and 70% ANS. The U.S. Gulf Coast will refine light oil and Caribbean blended heavy. A few Midwest refineries will refine Canadian blended crude (bitumen, upgraded bitumen, and diluent) and light crudes. The price of heavy oil at the refinery gate will limit refining of AHO in California, as refiners will find imported Caribbean medium and heavy oil at a much lower price than AHO or will refine imported light and medium crude and make a better rate of return.

A number of EOR technologies for production of AHO have been reported in the literature, including gas, CO₂, in situ combustion, and steam. Thermal production of heavy oil (hot water/steam) has been attempted, but the results of the field pilot have not been made public. Constraints on producing heavy oil in Alaska indicate that even with significant economic incentives and a significant increase in oil prices, little of the heavy oil in Alaska will be produced. If the current production decline and lack of further investment continue because of lack of access to explore and develop light oil reservoirs and better prospects elsewhere in the world, it is very likely that there will not be sufficient infrastructure or light oil diluent (for blending with heavy oil to lower viscosity) available for the development, production, and transport of Alaska's heavy oil resource.

Limitations are also imposed by the harsh environment of Alaska. The fragile Arctic tundra is supported by thick permafrost that must be maintained since the artificial islands in the permafrost are the support (base) for all drilling and production operations. This limits thermal recovery of the shallow heavy oil that is found scattered in the shallow fluvial-dominated formations on the North Slope that lay above lighter oils that are currently being produced. Reinjection of produced gas mandates that the heavy oil will be some of the last resources developed because natural gas will be used to supplement pressure and as a solvent to recover more valuable lighter crude oil on the North Slope. Interior basins of Alaska are still unexplored, and significant potential exists outside current fields for discovery of significant light, medium, and heavy oils. Minimum throughput (300,000 BOPD, $4.8 \times 10^4 \text{ m}^3/\text{d}$) on the TransAlaska Pipeline is a concern, but heavy

oil will not keep the pipeline full because the line was not designed to transport viscous heavy oil.

On the basis of publicly available data, this study determined that little of the heavy oil in Alaska is likely to be developed without significant economic incentives and even then the cost may be prohibitively expensive compared with that for heavy oil development in other parts of the United States or the world; thus most of Alaska's heavy oil may be unproduced. This oil has to compete on the world oil market even though legislative constraints mandate that ANS must be sold to the United States. This constraint mandates that produced AHO must be refined either in Alaska or in the heavy oil refining areas of California or the U.S. Gulf Coast. This makes AHO compete directly with heavy oil produced in California where the transportation cost of AHO to California may exceed \$10/bbl (\$62/m³).

With current constraints, the heavy oil fields in California, Wyoming, and the Gulf Coast states (Texas, Arkansas, Louisiana, and Mississippi) will be developed long before Alaska's.

Heavy Oil Database

Research is progressing on developing a national relational heavy oil reservoir database scheduled for completion in the spring of 1993.

References

1. D. K. Olsen, E. C. Taylor, and S. M. Mahmood, *Feasibility Study of Heavy Oil Recovery Production, Marketing, Transportation, and Refining Constraints to Increasing Heavy Oil Production in Alaska*, DOE Report NIPER-610, October 1992.
2. Group of Experts, *UNITAR Proposal for the Definition of Heavy Crude and Tar Sands and Addendum*, presented at the Second International Conference on Heavy Oil and Tar Sands, Caracas, Venezuela, February 1981.
3. Production Statistics, *Oil Gas J.* (Oct. 6, 1992).
4. R. E. Krause, R. H. Lane, D. L. Kuehne, and G. F. Bain, *Foam Treatment of Producing Wells to Increase Oil Production at Prudhoe Bay*, paper SPE/DOE 24191 presented at the Eighth SPE/DOE Enhanced Oil Recovery Symposium, Tulsa, Okla., Apr. 22-24, 1992, *Proceedings*, Vol. 2, pp. 359-368.
5. G. Moritis, EOR Increases 24% Worldwide; Claims 10% of U.S. Production, Biennial EOR Production Report, *Oil Gas J.*, 90(16): 51-79 (Apr. 20, 1992).
6. Alaska Oil and Gas Conservation Commission, Anchorage, Alaska, personal communiqué, July 9, 1992.
7. M. R. Werner, Tertiary and Upper Cretaceous Heavy-Oil Sands, Kuparuk River Unit Area, Alaskan North Slope, Exploration for Heavy Crude Oil and Natural Bitumen, *AAPG Stud. Geol.*, 25: 537-547 (October/November 1984).
8. G. D. Sharma, *Reservoir Description and Summary of Petroleum Resources on the Alaskan North Slope*, Topical Report, Petroleum Development Laboratory, University of Alaska, Fairbanks, August 1990.
9. ARCO Maps Plans for West Sak Thermal Project, *Oil Gas J.*, 81:78 (November 1983).
10. C. P. Thomas, T. C. Doughty, D. D. Faulder, W. E. Harrison, J. S. Irving, H. C. Jamison, and G. J. White, *Alaska Oil and Gas: Energy Wealth or Vanishing Opportunity?* DOE Report DOE/ID/01570-HI., January 1991.
11. V. A. Kamath and G. D. Sharma, *Summary of Petroleum Resources on the North Slope, Alaska and Their Recovery Annual Report*, Petroleum Development Laboratory, University of Alaska, 1986.
12. R. J. Hallam, E. J. Piekenbrock, A. S. Abou-Sayed, A. M. Garon, T. W. Putnam, M. C. Weggeland, and K. J. Webb, *Resource Description and*

Development Potential of the Ugnu Reservoir, North Slope, Alaska, paper SPE 21779 presented at Western Regional Meeting, Long Beach, Calif., Mar. 20-22, 1991.

13. G. J. Carman and P. Hardwick, Geology and Regional Setting of the Kuparuk Oil Field, Alaska, *Oil & Gas J.*, 80: 152-158 (Nov. 22, 1982).
14. M. W. Hornbrooke, K. Dehghani, S. Qadeer, R. D. Ostermann, and D. O. Ogbe, Effects of CO₂ Addition to Steam on Recovery of West Sak Crude Oil, paper SPE 18753, *SPE Reserv. Eng. J.*, 6: 278-286 (August 1991).

SIMULATION ANALYSIS OF STEAM-FOAM PROJECTS

**Cooperative Agreement DE-FC22-83FE60149,
Project SGP58**

**National Institute for Petroleum
and Energy Research
Bartlesville, Okla.**

**Contract Date: June 1, 1992
Anticipated Completion: May 31, 1994
Funding for FY 1993: \$321,000**

**Principal Investigator:
Partha Sarathi**

**Project Manager:
Thomas Reid
Bartlesville Project Office**

Reporting Period: Oct. 1-Dec. 31, 1992

Objectives

The objectives of this research program are to (1) conduct a study on the viability of the steam-foam process by analyzing data from selected completed steam-foam projects and (2) assess under what conditions the process is likely to succeed, both technically and economically.

Summary of Technical Progress

Several base case steam injection simulations were performed this quarter, and the results were history matched with the reported field data. The Computer Modeling Group's (CMG) STARS simulator was used to conduct a base case history match and to simulate field response to foam. STARS is a compositional thermal simulator with the ability to simulate steam drives as well as capture the many features of steam-foam pilots in real reservoirs. Because of the exploratory nature of the simulations, only the basic features available in STARS were used for these simulations.

The simulation was conducted with data from Section 26-C of Midway-Sunset field, California. For this field, a complete set of reservoir and production data is available in the literature for both base runs as well as steam-foam tests.¹⁻³ The

simulation study consisted of two stages. First, a representative model of the reservoir was constructed and 2 yr of steam injections prior to foam injection were performed to obtain results for history match with actual field performance. In the second stage, the model results were compared and matched with field results.

Base History Match

An idealized three-dimensional, 9 × 5 × 4, grid was used to represent one-eighth of an inverted 5-spot pattern of the pilot. The injection well was located at the center of the grid and was modeled as one-eighth of the field well. The rock and fluid properties used were those of Gomaa et al.¹ and were typical for the Monarch Sand of Midway-Sunset field. The grid dimensions and rock fluid properties of Midway-Sunset field are shown in Table 1.

TABLE 1

Reservoir and Fluid Properties of Monarch Sand (Section 26C), Midway-Sunset Field, Calif.*

Average depth, ft	1,200
Gross thickness, ft	600
Average net oil sand, ft	260
Porosity	0.27
Permeability, mD	1,390
Initial oil saturation	0.66
Oil saturation in the depleted zone	0.36
Oil gravity, °API	14
Reservoir temperature, °F	105
Oil viscosity, cP @ 40 °C	1,500
Oil viscosity, cP @ 148.9 °C	10
Current reservoir pressure, kPa (psig)	75
Grid dimensions	ΔX = 50 ft, ΔY = 40 ft, ΔZ = 15 ft
Injection location	(I = 5, J = 5, K = 1)
Producer A	(I = 1, J = 5, K = 2)
Producer B	(I = 9, J = 5, K = 2)
Observation well	(I = 5, J = 1, K = 3)

* See references 1 and 3.

The history match consisted of predicting and matching steamflood performance for 2 yr prior to foam injection. The predicted results were compared with field results prior to and after the history match in Table 2. The history match consisted of matching the injection pressures, the average reservoir pressures and temperatures, and the oil and water production. The match was obtained after adjusting a number of input parameters, such as the absolute permeability, water and oil saturation in the injection and production blocks, and the water and oil relative permeabilities in the reservoir. Substantial efforts were focused on matching the injection and the average reservoir pressures to realistically model the formation transmissibility. The injection and production constraints

TABLE 2

Comparison of Simulation Results with Field Values Before and After History Match

Parameters	Field value	Predicted value	
		Before history match	After history match
Cumulative oil production	6,185	5,453	6,137
2 yr, m ³ (bbl)	(38,900)	(34,300)	(38,600)
Cumulative water production, m ³ (bbl)	35,931 (226,000)	39,906 (251,000)	35,454 (223,000)
Average production well temp., °C (°F)	126.6 (260)	119.4 (247)	125 (257)
Average temp. at observation well, °C (°F) (after 2 yr)	199 (390)	207 (405)	200 (392)
Average pressure at observation well, (after 2 yr), kPa (psia)	1,655 (240)	1,551 (225)	1,641 (238)

input into the model were (1) the injection well is a constant rate well, where the bottomhole injection pressure is not to exceed 560 psi, this being the formation fracture pressure, and (2) a gross fluid production rate was assigned to the production well on a monthly basis. Simulation of steam-foam tests are planned for the next quarter. Steam-foam tests will be history matched with the parameters obtained from the base case steamflood history match. Surfactant properties and foam mobility reduction parameters will be included during this phase.

References

1. E. E. Goma, J. H. Duerksen, and P. T. Woo, *Designing a Steamflood Pilot in the Thick Monarch Sand of the Midway-Sunset Field*, paper SPE 5853 presented at the 51st Annual Fall Technical Conference of the SPE, New Orleans, La., Oct. 3-6, 1976.
2. J. H. Duerksen and E. E. Goma, *Status of the Section 26C Steamflood, Midway-Sunset Field, California*, paper SPE 6748 presented at the 52nd Annual Fall Technical Conference of the SPE, Denver, Colo., Oct. 9-12, 1977.
3. J. F. Ploeg and J. H. Duerksen, *Two Successful Steam-Foam Field Tests, Sections 15A and 26C, Midway-Sunset Field*, paper SPE 13609 presented at the SPE California Regional Meeting, Bakersfield, Calif., Mar. 27-29, 1985.

FIELD APPLICATION OF FOAMS FOR OIL PRODUCTION SYMPOSIUM

Cooperative Agreement DE-FC22-83FE60149,
Project SGP63

National Institute for Petroleum
and Energy Research
Bartlesville, Okla.

Contract Date: July 1, 1992
Anticipated Completion: June 30, 1993
Funding for FY 1993: \$39,000

Principal Investigator:
David K. Olsen

Project Manager:
Thomas Reid
Bartlesville Project Office

Reporting Period: Oct. 1-Dec. 31, 1992

Objectives

The objectives of the symposium on Field Application of Foams for Oil Production are to (1) document updates in field application of foams technology, (2) provide a means of information exchange on field application of foams to improve production of crude oil, and (3) enhance the development of this technology through the reports and discussion on success and failure of applications of foam.

Summary of Technical Progress

The Department of Energy (DOE) and the National Institute for Petroleum and Energy Research (NIPER) will co-sponsor a 1½-day symposium on *Field Application of Foams for Oil Production* at the Red Lion Inn in Bakersfield, Calif., on Feb. 11-12, 1993. This symposium will follow the SPE 1993 International Thermal Operations Symposium scheduled for Feb. 8-10, 1993, in Bakersfield. The program will include 13 papers and 6 poster presentations. A panel discussion of the pros and cons of field application of foams has been scheduled. Preprints of the papers and abstracts of the posters will be available for registered participants at the meeting. The proceedings of the meeting, panel discussion, and responses to questions and authors' responses will be compiled and published by DOE as a Fossil Energy report.

RESEARCH ON OIL RECOVERY MECHANISMS IN HEAVY OIL RESERVOIRS

Contract No. DE-FG22-90BC14600

**Stanford University
Petroleum Research Institute
Stanford, Calif.**

**Contract Date: Feb. 23, 1990
Anticipated Completion: Feb. 22, 1993
Government Award: \$740,000
(Current year)**

Principal Investigators:

**W. E. Brigham
K. Aziz
H. J. Ramey
L. M. Castanier**

Project Manager:

**Thomas Reid
Bartlesville Project Office**

Reporting Period: Oct. 1–Dec. 31, 1992

Objectives

The goal of the Stanford University Petroleum Research Institute (SUPRI) is to conduct research directed toward increasing the recovery of heavy oils. Presently SUPRI is working in five main directions:

1. Flow properties research—to assess the influence of different reservoir conditions (temperature and pressure) on the absolute and relative permeability to oil and water and on capillary pressure.
2. In situ combustion studies—to evaluate the effects of different reservoir parameters on the in situ combustion process. This project includes the study of the kinetics of the reactions.
3. Additives to improve steam injection—to investigate the mechanisms of the process using commercially available surfactants for reduction of gravity override and channeling of steam.
4. Reservoir definition—to investigate and improve techniques of formation evaluation, such as tracer tests and pressure transient tests.
5. Field support services—to provide technical support for design and monitoring of DOE-sponsored or industry-initiated field projects.

Summary of Technical Progress

Flow Properties Studies

End effects as a result of capillary forces can cause important errors in measuring relative permeability. Previous work

performed on Berea cores with a computerized axial tomography (CAT) scanner has shown that the saturation distribution in the core during unsteady state measurements is crucial. Based on the data, calculations of correct relative permeability curves may require three-dimensional (3-D) simulation. A new series of drainage and imbibition runs has been completed with the new epoxy Teflon core assembly. The rates were varied between 2 and 8 cm³/min in a 2-in. diameter Berea core. No recurrence of the channeling problem was observed. Simulations of these experiments are in progress for history matching of the results with the commercial simulator ECLIPSE.

Fractured reservoirs are an important resource. Studies of the fluid transfer between the matrix and the fracture network have been initiated and will continue during the next period of performance. Most of the work performed this quarter has been review of the literature and preliminary fine grid simulations for design of a new experiment.

Development of the software package for computerized tomography (CT) data interpretation and display (IDL) was purchased from IMSL. Three-dimensional reconstruction of cores can now be constructed from a set of two-dimensional (2-D) cross sections.

In Situ Combustion

Notes gathered from the In situ Combustion Forum in Tulsa, Okla., in April will be included as a section of the annual report.

The experimental research on the kinetics of combustion has continued. Fourteen kinetic runs were performed on crude oils from Cold Lake (Canada), Hamaca (Venezuela), and Huntington Beach (California). In addition, differential scanning calorimetry and thermogravimetric analysis results for the same oils were obtained from Pr Okandan at the Middle East Technical University of Ankara, Turkey. The main results to date are

- The reactions can be modeled by a set of two reactions only.
- The fuel burned at high temperature is an oxygenated hydrocarbon.
- The physics of combustion in a kinetic cell are different from those of tube run and field processes.

Tube runs on the same oil/matrix materials used for the kinetics studies are in progress.

Steam with Additives

Mathematical analysis of the model developed for one-dimensional (1-D) transient foam flow in porous media has been finalized. A paper on this project was presented at the SPE Fall meeting in Washington, D.C., in October. A report summarizing this project has been published by DOE.

A report on the model design and construction for the 3-D steam injection model under CAT scan was published by DOE. Numerical simulation of the steam injection runs has

continued using STARS, a commercial simulator. The preliminary results have shown a steam zone growth slower than the experimental results. As STARS is not well adapted to simulation of laboratory experiments, comparison of the heat losses from the model with the simulator data were difficult. STARS has now been modified to solve this problem. A report on the simulation is planned for summer 1993.

Design of the experimental apparatus to study steam flow in fractured systems has been finalized. Polysulfone plastic was selected as the core holder material because of its thermal resistance (up to 350 °F), its coefficient of dilatation, and its properties under CAT scan. A mock-up of the model was built in order to verify the feasibility of measurements of saturations by scanning. The results were satisfactory as position of the fracture and two-phase saturations were accurately measured in the mock-up model at room temperature. Construction of the final version of the model is in progress. The first test runs are scheduled for the second quarter of 1993.

Formation Evaluation

Numerical simulation of gravity drainage well testing has continued. The problems in adapting existing numerical mod-

els to solve this complex system of equations have been corrected. Setting the correct boundary conditions is, however, especially difficult and work is in progress on this problem. A report on the simulation of gravity drainage well testing is planned for the summer of next year. In parallel, analytical techniques to solve a simplified set of gravity drainage well testing equations are being developed.

Field Support Services

A report on the tests of an ultrasonic flowmeter is in the draft stage. This method seems to be promising for measuring two-phase flow rates in wells. More work is needed on this topic.

Another report on multivariate optimization of a single-well reservoir system including surface facilities is also in the draft stage and will be presented to DOE for review shortly.

The semianalytical steam injection model has been extended to include a layered system. Present work is focusing on two noncommunicating layers as a first step. Heat transfer from the steam swept from the most permeable one to the less permeable one is included in the model. Verification of the model by comparison with STARS results is now in progress.

GEOSCIENCE TECHNOLOGY

MEASURING AND PREDICTING RESERVOIR HETEROGENEITY IN COMPLEX DEPOSIT SYSTEMS

Contract No. DE-AC22-90BC14657

**West Virginia University
Appalachian Oil and Natural Gas
Research Consortium
Morgantown, W. Va.**

**Contract Date: Sept. 20, 1990
Anticipated Completion: Sept. 20, 1993
Government Award: \$1,915,000**

Principal Investigators:

**Alan C. Donaldson
Robert Shumaker
Milton Heald
Kashy Aminian
Michael Ed. Hohn**

Project Manager:

**Edith Allison
Bartlesville Project Office**

Reporting Period: Oct. 1–Dec. 31, 1992

Objectives

The recovery of additional oil from existing fields in the Appalachian basin is hampered by poorly known permeability barriers within the reservoirs. Vertical barriers, caused by stacking of sandstones separated by shale breaks, are relatively easy to recognize in a given well but difficult to project laterally. Lateral barriers caused by facies changes are more difficult to predict, and subtle changes within the reservoir caused by diagenetic changes are the most difficult of all. Thus several scales of heterogeneity exist, from those imposed by shifts in depositional environments to the pore throat barriers developed during diagenesis. The result is that the oil reservoirs consist of a complex series of flow systems dependent on lithology, sandstone genesis, and structural and thermal history.

The proposed research is designed to use a multidisciplinary approach to measure and map heterogeneity at various scales and ultimately to develop tools and techniques to predict heterogeneity, both in existing fields and in undrilled areas. The stratigraphic unit chosen for this research is the fluvial-deltaic Big Injun sandstone (Mississippian) in West Virginia.

The main goal of this research project is to understand reservoir heterogeneity sufficiently to allow prediction of optimum drilling locations vs. high-risk locations in a given field so that the most cost-effective infill-drilling programs can be recommended.

Summary of Technical Progress

Stratigraphy

Maccrady Big Injun sandstones are enclosed in redbeds, whereas Pocono Big Injun sandstones occur stratigraphically below the Maccrady units. Descriptions of cuttings (geologs) from wells indicate that the reservoir sandstone for the three-county area containing the Granny Creek, Lizemores, and Tariff oil fields is the Pocono Big Injun, whereas the reservoir sandstone for the Rock Creek and Blue Creek fields is the Maccrady Big Injun sandstone. Both Pocono and Maccrady Big Injun sandstones are reservoir rocks in Pond Fork field. Preliminary findings indicate that oil pay zones mainly occur in the subfacies of the distributary-mouth bar depositional environment for both the Pocono Big Injun of Granny Creek field and the Maccrady Big Injun of Rock Creek field. Also, the pre-Greenbrier unconformity truncates the tops of the reservoirs in both fields. Although no coarse-grained sandstones occur in cores studied in Rock Creek field, geophysical log characteristics from wells in the western part of the field suggest that a coarse-grained unit (possibly fluvial channel fill) overlies the fine-grained sandstone (distributary-mouth bar), similar to the vertical sequence in Granny Creek field. Although similarities seem to occur, known differences between the reservoir rocks of Granny Creek and Rock Creek fields include (1) progradation of the Pocono distributary-mouth bars toward the west, whereas the Maccrady Big Injun prograded toward the east into a marine environment a longer distance from the river source; (2) Granny Creek sediments probably were supplied by a small (intrabasinal) drainage basin extending eastward across the West Virginia dome, compared with Maccrady Big Injun sandstone of Rock Creek field, which received its sediment from a large (extrabasinal) drainage basin that extended northward across the craton as well as eastward to the orogenic belt; and (3) the sandstones never were laterally continuous from field to field.

Structural Geology

A regional structure map on the Big Lime (Greenbrier Group) between the Granny Creek and Rock Creek fields was completed, and detailed structure maps were modified by the addition of more well data in both fields. A preliminary structure map on the basement shows that both fields are near or above basement faults that have large offset at the Cambrian level but are expressed only as low-relief flexures at the Big Lime level.

The acquisition of additional seismic data over Granny Creek field began during the late part of the quarter. Initial field tests revealed that a broad bandwidth was being received from the target Big Injun interval. Frequencies at 150 Hz are about 20 dB down from peak amplitudes and are expected to be recovered as usable data in the final stack. Although the resolution limit will be close to 30 ft, rather than the approximately 58 ft now in the Vibroseis data, the response of the reservoir interval is complicated because of interference from large impedance contrasts in the overlying carbonate section.

The composite nature of the seismic response at the Big Injun travel time requires an evaluation of the possible influence of impedance variations in the shallower carbonate section. This is being done by introducing impedance variations that are laterally and vertically variable into the overlying section. Lateral variations are introduced in fractions or multiples of the Fresnel zone radius at the reservoir depth.

Time-difference measurements between major reflection events in the Paleozoic section have been subdivided on the basis of their relationship to deeper basement structures. Net relative subsidence, uplift, or rotation of these subdivisions has been plotted for each of the seismic lines as a function of time through the Paleozoic. On some lines the intensity of tectonic activity appears to decrease nearly exponentially with time following the Middle Cambrian development of the Rome Trough, whereas on other lines periods of increased tectonic activity occur. Post-Big Injun reactivation of these structures also has been observed. The implications of this observation include possible syndepositional effects on the Big Injun and post-depositional structural interruption of the reservoir.

Petrology

Fifty-three samples were collected from wells partially sampled earlier to obtain additional thin sections of significant diagenetic features. These thin sections have been point counted for mineralogy and grain size measurements. Initial point counts and grain size analysis of all 411 thin sections have been completed.

The data are being organized into several workable files to facilitate close integration of data from other areas of the project. Depositional environments proposed by project stratigraphers may have controlled many petrographic properties, which accounts for important variations in porosity and permeability in the Big Injun sandstone.

Average grain size was determined for the different facies in each well in Granny Creek field (Table 1). The smaller grain size

TABLE 1
Average Grain Size for Various Facies in Ten Cores*

Well No.	Channel	Fluvial infl.†	Marine infl.†	Distal bar
1107	0.232	—	0.169	0.146
1108	0.241	0.137	0.131	0.137
1109	0.395	—	0.152	0.103
1110	0.299	0.130	0.145	0.131
1128	0.384	—	0.151	0.116
1130	0.391	—	0.144	0.147
1132	0.337	—	0.147	0.119
1133	0.350	—	0.142	0.103
1134	0.552	—	0.137	0.148
1052	0.261	0.166	0.150	0.132
Average	0.344	0.144	0.147	0.128

*Data in millimeters.

†Infl. = influenced.

in the distal part of the mouth bar is one of the more important factors accounting for low permeability in this facies.

Reservoir Engineering

Development of Reservoir Models

The objective of this subtask is to develop a systematic reservoir model for heterogeneous reservoirs. Work on this task was directed toward continued interpretation of data and development of a computer model.

New correlation charts using log vs. core porosity values were completed. Reservoir data were compiled for a newly selected, five-spot water injection area, called P3. A 9×10 grid was selected and formation properties were assigned to individual blocks in the five-spot study area. The reservoir fluid properties and operating conditions in the five-spot water injection area were compiled and used as input to the BOAST model. Several preliminary runs were conducted and a final history match was obtained for cumulative oil production from well Clay 1439, located in the center of the five-spot area. Figure 1 shows the results of the final history match of cumulative production.

Work continued on simulation of Columbia's waterflood project in Granny Creek field. The study was expanded to five-spot P3, a third five-spot pattern adjacent to P1 and P2

patterns. Figures 2 and 3 show the location of the patterns as well as a projected natural fracture between an injection well in the P1 pattern and the production well in the P2 pattern. The orientation of this fracture is in agreement with seismic interpretations and agrees with injection pressure data at six injection wells in these two patterns. The injection pressure in well I-4 was considerably lower than those of injection wells I-1 through I-6 (400 psi compared to 950 psi).

Figures 4 and 5 show the simulation results achieved in these three patterns. Good agreement exists between field data and simulation results for both oil and water production in all three patterns. A closer look at Fig. 4 shows that, although these patterns have comparable pore volumes, the injection rates and pressures in all three patterns are quite comparable, and production schemes are the same. The amount of oil and water being produced from these patterns, however, is by no means similar. For example, oil and water production in the P2 pattern can be explained by the existence of a high-permeability fracture that connects the production well in the P2 pattern to an injection well somewhere in the field (perhaps I-4). Comparison of oil and water production of the P1 and P3 patterns shows that, although neither of these patterns produces water, their oil productions are quite different. This phenomenon could be linked to a number of heterogeneities. It is possible that there are fractures present in the P3 pattern

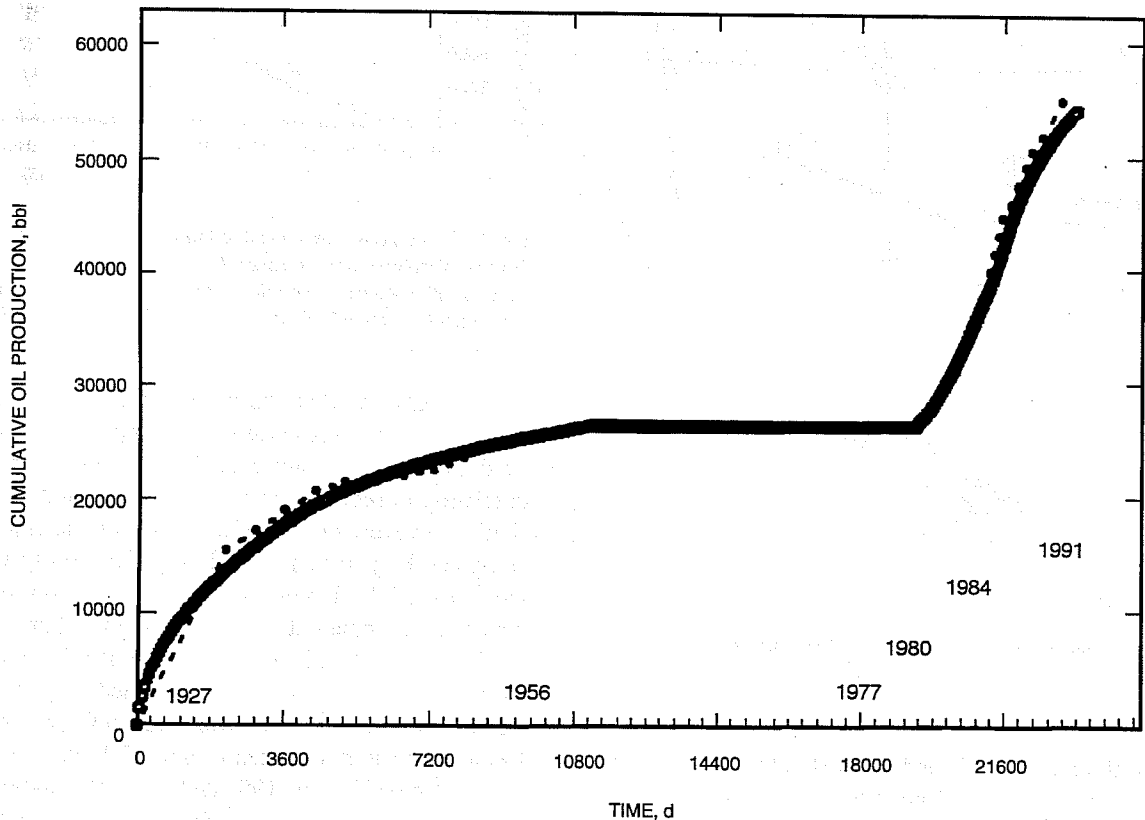


Fig. 1 History match results for the five-spot waterflood study area, Granny Creek field, Roane and Clay Counties, West Virginia. Oil production for Well 1439 (shut down in 1956 and reopened in 1980). Well permit No. 1185, date of injection, 1977; well permit No. 1603, date of injection, 1980; well permit No. 1630, date of injection, 1981; and well permit No. 2253, date of injection, 1984. ●, real production. □, simulated.

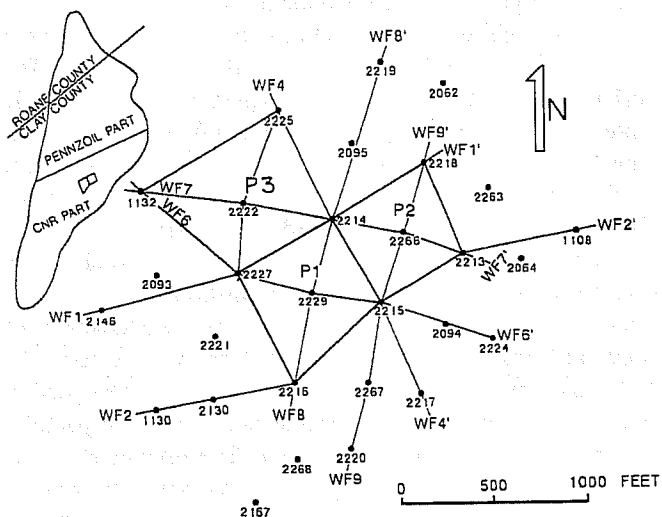


Fig. 2 Waterflood patterns P1, P2, and P3 in Granny Creek field.

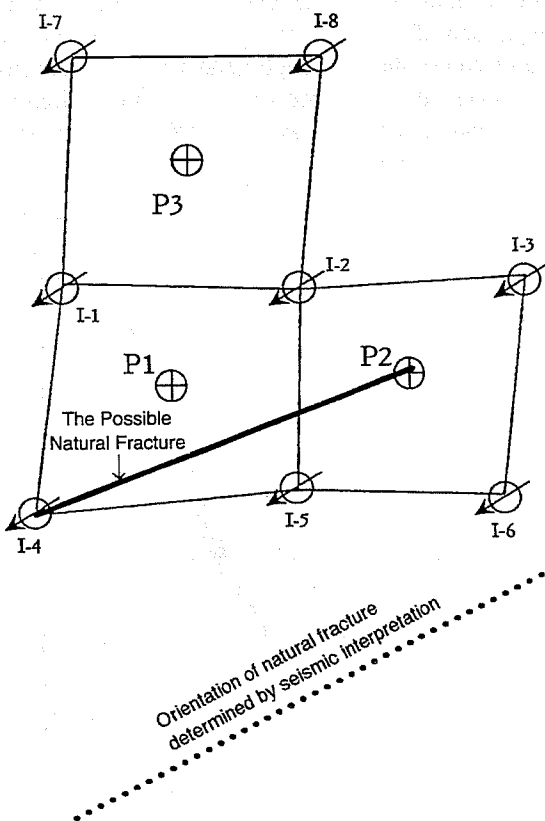


Fig. 3 Orientation of a possible natural fracture with respect to P1 and P2 flood patterns determined by seismic interpretation.

that act as thief zones and conduct most of the injected water out of the pattern. Alternatively, compartments in the field could have disrupted the uniform distribution of pressure and/or saturations throughout the field during primary production. This would mean that heterogeneous distribution of pressure and/or saturation occurred within the field prior to waterflooding.

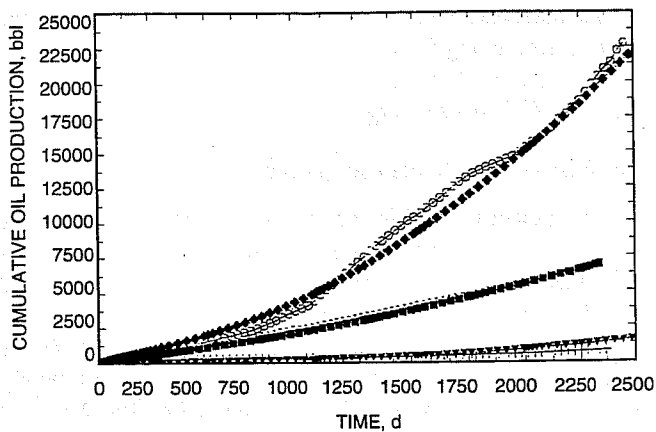


Fig. 4 Cumulative oil production in the three flood patterns, field data vs. simulated data. Granny Creek field, Columbia lease. \circ , field data for P1 pattern. \blacklozenge , simulated data for P1. $+$, field data for P2. \blacktriangledown , simulated data for P2. $+$, field data for P3. \blacksquare , simulated data for P3.

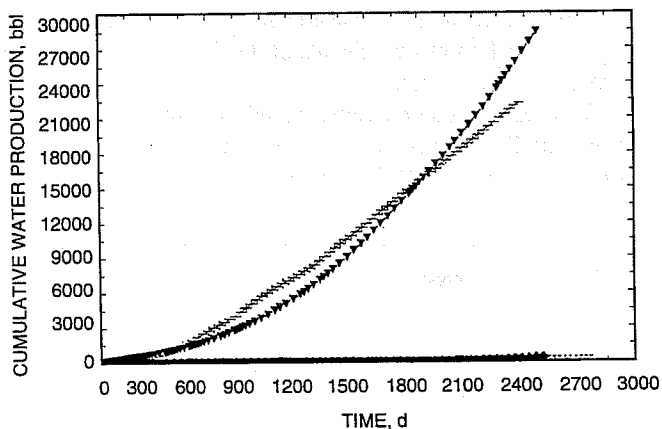


Fig. 5 Cumulative water production in the three flood patterns, field data vs. simulated data. Granny Creek field, Columbia Lease. \circ , field data for P1 pattern. \blacklozenge , simulated data for P1. $+$, field data for P2. \blacktriangledown , simulated data for P2. $+$, field data for P3. \blacksquare , simulated data for P3.

Another important observation noted during this simulation study is the presence of high injection pressure in the field. Permeability values used in the simulation study were obtained from cores and vary from 5 to 15 mD throughout the field. However, pressures observed in the injection wells could not be justified with these permeability values. This gave rise to the hypothesis of localized, low-permeability zones in the immediate vicinity of the wellbore.

To investigate this matter in more detail, fall-off test data from two injection wells were obtained. Figure 6 shows the test data for well 21975 (permit number Clay 2499), which is located in the northern portion of the Columbia lease. This test was performed in June 1991 and lasted about 400 h. Analysis shows that an area with a radius of 300 ft was investigated during the test. Effective permeability was calculated to be 0.31 mD with a skin factor of -2.5 , which implies some kind of well stimulation prior to the test. It must be noted that 0.31 mD is the effective permeability throughout the area that

was investigated. This means that the area closer to the wellbore must have a much lower permeability if the area away from the wellbore has a permeability of 5 to 15 mD, as measured from cores. These findings were further confirmed by analyzing a second set of fall-off test data from well 2055, which is located in the southern part of Columbia's lease (Fig. 7). This test was performed in September 1988 (well after the waterflood project had started) and lasted about 200 h. Analysis of this test shows a radius of investigation of about 240 ft with an effective permeability of 0.4 mD. This well also has been stimulated and the skin factor was calculated to be -3.1 , which implies a greater degree of stimulation when compared to well 21975.

These results confirm the localized, low-permeability zones hypothesis. The next step will be to identify the cause. Because the presence of clay minerals in amounts that could cause enough swelling to justify the observed high injection pressures is not substantiated by optical microscopy studies, two other possibilities should be taken into consideration. First, the presence of small particles and/or specific reactive chemicals in the injection water may cause partial plugging of the formation, especially around the wellbore. The second possibility is the presence of clay in the formation in forms that might not be detected by optical microscopy.

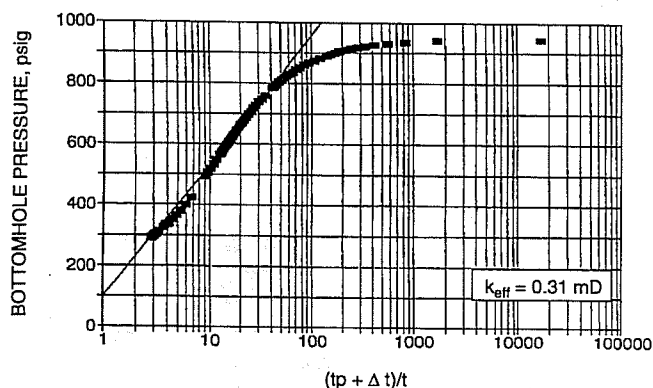


Fig. 6 Injection fall-off test data for well 21975. k_{eff} , effective permeability.

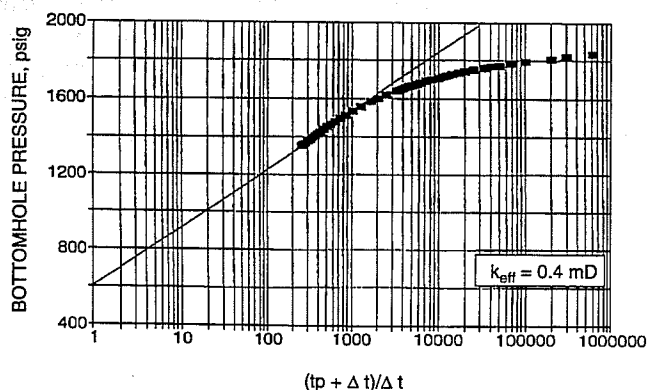


Fig. 7 Injection fall-off test data for well 2055. k_{eff} , effective permeability.

Geostatistics and Modeling

Efforts were concentrated on three objectives: (1) modeling of reservoir properties at the field scale for Granny Creek, (2) assessment of various schemes for the stratigraphic subdivisions of the Big Injun, and (3) preliminary modeling and mapping of Big Injun reservoir properties in Rock Creek.

In October and November, cumulative oil production data for the southern part of Granny Creek field were entered into the West Virginia Geological Survey's Oil and Gas database; data collection for this field is now complete. Ten-year cumulative production was computed for each well completed before 1960, and a contour map was drawn. Earlier work in the northern part of this field showed a distinct north-south band of above-average production along the western margin of the field; the new map shows that this trend also is present in the southern part of the field but is less distinct. The largest concentration of high-producing wells is in the northern part of Granny Creek field.

All wells in Granny Creek with both gamma-ray and density logs were correlated by computer and density values were converted to porosity. Multidimensional scaling techniques were then used to produce a horizontally flat data set for the field representing volumetric log porosity for the Big Injun interval. A number of porosity cross sections were created and compared to production and initial production (IP) maps. The only observed trend was a tendency for log porosity in the fine-grained portion of the Big Injun to be reduced (10 to 15%) in areas of high IP; the average log porosity for the Big Injun in Granny Creek is approximately 18%. Variography on the porosity data yielded a range of 800 to 1000 m with a fairly well-defined E-W anisotropy.

Statistical analyses were carried out on two schemes proposed for stratigraphic subdivisions of the Big Injun: a four-fold scheme based on proposed environments of deposition and a six-fold scheme based on microfacies. Lithologic descriptions, core analyses, well logs, and petrographic data from four "type" wells in Granny Creek were analyzed to determine which method of subdividing the Big Injun was most reproducible using computer techniques. Division of the Big Injun into six lithofacies could be reproduced by computer with a success rate of only 48% (70% is the minimum acceptable rate) using gamma-ray and density response. Division of the Big Injun strata into four depositional environments could be reproduced with a success rate of 67%. With the use of mathematically transformed values of gamma-ray and density response, the success rate was improved to 72%.

At the same time, cluster analysis was applied to data from the "type" wells to see if a more appropriate method of subdividing the Big Injun could be found. Subdivisions of the Big Injun into four or five "electrofacies" based solely on gamma-ray and density response have been reproduced by computer with success rates as high as 98%. Work is continuing to apply these electrofacies to the entire field.

Preliminary correlation of wells from Rock Creek was completed and indicated the presence of several types of

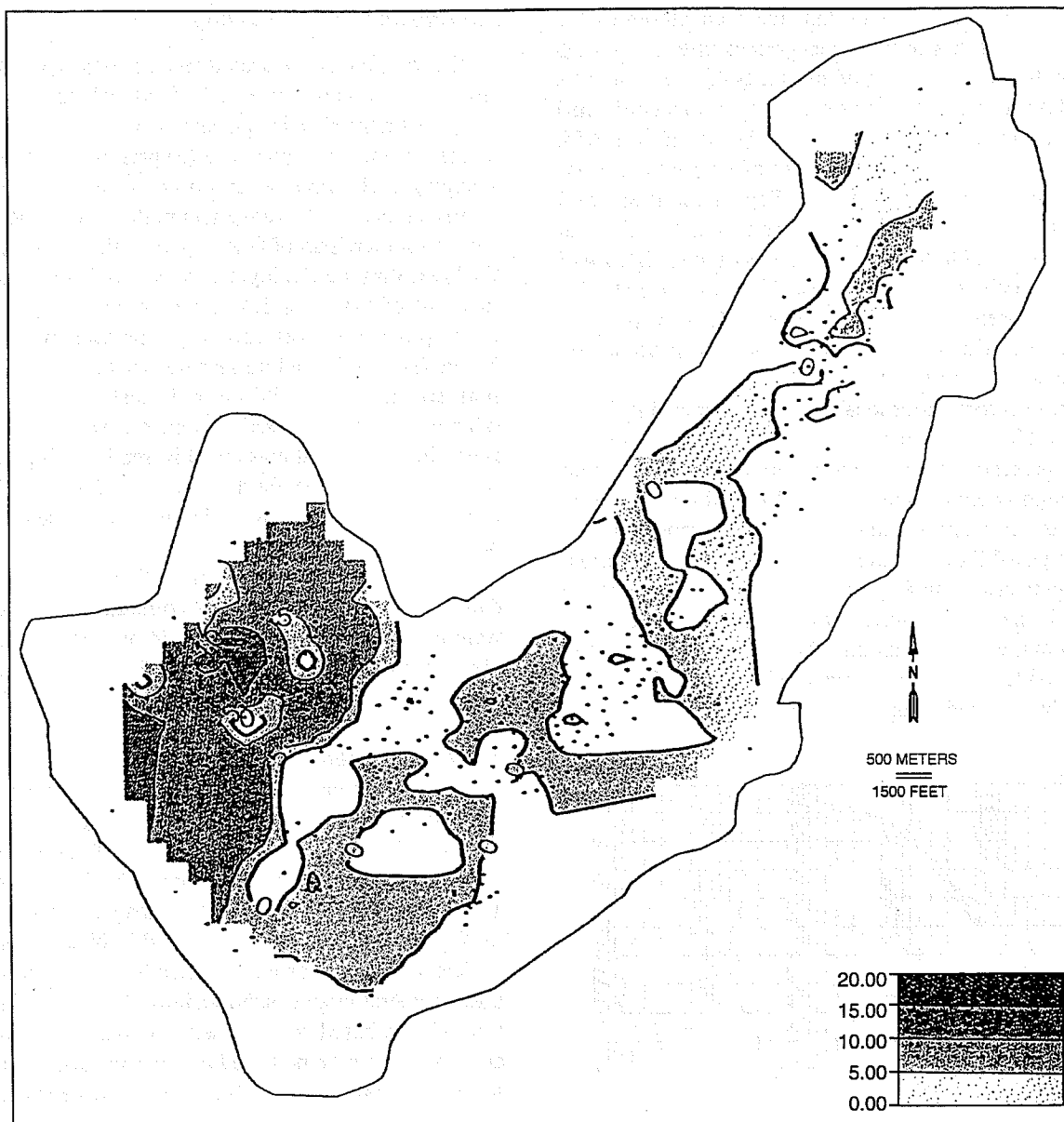


Fig. 8 Preliminary isopach map of shales contained within the Big Injun interval in Rock Creek. Contour interval is 5 ft.

heterogeneity in the Big Injun interval. Shales and zones of increased cementation are common throughout the field. These shales are thin (≤ 2 ft) in the eastern portion of the field but thicken markedly (≥ 5 ft) to the west (Fig. 8). These units cause the available reservoir to shrink from over 40 ft to less

than 20 ft in total thickness. Available reservoir in the western and northeastern portions of the Rock Creek field is increased by the presence of a porous zone at the base of the Greenbrier Limestone (Fig. 9). Although porosity in this unit rarely exceeds 10%, its thickness may exceed 30 ft locally.

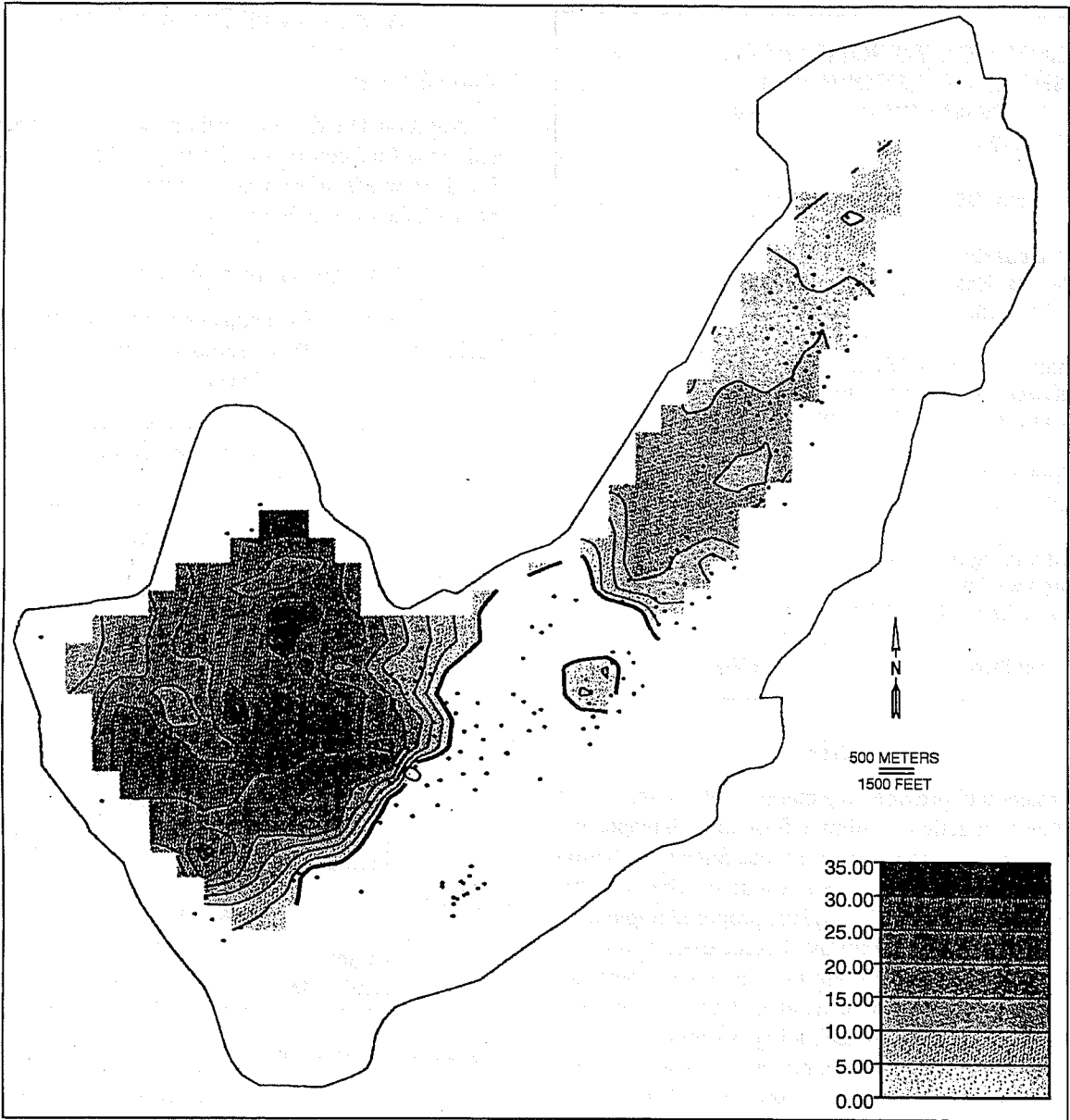


Fig. 9 Preliminary isopach map of the porous unit at the base of the Greenbrier Limestone in Rock Creek. Contour interval is 5 ft.

**RESEARCH ON IMPROVED AND
ENHANCED OIL RECOVERY IN
ILLINOIS THROUGH RESERVOIR
CHARACTERIZATION**

Contract No. DE-FG22-89BC14250

**Illinois Department of Energy
and Natural Resources
Springfield, Ill.**

**Contract Date: June 29, 1989
Anticipated Completion: June 27, 1993
Government Award: \$373,000**

**Principal Investigator:
Donald F. Oltz**

**Project Manager:
R. Michael Ray
Bartlesville Project Office**

Reporting Period: Oct. 1–Dec. 31, 1992

Objective

This project will provide information that can maximize hydrocarbon production, minimize formation damage, and stimulate increased production in Illinois. Such information includes definition of hydrocarbon resources, characterization of hydrocarbon reservoirs, and the proposed implementation of methods that will improve hydrocarbon extractive technology. Increased understanding of reservoir heterogeneities that affect oil recovery can aid in identifying producible resources. The transfer of technology to industry and the general public is a significant component of the program. The project is designed to examine selected subsurface oil reservoirs in Illinois. The research team uses advanced scientific techniques to gain a better understanding of reservoir components and behavior and addresses ways of potentially increasing the amount of recoverable oil. In the Illinois Basin as much as 60% of the oil in place can be unrecoverable with standard operating procedures. Heterogeneities (geological differences in reservoir makeup) affect the capability of a reservoir to release fluids. Bypassed mobile and immobile oil remains in the reservoir. To learn how to get more of the oil out of reservoirs, the Illinois State Geological Survey (ISGS) is studying the nature of Illinois reservoir rock heterogeneities and their control on the distribution and production of bypassed, mobile oil.

Summary of Technical Progress

Field Studies

Additional field studies in the series that have been submitted to the final editing and drafting process include Tamaroa Field, Stewardson Field, and Energy Field. These studies will be published in the first quarter of 1993.

Oil and Gas Development Maps

Development of a computer-generated series of maps to replace the older ISGS series of hand-drawn oil and gas development maps continues.

Maps completed to date

Alto Pass	McLeansboro
Benton	Mt. Vernon
Carbondale	Murphysboro
Carlyle	Nashville
Cave-In-Rock	New Burnside
Centralia	Noble
Clay City	Patoka
Du Quoin	Pinckneyville
Effingham	Roaches
Fairfield	Rosiclare
Goreville	Shelbyville
Kinmundy	Thompsonville
Mattoon	Xenia

Maps in progress

Carmi
Louisville

Technology Transfer

The two committees advisory to this project, the Petroleum Advisory Committee (PAC) and the Technical Advisory Committee (TAC), met with project teams on November 18 in Mt. Vernon, Ill. The committees reviewed project progress and attended the second workshop "Working Toward Improved Recovery of Mobile Oil in Illinois Reservoirs."

The workshop was attended by 145 independents and included presentations on the overall work plan, detailed field studies on Storms Consolidated, Energy Field, Dale Consolidated, seismic at King Field, and outcrop work on the Cypress Formation. Poster sessions exhibited work on Lawrence, Mattoon, Xenia, Dale, and Tamaroa Fields. Hands-on demonstrations of BOAST and Questor (the Survey's database) were also conducted.

ELECTRICAL AND ELECTROMAGNETIC METHODS FOR RESERVOIR DESCRIPTION AND PROCESS MONITORING

Lawrence Berkeley Laboratory
University of California
Berkeley, Calif.

Contract Date: Oct. 1, 1990
Anticipated Completion: Sept. 30, 1993
Government Award: \$195,000

Principal Investigators:

H. Frank Morrison
Ki Ha Lee
Alex Becker

Project Manager:

Robert Lemmon
Bartlesville Project Office

Reporting Period: Oct. 1–Dec. 31, 1992

Objectives

This project is part of an integrated effort by Lawrence Berkeley Laboratory (LBL)—University of California at Berkeley (UCB), Lawrence Livermore National Laboratory (LLNL), and Sandia National Laboratories (SNL) in the electrical and electromagnetic (EM) geophysical method development research and development (R&D) program for petroleum reservoir characterization and process monitoring. The overall objectives of the program are to (1) integrate research funded by the Department of Energy (DOE) for hydrocarbon recovery into a focused effort to demonstrate the technology in the shortest time with the least cost, (2) assure industry acceptance of the technology developed by having industry involvement in the planning, implementation, and funding of the research, and (3) focus the research on real-world problems that have the potential for solution in the near term with significant energy payoff.

Research conducted through this integrated effort focuses on five general activities:

1. EM forward modeling development.
2. Data interpretation methods development.
3. Hardware and instrumentation development.
4. Enhanced Oil Recovery (EOR) and reservoir characterization.
5. Controlled field experiments.

Lawrence Berkeley Laboratory—University of California at Berkeley research is focused on activities 1, 2, and 5. The primary focus is in the development of reliable inversion and imaging schemes that can yield conductivity distribution from measured electrical and electromagnetic field data. The development of accurate forward modeling algorithms and the

acquisition of high-quality scale-model data are necessarily the early part of the inversion scheme development for ultimately monitoring the front tracking in existing reservoirs.

Summary of Technical Progress

The highlight of this quarterly report includes the continued development in the diffusion-to-wavefield transform and its application to high-resolution conductivity imaging. The effort on this subject has been very successful and the initial numerical result for the wavefield transform and subsequent tomographic imaging of electrical conductivity will be published in the June 1993 issue of *Geophysics*.¹

In spite of the initial success, a great deal of research needs to be carried out before the q-domain technique can be practical. The numerical method is continuously improved, but at the same time the stringent requirement for the time-domain data needs to be relaxed further. The transform now requires two decades of time-domain data with its first sample collected as early as a few microseconds. A maximum allowable noise is 3% over the entire band. Important subjects to be studied include the analysis of the effect of the source waveform on reconstructed travel-time data, the anticipated difficulty in imaging conductivity of a high-contrast medium, and extension of the method to the surface-to-borehole configuration. An alternative approach is also being considered in which the wavefield transform would be achieved using the frequency-domain data. Most importantly, the evident success of the q-domain imaging technique argues very strongly for the development of a new wide-band borehole time-domain electromagnetic (TEM) system. In this quarterly report the effect of the source waveform will be examined and a scheme will be proposed in which travel-time data can be obtained using the frequency-domain data.

Source Waveform

In numerical simulations the magnetic field at the receiver is calculated by assuming that the current in the transmitter coil (magnetic dipole) is an impulse described by a delta function. The same result can be achieved if the voltage across the receiver coil is measured after direct current in the transmitter is turned off instantly. In reality, it is impossible to turn off the current instantly, and therefore it is necessary to examine the effect of the source current waveform on fields which, in turn, will be transformed to wavefields.

The basic equation for the transform is

$$H(t) = \frac{1}{2(\pi t^3)^{1/2}} \int_0^{\infty} q e^{-q^2/4t} U(q) dq$$

where H is the transient magnetic field caused by an impulse current source and U is the transformed wavefield satisfying

a wave equation. If the current waveform is other than delta function, this equation should be modified to

$$H^*(t) = H(t) \otimes W(t)$$

$$= \left[\frac{1}{2(\pi t^3)^{1/2}} \int_0^\infty q e^{-q^2/4t} U(q) dq \right] \otimes W(t)$$

Here $H^*(t)$ is the magnetic field that would be measured by a receiver and \otimes denotes convolution. $W(t)$ is the source waveform. Two possible ways of wavefield construction may be considered. The first one involves direct transform of the convolved field $H^*(t)$. This approach is easy to handle, but travel-time data estimated from a thus transformed wavefield may not be correct. In the second approach the data will first be deconvolved with the current waveform $W(t)$ and then transformed to wavefields. It would be ideal if the second approach could be followed, but this approach may suffer from numerical instability inherent to the deconvolution operation.

The first approach was tested with a boxcar current waveform with varying pulse widths. Magnetic fields corresponding to this type of source are equivalent to voltages in the receiving coil because of a source current in the transmitter coil that is turned off linearly over a short period of time. Initial results show that data obtained from a source current with a pulse width of 2 to 3 μ s can be transformed to wavefields whose travel time seems to be reasonably accurate for tomographic inversion purpose.

A TEM scale-model facility is under development at LBL, and some experimental data have been obtained from the preliminary setup. The effort in transforming these data has not been successful so far. One of the reasons for this is that the source current turnoff time is not short enough—on the order of 5 μ s.

Frequency-Domain Data

In this study the wavefield transform methodology will be extended to include frequency-domain data that may be available only at a few frequencies. To begin, first Fourier transform (from t to ω) the original integral equation to obtain the transform equation in the frequency domain

$$\tilde{H}(\omega) = \int_0^\infty e^{-(i\omega)^{1/2} q} U(q) dq$$

The following approximation is then introduced to the wavefield $U(q)$

$$U(q) = \sum_{i=1}^N a_i \delta(q - q_i)$$

where $\delta(\cdot)$ is the Dirac delta function, and the coefficient a_i may be considered as the strength of the i th delta function. The approximation should approach the exact value as the number of terms N is increased. Substituting the approximation into the frequency-domain integral equation, the following is obtained

$$\tilde{H}(\omega) = \sum_{i=1}^N a_i e^{-(i\omega)^{1/2} q_i}$$

Here the series $\{a_i\}$ is called the “pseudo-impulse” response, and it depends on the reflection and transmission coefficients of the wavefield $U(q)$ at inhomogeneous boundaries within the heterogeneous medium. The equation can be used, in principle, to compute the pseudo-impulse response $\{a_i\}$ corresponding to events that take place at $\{q_i\}$. The first arrival may be identified by q_1 , and it corresponds to the “travel time” required for the wavefield to travel the distance between the transmitter and receiver.

It is proposed in this report that travel time in the wavefield domain will be obtained using the frequency-domain data following the procedure described previously. Because of the highly nonlinear nature of the equation, however, numerical methods need to be examined that would lead to acceptable solutions for the parameters $\{a_i\}$ and $\{q_i\}$.

Reference

1. K. H. Lee and G. Q. Xie, A New Approach to Imaging with Low-Frequency Electromagnetic Fields, *Geophysics* (June 1993).

GEOPHYSICAL AND TRANSPORT PROPERTIES OF RESERVOIR ROCKS

Contract No. DE-AC22-89BC14475

University of California
Berkeley, Calif.

Contract Date: Sept. 22, 1989
Anticipated Completion: Aug. 21, 1993

Principal Investigator:
Neville G. W. Cook

Project Manager:
Robert Lemmon
Bartlesville Project Office

Reporting Period: Oct. 1–Dec. 31, 1992

Objectives

The definition of reservoir characteristics, such as porosity, permeability, and fluid content, on the scale of meters, is the key to planning and control of successful enhanced oil recovery (EOR) operations. Equations relating seismic and electrical properties to pore topology and mineral–fluid interactions are needed to invert geophysical images for reservoir management. Both the geophysical and transport properties of reservoir rocks are determined by pore topology and the physics and chemistry of mineral–fluid and fluid–fluid interactions.

The objective of this research is to understand, through analysis and experiment, how fluids in pores affect the geophysical and transport properties of reservoir rocks.

Summary of Technical Progress

During the reporting period, research was carried out in the following areas: formation factor and the distribution of a wetting phase in the pore space of Berea sandstone and numerical simulations of fluid flow in porous rock using graph theory. A comprehensive report entitled “Measurements and Analysis of Seismic Properties” on the seismic measurements and their analysis was completed.

Formation Factor and the Distribution of Wetting Phases in Pore Space of Berea Sandstone

In summary, laboratory electrical conductivity data for fully and partially saturated samples of Berea sandstone with a wetting fluid are presented. In these studies, a wetting fluid (paraffin wax) is used that can be frozen in place at controlled saturations to allow examination of the occupied pore space after the experiment. The effective formation factors for an electrolyte in the pore spaces not occupied by the paraffin are measured at various saturations after solidifying the paraffin in place. The effect of clay and other surface-reactive minerals on Berea sandstone formation factor is first isolated and their surface conductance contribution to overall conductivity assessed. The electrical conductivity experimental data are analyzed in light of the role of the pore structure on the wetting fluid invasion process with the aid of direct observation of fluid distributions at each saturation regime, a complete pore cast, and its corresponding rock section.

Effect of Pore Structure and Topology

The electrical conductivity data (Fig. 1) have been studied in light of the wetting fluid distributions at each saturation regime (Figs. 2, 3, and 4) with the aid of a complete rock pore cast (Fig. 5) and its associated rock section (Fig. 6) to explore how pore structure and topology control the transport property of consideration. The rock pore cast was obtained from a rock specimen that had been fully impregnated with Wood’s metal alloy and the quartz grains removed by hydrofluoric acid. The rock pore cast and its associated rock section clearly reveal that the pore space is composed by grain contact porosity (thin

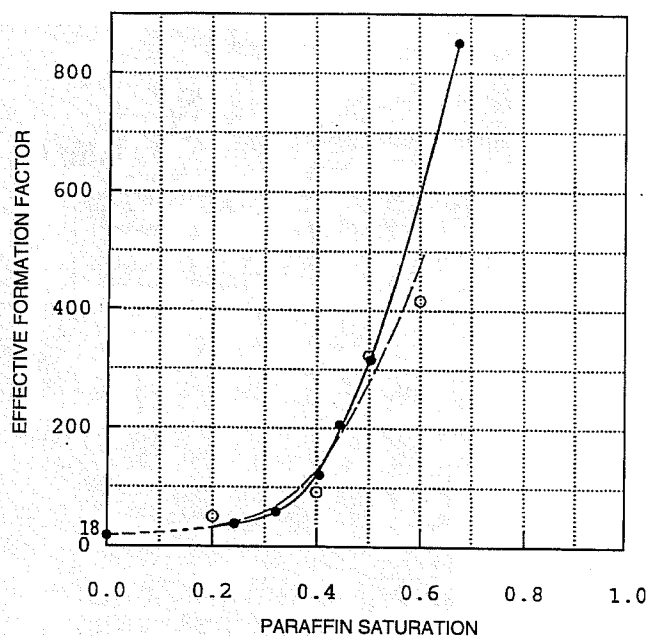


Fig. 1 Effective formation factor vs. hydrocarbon paraffin saturation for Berea sandstone. The pore space was partially saturated with hydrocarbon paraffin. The remaining portion of the pore space was filled with a 0.5M zinc nitrate solution. Cases A (○) and B (●) correspond to experimental data on samples subjected, or not subjected, to a formation factor measurement previous to paraffin application, respectively.

sheets and micropores) and intergranular porosity. Figure 2 shows a scanning electron microscope (SEM) micrograph collage of a section of Berea sandstone that has been partially saturated with approximately 20 to 30% paraffin. The gray phase corresponds to quartz grains, the white phase corresponds to pores that have been impregnated with paraffin, and the black phase corresponds to the remaining pore space filled with blue epoxy for imaging purposes. The paraffin has invaded grain contact pore space (i.e., thin sheets and micropores) and intergranular pore space connected by smaller throats while only coating available intergranular channels connected by larger throats. A substantial effect on effective formation factor is observed. Therefore, the fraction of the pore structure connected by smaller constrictions (e.g., grain contact pore space) provides important alternative routes to intergranular conduits connected by larger throats for the ions to travel. Figure 3 displays an SEM collage of a rock section partially saturated with approximately 40 to 50% paraffin. At this stage, intergranular conduits connected by the larger throats are being filled. Also, a portion of the electrolyte has apparently lost continuity as the paraffin saturation is increased over ~30% so that the resistivity increased at a faster rate. Hence, a larger effect on effective formation factor is observed. Figure 4 displays an SEM collage of a rock section partially saturated with approximately 60 to 70% paraffin. Almost all intergranular conduits connected by larger throats have been filled. A few intergranular pores not well connected still remain unfilled. When paraffin saturation is about 70% the whole pore structure behaves as disconnected.

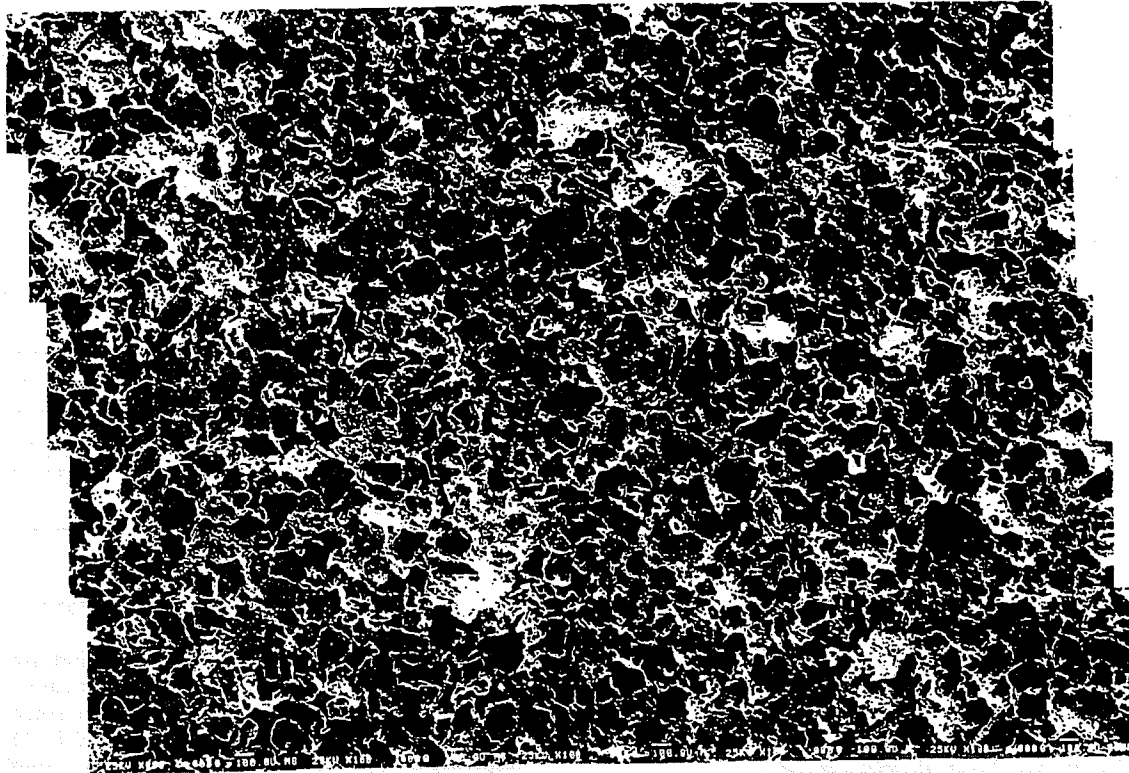


Fig. 2 Scanning electron micrograph collage of a Berea sandstone section impregnated with approximately 20 to 30% paraffin. Actual width of field is about 6 mm. The gray phase denotes quartz grains, the white phase denotes pores saturated with paraffin, and the black phase denotes remaining pores filled with blue epoxy for imaging purposes.

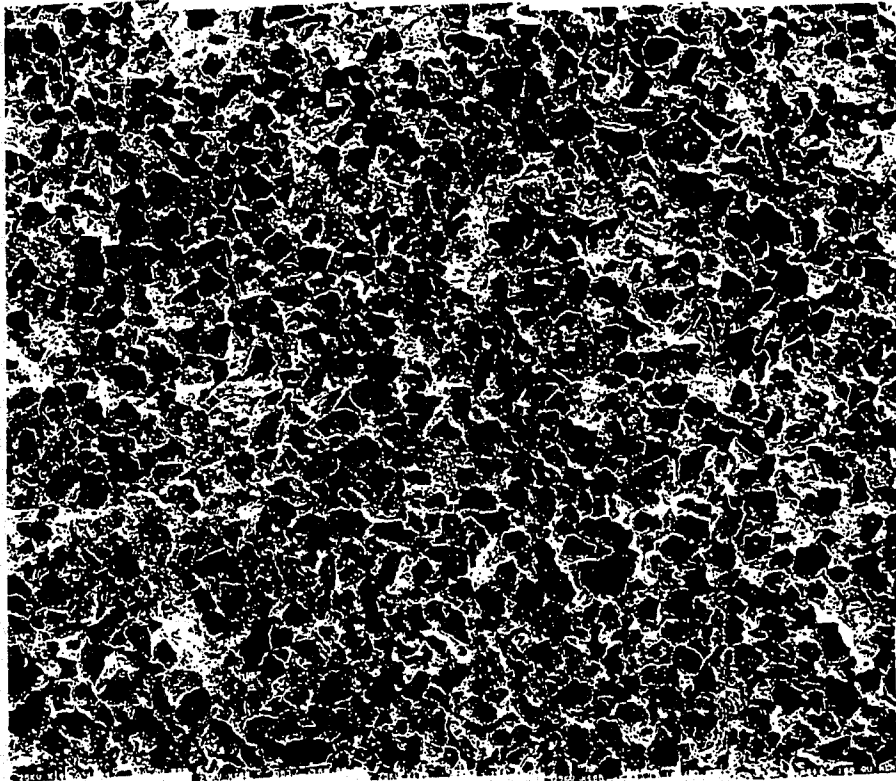


Fig. 3 Scanning electron micrograph collage of a Berea sandstone section impregnated with approximately 40 to 50% paraffin. Actual width of field is about 6 mm. The gray phase denotes quartz grains, the white phase denotes pores saturated with paraffin, and the black phase denotes remaining pores filled with blue epoxy for imaging purposes.

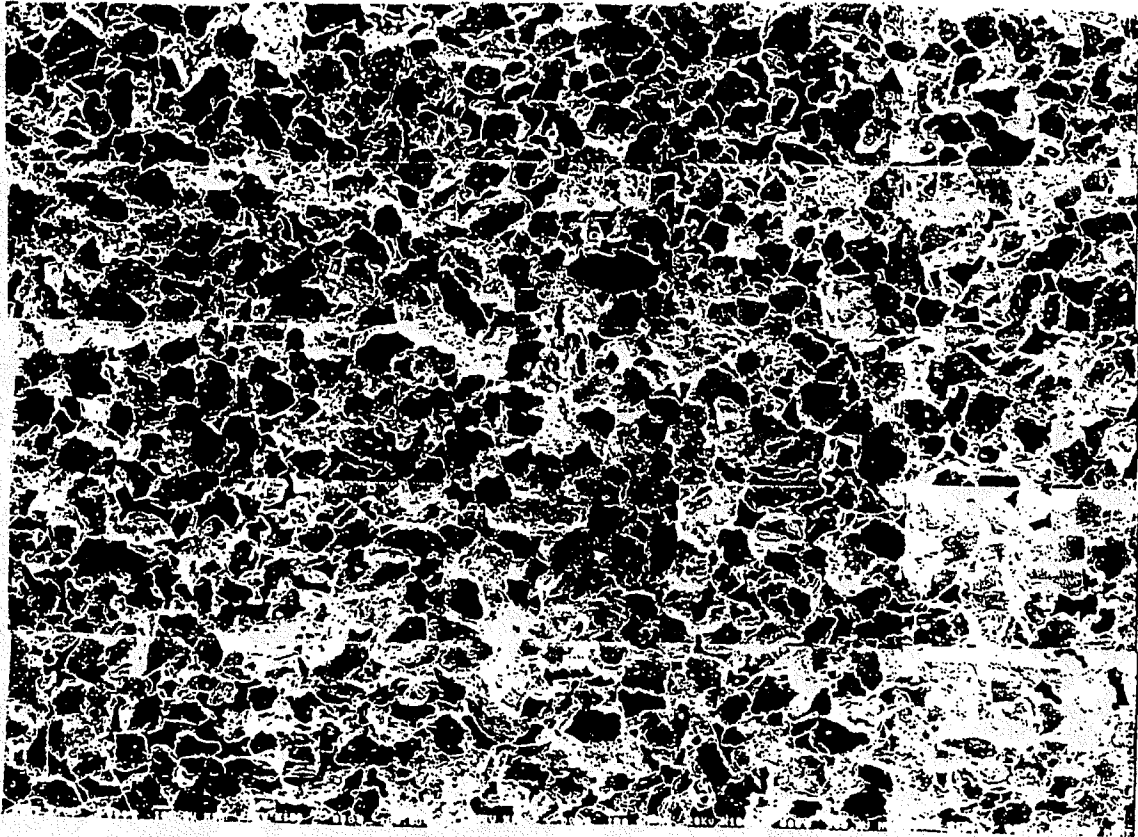


Fig. 4 Scanning electron micrograph collage of a Berea sandstone section impregnated with approximately 60 to 70% paraffin. Actual width of field is about 6 mm. The gray phase denotes quartz grains, the white phase denotes pores saturated with paraffin, and the black phase denotes remaining pores filled with blue epoxy for imaging purposes.

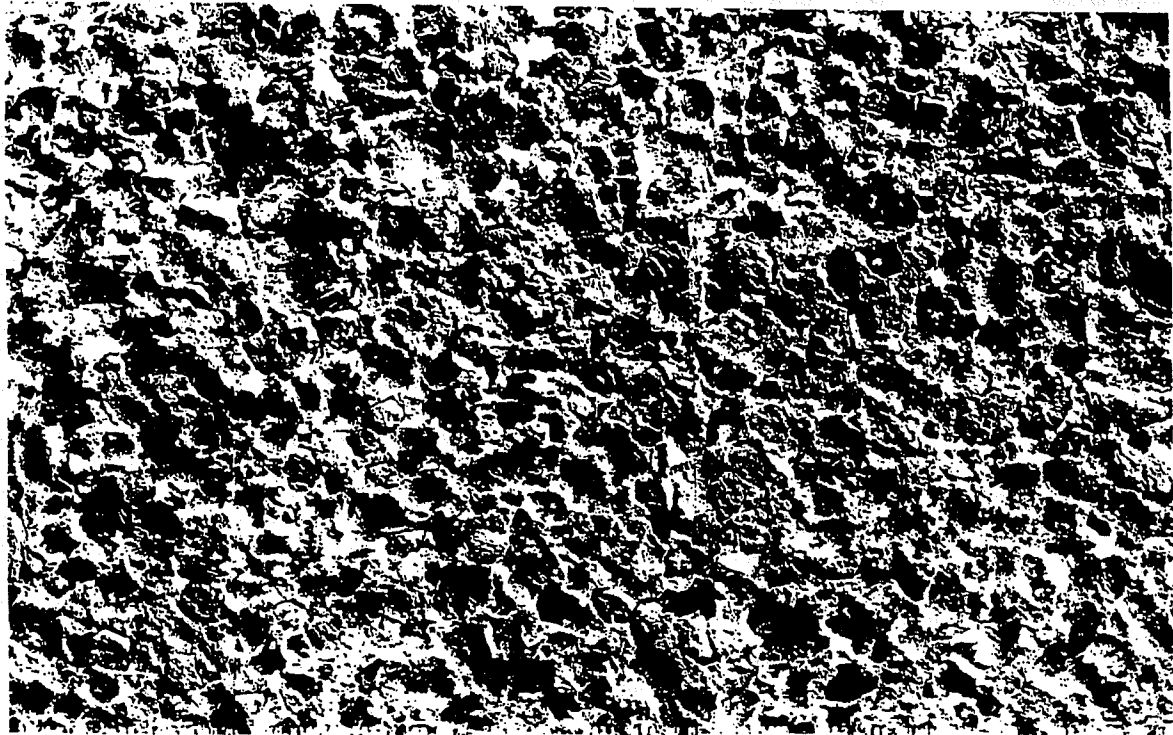


Fig. 5 Scanning electron micrograph collage of a Berea sandstone pore cast. Actual width of field is about 6 mm. The rock pore space was filled with Wood's metal alloy and the quartz grains removed by hydrofluoric acid to allow direct observation of the pore structure.

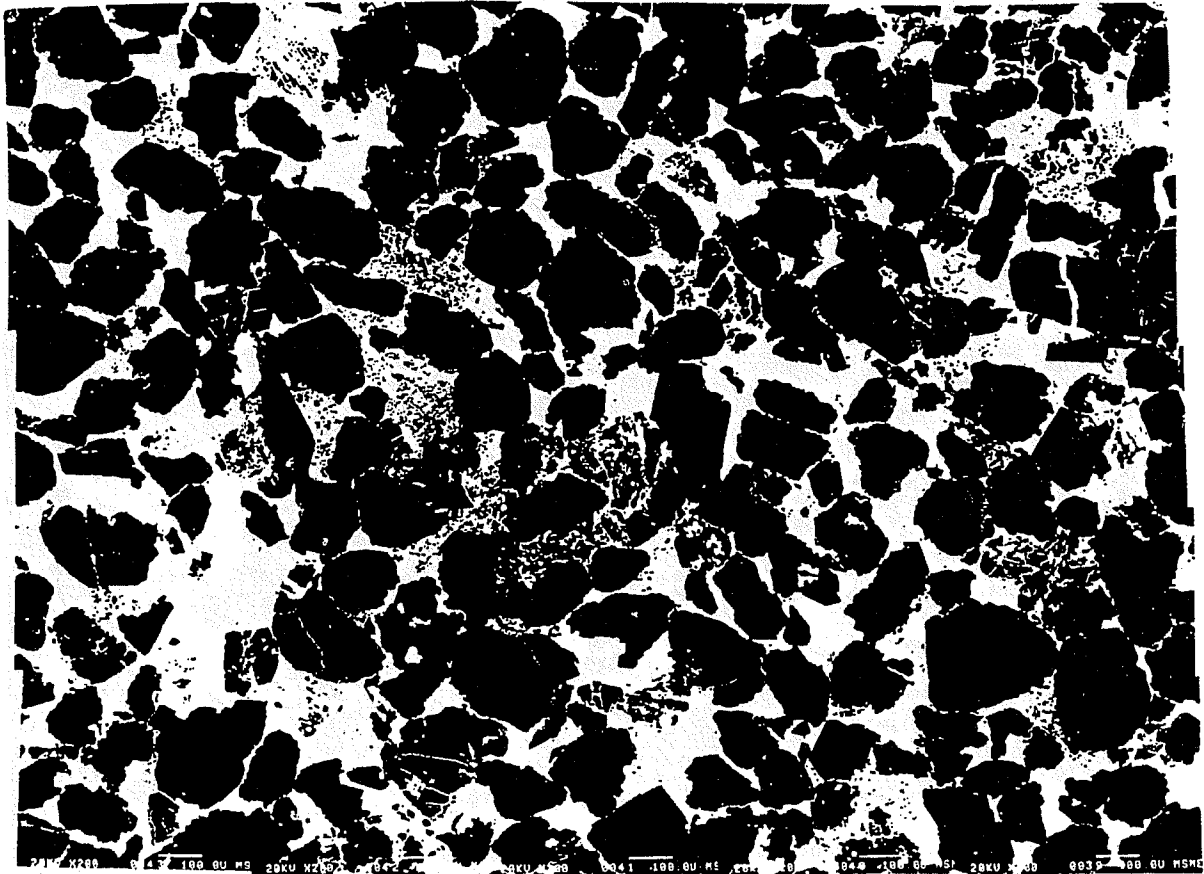


Fig. 6 Scanning electron micrograph collage of a Berea sandstone rock section fully impregnated with Wood's metal alloy. Actual width of field is about 3 mm. The gray phase denotes quartz grains and the white phase denotes pores saturated with the alloy. The section reveals that the pore space is composed by grain contact (i.e., thin sheets and micropores) and intergranular porosity.

Application of Graph Theory to Two-Phase Flow in Rock Matrix

Work continued on the refinement of computer programs to simulate flow in stochastic and spatially correlated network models of pore structure and topology.

Seismic Wave Propagation

Measurements reported earlier have been consolidated into a single report and the results have been analyzed with a newly developed Boundary Integral Code to simulate wave propagation in granular media. Much of the period was spent performing the numerical calculations and writing the report entitled "Measurements and Analysis of Seismic Properties," which was then submitted to the Department of Energy.

Bibliography

- Anderson, W. G., 1986, Wettability Literature Survey. Part 3: The Effects of Wettability on the Electrical Properties of Porous Media, *J. Petrol. Technol.*, 12: 1371-1378.
- Archie, G. E., 1942, The Electrical Resistivity Log as an Aid in Determining Some Reservoir Characteristics, *Trans. Am. Inst. Min. Eng.*, 146: 55-62.
- Khilar, K. C., and H. S. Fogler, 1984, The Existence of a Critical Salt Concentration for Particle Release, *J. Colloid Interface Sci.*, 101: 214-224.
- King, M. S., R. W. Zimmerman, and R. F. Corwin, 1988, Seismic and Electrical Properties of Unconsolidated Permafrost, *Geophys. Prospect.*, 36: 349-364.
- Schlueter, E., 1991, *The Effect of Clay on Rock Resistivity and the Mechanisms Affecting Clay-Fluid Electrolytic Conduction*, Soil Surface and Colloid Chemistry Course (SS 221) Report, University of California, Berkeley.
- Schlueter E., L. R. Myer, N. G. W. Cook, and P. A. Witherspoon, 1992, *Relative Permeability and the Microscopic Distribution of Wetting and Non-Wetting Phases in Pore Space of Berea Sandstone*, Lawrence Berkeley Laboratory Report, in preparation.
- Schlueter, E., L. R. Myer, N. G. W. Cook, and P. A. Witherspoon, 1992, *Formation Factor and the Microscopic Distribution of Wetting Phase in Pore Space of Berea Sandstone*, Lawrence Berkeley Laboratory Report.
- Sposito, G., 1984, *The Surface Chemistry of Soils*, Oxford University Press, New York.
- Suarez-Rivera, R., 1991, personal communication.
- Williams, D. J. A., and K. P. Williams, 1978, Electrophoresis and Zeta Potential of Kaolinite, *J. Colloid Interface Sci.*, 65: 79-87.
- Wyllie, M. R. J., 1963, *The Fundamentals of Electric Log Interpretation*, Academic Press, Inc., New York.

RESERVOIR CHARACTERIZATION OF PENNSYLVANIAN SANDSTONE RESERVOIRS

Contract No. DE-AC22-90BC14651

**University of Tulsa
Tulsa, Okla.**

**Contract Date: Aug. 9, 1990
Anticipated Completion: Aug. 8, 1993
Government Award: \$108,207**

**Principal Investigator:
Balmohan G. Kelkar**

**Project Manager:
Rhonda Lindsey
Bartlesville Project Office**

Reporting Period: Oct. 1–Dec. 31, 1992

Objectives

The overall objectives of this work are to (1) investigate the importance of various qualities and quantities of data on the optimization of waterflooding performance and (2) study the application of newly developed, geostatistical techniques to analyze available production data to predict future prospects of infill drilling.

Specifically, to satisfy the first objective, the feasibility of applying fractal geometry concepts to characterize individual formations will be studied; a three-dimensional (3-D) conditional simulation program to define reservoir properties at various scales will be developed; a method to integrate the data collected at various scales, including the well test and the core data, will be established; and the use of outcrop data in describing subsurface reservoir details will be investigated. To satisfy the second objective, various techniques to utilize the production data, including initial potential and the production decline, will be investigated so that a possible location for a future infill well can be proposed. The techniques investigated will include geostatistical analyses. The study will be restricted to Pennsylvanian sandstone reservoirs commonly found in Oklahoma.

Summary of Technical Progress

Collection of Data

The data collection phase is complete. The data were collected from the Burbank and the Glenn Pool fields. The data include core and log data as well as production history from both fields.

Waterflooding Optimization

Characterization with the Use of Fractals

The primary goal of this work is to study the feasibility of applying the fractal geometry technique to characterize producing formations. This work has been completed. The main conclusions of this work can be summarized as follows:

- On the basis of these results, rescaled range (R/S) analysis and box counting are the two most reliable methods for determining the intermittency exponent H (Ref. 1). Of these two methods, the box counting method seems to fit the variogram data best. As a result, the box counting method for analyzing vertical wellbore data has been recommended.
- Most of the wellbore data include the effect of geological environment as indicated by localized trends in the data. When the trends are removed before analyzing the vertical data, the analysis indicates a much more consistent trend for intermittency exponent values. The typical values for both the carbonate and the sandstone fields lie between 0.75 and 0.8 (Refs. 2 and 3).
- On the basis of exhaustive comparisons between the field wellbore data and the simulated wellbore data (using the method of conditional simulated annealing), it was observed that, in general, the fractional Gaussian noise (fGn) models do a better job describing the areal heterogeneities in carbonate reservoirs, whereas the fractional Brownian motion (fBm) models adequately describe the sandstone reservoirs. This observation may be important in constructing three-dimensional (3-D) reservoir descriptions when very limited data are available.

Three-Dimensional Conditional Simulation

A method of simulated annealing was selected to describe the reservoir in three dimensions. Originally proposed by Farmer,⁴ the method is based on the principle of swapping randomly generated values having the same histogram as the sampled values. After every swap, a predefined energy function is calculated and compared with the energy function in the previous step. If the new function is smaller, the swap is accepted. If the new energy function is greater, the swap may still be accepted, depending on the probability of acceptance. The process of swapping will continue until a desired level of energy function is reached. The method is flexible and allows incorporation of various constraints when generating the reservoir properties.

Although the technique of annealing is robust, one of the potential problems in using annealing simulation is its speed. Compared to other simulation programs, the program of annealing is relatively slow. One of the alternatives that has shown promising results is the use of a different initial distribution. In this approach, instead of using a completely random distribution as the initial distribution, a distribution based on a simple linear interpolation is created. In three dimensions, data at each datum in each conditioning well are taken and a smooth surface at that datum is created with a

linear interpolation. A stack of surfaces will generate a 3-D distribution. After generation of the initial distribution, a random component at each location is added based on the average variance of the differences between the conditioning data points at each datum to match the generated distribution with the distribution of the conditioning data. The calculation of the initial distribution takes a few minutes and is a small overhead on the total computations. With this newly created distribution, a simulated annealing procedure is initiated. Instead of a conventional method, a greedy algorithm was used to increase the speed of the program. When compared with the conventional annealing method, this modified method takes only 15 to 20% of the time of the original method.

In addition to making the program faster and more flexible, an investigation is under way to determine the possibility of incorporating other types of data when describing reservoir characteristics. In addition to conditional data and the variogram models, well test data are another important input data that can be used for reservoir description. Well test data are collected over a much larger volume than the core data and are more closely representative of the grid block values than are the core data. Unfortunately, conventional kriging and associated conditional simulation methods cannot incorporate the well test data in reservoir description. Simulated annealing is flexible enough to accommodate the well test data through an appropriate objective function. This objective function should include the well test data as some representative average of nearby wellbore data.

The type of average the wellbore data represents needs to be determined before the representative average is used as an objective function. Recently, Oliver⁵ presented an analytical technique to estimate the well test permeability value for heterogeneous reservoirs. The method is restricted to certain simplifying assumptions. With the Oliver solution, the instantaneous permeability determined from the well test data was compared with different averaging schemes to calculate effective permeability from small-scale heterogeneities. For these purposes, the ECLIPSE 100 simulator was used. This procedure was tested over a wide range of heterogeneities. The Dykstra-Parsons coefficient was varied between 0.2 and 0.8, and the normalized scale length was varied between 0.0 and 0.5. The results indicate that Oliver's method is valid if the geometric average of the permeability values is used. In most cases, the difference between the well test value and the average value was less than 10%.

With the use of Oliver's solution, the well testing constraint was implemented in the simulated annealing program. The program requires the input of instantaneous well test permeability values at various times. With that as a constraint, the simulated annealing program is run; this honors the well test data. To validate the utility of the program, the well test was flow simulated with the generated distribution, and the pressure and the pressure derivative data of the "truth" case were compared with the simulated data. So long as early time data were included as a constraint, the comparison between the two data sets was satisfactory.

This program will be optimized by investigating the minimum number of times at which the well test values need to be defined. Also, the possibility of defining the Oliver's solution as a constraint in a different manner is being investigated. Eventually, a field well test will be used to compare and validate the results.

Effective Properties for a Grid Block

Reservoir properties are measured on various scales. Core data are collected on a size of 2 in., whereas the well test data are collected on a reservoir size of thousands of cubic feet. From a simulation point of view, determination of the grid block properties is of interest to us. A typical grid block size may vary between 10 and 1000 ft in size.

The estimation of an effective property of a grid block is being investigated with both analytical and numerical methods. On the analytical side, a method has been developed to predict an effective tensor of a grid block with the small-scale heterogeneities present in the grid block as two-dimensional (2-D) distributions. The method is fast and flexible and compares very well with the numerical results. When compared with other literature methods, such as power averaging and renormalization methods, the effective tensor method predicts the miscible displacement performance much better than any other method.

The method has also been tested for immiscible displacements. Again, compared with other literature methods, the effective tensor method predicts the effect of small-scale heterogeneities on upscaling much more consistently than other methods.

As an extension of this work, a scheme has also been developed to incorporate the permeability tensor in conventional reservoir simulators. The scheme is based on finite-element principles. The method is generalized, and it reduces to the methods proposed in the literature under certain simplified conditions. The method has been tested by incorporating it in a black oil simulator. A good comparison between simulated results using the detailed heterogeneity model and simulated results using the upscaled heterogeneity model indicates the usefulness of the method.

Extending the method to 3-D grid blocks is under way. The preliminary analysis has already started and some results are expected before the next report.

Outcrop Studies

An outcrop called a Bluejacket sandstone located approximately 45 miles northeast of Tulsa has been selected for further studies. It contains the same Red Fork sand as the sand from which Glenn Pool field is producing. The outcrop has been surveyed and the facies mapped using a mapping program.

In addition to the collection of permeability data, 12 wells have been drilled behind the outcrop. A typical distance between two wells is less than 50 ft with an exception of one well that is drilled about 400 ft away behind the outcrop to get a complete geological section. The typical depth of a well is

in the range of 50 to 80 ft. All these wells have been cored and a suite of logs has been run in these wells, including gamma-ray and neutron density. In addition, a Formation Micro-Scanner (FMS) log has been run through one of the wells.

The whole cores have been slabbled and photographed. The cores have also been logged with a gamma-ray device. In addition, more than 1000 minipermeameter readings have been taken to quantify the vertical variability of permeability distributions. Approximately 200 1-in. core plugs, some of them vertical, have been taken. Additionally, a large number of minipermeameter readings have been collected on the outcrop by investigating the horizontal and several vertical transects.

To validate the minipermeameter results, the permeability values measured with the conventional core analysis were compared with the permeability values measured with the minipermeameter. The results indicate an excellent match. Vertical variograms were also generated for each well using the minipermeameter readings as well as the gamma-ray logs. The results indicate that the average dimension of a geologic unit can be estimated using the variogram structure as a basis. If the hole effect in the variogram structure is observed and then compared with the distance at which the minimum value is reached in the hole, that distance correlates very well with the average geological unit as described by the geologist. This method may prove to be useful in quantifying and validating the geological interpretation of a well log.

Infill Drilling

A synthetic reservoir was used to develop a procedure to locate infill drilling prospects. The main advantage of a synthetic reservoir is that production and operational constraints imposed upon the actual production are not a concern. Further, drilling and location of the wells can be controlled.

With these simulations, the data will be analyzed to predict possible in-fill locations within the reservoir. One of the techniques currently being explored is the use of connectivity function to define relative continuity in the reservoirs. On the basis of such reservoir performance parameters as breakthrough, water/oil ratio, or injection rate, the reservoir continuity can be qualitatively described. If this continuity can be quantified, this information can be used in a conditional simulation method to describe the reservoir. One method flexible enough to incorporate this continuity function is simulated annealing.

At present, several simulation runs have been conducted using synthetic data. Some of the performance parameters have been related to the continuity functions. Results indicate that the continuity function is closely related to the performance of the reservoir. Also, if the continuity function is incorporated in the annealing program, the level of uncertainty in the reservoir performance can be reduced. This function has been incorporated in a simulated annealing program. The comparison between the "truth case" simulation and the simulation carried out using alternate images of

the reservoir indicates that the continuity function is extremely important in characterizing flow behavior of the reservoir. One disadvantage of adding additional constraint in the annealing program is that it slows down the speed of the program. However, by making some additional simplifications, a code has been developed that only takes 10 to 20% more time to generate the reservoir description incorporating the connectivity function.

Once the production parameters are related to continuity parameters for water flooded reservoir, the primary production from a synthetic reservoir will be investigated and its relationship to the continuity as well near wellbore parameters.

References

1. T. A. Hewett, *Fractal Distributions of Reservoir Heterogeneity and Their Influence on Fluid Transport*, paper SPE 15386 presented at the 1986 SPE Annual Technical Conference and Exhibition, New Orleans, La., Oct. 5-8, 1986.
2. Quarterly DOE Report, *Reservoir Characterization of Pennsylvanian Sandstone Reservoirs* (Contract No. DE-AC22-90BC14651), Jan. 1-Mar. 31, 1992.
3. Quarterly DOE Report, *Reservoir Characterization of Pennsylvanian Sandstone Reservoirs* (Contract No. DE-AC22-90BC14651), July 1-Sept. 30, 1992.
4. C. L. Farmer, *Numerical Rocks*, paper presented at the Joint IMA/SPE European Conference on the Mathematics of Oil Recovery, Robinson College, Cambridge University, July 25-27, 1989.
5. D. S. Oliver, *Estimation of Radial Permeability Distribution from Well Test Data*, paper SPE 20555 presented at the 1990 SPE Annual Technical Conference and Exhibition, New Orleans, La., Sept. 23-26, 1990.

LAWRENCE BERKELEY LABORATORY/ INDUSTRY HETEROGENEOUS RESERVOIR PERFORMANCE DEFINITION PROJECT

Lawrence Berkeley Laboratory
University of California
Berkeley, Calif.

Contract Date: Apr. 1, 1992
Anticipated Completion: September 1995
Government Award: \$275,000

Principal Investigators:

J. C. S. Long
E. L. Majer
L. R. Myer

Project Manager:

Robert Lemmon
Bartlesville Project Office

Reporting Period: Oct. 1-Dec. 31, 1992

Objectives

The purpose of this work is to validate geophysical and hydrological techniques for characterizing heterogeneous reservoirs in the most optimal (economic) manner. The overall goal of the project is to develop a methodology that can be used by the petroleum industry in a variety of heterogeneous regimes for characterizing and predicting the performance of petroleum reservoirs.

This will be accomplished through a cooperative research program between Lawrence Berkeley Laboratory (LBL), British Petroleum, Inc. (BP), and the University of Oklahoma (OU), which is focused on the characterization of heterogeneous reservoirs in a meander belt porous medium formation. BP has done characterization and data integration at several test facilities. The present program will continue BP's multiyear efforts at the Gypsy site in northeastern Oklahoma. The resulting research will integrate various geophysical and hydrological methods and apply them at a well-calibrated and characterized site, where their utility can be assessed. This cooperation will allow techniques developed for waste storage and geothermal energy to be adapted for use in heterogeneous and fractured reservoirs. The work will be coordinated with the crosswell Electromagnetic Research and Development (EM R&D) Project and the LBL/Morgantown Energy Technology Center (METC) Reservoir Performance Definition Project.

Summary of Technical Progress

Hydrologic-Related Work

The assessment of the Gypsy subsurface pilot-site well-test data continued as described in the previous quarterly report. An example of a strategy for cross-validation of the hydrologic inversions is outlined. Changes were made to the computer program that will be used for the inversions for treating the pilot-site data.

The conceptual model of the subsurface pilot site indicates that the lower sand channel is hydrologically isolated from the upper and middle sand channels, and the plan for hydrological inversion involves an examination of well tests conducted solely in the lower sand channel first. A total of five well tests were done using lower-channel intervals; these yielded five pressure transients recording buildup in pumping wells and twelve pressure transients recording drawdown and recovery in observation wells. The pressure transients available for the hydrologic inversion are illustrated schematically in Fig. 1. A line connecting two wells indicates that an interference test was conducted between these two wells using lower-channel intervals. For example, the connection between wells 8 and 9 represents the test in which the lower interval of well 8 was pumped and pressure was observed in the lower interval of well 9. For three of the connections (well-1-to-well-5, well-1-to-well-11, and well-1-to-well-7), two well tests were done, which provided redundant information and enabled a deter-

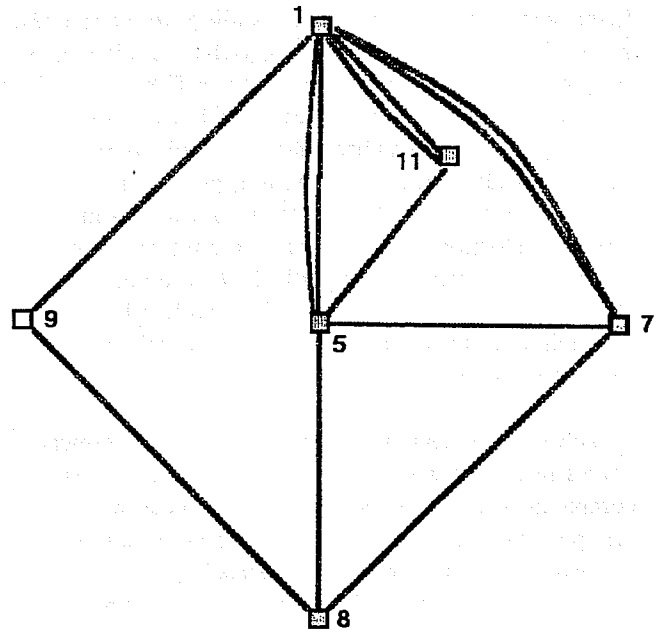


Fig. 1 Schematic diagram illustrating the well tests conducted in the lower sand channel of the Gypsy subsurface pilot site. □, well. ◻, buildup test. —, interference test.

mination of the precision of the flow rate and pressure measurements. This leaves nine unique interference-test pressure transients to use in the inversions.

In cross-validation an inversion is done using some of the pressure transients, then subsequent checks are made of the resulting model by trying to predict the remaining pressure transients. The difficulty of the cross-validation exercise can be controlled by choosing how much and which data to omit from the inversion. Figure 2 shows schematically where the hydrologic properties have the greatest impact on a well test in which well 5 is pumped and pressures are observed in wells 1 and 7. Conversion of the lines in Fig. 1 to broader elliptical regions allows visualization of the information on the hydrologic property distributions gained by the various interference tests done on the lower sand channel, and thus their relative importance to the inversion process. For example, a cross-validation that inverts interference data from all five well tests together but omits the well-1-to-well-11 data would be likely to be successful (i.e., able to predict the missing data) on the basis of information gained from the well-1-to-well-7 data. In contrast, a cross-validation that omits the well-9-to-well-1 and well-9-to-well-8 data would be much more difficult because none of the other tests focus on the region around well 9. A variety of cross-validation exercises has been devised, successively omitting different subsets of the pressure transients shown in Fig. 1. An analogous analysis has been done for the upper/middle sand channel. Inversion using pressure transients from buildup tests requires special care because wellbore effects can mask the impact of hydrologic properties. Therefore, it may be preferable to do cross-validation by omitting the buildup data and trying to predict it rather than the other way around.

in much more significant improvements in execution time, on the order of a factor of 100.

Seismic-Related Work

In the last quarterly report, it was noted that the mini cross-hole seismic survey could not be carried out at the Gypsy outcrop site because the boreholes would not hold water for a long enough period of time. Means to seal the boreholes have been investigated and a decision was made to use an impermeable liner that can be emplaced for the test and then removed afterward. Such liners are being used at Lawrence Livermore National Laboratory for studies being carried out in conjunction with a soil steam-cleaning project. The mini cross-hole seismic survey will be conducted later this year.

Reference

1. J. C. S. Long, C. Doughty, K. Hestir, and S. Martel, Modeling Heterogeneous and Fractured Reservoirs with Inverse Methods Based on Iterated Function Systems, in *Proceedings of the Third International Reservoir Characterization Technical Conference*, Tulsa, Oklahoma, November 3-5, 1991; also published as Report LBL-31333, Lawrence Berkeley Laboratory, 1992.

GEODIAGNOSTICS FOR RESERVOIR HETEROGENEITIES AND PROCESS MAPPING

Sandia National Laboratories
Albuquerque, N. Mex.

Contract Date: Oct. 1, 1987
Anticipated Completion: Sept. 30, 1993
Government Award: \$200,000

Principal Investigators:

M. W. Scott
A. J. Mansure
J. R. Waggoner

Project Manager:

Robert Lemmon
Bartlesville Project Office

Reporting Period: Oct. 1-Dec. 31, 1992

Objective

The objective of this project is to increase the producibility of existing oil resources by better definition of reservoir heterogeneities and monitoring of oil recovery processes through the application of advanced geodiagnostics systems. This project provides a geologic and reservoir engineering perspective for the integrated Electromagnetic Geophysical

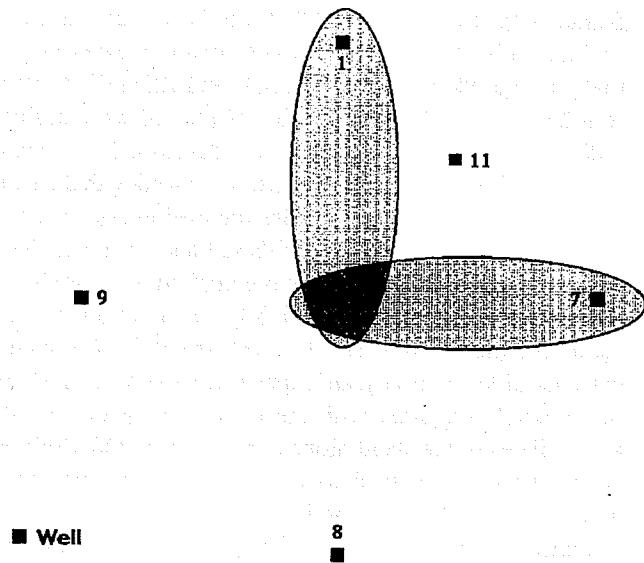


Fig. 2 Schematic diagram showing where hydrologic properties have the most impact on a well test in which well 5 is pumped and pressure changes are observed in wells 1 and 7.

An inverse method based on iterated function systems (IFS)¹ will be used to analyze the well-test data. Two coding changes are being made to the IFS inversion computer program for treating the subsurface pilot-site well-test data. First, the IFS inversion code includes a finite-element model called TRINET to do the forward calculation (i.e., numerically simulate the well test) each iteration. Currently TRINET requires either constant-flow-rate or constant-head boundary conditions at pumping wells. To analyze the subsurface pilot-site well tests, which contain several short pulses followed by a constant flow rate and then a shut-in period, time-varying flow rates need to be specified as boundary conditions at pumping wells. Second, the current version of the IFS inversion code only inverts one well test at a time (although one well test may contain multiple pressure transients corresponding to multiple observation wells). Different combinations of pumping and observation wells in a sequence of tests provide information on a more extensive region than does a single test, so the capability to co-invert multiple well tests is also being added to the code. In a sense, co-inverting multiple tests may be thought of as inverting one long test in which flow rates change with time as different wells are pumped and shut in to be used as observation wells. However, some generality is lost in the treatment of multiple tests as one long test, so alternative coding options are being considered as well. All the coding changes required to analyze the subsurface pilot-site well-test data are simple in principle and should be straightforward to complete.

Efforts are also under way to improve the efficiency of the IFS inversion code. Preliminary streamlining has resulted in a factor of 2 to 3 speedup for execution of a sample problem. A more significant change in the architecture of the code should allow it to run on a parallel computer and could result

Method research and development program being coordinated by the Department of Energy at Sandia National Laboratories, Lawrence Livermore National Laboratory, Lawrence Berkeley Laboratory, and the University of California at Berkeley. FY92 tasks include (1) develop and apply an oil-field recovery/resistivity simulator (ORRSim) system, (2) apply reservoir characterization concepts to bulk resistivity and electromagnetic (EM) field data interpretation, (3) acquire and characterize an industry field site, and (4) field test reservoir characterization data collection.

Summary of Technical Progress

During most of this quarter, this project was inactive in order to reserve resources for the large data interpretation effort anticipated later in the fiscal year. Late in the quarter it was decided that a code development task should be started to prepare for the upcoming data interpretation task and to provide a technology transfer solution. As reported in the May and June 1992 monthly reports, industry has approached

Sandia with questions about ORRSim. To address this industry interest in ORRSim, work was started to create a subroutine package incorporating TRACK and RESIST, to be referred to as ORRSub, that can be transferred more easily to industry. Previously, ORRSim was developed as a stand-alone post-processing program that interfaced with the simulation program through data files dumped every time step. Because of the very large size of these files, it was decided to create a subroutine package that is compiled with the simulation program. This results in slightly larger storage requirements for the TRACK and RESIST specific data, such as concentration, resistivity, and input data. However, this should be minimal compared with the huge amount of data that accumulates in the stand-alone configuration. ORRSub will be functionally identical to ORRSim, so previous reports describing ORRSim are applicable to ORRSub as well. This response to industry is a critically important part of the overall program goal to transfer EM technology to the petroleum industry.

ADVANCED SEISMIC GEOCHARACTERIZATION— BOREHOLE ACOUSTIC SOURCE

Los Alamos National Laboratory
Los Alamos, N. Mex.

Contract Date: Mar. 1, 1988
Anticipated Completion: Sept. 30, 1993
Government Award: \$200,000
(Current year)

Principal Investigators:
Robert O. Hedges
Ray Engelke

Project Manager:
Robert Lemmon
Bartlesville Project Office

Reporting Period: Oct. 1–Dec. 31, 1992

prototype tool include providing many repetitive detonations that can be fired during one trip in the wellbore; downhole mixing, encapsulation, and detonation of individual charges; and operation on a standard 7-conductor wireline. The seismic source and its associated instrumentation will not exceed 108 mm (4.25 in.) in diameter and 5.5 m (18 ft) in length.

Summary of Technical Progress

A highly energetic source is required to maximize the distance between the seismic source and the receivers from which useful data can be obtained. To satisfy the high energy requirement, the source will use an insensitive explosive that can only be initiated by sophisticated, but nonetheless low-cost, technical means. Because the source is explosive, a major consideration is the design of a tool that is inherently safe. To accomplish this, the explosive will be manufactured downhole, in single-shot quantities, using two chemicals, neither of which is classified as explosive by the U.S. Department of Transportation.

During the first quarter there was further reassessment of requirements that will make this seismic source more useful to the oil industry. The ability to operate in as great a number of wells as possible and the need to obtain useful data at greater well spacings were the problems assessed. As a result, the outside diameter requirement was further reduced to 4.25 in. from 4.50 in. and the explosive charge size was modified from an exclusive 1-g charge to a range of 1 to 10 g, which can be selected prior to each trip in a wellbore. These changes to requirements, in addition to increasing the technical challenge for design of the tool, will also greatly increase the usefulness of this seismic source, particularly for crosswell tomography applications.

Objective

The goal of this effort is to develop and field test a prototype seismic source that will meet oil-field requirements for low-cost, high-resolution characterization of rock masses between wellbores. The source must deliver sufficient energy to transmit a high-frequency signal over 300 to 900 m (1,000 to 3,000 ft) between boreholes in typical oil reservoirs comprised of sandstone or limestone, at depths ranging from 100 m (300 ft) to 4,600 m (15,000 ft). The goals for the

The underwater firing of slappers and the underwater detonation of the liquid explosive mixture were accomplished during this period. Two slapper assemblies without explosive were fired to investigate the possibility of voltage breakdown in water. The slappers performed flawlessly at 5000 V and at 8000 V. An explosive assembly with the liquid contained in a thin Teflon "sack" was detonated at 5000 V. A second explosive assembly did not detonate at 4750 V, which is the lower threshold at which detonation has been achieved for this containment configuration in air. These tests demonstrate that operation in wellbore fluids does not present basic problems for the slapper/explosive system that has been chosen for this project.

Test assemblies of the tamper, slapper, barrel, and barrier were pressure tested to establish response to actual hydrostatic pressure. Four assemblies representing the actual configuration that will be used in a tool were subjected to hydrostatic pressures up to 10,000 psi. (The operational goal is 6,500 psi, equivalent to 15,000 ft well depth.) One of the assemblies was damaged because of leakage of pressure between the tamper and the slapper. The other three assemblies were undamaged and did not leak, even though one specimen received an overpressure surge as a result of an equipment malfunction. These tests confirm that the chosen materials for the barrel and barrier will perform as expected but that extreme care must be taken to ensure proper assembly.

Small-scale safety tests were performed with the explosive liquid mixture which indicate that this explosive is stable to at least 130 °C and probably to higher temperatures. Additional testing will be done to establish a more specific upper temperature limit. This testing indicates that normal wellbore temperatures will not be a problem for this explosive source.

A complete, formal response to the Request for Quotation for a test contractor was received and a complete evaluation of the technical and cost quotation has been prepared. An actual contract should be placed by mid-January. This contract consists mainly of testing to characterize the performance of the slapper/explosive system at elevated temperatures and hydrostatic pressures. A pressure test chamber in which these firings at elevated temperatures and hydrostatic pressures can be conducted has been completed. This chamber is available for the contractor to begin testing as soon as possible.

On Dec. 10, 1992, a presentation of the status of this project was made to the annual meeting of the Crosswell Seismic Forum. The result of the Forum's evaluation of progress made on this project has not been announced as of the date of this report. Los Alamos is proceeding with the project with the goal of demonstrating repetitive loading and firing of charges by the end of FY93.

THREE-PHASE RELATIVE PERMEABILITY RESEARCH

**Cooperative Agreement DE-FC22-83FE60149,
Project BE9**

**National Institute for Petroleum
and Energy Research
Bartlesville, Okla.**

**Contract Date: Oct. 1, 1985
Anticipated Completion: Sept. 30, 1993
Funding for FY 1993: \$340,000**

**Principal Investigator:
Dan Maloney**

**Project Manager:
Rhonda Lindsey
Bartlesville Project Office**

Reporting Period: Oct. 1–Dec. 31, 1992

Objectives

The objectives of this project are to (1) improve the reliability of laboratory measurements of three-phase relative

permeability for steady- and unsteady-state conditions in core samples; (2) investigate the influence of rock, fluid, and rock-fluid properties on two- and three-phase relative permeabilities; and (3) expand the state of the art for measuring relative permeabilities at higher temperatures and pressures.

Summary of Technical Progress

Milestone 1

Tasks by project staff members to complete this milestone were finished during the reporting period. A safety assessment of the project was made, and the results were reported.¹ The status report describes environmental, safety, and health (ES&H) aspects relative to the project and explains how the project staff intends to meet ES&H objectives.

Milestone 2

Only slight progress was made toward accomplishing this milestone because of equipment failures. Permission was received to change the milestone completion time to February. The microwave klystron failed and was replaced. One of the tubes in the microwave power supply broke when the power supply was shipped by the manufacturer back to the National Institute for Petroleum and Energy Research (NIPER) after routine maintenance. The tube was replaced. The high-voltage tank assembly in the X-ray generator failed. The

assembly was replaced. Manpower was expended repairing equipment and in several attempts to restart the experiment between breakdowns. The scanning system was fully operational by the end of December.

Several unsteady-state relative permeability tests were conducted. Automated systems for recording oil and brine production, time, and pressure data during unsteady-state relative permeability tests were assembled and tested. An oil-water system was built using a separator based on the weight method described in a previous topical report.² Two 1800-g-capacity balances are used for weight measurements. The balances feature RS232 communication capabilities and measure weights with 0.01-g precision. An oil-gas separator was built that uses an electronic balance for oil production measurement and a ClaMar® Model 200 Gas Meter to measure gas production. The measurement concept is similar to that used by Gash and others.³ Pressures and fluid production volumes are recorded by a computer. The systems worked well for tests with clean laboratory fluids (synthetic brine and refined oil) and provided excellent production and pressure vs. time data. A more difficult test was performed with Berea sandstone using crude oil and a low-salinity brine. The test was performed at a temperature of 49 °C with 2.17 MPa back pressure. The system worked well even though the oil and brine effluent from the core plug did not separate quickly. One of the advantages of the measurement technique is that it can tolerate slow-breaking emulsions without loss of accuracy. Compared to typical unsteady-state tests in which manual measurements yield at best 15 to 20 data points, more than 8500 data points were recorded during the Berea sandstone test. Figure 1 shows oil production vs. time from the test. Results indicate that approximately 3700 s into the test, clay swelling and fines migration from the low-salinity brine began to affect the flow characteristics of the sample. The "noise" in Fig. 1 around $T = 4000$ s is probably because of pressure fluctuations either

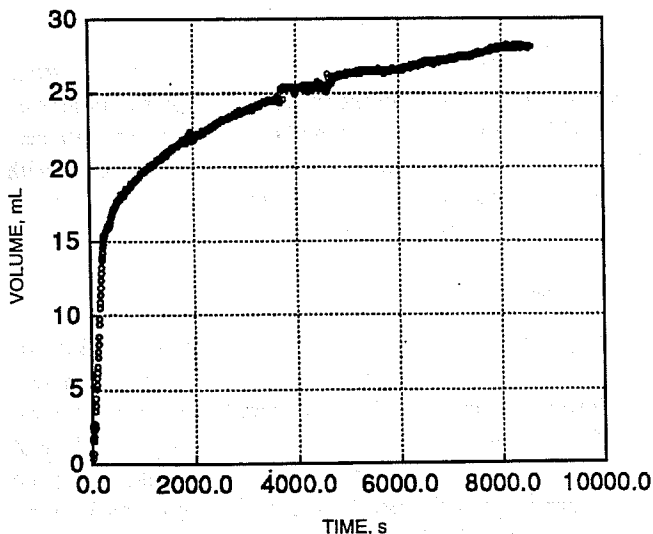


Fig. 1 Oil production vs. time from an unsteady-state crude oil-brine relative permeability test with Berea sandstone.

from fines migration and plugging or from the operating characteristics of the back-pressure regulator.

Back-pressure regulators seem to control pressures with minimum fluctuation when only a single fluid flows through the regulator. Equipment configurations for measuring oil production upstream from the back-pressure regulator were designed to minimize back-pressure fluctuations and to provide for performing oil-water and gas-oil unsteady-state tests at high temperatures. These techniques may be tested when conducting unsteady-state measurements for Milestone 6.

The unsteady-state data were used to check the computer program that is used for unsteady-state calculations. The program uses the Johnson-Bossler-Naumann (JBN) method.⁴ Results were also checked using the method described by Jones and Roszelle.⁵ A possible method for measuring the volumes of oil, gas, and brine in a closed-loop separator was developed. Equipment was ordered to test the laboratory fluid separator design. The equipment is expected to arrive in January.

Milestone 3

A consortium meeting was held during the first week of December. Fontainebleu sandstone was selected as the rock for use in FY93 activities. The rock is a clean sandstone and porosities and permeabilities of Fontainebleu sandstone samples are reported to be well correlated. Samples of the rock are available at NIPER. Characterization will begin in January.

Milestone 4

Fluid design criteria were discussed during the consortium meeting. One conclusion from the discussion was that a binary condensate fluid system using 1-bromopropane as one of the hydrocarbon fluids might provide good test characteristics. The 1-bromopropane should provide good X-ray absorption contrast between the brine and hydrocarbon phases because bromine has a fairly high X-ray mass attenuation coefficient. Work is in progress to prepare a laboratory for the combined pressure-volume-temperature and interfacial tension measurement systems.

Technology Transfer

Several of the topical reports from the project were given to one of the staff members of INTEVEP during a trip to Venezuela. A summary of X-ray saturation and steady-state relative permeability measurement techniques was presented during a visit with personnel at a major oil company laboratory in Houston. Technology exchange was accomplished among the project staff and representatives from the Department of Energy and three major oil-producing companies during the consortium meeting in December.

References

1. D. Maloney, *Environmental, Safety, and Health Assessment of FY93 Tasks for Project BE9*, DOE Report NIPER-655, December 1992.

2. D. Maloney and A. Brinkmeyer, *Three-Phase Relative Permeabilities and Other Characteristics of 260-mD Fired Berea*, DOE Report NIPER-581, pp. 22-23, 1992.
3. B. Gash, R. Volz, G. Potter, and J. Corgan, *The Effects of Cleat Orientation and Confining Pressure on Cleat Porosity, Permeability, and Relative Permeability in Coal*, paper SCA 9224 presented at the 33rd Annual Symposium of the Society of Professional Well Log Analysts, Oklahoma City, June 15-17, 1992, Vol. III.
4. E. Johnson, D. Bossler, and V. Naumann, Calculation of Relative Permeability from Displacement Experiments, *AIME Trans.*, 216: 370-372 (1959).
5. S. Jones and W. Roszelle, Graphical Techniques for Determining Relative Permeability from Displacement Experiments, *J. Pet. Technol.*, 30: 807-817 (May 1978).

Summary of Technical Progress

Milestone 1

Milestone 1 consists of evaluation of the environmental, safety, and health aspects of the procedures, activities, and equipment required to conduct the tasks planned for FY 1993. The environmental, safety, and health assessment report¹ for Project BE12 was completed and delivered to DOE.

Milestone 2

Milestone 2 consists of investigation of using single and multi-energy scans for rapid characterization of cores. Forty-six 2.54-cm-diameter sandstone core plugs of known porosity and permeability from Muddy and Almond formation outcrops in Wyoming and Blue Jacket formation outcrops in Oklahoma were scanned at 96-, 125-, and 141-kV X-ray beam energies both in dry and brine-saturated states. Very good correlations ($R > 0.96$) between the CT attenuation and porosity were observed for both the dry samples (Fig. 1) and the saturated samples (Fig. 2) for the 125- and 141-kV X-ray beam energies. The correlation for the 96-kV X-ray beam energy was not as good because the attenuation exceeded the highest value (1024 Hu) for the lower porosity samples. By constructing a database for different rock types, the direct CT attenuation-porosity correlation can provide a rapid, detailed porosity profile for cores to be used for log calibration and can provide a selection of representative core plugs for special core analysis. With the use of the porosity-permeability correlation (Fig. 3) together with the porosity profile, a detailed whole core permeability profile can be generated for improved scaling up from core to simulator grid block.

Milestone 3

Milestone 3 consists of application of imaging technology to derive scaleup procedures for permeability and relative permeability in large heterogeneous samples. The feasibility of BOAST-VHS reservoir simulator, adapted previously for coreflood simulations, has been investigated for its applicability to study the effect of relative permeability variations on the prediction of flow in heterogeneous cores. While satisfactory matches between the simulation and the CT-measured results have been obtained, further improvements are needed. They can be made by incorporating the dispersion effects, refining the grid block sizes, and performing three-dimensional (3-D) simulations. All these improvements require increased computing speed and larger random access memory (RAM).

Modifications of the hardware and of the calibration and measurement procedures performed allow minipermeameter measurements on large heterogeneous rock samples at the average rate of one measurement every 2 min with immediate permeability reading.

The environmental, safety, and health aspects have been considered in designing and building the experimental setup

IMAGING TECHNIQUES APPLIED TO THE STUDY OF FLUIDS IN POROUS MEDIA

Cooperative Agreement DE-FC22-83FE60149,
Project BE12

National Institute for Petroleum
and Energy Research
Bartlesville, Okla.

Contract Date: Oct. 1, 1987
Anticipated Completion: Sept. 30, 1993
Funding for FY 1993: \$350,000

Principal Investigator:
Liviu Tomutsa

Project Manager:
Robert Lemmon
Bartlesville Project Office

Reporting Period: Oct. 1-Dec. 31, 1992

Objectives

The objectives of this project are to (1) develop and correlate reservoir engineering parameters from petrographic image analysis, computerized tomography (CT) scanning, and nuclear magnetic resonance (NMR) imaging; (2) investigate the applicability of imaging technologies in the development of scaleup procedures from core plug to whole core to interwell scale; (3) develop an industry consortium or industrial advisory panel organized to help plan, review, and participate in the research through the work-for-others program and to provide for effective technology transfer; and (4) strongly encourage collaborative research by industrial participants.

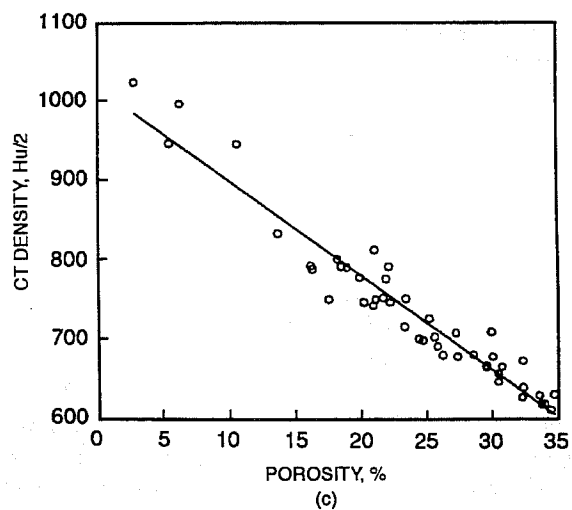
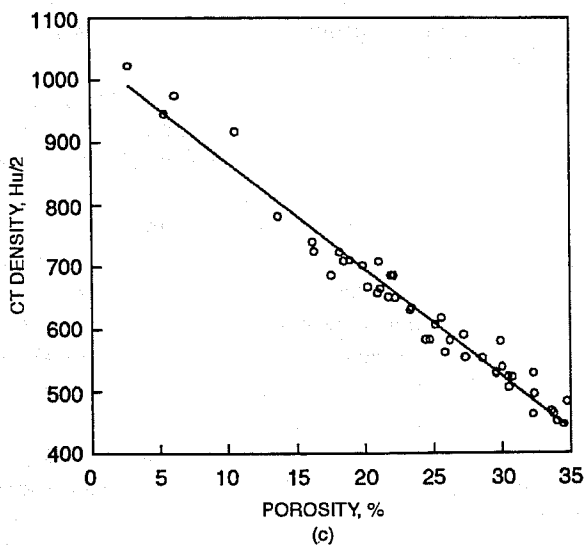
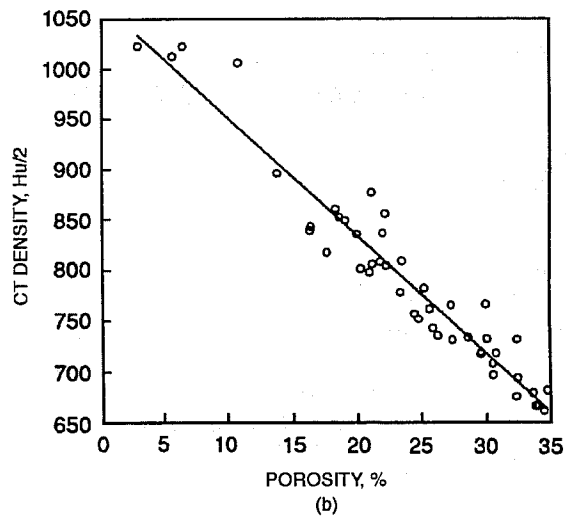
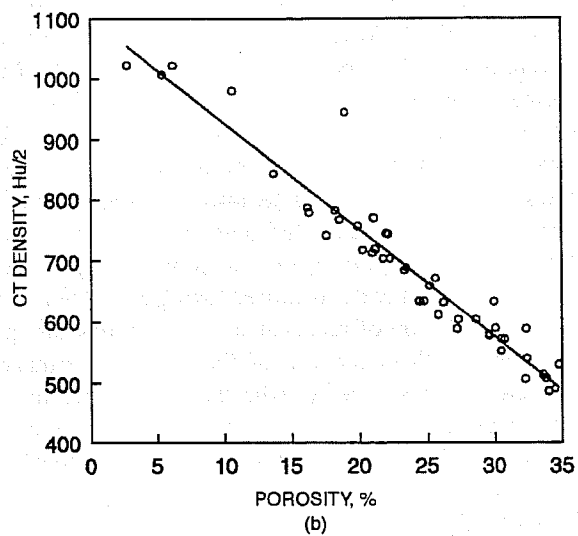
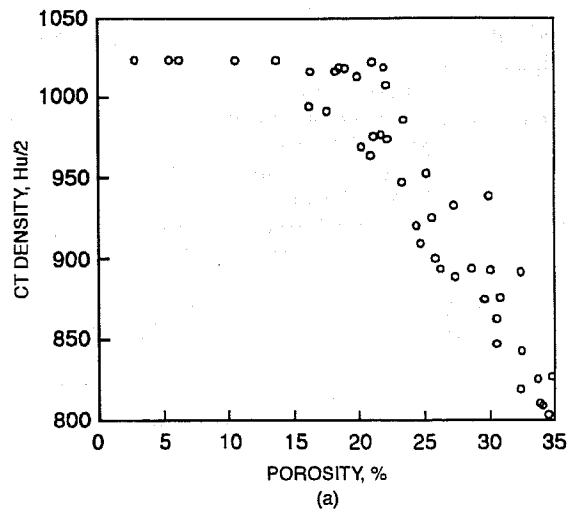
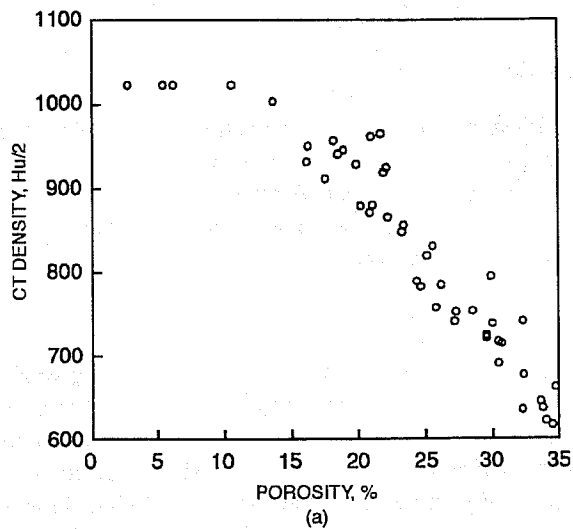


Fig. 1 Computerized tomography (CT) density vs. core plug porosity for dry core plugs: (a) 96-kV, (b) 125-kV, and (c) 141-kV X-ray beam energy.

Fig. 2 Computerized tomography (CT) density vs. core plug porosity for saturated core plugs: (a) 96-kV, (b) 125-kV, and (c) 141-kV X-ray beam energy.

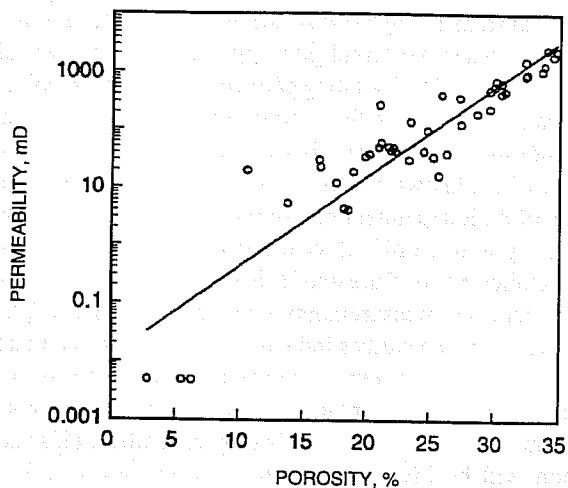


Fig. 3 Permeability vs. porosity for core plugs.

for using the mercury injection apparatus. This apparatus will be used in pore throat characterization of small volume (less than 1 cm³) samples representative of the heterogeneities present in a large heterogeneous Tallant sample monitored by CT. The construction of necessary protective equipment and the installation of the mercury injection apparatus have been completed.

Construction of new equipment and testing of new procedures were initiated for improving the image quality generated by CT scanning of large rectangular shape rock blocks needed for scaleup from centimeter to meter scales.

Milestone 4

Milestone 4 consists of investigations of the applicability of NMR spectroscopy and microscopy to study rock-fluid interactions affecting wettability.

An upgrade of the FORTRAN compiler for the i860 board was obtained along with an enhancement package which includes a source code debugger, a source code profiler, a vector math library, and a graphics library. The upgrade includes drivers for compiling and running programs for the i860 from OS/2 2.0. This is very helpful because the data processing can be started from OS/2 and run on the i860 board leaving the main computer free for other tasks.

There are several different techniques for acquiring 3-D images with NMR imaging equipment: (1) slice imaging sequences in which successive slices are captured, (2) 3-D Fourier transform imaging (3D-FFT) in which two-phase gradients are stepped in value to map 3-D image space, and (3) 3-D projection reconstruction imaging in which a constant magnitude gradient is stepped through different directions to map 3-D image space. These image techniques are also listed in the order of decreasing length of the pulse sequence required to acquire each image element. Projection reconstruction has been used at the National Institute for Petroleum and Energy Research (NIPER) because only one gradient (three orthogonal components) needs to be switched

on and off during the pulse sequence leading to the shortest possible sequence times. This is particularly important for samples of fluids in porous rock where short spin-spin relaxation times (T_2) lead to low signal/noise ratios for longer echo times. However, this sequence requires stronger radio frequency (RF) pulses with shorter 90° pulse lengths to adequately irradiate the entire sample space in the presence of the strong gradients. Also, the data processing algorithms are more complex, requiring more steps and longer computer processing times to recover the image.

The NMR imaging hardware has been modified to permit the use of the 3D-FFT pulse sequence. This involved modifying the digital-to-analog output board which supplies the three X-, Y-, and Z-gradient values to the gradient coils so that the three gradient signals could be shaped with a pre- and post-gradient component. Figure 4 shows in schematic form this pulse sequence with the timing relationships between the RF pulses and the shaped gradients. The gradient pulse has a finite rise time and fall time controlled by electrical, material, and mechanical factors in the gradient coil, RF probe, and NMR magnet assembly. With use of a pre-gradient pulse value twice as large and reduction of it to the desired value at a time equal to half the rise time, the apparent rise time can be reduced to half its actual value. The same principle applies to the post-gradient pulse which reverses the gradient signal to effectively damp the gradient in half the time. This process can shorten total pulse sequence times by several milliseconds. Because the RF pulses occur in the absence of the gradients, they are not required to irradiate a wide frequency bandwidth and can have lower power levels.

A modified data acquisition program was written to provide the pre- and post-gradient pulse values to the gradient pulses and provide the proper timing relationships between

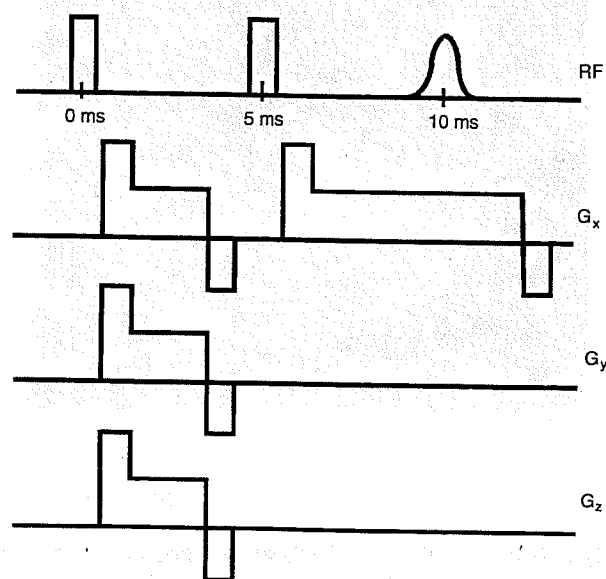


Fig. 4 Schematic diagram of 3D-FFT pulse sequence showing timing between the three gradients and the radio frequency (RF) transmitter pulses and signal echo.

the RF pulses, gradient pulses, and signal acquisition trigger for acquiring the image data. A new computer program was written to process the 3D-FFT image data file and recover the image. This 3D-FFT processing proved to be two to five times faster than processing an equivalent 3-D projection reconstruction image data file. Figure 5 shows one cross-sectional slice from a 3-D image of an oil-saturated polymer beadpack. The polymer beads ranged in size from 125 to 1000 μm in diameter. The figure shows the oil between the beads in lighter shades with the beads shown as the darker circular areas. The large circular dark area in the lower left-hand quadrant is the silhouette of an air bubble in the beadpack. The beadpack had a diameter of 12.5 mm, and the natural line width of the oil signal in the beadpack was 300 Hz. The image has 128×128 pixels for a resolution of about 150 μm per pixel. This image was acquired using 128 steps in the Y-gradient and 64 steps in the Z-gradient with 128 complex points in the acquisition of the signal. The shielded gradient coil was used with the standard 15-mm NMR probe. The gradient rise times for this combination were about 2 ms, so the pre- and post-gradient pulse periods were set at 1 ms. Total gradient pulse lengths were 5 ms, so the time-to-echo was about 10 ms.

A literature search was completed for references to measurement of wettability by NMR. Work by other investigators indicates that the spin-lattice relaxation times (T_1) for water in water-wet reservoir rock are significantly shorter than those for water in oil-wet rock. Wettability is determined for a given

rock system by measuring the water relaxation time for a known water-wet condition and that for a known oil-wet condition and interpolating between these two endpoint relaxation values to get the wettability of a particular sample. Criticism of this approach is directed at what the true wettability state of the known oil-wet or water-wet conditions might be. Use of an independent measure of wettability for these endpoint systems would alleviate some of this uncertainty. Use of the United States Bureau of Mines (USBM) method of capillary pressure measurements with centrifugation is planned. However, some studies indicate that at higher magnetic field strengths, the differences between T_1 values for oil-wet vs. water-wet rock systems tend to decrease, making T_1 measurements unreliable for distinguishing wettability. This phenomenon will be investigated with measurements of T_1 using NMR instruments operating at lower frequencies (20 and 85 MHz) than those of this instrument, which operates at 270 MHz.

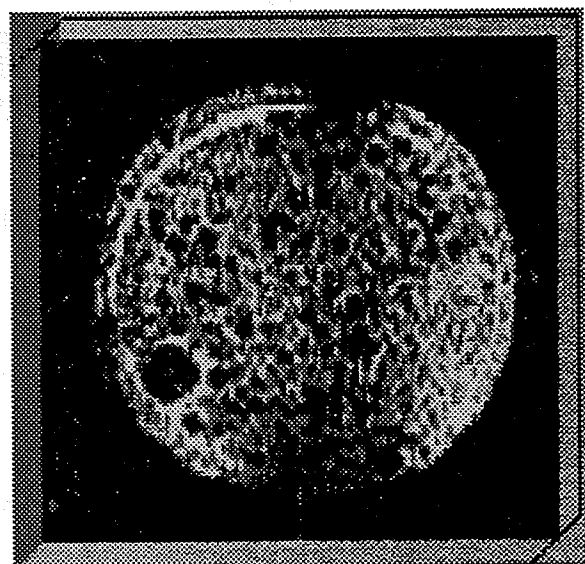
Milestone 5

Milestone 5 consists of technology transfer work. Industry members of the Relative Permeability Consortium were given a tour of the Rock-Fluid Imaging Laboratory, and questions were answered regarding the hardware, software, and procedures in image acquisition and processing. Assistance was provided to one participant company with information toward upgrading its hardware and software for CT image processing to make it more compatible for processing and exchange of image files. A brief presentation of the research on the effect of small-scale heterogeneity on oil trapping and recovery and simulation results was made and a presentation on the use of CT technology in performing unsteady-state relative permeability measurements. An outline of the presentations for the fluid imaging part to be presented in a joint workshop with the reservoir characterization project, in spring 1993, was written. Contacts were continued with an oil company toward establishing closer cooperation to help plan, review, and participate in research through the work-for-others category of the cooperative agreement and to provide for effective technology transfer.

An abstract was submitted and accepted for an invited presentation at the American Chemical Society (ACS) National Spring Meeting Symposium on Applications of Magnetic Resonance Imaging in Enhanced Oil Recovery, Denver, Colo., Mar. 28–Apr. 2, 1993. The title of the presentation is "Pore-Scale Fluid Imaging in Reservoir Rock by NMR Microscopy," by Daryl A. Doughty, Liviu Tomutsa, and Michael P. Madden.

Reference

1. L. Tomutsa, *Environmental, Safety, and Health Assessment of FY93 Tasks for Project BE12*, DOE Report NIPER-656, December 1992.



1500 microns

Fig. 5 Horizontal slice through oil-saturated polymer beadpack. Silhouettes of the beads appear dark; the oil appears white.

**CHARACTERIZATION AND MODIFICATION
OF FLUID CONDUCTIVITY IN
HETEROGENEOUS RESERVOIRS TO
IMPROVE SWEEP EFFICIENCY**

Contract No. DE-AC22-89BC14474

**University of Michigan
Ann Arbor, Mich.**

**Contract Date: Sept. 26, 1989
Anticipated Completion: Sept. 26, 1993**

**Principal Investigator:
H. Scott Fogler**

**Project Manager:
Robert Lemmon
Bartlesville Project Office**

Reporting Period: Oct. 1–Dec. 31, 1992

Objective

The objective of the experimental work performed this quarter was to study one aspect of the formation of the foamed gel formed in a porous medium. Specifically, the focus of the work was to investigate the change of foam texture and the configuration of the gelling phase during the gelation period.

Summary of Technical Progress

Introduction

A foamed gel is a dispersion of gas bubbles in a continuous gelled phase. Foamed gels are currently used for a wide variety of applications, including fracturing oil-field reservoirs, stabilizing of earthen formations, and plugging high-permeability streaks.¹⁻⁶ In these cases foamed gel may be generated in situ or externally before injection into the porous medium. The major difference between foamed gel and aqueous foam is that after some time the external phase of the foamed gel cross-links and thus greatly enhances the stability as well as the mechanical strength of the foam system. This added stability improves the lifetime of the foam in fractures and prevents foam collapse during water-flood treatments as opposed to aqueous foams.

Successful application of a foamed gel system requires a well-designed treatment based on knowledge of the behavior of the foamed plug as well as the physical characteristics of the foamed gel in the pore space. A recent study (performed under this grant) shows that foamed gels can plug porous media effectively and has also delineated both the mechanism of fluid flow through the foamed gel and the influences of the pertinent physical characteristics of the foamed gel and the porous media on the effectiveness of a foamed gel

plug.⁷ The physical characteristics (quality, texture, and location of gel) of a foamed gel after the external phase has gelled are particularly important because the location and amount of the gel at the pore level and the bubble size will strongly influence the behavior of the foamed gel plug. No studies have been reported that consider the physics of formation of a foamed gel and attempt to estimate the quality and texture of the aged foamed gel.

Background

Changes in foam texture occur by two primary mechanisms: (1) rupture of inter-bubble films and (2) inter-bubble diffusion between bubbles of different sizes.^{8,9} Many factors lead to film rupture, including poor stabilizing effect of surfactant, gravity drainage, pressure shocks, and bubble rearrangement,¹⁰⁻¹² and exceeding a limiting capillary pressure.¹³ Careful experimental design can eliminate these film-rupture mechanisms. Disproportionation that results from inter-bubble gas transfer cannot be eliminated in an aqueous foam. Disproportionation occurs because inter-bubble gas diffusion causes small bubbles to shrink progressively as their gas diffuses to larger bubbles. The cause of inter-bubble gas diffusion is the result of the polydisperse nature of foam bubbles (causing gas pressure differences between different size bubbles) and the high diffusivity of gas through the liquid films separating bubbles.

Experimental Apparatus

Etched-glass micromodels were used to visualize the generation and subsequent disproportionation of the foamed gels. The general apparatus is depicted in Fig. 1. A Harvard Apparatus model 22 syringe pump was used to meter the foaming solution into the porous system. Nitrogen gas was mixed with the foaming solution stream just ahead of the foam generator or in the micromodel inlet if a foam generator was not used. The gas injection rate could be controlled with a mass flow controller or adjusted to a constant pressure and monitored with a Brooks 5860E mass flowmeter. The pressure at the inlet to the micromodel was measured with a Setra transducer. An Olympus SZ-11 stereozoom microscope equipped with a Panasonic Digital 5100 CCTV camera was used to magnify the micromodels for observation. The micromodel images were recorded with a Panasonic AG-7355 super VHS for further analysis.

Three micromodel pore configurations were used in this study. The first pore-space configuration had square pore bodies connected together with pore throats in a square lattice arrangement (Part a of Fig. 2). These micromodels were used to observe the final configuration of the foamed gel in an interconnected pore space after gelation. The second micromodel pore-space pattern consisted of one large channel (Part b of Fig. 2). These micromodels were called "thin cells." The thin cells allowed observation of the effect of foaming solution gelation on the evolution of the foam texture. They were designed to spread a regenerated

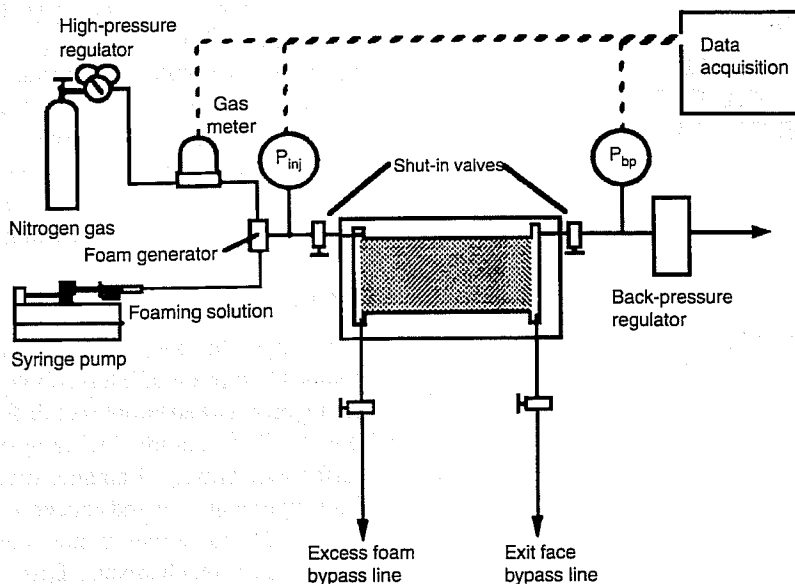


Fig. 1 Micromodel apparatus used for visualizing the formation of foamed gel.

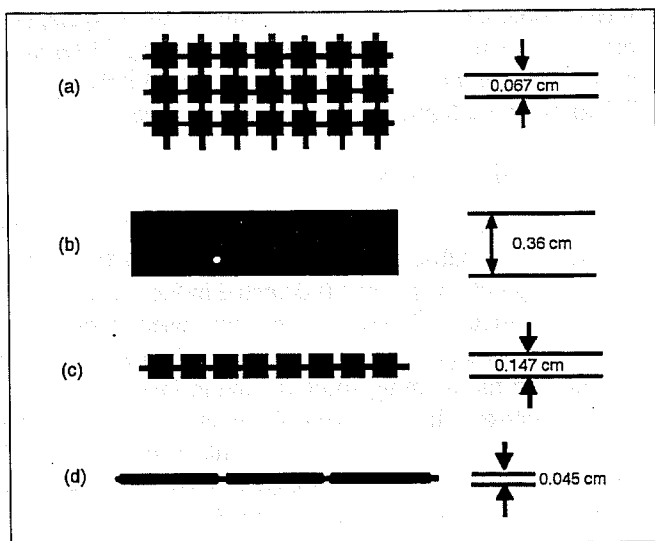


Fig. 2 Various micromodel patterns used in foam coalescence study (not drawn to scale). (a) Portion of interconnected pattern. (b) Thin cell. (c) Portion of $L/W = 1.1$ pattern. (d) Portion of $L/W = 12.8$ pattern.

foam into a monolayer for easy characterization. Additionally, the length and width of the thin cell were large enough that the growing bubbles would not be constrained by the boundaries of the system. The third micromodel pattern consisted of pore bodies connected in series by pore throats (Parts c and d of Fig. 2). All pore bodies were connected by identical size pore throats, and all pore bodies possessed the same etched volume. Two variations of this pattern were used. One pattern had square pore bodies ($L = 1.1W$) and the other had rectangular pore bodies ($L = 12.8W$), where L and W represent the length and width of the pore, respectively. The

purpose of these pore patterns was to study the influence of pore body geometry, in particular the aspect ratio of the pore body (L/W), on the texture of foamed gel.

Materials Used in Foamed Gel Systems

Two types of foaming gel systems were used for this experimental investigation.

1. *Polyacrylamide gel system.* Polyacrylamide from the Aldrich Chemical Company (approximate molecular weight, 5 million daltons; approximately 1% degree of hydrolysis) was mixed with deionized water and a cationic surfactant cetylpyridinium chloride (no interference with the polymer at a 10:1 polymer-to-surfactant weight ratio was observed). Chromium nitrate hydrate, $\text{Cr}(\text{NO}_3)_3 \cdot 9(\text{H}_2\text{O})$, was used as a cross-linker. By varying the concentration of polymer and cross-linker, the gelation time and thus the diffusivity of the gas can be varied. The gelation time was defined as the time at which the gel will not flow out of an inverted beaker.

2. *Colloidal silica gel system.* A 3.5 wt % sodium silicate solution with 2 wt % of a nonionic surfactant [Polyterg SL-62 (Olin Chemical Co.)] was mixed with a 50:50 mixture of deionized water and a 96 wt % ethyl acetate, 4 wt % formamide solution. The gelation time of the silica gel system could be varied by changing the ratio of the sodium silicate to ethyl acetate solutions mixed.

The purpose of using these two different gelling systems is as follows. The polyacrylamide gel formed elastic lenses when foamed, and the gelled lenses remained permeable to gas. In contrast, the silica gel formed rigid lenses after gelation and was much less permeable to gas. Hence the influence of the gelling characteristics on the evolution of foamed gel texture as a result of inter-bubble gas permeation could be studied.

Experimental Summary

The experimental findings are summarized as follows:

1. Foam injected into a porous medium, such as glass micromodels, will undergo disproportionation via gas bubble diffusion until an equilibrium state is achieved for disproportionation-dominated foams. The equilibrium state will be one bubble per pore body and one lens per pore throat when the pore body length-to-width ratio is small (see Fig. 3).

2. Rapid formation of a gas-impermeable gel (gelation dominated) and/or high aspect ratio pores will preserve foam texture (see Fig. 4).

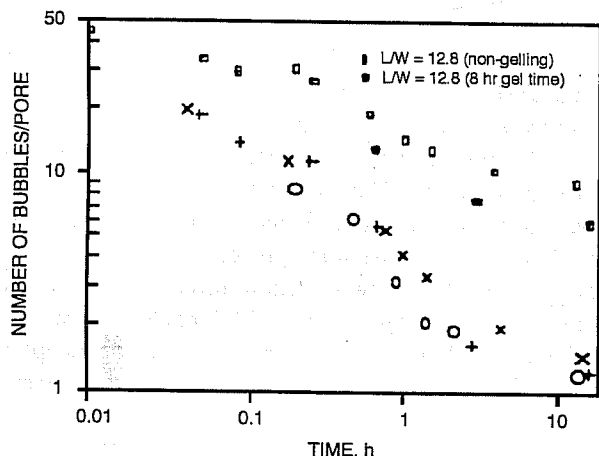


Fig. 3 Effect of the pore aspect ratio on the evolution of foam texture. ○, $L/W = 1.1$ (nongelling). +, $L/W = 1.1$ (8 h, gel time). ×, $L/W = 1.1$ (1 h gel time).

The experimental study underscores the factors that govern the texture of foamed gel in porous media. In a medium where the pore body length-to-width ratio is close to 1 (sandstone, sintered porous materials, and compacted soil), the disproportionation of foam will stop when the bubbles grow to the size of the pores or when the external phase of a gelation-dominated foam gels. In porous media with a large pore body length-to-width ratio (fracture networks), the disproportionation is limited by the aspect ratio of the fracture as well as the gelation of the external phase.

References

1. E. K. Watkins, C. L. Wendorff, and B. R. Ainley, *A New Crosslinked Foamed Fracturing Fluid*, paper SPE 12027 presented at the 58th Annual Technical Conference and Exhibition, San Francisco, Oct. 5-8, 1983.

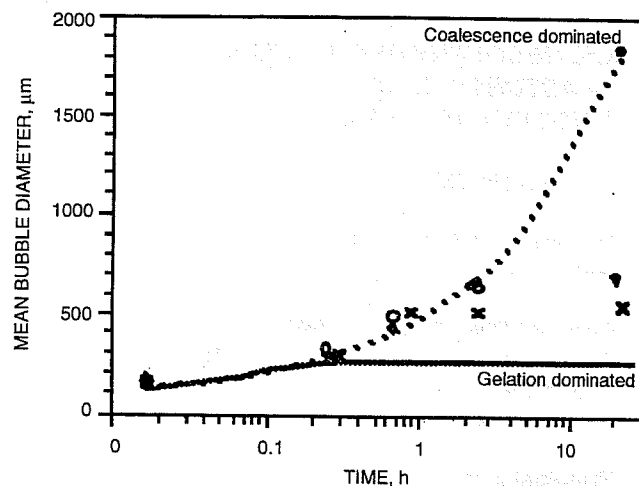


Fig. 4 Evolution of foam texture of a foamed silica gel at different gelation times. ○, infinite gelation time. △, ~2-h gelation time. ×, ~1-h gelation time.

2. R. D. Sydansk, *Foam for Improving Sweep Efficiency in Subterranean Oil-Bearing Formations*, U.S. Patent No. 5,105,884, Apr. 21, 1992.
3. R. L. Clampitt, *Foamable Compositions and Formation Treatment*, U.S. Patent No. 4,300,634, Nov. 17, 1981.
4. G. A. Scherubel and C. W. Crow, *Foamed Acid, A New Concept in Fracture Acidizing*, paper SPE 7568 presented at the 1978 SPE Annual Fall Technical Conference, Houston, Tex., Oct. 1-3, 1978.
5. W. G. F. Ford, *Foamed Acid—An Effective Stimulation Fluid*, *J. Pet. Technol.*, 1203-1210 (July 1981).
6. R. D. Hazlett and P. Shu, *Amino Resin Modified Xanthan Polymer Foamed with a Chemical Blowing Agent*, U.S. Patent No. 4,830,108, May 16, 1989.
7. M. J. Miller and H. S. Fogler, *A Mechanistic Investigation of Waterflood Diversion Using Foamed Gels*, paper SPE 24662 presented at the 67th Annual Technical Conference and Exhibition, Washington, D.C., Oct. 4-7, 1992.
8. A. Monsalve and R. S. Schechter, *The Stability of Foams: Dependence of Observation on the Bubble Size Distribution*, *J. Colloid Interface Sci.*, 97(2): 327-335 (February 1984).
9. D. S. H. Sita Ram Sarma, J. Pandit, and K. C. Khilar, *Enhancement of Stability of Aqueous Foams by Addition of Water-Soluble Polymers—Measurements and Analysis*, *J. Colloid Interface Sci.*, 124(1): 339-348 (July 1988).
10. G. C. Frye and J. C. Berg, *Interactions Between Surface-Active Species in Evanescent Foams*, *Chem. Eng. Sci.*, 43(7): 1479-1487 (1988).
11. J. W. Kim and W. K. Lee, *Coalescence Behavior of Two Bubbles Growing Side-by-Side*, *J. Colloid Interface Sci.*, 123(1): 303-305 (May 1988).
12. K. Malysa, *Wet Foams: Formation, Properties and Mechanism of Stability*, *Adv. Colloid Interface Sci.*, 40: 37-83 (1992).
13. Z. I. Khatib, G. J. Hirasaki, and A. H. Falls, *Effects of Capillary Pressure on Coalescence and Phase Mobilities in Foams Flowing Through Porous Media*, *SPE Reserv. Eng.*, 919-926 (August 1988).

OIL RECOVERY FROM NATURALLY FRACTURED RESERVOIRS BY STEAM INJECTION METHODS

Contract No. DE-AC22-90BC14661

**University of Texas at Austin
Austin, Tex.**

**Contract Date: Sept. 25, 1990
Anticipated Completion: Sept. 24, 1993
Government Award: \$312,773
(Current year)**

**Principal Investigators:
John C. Reis
Mark A. Miller**

**Project Manager:
Jerry Ham
Metairie Site Office**

Reporting Period: Oct. 1–Dec. 31, 1992

Objective

The objective of this study is to develop accurate models for predicting oil recovery in naturally fractured reservoirs by steam injection. This objective is being met through an integrated experimental, numerical, and analytical study of the recovery mechanisms that control oil recovery for this process. These mechanisms include capillary imbibition, thermal expansion, gas generation from chemical reactions, and temperature-dependent thermal properties.

Summary of Technical Progress

Recovery Mechanisms

During this reporting period the experimental validation of the closed-form analytical models for capillary imbibition into matrix blocks using the low-temperature apparatus has continued. A paper describing this imbibition model was written and has been submitted to the 1993 Annual Meeting of the Society of Petroleum Engineers. Development of a

model for the gas saturation distribution during gas generation continues.

Measurements at temperatures other than room temperature have begun. Initial air–water imbibition studies are being conducted with the low-temperature apparatus with chilled and hot water.

During the next quarter the experimental studies will continue with the low-temperature apparatus at different temperatures to validate the model for capillary imbibition. The resulting imbibition rates will be scaled with the analytical models to validate them. The development of the gas generation model will also continue.

Thermal Properties

The database of all published thermal conductivity and thermal diffusivity data is being studied to identify test conditions where more data are needed.

Development of the steady-state thermal conductivity apparatus was completed and reported in a Ph.D. dissertation. A review of measurements reported in the literature is being considered to determine what type of measurements to conduct for the study. A new student is also being trained to run the apparatus. In addition, some additional high-temperature relative permeability measurements will soon be completed. The existing apparatus is being calibrated, and a student is being trained to run it.

Fractured Reservoir Simulation

Two efforts were under way this quarter. The first was completion of the new approach to dual-porosity simulation for isothermal systems. This approach treats the matrix–fracture transfer flow in an explicit formulation that allows adding on of dual-porosity effects to existing single-phase simulation codes. The new approach also allows significant increases in accuracy, above that of most existing dual-porosity codes, with only modest increases in computational time. The final results of this work will be reported in a Ph.D. dissertation.

Work also continues on formulation of a dual-porosity thermal code. This formulation will take advantage of the techniques developed for the isothermal code and will include necessary energy transfer mechanisms. Anticipated coding will use fairly conventional approaches to thermal simulation.

DISPERSION MEASUREMENT AS A METHOD OF QUANTIFYING GEOLOGIC CHARACTERIZATION AND DEFINING RESERVOIR HETEROGENEITY

Contract No. DE-AC22-90BC14652

University of Oklahoma
Norman, Okla.

Contract Date: July 12, 1990
Anticipated Completion: July 11, 1993
Government Award: \$332,871

Principal Investigator:
Donald E. Menzie

Project Manager:
Gene Pauling
Metairie Site Office

Reporting Period: Oct. 1–Dec. 31, 1992

TABLE 1

Physical Properties of Berea Sandstones Used in Gas–Gas Dispersion Study

Core	Porosity, %	Permeability, mD	Diameter, cm	Length, cm
A5-2 + B5-2	20.0	300	38.1	29.14
D1 + D2 + D3	17.89	96	38.1	45.6

TABLE 2

Physical Properties of Gases Used in Gas–Gas Dispersion at T = 23 °C and P = 1 atm

Gases	Density, g/cm ³	Viscosity, cP	Molecular weight
Nitrogen	0.001154	0.0177	28.02
Helium	0.000163	0.0186	4.0

Objective

The objective of this research is to characterize and define reservoir heterogeneities by measuring dispersion in porous media. So far, almost all research in the area of dispersivity has been made with liquids flowing through the porous media. The measurement of dispersivity with gases will provide another opening to visualize the flow system of the reservoir rocks.

Summary of Technical Progress

With the experimental apparatus shown in Fig. 1, a series of gas–gas dispersion measurements were conducted on two consolidated Berea sandstone cores. The tests were designed to explore the dispersion of gas flow through porous media.

The specific characteristics of the cores measured in this study are shown in Table 1. The physical properties of gases used in the gas–gas dispersion measurements are shown in Table 2.

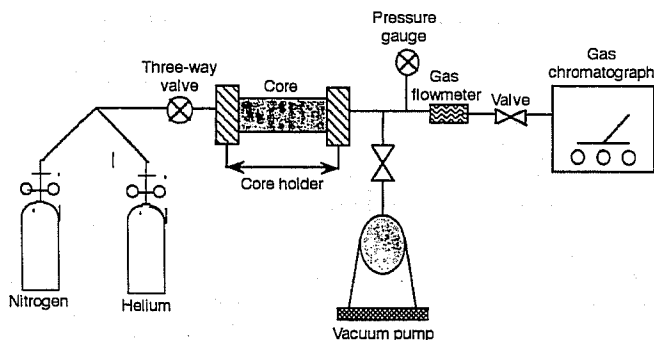


Fig. 1 Gas–gas dispersion apparatus.

A series of gas–gas displacement experiments with different pore flow velocities were conducted on each core used in this study. All the experiments were conducted within the range of laminar flow. The dispersion test results obtained for each core are depicted in Figs. 2 to 5.

Figures 2 and 3 show the measured breakthrough curves (S-shape curves) of nitrogen gas displacing helium gas with different pore flow velocities for each core. In these figures the y-axis is the relative concentration of the displacing gas and the x-axis is the pore volumes of displacing gas injected. Figures 4 and 5 depict the rate of concentration change of the displacing gas in the core effluent with respect to pore volume of displacing gas injected for various pore flow velocities. These curves were developed analytically by calculation of the slopes of the breakthrough curves. Although the data were obtained by a continuous monitoring technique, for comparison purposes the data are depicted as discrete points in these figures.

Figures 2 and 3 show that the “front-end” dispersion (area under the breakthrough curve at the vertical line at $V/V_p = 1$) and the “back-end” dispersion (area above the breakthrough curve and the vertical line at $V/V_p = 1$) are smaller for faster flow velocities. In other words, dispersion of the displacing gas is smaller at high pore flow velocity than at low pore velocity. These dispersion differences can also be seen in Figs. 3 and 4 where the spreading of the curves is less at high flow velocities than at low flow velocities. It is considered that the diffusion between gases becomes an important part of the dispersion measured through the breakthrough curves at low flow velocities. Therefore an attempt is currently being made to separate the gas diffusion from the dispersion measurements.

For a comparison of the gas–gas dispersion with liquid–liquid dispersion, the breakthrough curves obtained from the same core are shown in Fig. 6. The gas–gas dispersion has a much earlier breakthrough point and more spreading than the liquid–liquid dispersion under similar pore flow velocities.

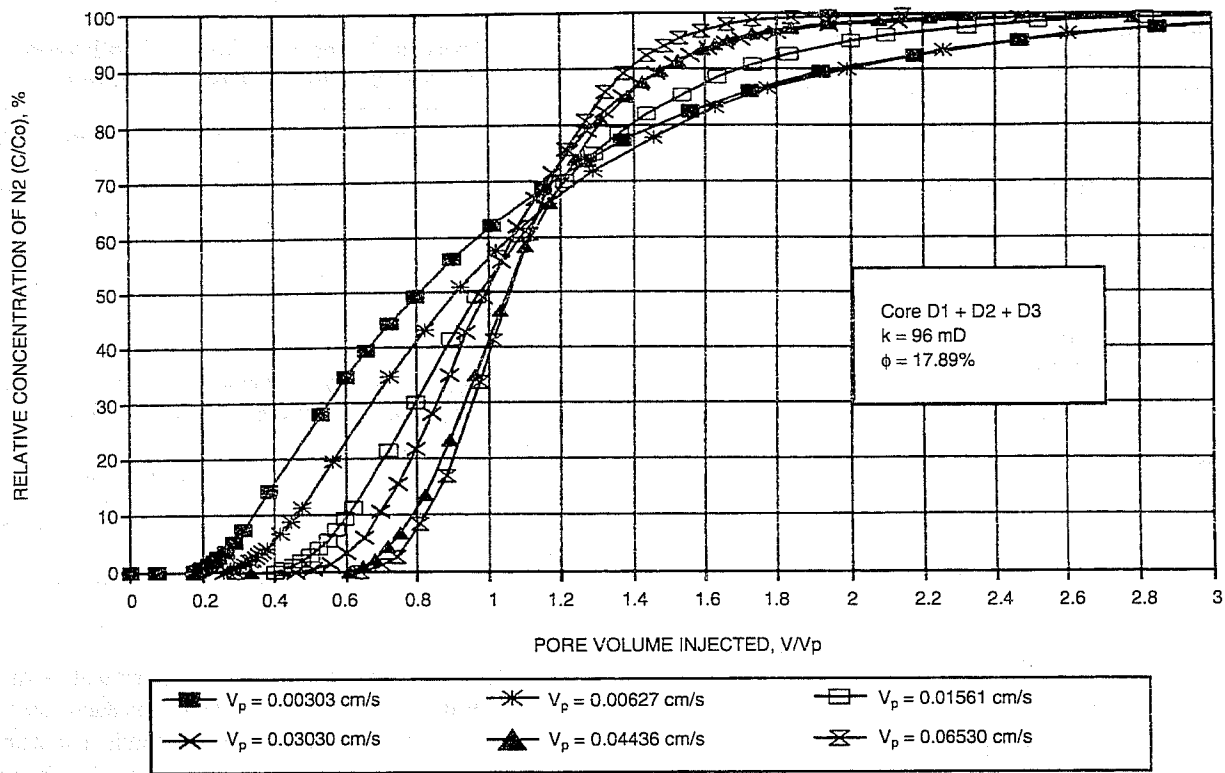


Fig. 2 Experimental displacing breakthrough curves (nitrogen displacing helium) using different pore flow velocities for Berea sandstone core number D1 + D2 + D3.

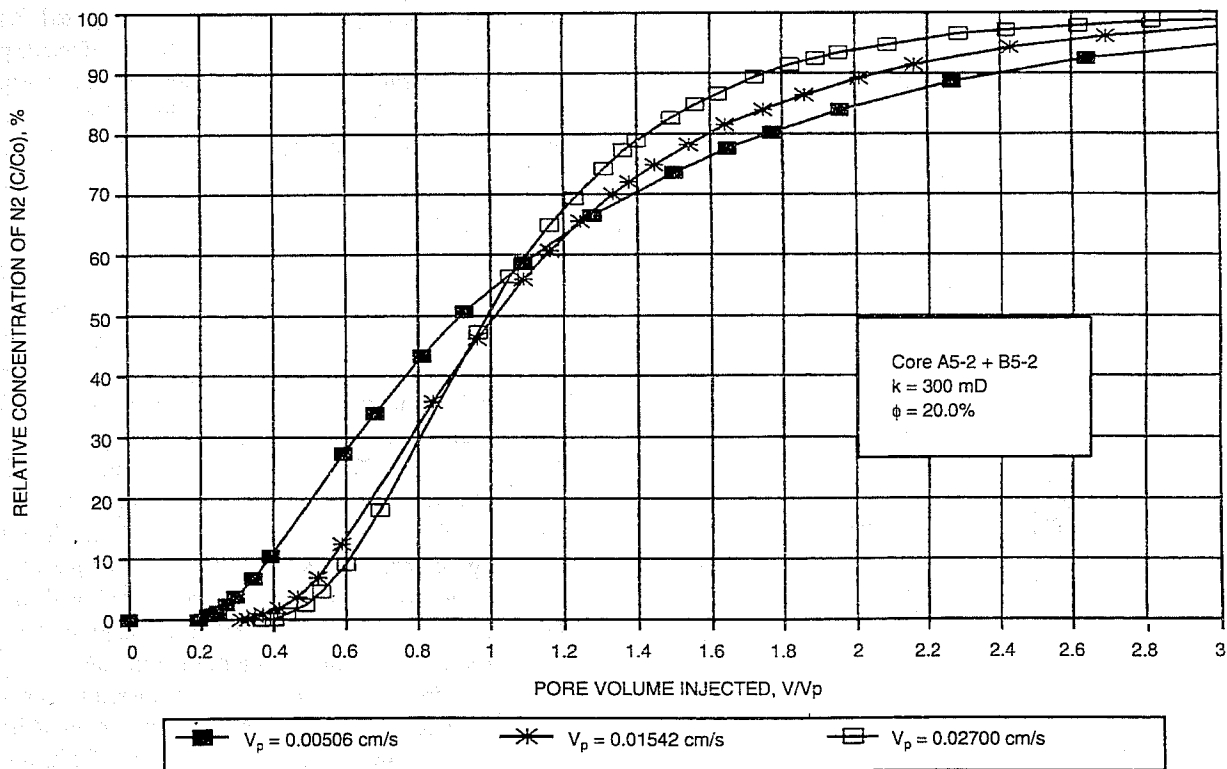


Fig. 3 Experimental displacing breakthrough curves (nitrogen displacing helium) using different pore flow velocities for Berea sandstone core number A5-2 + B5-2.

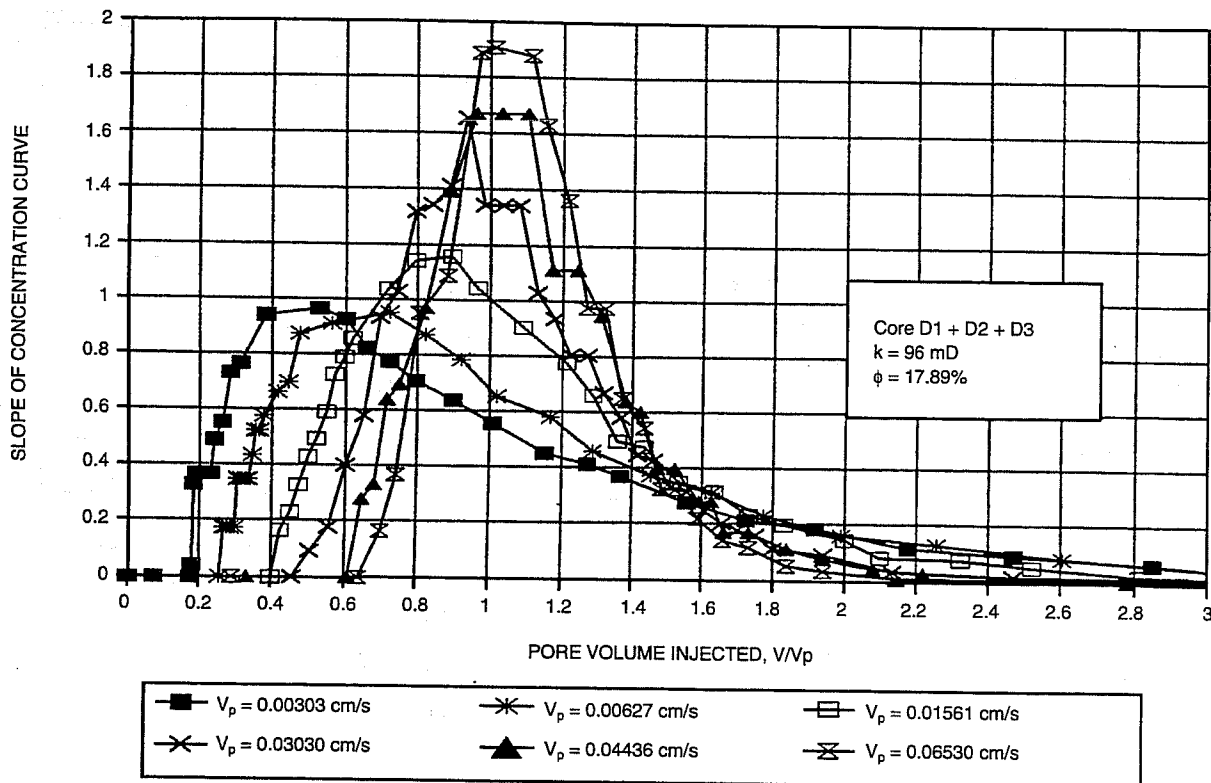


Fig. 4 Displacing breakthrough curves (nitrogen displacing helium) showing the rate of concentration change of the effluent gas vs. pore volume injected for Berea sandstone core number D1 + D2 + D3.

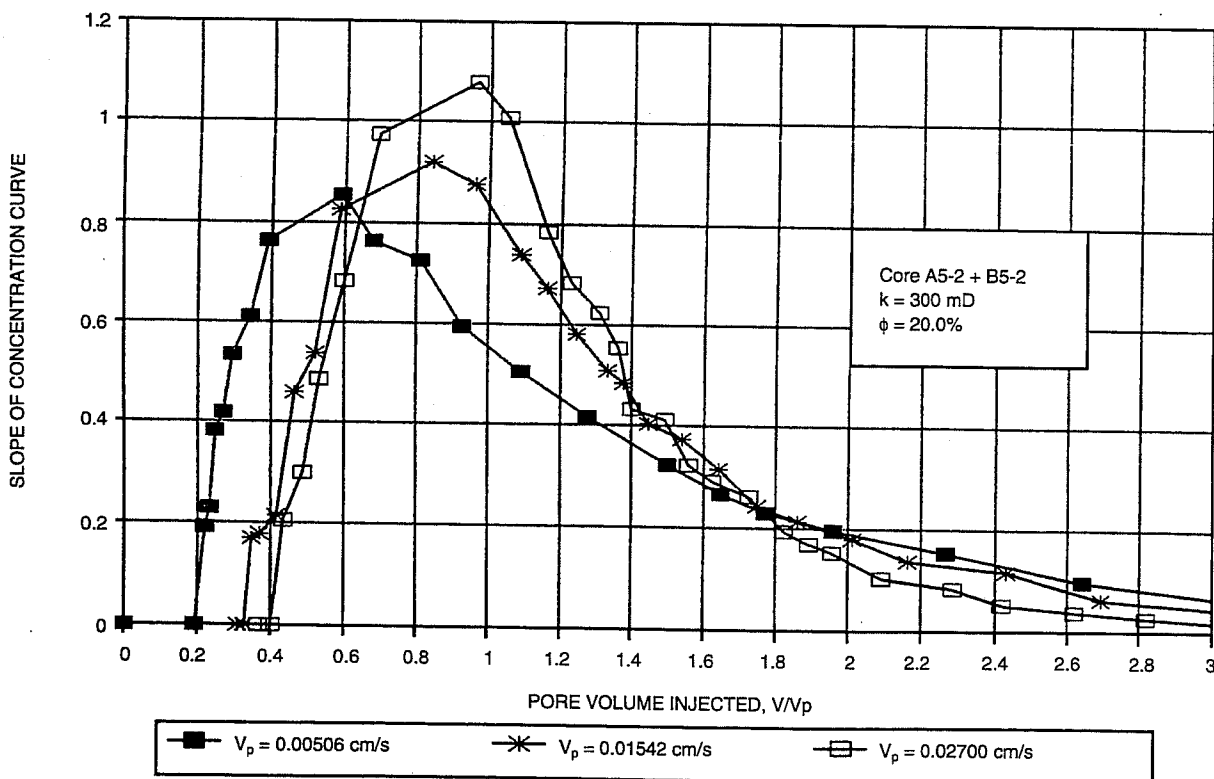


Fig. 5 Displacing breakthrough curves (nitrogen displacing helium) showing the rate of concentration change of the effluent gas vs. pore volume injected for Berea sandstone core number A5-2 + B5-2.

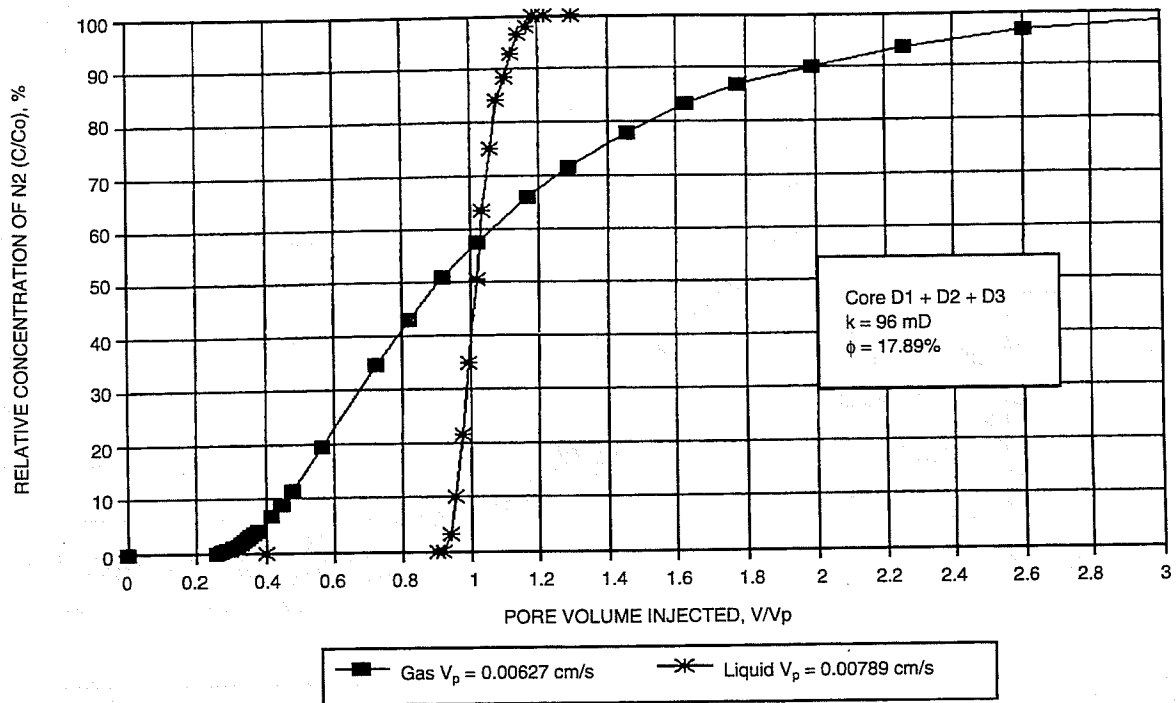


Fig. 6 Comparison of breakthrough curves of gas-gas dispersion with liquid-liquid dispersion.

RESOURCE ASSESSMENT TECHNOLOGY

RESERVOIR ASSESSMENT AND CHARACTERIZATION

Cooperative Agreement DE-FC22-83FE60149,
Project BE1

National Institute for Petroleum
and Energy Research
Bartlesville, Okla.

Contract Date: Oct. 1, 1985
Anticipated Completion: Sept. 30, 1993
Funding for FY 1993: \$795,000

Principal Investigator:
Susan R. Jackson

Project Manager:
Edith Allison
Bartlesville Project Office

Reporting Period: Oct. 1–Dec. 31, 1992

Objective

The objective of this project is to develop an improved methodology for effective characterization of barrier island reservoirs to predict oil saturations at interwell scales and flow patterns of injected and produced fluids.

Summary of Technical Progress

Effect of Geological Heterogeneities on Distribution of Primary Reserves and Oil Production

A rigorous examination was conducted of the distributions of two important types of heterogeneities in a sandstone reservoir, namely, the clay and carbonate cement content that have a strong effect on oil production from the UA-5B reservoir at Patrick Draw (Wyoming) field.¹ Heterogeneity measures obtained from frequency-domain analysis of gamma-ray and density logs along a profile across the sandstone deposit were correlated with core-derived porosity and permeability values and with cumulative primary oil production rates. The geological heterogeneities were then correlated with the distribution of primary reserves obtained from an analysis of the decline curves of primary oil production data with a sophisticated type-curve-matching program, MIDA.

Preliminary estimates were made of incremental oil recovery from waterflooding at certain well locations to identify geological heterogeneities that adversely affected waterflood sweep efficiency.

Lateral Variations in Clay and Carbonate- Cement Content of UA-5B Sandstones at Patrick Draw Field

Depositional and diagenetic processes have imparted large-scale lateral variations in pay thickness, sand continuity, and

the clay and carbonate-cement content in the producing UA-5B sandstones at Patrick Draw field.^{1,2} The lateral variations in the clay and cement content in the sandstones have affected porosity and permeability, which, in turn, have contributed to significant variations in the volumes and rates of oil production from different parts of the Patrick Draw field.² Reliable methods for mapping the lateral distributions of these heterogeneities as well as methods for predicting their distribution are important prerequisites for effective implementation of primary, waterflood, and enhanced oil recovery (EOR) operations.

It has been demonstrated that with proper precautions reliable estimates of the clay volumes in the UA-5B sandstones can be made from interpretations of gamma-ray logs.^{1,2} Similarly, because of significantly higher densities of carbonate rocks (around 2.71 g/cm³ or higher) compared with the matrix rocks (dominantly quartz and feldspars with an average density of around 2.65 g/cm³), the density or the sonic logs may be effectively used to estimate the relative amounts of carbonate rocks in the UA-5B sandstones.³ The presence of other heavier minerals like pyrite or siderite could adversely affect such estimations, but X-ray diffraction (XRD) analyses¹ indicate that such minerals occur in relatively very small quantities in the UA-5B sandstones and therefore will not be a significant factor in the estimation of carbonate rocks in the UA-5B sandstones.

Frequency-Domain Investigation Methods

For quantitative estimation of relative variations in clay and carbonate minerals across the reservoir sandstone at Patrick Draw field, a method based on the frequency-domain transformation of the digitized wireline log data discussed in paper SPE 24724 has been used.⁴ In this method the relative abundance of clay and carbonate or carbonate-cemented beds of different thicknesses are estimated along a profile across the sandstone deposit. The division of the pay thickness into heterogeneous (clay or carbonate cemented) beds of different thicknesses has been found very useful⁴ because clay and carbonate beds of different thicknesses respond differently to different fluid recovery operations. As an example, waterflood sweep efficiency, and therefore waterflood recovery, has an inverse relationship with the degree of thin clay bed stratification.

In this method the digitized wireline log data are first converted by Fourier transformation into a series of waves, each having a distinct amplitude and frequency. Although the conventional measure of frequency is cycles per second, in the analysis of depth domain wireline log data it is expressed as cycles per foot. In the frequency-domain representation, therefore, higher frequencies will imply the effect of beds of smaller thicknesses and lower frequencies will indicate the presence of thicker beds.

It has been demonstrated^{4,5} that the power spectrum (which is the distribution of the square of Fourier amplitudes as a function of frequency) of the frequency-transformed log data has certain very interesting properties. For example, in the

frequency domain the summation of the total power for all the frequencies is the variance of the wireline log data series in the depth domain. The power at a particular frequency implies variance contribution from a wave of that particular frequency (or period because frequency $f = 1/T$, where T is the period of the wave). The computation of the power spectrum of the digitized log series will give a continuous distribution of variances by beds of different thicknesses. For a quantitative estimation of the effects of beds of different thicknesses, the entire frequency scale from the lowest to the highest frequency was divided into four equal quadrants and the area under each quadrant calculated for each well. Quadrant 1 contains the thickest beds, quadrant 4 the thinnest, and quadrants 2 and 3 in between.⁴ In this way the area under each quadrant will give a measure of the relative abundance of beds of certain thicknesses present in the wireline log data.

Relative Abundance of Clay and Carbonate-Cemented Beds Across the Sandstone Deposit at Patrick Draw Field (Wyoming)

Gamma-ray and density logs in nine wells in the northern part of the Arch Unit were first digitized at 0.5-ft-depth intervals and then Fourier transformed for conversion of the depth data into continuous series of frequencies. The "power spectrum" was then estimated from each of the Fourier logs. The area within each quadrant of the power spectrum was then calculated for each well. The areas under the power curves for the gamma-ray and density logs from the nine wells across the sandstone deposit have been plotted in Figs. 1 and 2, respectively, as functions of cumulative oil production per foot of sand. All calculations were performed by using the computer program RESVER developed for frequency-domain analysis of wireline log data.⁶

For the gamma-ray logs (Fig. 1), the power distributions under quadrant 1 and under quadrants 1 and 2 combined were investigated because the abundance of thick clay-filled beds strongly controls the primary oil production.⁴ Core-derived geometric average permeabilities at different wells and the Dykstra-Parsons coefficients, which are a measure of the vertical variability of permeability, are plotted in Fig. 1.

Except for well Arch 103, the areas under the gamma-ray power curve show a strong inverse relationship with permeability and have an overall decreasing trend with the increase in cumulative oil production. The poor correlation of Dykstra-Parsons coefficients with primary oil production is thought to result from permeability distributions that reflect the variations in lithological and mineralogical composition and deviate significantly from a log normal. The relatively high geometric average permeability in well Arch 103 (41.8 mD) is because the lower part of the sandstone in this well is very clean, whereas the upper part is relatively much more clayey. The sharp difference in clay content between the two parts of the sandstone in well Arch 103 has raised the variance in this well compared with that of the other wells in the general vicinity where the sandstones have much more uniform distribution of clays.

The relative abundance of carbonate or carbonate-cemented layers of different thicknesses was determined by plotting the areas under quadrant 4, under quadrants 3 and 4 combined, and under all four quadrants (total density) at the different well locations (Fig. 2). The areas under quadrant 4 that average the effect of the highest frequencies (i.e., beds of smallest periods) will represent the effect of thin carbonate bed stratification. The cumulative oil production is affected by the amount of carbonate content in the sandstone pore spaces (Fig. 2), and a good quantitative measure of this is given by the areas in quadrants 3 and 4. The average core-derived porosity thickness (ϕh) product at different well locations is plotted in Fig. 2.

Figures 1 and 2 give a relative measure of the abundance of clay and carbonate beds of different thicknesses across the sandstone deposit. Lateral variations of these heterogeneities

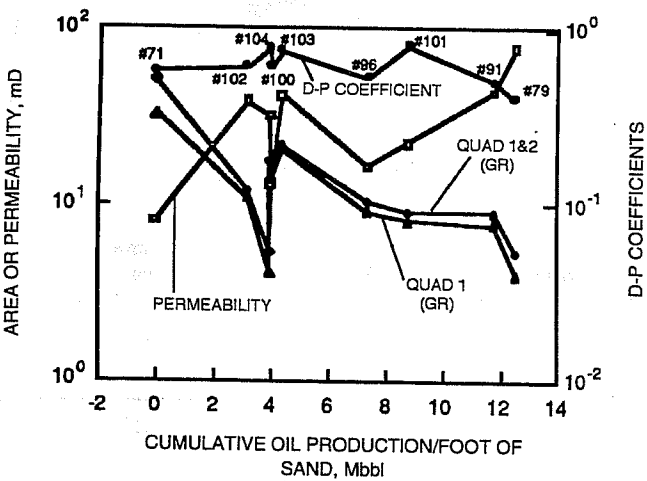


Fig. 1 Distributions of permeability, Dykstra-Parsons coefficients and the areas under the power curves in the different frequency quadrants of gamma-ray logs plotted as a function of cumulative oil production rates per foot of sand at different well locations in Patrick Draw Field (Wyoming).

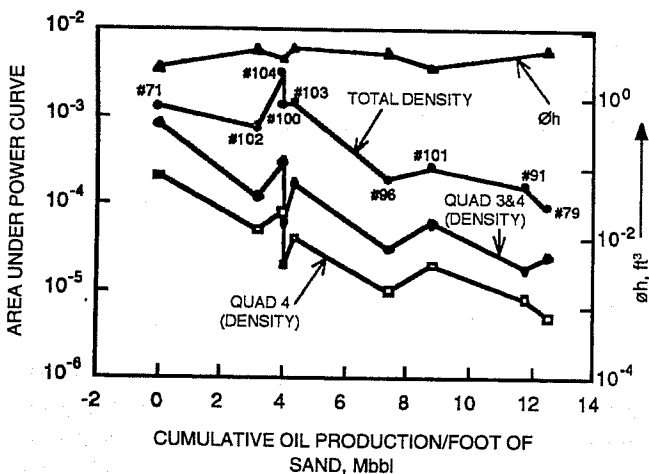


Fig. 2 Distributions of porosity thickness (ϕh) product and the areas under the power curves in the different frequency quadrants of density logs plotted as a function of cumulative oil production rates per foot of sand at different well locations in Patrick Draw Field (Wyoming).

have affected distributions of petrophysical properties and appear to have locally resulted in compartmentalization of the reservoir, possibly caused by faulting of brittle carbonate rocks. This will be investigated from decline-curve analysis of primary production data discussed in the following text.

Decline-Curve Analysis of Primary Production Data

The estimation of ultimate recovery by extrapolation of a performance trend is made from a graph of the rate of oil production as a function of time. The graphical extrapolation of the apparent production trend until the economic production limit is reached will give an estimate of the remaining reserves. The basic assumption in this procedure is that whatever causes governed the trend of the curve in the past will continue to govern its trend in the future in a uniform manner. This extrapolation procedure is strictly of an empirical nature, and a mathematical expression of the curve based on physical considerations of the reservoir can only be set up for a few simple cases.⁷ The decline-curve analysis will give estimates of oil reserves during the primary phase of an oil-producing reservoir. Reserves that may be obtained by secondary recovery methods or fluid injection programs cannot be estimated from this analysis.

Theory of Decline-Curve Analysis Using Type Curves

Decline-curve analyses of production data from Patrick Draw field were performed with the computerized type-curve-matching program, MIDA.⁸ The sophisticated technique of type-curve matching is rapidly gaining wide acceptance because of its greater reliability over other decline-curve analysis methods like the curve-fitting techniques. The type-curve analysis technique was first presented by Fetkovich in 1973,⁹ but until recently its use has been restricted because when performed manually type-curve matching is slow and awkward and consequently impractical for most engineers who deal with large numbers of wells. Through the use of computerized type curves, the engineer is provided with a diagnostic power and reliability not inherent in other decline-curve analysis techniques.⁸ In addition to the analysis of oil and gas production decline data, another major advantage of the type-curve matching method is that it can be used to estimate reservoir parameters like porosity, permeability, and skin factor. The important difference between the two main types of decline-curve analysis techniques (i.e., the type curve and curve fitting) is that in the latter method a nonlinear regression of the decline is made on the basis of the Arp's depletion equation given by:

$$q(t) = \frac{q_i}{(1 + bD_i t)^{1/b}} \quad (1)$$

- where $q(t)$ = production rate at time t
- q_i = initial production rate
- b = Arp's decline curve exponent
- D_i = initial decline rate
- t = time, d

Equation 1, however, characterizes oil and gas performance during the depletion period under constant flowing bottomhole-pressure conditions. The effort to curve fit production with Arp's equation on the entire production history of a well irrespective of the nature of decline has had mixed results because the data set may contain partly transient and partly depletion data.⁸ The Arp's equation only applies to the depletion portion, but curve-fitting routines are unable to distinguish between the two types of declines. The results almost invariably lead to misinterpretation of the overall trend and erroneous extrapolation.⁸ Type-curve matching of oil and gas production data does not suffer from these weaknesses. Inherent in the type-curve-matching program is the ability to discern the portion of the data that indicates transient conditions and the portion that indicates depletion conditions.

In the type-curve analysis program introduced by Fetkovich,^{8,9} the empirical equation of Arp is combined with the analytical constant-terminal pressure solutions of the diffusivity equation developed by Hurst, Van Everdingen, and others.⁹ Fetkovich combined the analytical and empirical data by defining a decline-curve dimensionless rate (q_{Dd}) and a decline-curve dimensionless time (t_{Dd}) as follows:

$$q_{Dd} = q(t)/q_i \quad (2)$$

and

$$t_{Dd} = D_i t \quad (3)$$

Equations 2 and 3 allow the integration of the transient and depletion envelopes. This greatly facilitated the curve-matching process in the computer. A large number of curves are available in the computer program MIDA for different values of b (Arp's decline-curve exponent) and the parameter $R_d = r_e/r_w$ (where r_e is the drainage radius and r_w is the effective wellbore radius) for accurate matching of any oil and gas data under primary operations. This will be illustrated by actual computations on data from Patrick Draw field.

Analysis of Production Data from Patrick Draw Field

Decline-curve analyses were performed on primary production data from 24 wells from the Arch Unit and 2 wells from the Monell Unit of Patrick Draw field. The primary objective of these analyses was to determine primary reserves distribution in the northern part of the Arch Unit, and a secondary objective was to determine lateral distribution of incremental recovery from waterflood and to understand causes for the large variations in waterflood production. As an example, the production decline of well Arch 40 using the computer program MIDA will be discussed.

Figure 3 gives the oil production rates in Arch 40 from the northern Arch unit from 12/1/61 to 7/1/75. Water injection in the neighboring wells commenced during 1967 and 1968. The sudden increase in oil production toward the end of 1969 was due to waterflooding, and the minor improvement in

production during the early part of 1965 could have been caused by acidization. The computer program MIDA automatically computes the dimensionless production rates (q_{Dd}) and times (t_{Dd}). A pair of curves corresponding to the analytical portion of the decline controlled by the R_d values and the empirical portion of the decline given by the b values were selected that best matched the input data for Arch 40 (Fig. 4).

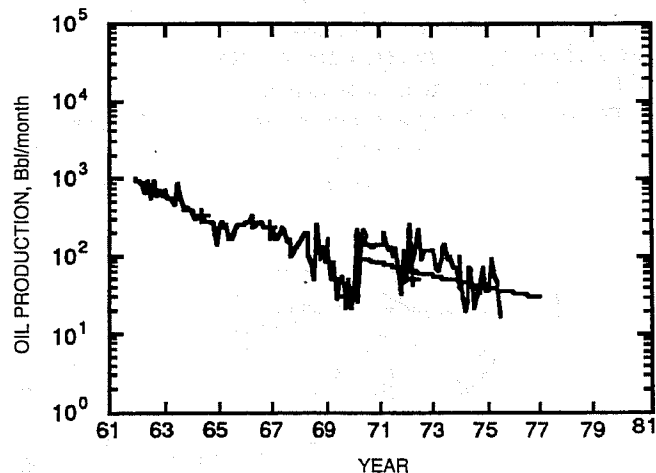


Fig. 3 Distribution of oil production rates in well Arch 40 in Patrick Draw field (Wyoming) and forecast of primary production until the economic limit rate is reached.

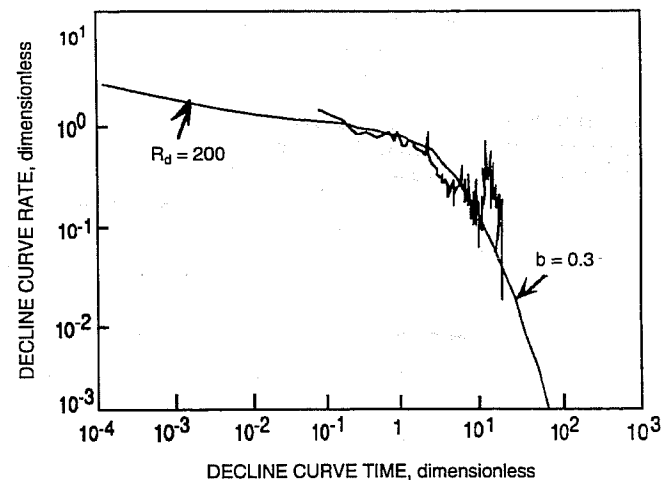


Fig. 4 Matching of primary field production data of Arch 40 with the composite of empirical and analytical decline curves given by the b and R stem values.

The values of R_d and b that gave the best match with the production data were 200 and 0.3, respectively. From this estimated trend, a forecast was made of primary production commencing at the time when the effect of waterflooding was just being noticed and terminating at the time when the production rate fell to 30 bbl/month (see Fig. 3 for extrapolation trend). Note that in the selection of the trend for production forecast, the higher production level in the postacidization

period was used. Note also that the falloff of oil production rates in the pre- and postacidization periods was the same as that observed in many other reservoirs.⁸ The total projected ultimate primary recovery from this extrapolation is 38,975 bbl, of which 30,144 bbl were produced before the onset of effects caused by waterflooding and 8,831 bbl is the projected production if the well had been only under primary production. The total primary and waterflood production in the well was 37,515 bbl, which indicates that there was no incremental oil recovery from waterflooding in this well. The oil recovery during 1974 and 1975 was very sluggish in this well, and one of the reasons may be the damage to the formation that resulted in a sharp decrease in the formation permeability. Well-log and core correlations indicate that the producing sand in this well is only 11 ft thick with an average porosity of 21.5% and a geometric average permeability of 44 mD. Reservoir compartmentalization that reduced the drainage area of this well could have contributed to the low primary reserves of this well because a number of faults have been mapped in the general area by seismic and well-log data (see the following discussion).

Distribution of Primary Oil Reserves from Decline-Curve Analysis

From decline-curve analyses of 23 wells from the northern part of Arch Unit in Patrick Draw field, contours showing the variations in primary oil reserves have been drawn (Fig. 5). The primary oil reserves computed for a well are affected by several factors, such as pay thickness, porosity, drainage area, oil saturation, and reservoir pressure. The highest primary reserves in the northern Arch Unit were calculated for well Arch 16 with a reserve of 462 Mbbl compared to 1014 Mbbl for well Arch 44 in the southern Arch Unit and 760.0 Mbbl for well Monell 14. The pay thickness, porosity, and calculated reserves for seven wells from Patrick Draw field are shown in Table 1. The effect on primary reserves estimates of reservoir

TABLE 1
Distribution of Reservoir Properties in Seven Wells from Patrick Draw Field (Wyoming) That Affect Primary Reserves Estimated from Decline-Curve Analysis

Well No.	Thickness of UA-5B sandstones, ft	Porosity, %	Primary reserves, Mbbl
Arch 24	13	21.4	198.1
Arch 44	24	19.5	1014.1
Arch 40	11	21.5	39.0
Arch 16	20	21.5	462.0
Arch 33	19	22.1	292.0
Arch 11	14	20.1	54.0
Monell 14	30	22.8	760.0

pressure variations or of reservoir compartmentalization brought about by structural, diagenetic, or stratigraphic causes is not indicated in Table 1 but could be significant considering the abrupt variations in the calculated reserves within short lateral distances (Fig. 5). A number of faults with very small throws (around 10 to 30 ft) have been mapped in Patrick Draw field with seismic and log data (see Fig 4.2, ref. 2). Some of these faults may divide the producing UA-5B sandstone into compartments in certain parts of the field. Significantly higher oil reserves in Arch 44 and Monell 14 are thought to be primarily caused by higher formation pressure that is possibly the result of gas-cap expansion and relatively large drainage volume, respectively.

Note in Figs. 1 and 2 that sandstone with low calcite cementation and clay (wells 96, 101, 91, and 79) coincide with the flat area in the primary reserves map (Fig. 5). The wells with higher carbonate cements (wells 71, 102, 104, and 103) in Fig. 2 could be prone to faulting and fracturing because of the brittle nature of the rocks, and this may be responsible for compartmentalization of the reservoir resulting in rapid variations in the primary reserves distribution (Fig. 5) in the northern part of the mapped area. Well Arch 104 also appears to be relatively clean (relatively smaller area under the power curve, Fig. 1) compared with the other wells in the general vicinity, although it has the maximum amount of total carbonate rocks (Fig. 2). Reliable estimates of primary reserves could not be made for this well because the well started production during October 1967 and a reliable primary production trend could not be deciphered because of the short duration of production. The effect of higher clay content in the producing sandstone is to reduce the effective porosity, and this will also decrease the primary oil reserves.

Incremental Oil Recovery As the Result of Waterflood

A preliminary investigation of the effect of geological heterogeneities on the waterflood recovery efficiency has been made from the estimated primary reserves and

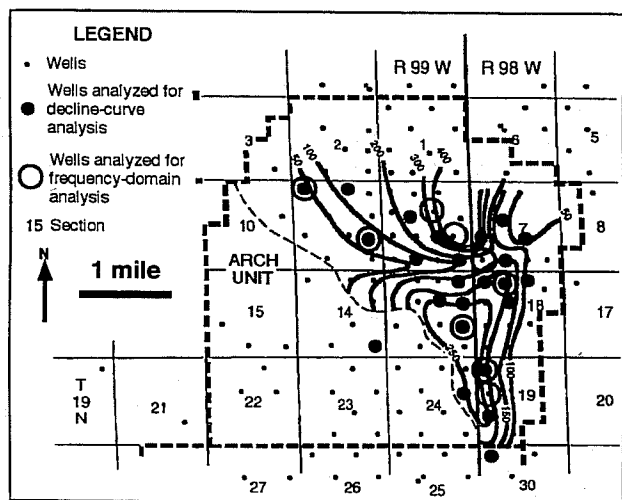


Fig. 5 Contours (in thousand barrels) showing the distribution of primary oil reserves in the northern Arch Unit obtained by decline curve analysis of primary production data.

production after initiation of waterflood. The incremental oil recovery from waterflooding was determined by subtracting the primary oil reserves from the total volume of oil produced by primary and waterflood operations. Total oil production, primary reserves, incremental oil recovery from waterflooding, and incremental recovery as a fraction of primary reserves for six wells from Patrick Draw field are shown in Table 2. The highly erratic waterflood recovery pattern is a reflection of the strong control the geological heterogeneities have on the sweep efficiency of the injected water. The best recovery as a fraction of the total primary reserves is observed in Arch 36 (87% of primary reserves) followed by Monell 1, which had a recovery of 23.3% of the primary reserves. Well Arch 36 has only slightly better petrophysical properties compared to well Arch 40, and the two wells have comparable primary reserves (Table 2), but the waterflood recovery efficiency in Arch 40 is much poorer, which could possibly be the result of poor sweep of the injected water caused by faulting in the neighborhood of this well. Similarly, well 79, which has the least amount of clay and carbonate rock stratification (Figs. 1 and 2), has very good primary reserves but very poor waterflood recovery, and this also could be caused by poor sweeping of the reservoir. Waterflood recoveries for other wells from the Arch Unit in Table 2 were significantly less.

TABLE 2

Incremental Oil Recovery from Waterflooding from Wells in Patrick Draw Field (Wyoming)

Well No.	Total production, Mbbl	Primary reserves, Mbbl	Incremental recovery, Mbbl	Incremental recovery as a fraction of primary reserves
Arch 44	1063	1014.6	48.4	0.05
Arch 100*	75.8	66.8	9.0	0.13
Arch 40	37.5	39.0	-1.5	-0.04
Arch 36	100.00	53.5	46.5	0.87
Arch 79†	287.7	282.8	4.9	0.02
Monell 1	146.6	118.7	27.7	0.233

*Drilled in 1967, "primary reserve" estimate is approximate.

†Drilled in 1964, "primary reserve" estimate is approximate.

References

1. R. A. Schatzinger, M. J. Szpakiewicz, S. R. Jackson, M. M. Chang, B. Sharma, and M. K. Tham, *Integrated Geological-Engineering Model of Patrick Draw Field and Examples of Similarities and Differences Among Various Shoreline Barrier Systems*, DOE Report NIPER-575, 1992.
2. S. R. Jackson, R. A. Schatzinger, M. Szpakiewicz, M. M. Chang, and B. Sharma, *Integration of the Geological/Engineering Model with Production Performance for Patrick Draw Field*, DOE Report NIPER-634, September 1992.
3. E. R. Crain, *The Log Analysis Handbook*, pp. 115-247, Pennwell Books, Tulsa, Okla., 1986.

4. B. Sharma, *A New Technique To Estimate Vertical Variability of Rock Properties for Reservoir Rock Evaluation*, SPE paper 24724 presented at the 1992 SPE Annual Technical Conference and Exhibition, Washington, D.C., Oct. 4-7, 1992.
5. G. M. Jenkins and Donald G. Watts, *Spectral Analysis and Its Applications*, pp. 141-257, Holden-Day, San Francisco, Calif., 1968.
6. B. Sharma, *Techniques for Mapping the Types, Volumes, and Distribution of Clays in Petroleum Reservoirs and for Determining Their Effects on Oil Production*, Final Report, DOE Report NIPER-646, 1992.
7. J. J. Arps, *Estimate of Primary Oil Reserves*, paper presented at the Petroleum Conference—Economics and Valuation, Dallas, Tex., 1956.
8. Mannon Associates Inc., *MIDA, Advanced Petroleum Software Manual*, Mannon Associates, 1991.
9. M. J. Fetkovich, *Decline Curve Analysis Using Type Curves*, *J. Pet. Technol.*, 32(6): 1065-1077 (1980).

TORIS RESEARCH SUPPORT

Cooperative Agreement DE-FC22-83FE60149, Project BE2

**National Institute for Petroleum and Energy Research
Bartlesville, Okla.**

**Contract Date: Oct. 1, 1983
Anticipated Completion: Sept. 30, 1993
Funding for FY 1993: \$340,000**

**Principal Investigator:
James F. Pautz**

**Project Manager:
Chandra Nautiyal
Bartlesville Project Office**

Reporting Period: Oct. 1-Dec. 31, 1992

Objective

The objective of this project is to provide research support to the Department of Energy Program Manager for the Tertiary Oil Recovery Information System (TORIS) in the areas of enhanced oil recovery (EOR) projects and reservoir database management, EOR project technology and trends analysis, and computer simulation.

Summary of Technical Progress

The first task of this project was to assess the potential hazards in the areas of environment, safety, and health that might be encountered while conducting the planned research. These areas were reviewed, and a report¹ was submitted.

SIMSTEAM is a wellbore heat-loss model developed by Scientific Software-Intercomp (SSI) under a subcontract with Kawasaki Thermal Systems, Inc. The model is designed to estimate the flow of two-phase steam-water systems in a

wellbore and related heat transfer from the wellbore fluid to the formation. This model was reviewed to determine what changes needed to be made before it is released to the public.

Minor deficiencies in documentation and programming were identified and specific recommendations were made to the Bartlesville Project Office (BPO).

The model was validated using "KTS TEMP," which was developed by Kawasaki Thermal Systems, Inc. Two other models^{2,3} in the literature were recommended for consideration because this did not appear to be an independent evaluation and validation. Once these corrections are made, the BPO will have a software tool to assist the thermal recovery industry in improving recovery efficiency.

Project Database

The BPO recently upgraded its computer and database management systems. This meant that the EOR project data needed to be transferred from the old system to the new INGRES system. In the last quarterly report, an entity relationship diagram was used to describe the new table structure for the EOR Project Database. This quarter the procedures to transfer and verify proper transfer of data are briefly described.

Data were unloaded from the S2k version of the database to tape that was consistent with the new table structure. Thirty-five separate files were created for each of the new INGRES tables containing all the entities of that table. After the data were transferred into the new data tables, random queries were made to determine that the data were properly loaded and that the tables were properly created and linked.

The following method was used to verify complete and accurate transfer. The first step was to create data files that mirrored all the data loaded into the INGRES tables. The files were then written to tape. The files on the tape were analyzed by cutting the first five and last five records for each of the 35 files. Each attribute in this abridged database was manually compared to a local working version. Because all the data compared favorably, it is believed that the data have been transferred properly to the INGRES version.

References

1. J. F. Pautz and C. A. Sellers, *Environmental, Safety, and Health of FY93 Tasks in Project BE2*, DOE Report NIPER-654, December 1992.
2. H. J. Ramey, Wellbore Heat Transmission, *J. Pet. Technol.* (April 1962).
3. K. C. Shui and H. D. Beggs, Predicting Temperatures of Flowing Wells, *J. Energy Resour. Technol.* (March 1980).

THIRD INTERNATIONAL RESERVOIR CHARACTERIZATION TECHNICAL CONFERENCE

**Cooperative Agreement DE-FC22-83FE60149,
Project SGP47**

**National Institute for Petroleum
and Energy Research
Bartlesville, Okla.**

**Contract Date: Dec. 1, 1990
Anticipated Completion: Feb. 1, 1993
Funding for FY 1993: \$33,000**

**Principal Investigator:
Bill Linville**

**Project Manager:
Edith Allison
Bartlesville Project Office**

Reporting Period: Oct. 1–Dec. 31, 1992

Objectives

The objectives of the Third International Reservoir Characterization Technical Conference were to (1) explore methods to integrate engineering and geological disciplines to improve the understanding of fluid flow in petroleum reservoirs; (2) review current practices, procedures, and technologies applied to reservoir characterization; (3) identify problems related to current practices and procedures for accurate reservoir descriptions and the information and technology required to solve the problems; (4) identify emerging technologies and promising directions for future research; and (5) provide a means for technology transfer.

Summary of Technical Progress

All the papers were delivered to PennWell Books, Inc., and publication of the Proceedings in a hardback book is scheduled for Feb. 1, 1993. A complimentary copy will be mailed to each registrant, except student registrants, of the conference.

UPGRADE THE BARTLESVILLE PROJECT OFFICE CRUDE OIL ANALYSIS DATA BANK

Cooperative Agreement DE-FC22-83FE60149,
Project SGP56

National Institute for Petroleum
and Energy Research
Bartlesville, Okla.

Contract Date: June 1, 1992
Anticipated Completion: May 31, 1993
Funding for FY 1993: \$106,000

Principal Investigators:

James F. Pautz
Carolyn Sellers
Johanna Shay

Project Manager:

Chandra Nautiyal
Bartlesville Project Office

Reporting Period: Oct. 1–Dec. 31, 1992

Objective

The purpose of this work is to (1) develop and maintain a crude oil analysis (COA) database online that maintains data integrity and system security and is available to the public, (2) upgrade and update crude oil analyses for inclusion in this database, and (3) participate in the United Nations Institute for Training and Research (UNITAR) analysis study group.

Summary of Technical Progress

Background

Crude oil analyses by a routine method have been conducted at the National Institute for Petroleum and Energy Research (NIPER) since the 1920s when the facility was part of the U.S. Department of the Interior, Bureau of Mines.¹ By 1965, more than 7000 crude oils had been analyzed, which created one of the largest collections of such information in the world.² The data were digitized by the late seventies, and a custom software application (COASYS) was implemented in 1980 (Ref. 3). The COASYS system gave the public access to the analysis information through telephone lines. This system is a traditional flat-file approach in which the data are created, updated, and accessed by programs written in a procedural programming language. Also, with this approach there is no standard system of data storage or data access, and all files are created and maintained separately.

Database Design

The first step in the database design process was to construct a data dictionary from the flat-file system. Initially,

scalar values (an individual data value that is atomic or nondecomposable) were identified. The scalars were then grouped together on the basis of their relations to each other. Each of these relations is expressed as an entity that may be viewed as an object in which interrelated data are stored. Ten entities emerged from this analysis. The next steps in the design process were to define relationships between entities and define the primary keys (pk) for each entity that serves as a link between entities.

At this point in database design, it becomes necessary to view the abstract entities in a manner that allows testing of assumptions of relationships. The Entity/Relationship (E/R) model approach introduced by Chen in 1976 (Ref. 3) and the E/R diagram were used to test the relationships. An E/R diagram is a technique for representing the logical structure of a database in a pictorial manner. The entities are the main building blocks within the E/R diagram. Figure 1 contains an E/R diagram for the COA database. This diagram uses the conventions and definitions of Chen and Date⁴ for entity relationships. Entities are depicted as rectangles, linking scalars are diamonds, and single or double lines represent the relationships between entities. The 1's and M's indicate the magnitude of relationship between entities. Ones indicate a one-to-one relationship and M's indicate a many-to-one or many-to-many relationship. For example, the relationship between entities State/Country Information and County Information is expressed as a one-to-many because there are

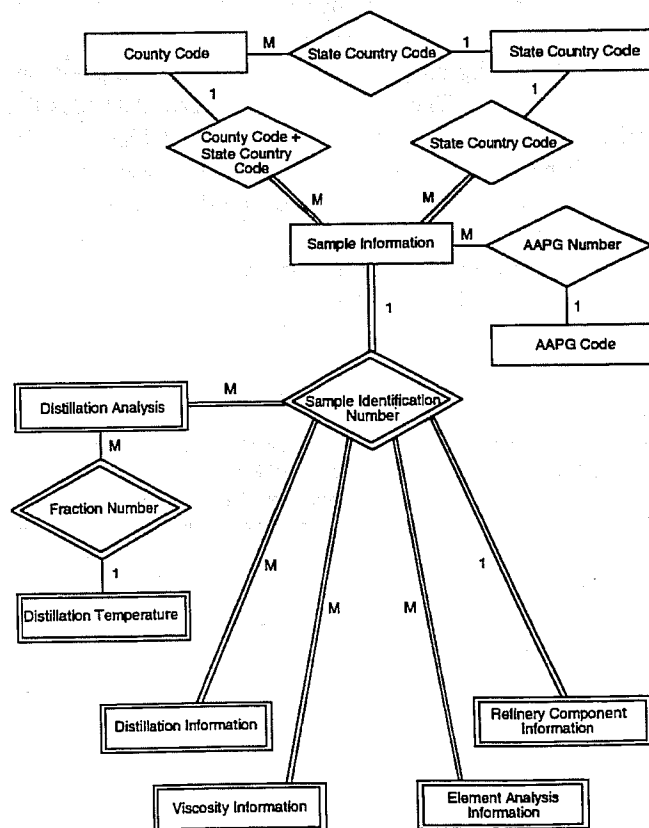


Fig. 1 Entity/Relationship diagram of the crude oil analysis database.

multiple occurrences of the scalar value State/Country Code in the County Information entity. Also indicated in the E/R diagram are instances of partial participation of entities and weak relations. Double-lined rectangles and diamonds indicate weak relations. A weak entity, according to Chen, is an entity that is existence-dependent on some other entity. It cannot exist if that other entity does not also exist. The entities Distillation Temperature, Distillation Analysis, Distillation Information, Viscosity Information, Refinery Component Information, and Element Analysis Information are all considered to be weak because their existence is dependent upon the existence of the Sample Information entity. Entities are viewed as participants in a relationship, and the number of participants in a given relationship is the degree of that relationship. Relationships may be partial or total. The degree of relationship is represented on the E/R diagram by a single (partial) or double (total) line. Data define these relationships as follows:

“Let R be a relationship type that involves entity type E as a participant. If every instance that E participates in includes at least one instance of R, then the participation of E in R is said to be total, otherwise it is said to be partial.”⁵

The final database design step involves the normalization of entities in accordance with the relational data structure. This type of data structure has the following properties:

1. A relation, that is, a table.
2. A tuple, which is a row of a table.
3. An attribute, which is a column of a table.
4. Cardinality, which is equal to the number of tuples.
5. Degree, which is equal to the number of attributes.
6. A primary key that serves as a unique identifier for the table and may be one or more columns.
7. A domain, which may be defined as a pool of values from which one or more attributes draw their actual value(s).

Normalization is a method for optimizing relational databases to eliminate data anomalies. This method involves breaking data in tables into smaller tables until the data values in each table depend only on the key or keys within the table. The normalization process is accomplished through the use of normal forms.⁶ Normal forms first, second, and third were applied to the design of the COA E/R model. The definition of normal forms is as follows:

- First normal form requires the elimination of repeating attributes or groups of attributes from a relation.
- Second normal form implies that the design is in first normal form and all non-key attributes are dependent on the primary key.
- Third normal form involves eliminating transitive dependencies, that is, the dependence of any non-key attribute on any other attribute except the primary key.

Currently the COA database tables, as displayed in Tables 1 to 10, are in third normal form with the exception of the Sample Information table. This table has redundant data in the attribute Field_Name, which is indicative of second normal form. To convert Sample Information into third normal form,

Field_Name must be removed and placed in a new table consisting of Field_Name and Field_Code (pk).

Input files are then generated from the original COA flat files. This requires extensive programming to match the data type and format in the old flat files and new relational tables.

TABLE 1
State_Country_Code

Attribute name	Data type	COA variable
state_country_code	integer	XLN
state_country_name	varchar(20)	

TABLE 2
County_Code

Attribute name	Data type	COA variable
state_country_code	integer	XLN
county_code	integer	NCTTY
county_name	varchar(25)	

TABLE 3
AAPG_Code

Attribute name	Data type	COA variable
aapg_no	integer	AAPGNO
geologic_age	varchar(35)	

TABLE 4
Sample_Info

Attribute name	Data type	COA variable
sample_id	integer	
depth_formation_top	integer	DEEP
depth_formation_bottom	integer	DEEP2
state_country_code	integer	XLN
county_code	integer	NCTTY
lab_code	char(1)	LAB
api_crude	float	APIG
color	char(2)	COLOR
field_code	char(9)	same as in projectdb
field_name	varchar(35)	FIELD
formation_code	char(4)	AAPGMN
formation_code_modifier	char(1)	AAPGMD
formation_name	char(4)	FORM
formation_name_modifier	char(1)	FORMMD
lithology	char(3)	FORTYP
geo_age	char(3)	AGE
aapg_no	integer	AAPGNO
pour_point_sign	char(1)	PRA
pour_point	integer	PRPT
specific_gravity_crude	float	SPGC

TABLE 5
Distillation_Temp

Attribute name	Data type	COA variable
fraction_no	integer	
cut_temperature	integer	

TABLE 6
Distillation_Analysis

Attribute name	Data type	COA variable
sample_id	integer	
fraction_no	integer	
recovered_vol_frac	float	VOL(I)
cloud_point_sign	char(1)	CLA(I)
cloud_point	integer	CL(I)
ref_index_d_line	float	RID(I)
ref_index_g_line	float	RIG(I)
specific_gravity_frac	float	SGR(I)
su_viscosity_frac_sign	char(1)	SUA(I)
su_viscosity_frac	integer	SU(I)

TABLE 7
Distillation_Info

Attribute name	Data type	COA variable
sample_id	integer	
atmospheric_press	integer	IATMPR
first_drop_temp	integer	IFDROP
first_vacuum_frac_no	integer	IVFRAC
stage_1_temp	integer	STAG1D
stage_2_temp	integer	STAG2D

TABLE 8
Viscosity_Info

Attribute name	Data type	COA variable
sample_id	integer	
su_viscosity	float	SU
su_viscosity_sign	char(1)	SUA
su_viscosity_temp	integer	

TABLE 9
Element Analysis_Info

Attribute name	Data type	COA variable
sample_id	integer	
element	char(2)	sulfur, nitrogen
element_wt_pcmt	float	SCR, CRN, SRES, NRES
element_wt_pcmt_sign	char(1)	SL
crude_or_residium	char(1)	

TABLE 10
Refinery Component_Info

Attribute name	Data type	COA variable
sample_id	integer	ID
carbon_residuum_wt	float	CRR
carbon_crude_wt	float	CRC
gas_oil_vol	float	GOVOL
lt_gasoline_vol	float	SVOL
gasoline_naphtha_vol	float	TGNVOL
vis_lub_distillate_vol	float	VLD
kerosine_distillate_vol	float	VOLKD
residuum_vol	float	VOLR
med_lub_distillate_vol	float	XMLD
non_visc_lub_dist_vol	float	NLD

The data now are in a test database using INGRES. This implementation is being tested before it is transferred to a production database that will be online to the public.

References

1. N. A. C. Smith, H. M. Smith, O. C. Blade, and E. L. Garton, The Bureau of Mines Routine Method for the Analysis of Crude Petroleum, *Bur. Mines Bull.*, 490 (1951).
2. H. M. Smith and J. H. Hale, Crude Oil Characterizations Based on Bureau of Mines Routine Analyses, *Bur. Mines Rep. Invest.*, 6846 (1966).
3. Peter Chen and Pin-Shan, The Entity-Relationship Model Toward a Unified View of Data, *ACM TODS 1*, No. 1 (March 1976) Republished in M. Stonebraker (Ed.), *Readings in Database Systems*, Morgan Kaufmann, San Mateo, Calif., 1988.
4. C. J. Date, *An Introduction to Database Systems*, Volume 1, Fifth Edition, Addison-Wesley Publishing Co., 1991.
5. C. J. Date, *An Introduction to Database Systems*, Volume 1, Fifth Edition, Chapter 22, Semantic Modeling, Addison-Wesley Publishing Co., 1991.
6. T. Kemm, A Practical Guide to Normalization, *DBMS*, 46-52 (December 1989).

**COMPILATION AND ANALYSIS OF
OUTCROP DATA FROM THE MUDDY
AND ALMOND FORMATIONS**

**Cooperative Agreement DE-FC22-83FE60149,
Project SGP69**

**National Institute for Petroleum
and Energy Research
Bartlesville, Okla.**

**Contract Date: Sept. 21, 1992
Anticipated Completion: May 31, 1993
Funding for FY 1993: \$23,750.10**

**Principal Investigator:
Susan Jackson**

**Project Manager:
Edith Allison
Bartlesville Project Office**

Reporting Period: Oct. 1–Dec. 31, 1992

Objectives

The objectives of this project are to compile outcrop data from the Muddy and Almond formations; supply missing data, interpretations, and analyses where needed; and put data in a transferable format so that the data can be used by those interested.

Summary of Technical Progress

Milestone 1

Field work was conducted at the Almond formation outcrops located near Rock Springs, Wyo., to supplement the measured sections previously completed at outcrop RH. Tidal inlet, tidal channel, and tidal delta facies could not be correlated from the two previously measured sections at outcrop RH, even though the sections were located approximately 1200 ft apart. A third section was measured in between the ones previously measured to allow better resolution on the lateral extent (dimensions) of the facies represented in the outcrop. The facies were traced laterally between the measured section to verify the correlations made when constructing the cross sections in the office and to document lateral changes within the facies. Measurements and interpretations made in the previous field season were checked, supplemented with additional data, and corrected where necessary.

In the field, outcrop RI, located approximately 1 mile to the south of outcrop RH, was investigated for potential use for facies dimensions determination. A striking termination of a flood tidal delta facies is exposed at this outcrop, where the facies thickness changes from greater than 30 ft thick to a few feet thick over a lateral distance of approximately 1500 ft. Outcrop RI is a good candidate for future work on the paleogeographic reconstruction of the Almond formation in the Rock Springs Uplift area and determination of facies geometry and dimensions.

MICROBIAL TECHNOLOGY

MICROBIAL ENHANCED OIL RECOVERY AND WETTABILITY RESEARCH PROGRAM

**Contract No. DE-AC07-76ID01570,
Project 5AC3**

**Idaho National Engineering Laboratory
EG&G Idaho
Idaho Falls, Idaho**

**Contract Date: Oct. 1, 1988
Anticipated Completion: Sept. 30, 1995
Government Award: \$600,000**

**Principal Investigator:
L. S. McCoy
Idaho Field Office**

**Project Manager:
Rhonda Lindsey
Bartlesville Project Office**

Reporting Period: Oct. 1-Dec. 31, 1992

Objectives

The objectives of this research program are to develop microbial enhanced oil recovery (MEOR) systems for ap-

plication to reservoirs containing medium to heavy oils and to evaluate reservoir wettability and its effects on oil recovery.

The MEOR research goals include

- Development of bacterial cultures that are effective for oil displacement under a broad range of reservoir conditions.
- Improved understanding of the mechanisms by which microbial systems displace oil under reservoir conditions.
- Determination of the feasibility of combining microbial systems with or following conventional enhanced oil recovery (EOR) processes, such as miscible and immiscible gas flooding, polymer and chemical flooding, and thermal methods.
- Development of an MEOR field process design.
- Implementation of an industry cost-shared field demonstration project.

The goals of the reservoir wettability project are to develop

- Better methods for assessment of reservoir core wettability.
- More certainty in relating laboratory core analysis procedures to field conditions.
- Better understanding of the effects of reservoir matrix properties and heterogeneity on wettability.
- Improved ability to predict and influence EOR response through control of wettability in reservoirs.

Summary of Technical Progress

MEOR Research and Field Application

Field application of MEOR requires field-specific evaluation, design, and engineering. Analysis of select small Minnelusa Sand formations in the Powder River Basin in Wyoming for potential field application of MEOR technology was conducted in FY 1990/1991. Subsequently, arrangements to conduct a cost-shared field demonstration of MEOR technology with the field owners, operators, and service companies of the Schuricht lease were made. National Environmental Protection Act (NEPA) documentation has been filed, and a letter agreement between the Idaho National Engineering Laboratory (INEL) and an independent owner/operator has been signed to allow for a two-phase field analysis of MEOR technology. Phase I will consist of four parts: (1) reservoir evaluation by pressure build-up testing, (2) injection of a brine blank (baseline control), (3) a shut-in period, and (4) a production period. Phase I will establish a baseline to which the following microbial process (Phase II) will be compared. The brine blank will be shut in for the same time period as planned for the microbial process and produced. Injection pressure, injection rate, produced brine composition, and fluid production rates will all be carefully monitored. This phase will begin around April 1993 and continue through the summer months.

Phase II will mimic Phase I with the exception of the injected fluid. The Phase II injected fluid will be a specifically designed microbial system. Total fluid production rate and oil production rate will be compared to those of Phase I. Success of the microbial process will be discerned by parameters such as increase in oil production (compared to the control phase) or successful injection, stimulation, and growth of organisms in situ. This phase is planned to take place in the spring and summer of 1994. Evaluation of this phase will be by comparison to the control process injected the previous summer and to mathematically simulated predictions.

Injection fluids and media formulation for the Schuricht field process will be based on water from a livestock supply well located approximately 5 miles south of the Schuricht lease. The well is currently being used as a source of injection water for secondary recovery technologies in the Moorcroft West lease. Water analysis has been previously completed. Cations (Na^+ , Ca^{2+} , Mg^{2+} , Fe^{total}) were analyzed by atomic adsorption (flame) spectroscopy (Perkin-Elmer 2280). Chlorides, hardness (as CaCO_3), and alkalinity (pH) were analyzed by titration. Sulfates were analyzed turbidimetrically as barium salts at 415 nm. Total dissolved solids (TDS) were estimated by mathematical summation. Analysis of injection water from the Moorcroft West Unit is presented in Table 1. No water is produced or injected at the Schuricht Well. Reported data are average values compiled from August 1989 to September 1991. On the basis of this analysis, the water is a suitable make-up water for media formulation.

TABLE 1
Water Analysis

Location	Section 12-51N-68W
Formation	Unknown shallow sand
Depth, ft	200 ft subsurface
Sample point	Wellhead
pH	7.3
TDS	366 mg/mL
Hardness (as CaCO_3)	21 mg/mL
Na^+	93.0 ppm
Ca^{2+}	31.3 ppm
Mg^{2+}	14.6 ppm
Fe^{total}	0
Cl^-	1.94 ppm
SO_4^{2-}	101 ppm

Evaluation of Reservoir Wettability and Its Effects on Oil Recovery

Activities for this quarter were focused on Schuricht crude oil. This crude oil, like others previously reported, alters the wetting of sandstone cores to weakly water-wet, and oil recovery improves with decreasing Amott index to water. Results of adhesion mapping indicate strong dependence of the transition between adhesion and nonadhesion on both pH and ionic strength. The dependence on brine ionic composition is more pronounced than is usually observed for crude oils and, at the low end, the transition pH is unusually high. Measurements with coreflooding brine (2.5% NaCl + 0.5% CaCl_2) were strongly adhesive, although two compositions containing calcium ion (those at the highest ionic strengths) were not.

Measurements of water and decane contact angles on glass surfaces equilibrated in various brines then aged in Schuricht crude at 80 °C have been performed. For Schuricht crude, complex behavior is observed for water advancing angles. The surfaces first wetted with low-pH brine (pH 4) gave moderately high advancing angles after several days of aging time. When the brine pH was increased to 6, the results were more dependent on sodium ion concentrations. Low ionic strength brine treatment gave steadily increasing and quite high advancing angles. Higher ionic strength brine results showed lower advancing angles that changed little with aging time. High-pH (pH 8) brine gave the least reproducible and most unusual results. Some advancing angles in this system actually appeared to decrease with increases in aging time.

Surface studies and two-dimensional micromodel displacements show that wetting is altered on surfaces contacted with Schuricht crude oil, but in ways that are complex and do not readily lead to prediction of waterflood results. The added complexity of an adverse mobility ratio requires further study in porous media.

NEW MICROORGANISMS AND PROCESSES FOR MICROBIAL ENHANCED OIL RECOVERY

Contract No. DE-AC22-90BC14663

Injectech, Inc.
Ochelata, Okla.

Contract Date: Aug. 1, 1990
Anticipated Completion: July 31, 1992

Principal Investigators:
Penny L. Sperl
George T. Sperl

Project Manager:
Rhonda Lindsey
Bartlesville Project Office

Reporting Period: Oct. 1–Dec. 31, 1992

Objective

The objective of this research is to study new microorganisms and processes for microbial enhanced oil recovery (MEOR) that have been successful in several key aspects. The research has isolated and characterized sulfate-reducing bacteria and denitrifying *Thiobacillus* sp. from oil-field waters that can use volatile fatty acids (VFAs) and dissolve carbonates found in these waters and formations. It has also been shown that these cultures can feed each other in sequential cultures and survive in mixed culture so long as sterile conditions are maintained. When nonsterile conditions are present, both organism types are only successful to a limited degree, and additional microflora belonging to the heterotrophic denitrifying bacteria develop. These microorganisms appear to be potentially useful in new MEOR processes through the production of pressure-forming gases, viscosifying agents, and the removal and prevention of *de novo* synthesis of hydrogen sulfide, and research on them is currently being pursued. They are capable of producing large amounts of gas, predominantly nitrogen and carbon dioxide, and also form viscosifying agents under conditions that can easily be maintained in an oil reservoir. In this report these are also shown to be potent agents for the control of sulfate-reducing bacteria (SRB) growth and the development and production of sulfide.

Summary of Technical Progress

Introduction

Because of experimental difficulties, coreflooding progress during this quarter was limited. Previous coreflood studies have shown that sandstone cores that have been flooded with crude oil and then washed yielded about 10 to 30% more oil

on flooding with a mixture of SRB and denitrifying bacteria with VFAs as the carbon and energy source. Similar results were obtained from sandpack studies as reported earlier.

Enhanced Oil Recovery and Sulfate-Reducing Bacteria

The competition between reservoir SRB and denitrifying bacteria was extensively studied this quarter. In past experiments a water obtained from one of the North Slope Alaskan oil fields was used. During this quarter water was obtained from other oil fields and the water samples were analyzed for their ability to support denitrifying bacteria and the resultant expected oil production because of their metabolic action. The results of the characterization of these water samples are shown in Table 1. Some of the information was supplied by the operators of the fields.

Sulfide was determined with an ion-specific electrode. Sulfate was determined with a wet chemical method. Acetate and propionate were determined by a gas chromatographic method. Total dissolved solids were determined by residue after evaporation. Analysis of P and N, which were not expected, showed that they were not detectable in most of the samples. Samples from these produced waters were injected into the medium that supports the growth of SRB. This medium contained 3.5% salt. Media with acetate and a mixture of acetate–lactate as the carbon and energy source were used. A rough titer was determined by serial dilution techniques. The results are shown in Table 2.

After these data were collected, a series of cultures were set up to determine if heterotrophic denitrifying bacteria were present and what their effect on SRB and sulfide was. Fifty milliliters of each water sample was put into a 100-mL serum bottle and sparged with helium for 15 min to drive off nitrogen and oxygen gas. The bottle was then capped with a butyl rubber stopper, and a deaerated solution containing $\text{NH}_4\text{H}_2\text{PO}_4$ and NH_4NO_3 was introduced with a 10-mL syringe. The syringe was left in the stopper to collect produced gas. This was chromatographically separated by gas chromatography (GC) and quantified. If denitrifying bacteria were present, they would consume the acetate and produce N_2O and N_2 . In addition, they should also inhibit the formation of sulfide by

TABLE 1

Analysis of Oil-Field-Produced Water*

Sample location	TDS, %	Sulfide	Sulfate	Acetate	Propionate	pH
Alaska #1	2.2	12	140	1000	80	8.1
Alaska #2	2.4	22	95	1100	79	8.1
California #1	12.3	0	5	60	0	7.6
California #2	7.6	21	250	200	12	7.7
California #3	4.8	23	65	710	44	8.4
Texas #1	3.6	17	120	920	37	8.2
Texas #2	11.5	23	30	80	2	8.5
Oklahoma #1	18.2	0	50	0	0	7.9
Oklahoma #2	15.1	11	23	10	0	8.0

*Sulfide, sulfate, acetate, and propionate are expressed as ppm.

SRB and reduce the number of viable SRB remaining in the system. The addition of nitrate to this system indeed caused the level of SRB in the system to drop to <100/mL and the heterotrophic denitrifying bacteria increased to about 10⁸/mL. Sulfide dropped dramatically, and there was no apparent new sulfate reduction. The results are presented in Table 3.

The data reveal two very interesting trends. First, the injection of nitrate into these waters helps remove sulfide. The mechanism is not apparently obvious with these data. Second, high salt (i.e., >5 to 7%) inhibits the growth of denitrifying bacteria. There are halotolerant (up to 8% salt) denitrifiers and very halophilic (up to saturation) denitrifiers reported in the literature. However, these microbes may not be present in oil-field-produced waters. Clearly, the denitrifiers not only remove existing sulfide but also prevent *de novo* sulfide production. This action extends to the inhibition of SRB growth and possibly acts to kill viable SRB cells. These results offer a promise to treat oil fields for the control of microbial induced corrosion.

TABLE 2

Presence of Sulfate-Reducing Bacteria in Produced Waters

Water sample	SRB	SRB, titer/mL
Alaska #1	+	10 ⁵
Alaska #2	+	10 ⁵
California #1	-	<1
California #2	+	10 ⁵
California #3	+	10 ³
Texas #1	+	10 ³
Texas #2	+	10 ³
Oklahoma #1	-	<1
Oklahoma #2	+	10 ⁴

TABLE 3

Inhibition of Sulfate-Reducing Bacteria by Denitrifying Bacteria

Sample	Acetate	Sulfide	N ₂	N ₂ O	SRB/mL	DB/mL
Alaska #1	0	<5	+	-	<10	>10 ⁷
Alaska #2	0	<5	+	+	<10	>10 ⁷
California #1	55	0	-	-	<10	0
California #2	0	<5	+	-	<10	>10 ⁷
California #3	0	<5	+	-	<10	>10 ⁷
Texas #1	0	<5	+	+	<10	>10 ⁷
Texas #2	70	15	-	-	<10	0
Oklahoma #1	0	0	-	-	<10	0
Oklahoma #2	10	15	-	-	<10	0

Conclusions

The following contain goals for future pursuit of the project. It will be necessary to redirect the focus of some of the original goals to be successful.

1. Determine the ability of the heterotrophic denitrifying bacteria to produce gas in cores and sandpacks and the effect of this gas on oil release from these cores.

2. Study the ability of heterotrophic denitrifiers to produce viscosifying agents in situ. Identify the conditions necessary for the production of these viscosifying agents.

3. Because the fuel for denitrification by heterotrophic bacteria is dissolved organic material in water, when this organic material is depleted, *T. denitrificans* will then become active. The progression of these organisms as the organic nutrients become depleted will be studied, and the environmental parameters required will be monitored and adjusted to obtain maximum oil production.

QUANTIFICATION OF MICROBIAL PRODUCTS AND THEIR EFFECTIVENESS IN ENHANCED OIL RECOVERY

Contract No. DE-AC22-90BC14662

University of Oklahoma
Norman, Okla.

Contract Date: Aug. 21, 1990
Anticipated Completion: Aug. 20, 1993
Government Award: \$97,467
(Current year)

Principal Investigators:
Michael J. McInerney
Roy M. Knapp

Project Manager:
E. B. Nuckols
Metairie Site Office

Reporting Period: Oct. 1-Dec. 31, 1992

Objective

The goals of this project are to determine the growth kinetics and the relationships that exist among microbial growth, microbial product formation, and oil recovery and to develop mathematical models that predict microbial activity in porous materials.

Summary of Technical Progress

Oil Recovery Related to Microbial Product Formation

The studies on the influence of microbial growth and product formation on the recovery of residual oil from Berea sandstone cores were continued this quarter. The experiments

were carried out at 36 °C using the high-pressure core apparatus described previously. Four microbial and nutrient treatments were carried out on a single Berea sandstone core using the microorganism *Clostridium acetobutylicum* suspended in a glucose–mineral salts medium. The experimental conditions used are listed in Table 1. Microbial growth in the core was monitored by following pore pressure changes.

In the first treatment the pore pressure did not increase during the first 35 h of incubation. During the next 20 h the pressure increased by 175 psig. After a further 75 h of incubation, the pressure decreased, possibly because of the microorganism, *C. acetobutylicum*, switching its metabolism from organic acid production to solvent production, which involves the uptake of hydrogen gas. Biochemical analysis of the effluent showed that 16 mM of glucose was degraded with the production of acetate, butyrate, ethanol, butanol, and CO₂ (Table 2), products characteristic of sugar metabolism by *C. acetobutylicum*. The effective permeability did not change markedly during this treatment (42 to 40 mD), and only 1 mL (about 3%) of the residual oil was produced.

During the second treatment an increase in pressure was observed after only 22 h of incubation as opposed to 35 h for the first treatment. This shorter lag time was probably the result of active microbial population being present from the first treatment. The core pressure again increased by 175 psig over a 36-h period, after which an immediate pressure decrease of 125 psig was observed (Fig. 1). Biochemical analysis of the effluent showed that 60 mM of glucose was degraded, and a corresponding production of acetate, butyrate, ethanol, butanol, and CO₂ was observed (Table 2). Again, only 1 mL (3%) of the residual oil was recovered. The effective permeability increased from 40 to 57 mD. The increase in permeability may be the result of dissolution of carbonate minerals caused by the production of the organic acids.

The lag phase of the third treatment was estimated to be about 3 to 5 h. The length of the lag phase was so short that it could not be accurately estimated because the increase in pressure that results from microbial gas production overlapped that from thermal expansion of the injected liquids. Thermal expansion is estimated to account for 150 psig

TABLE 1
Berea Core Experimental Conditions

	1st treatment	2nd treatment	3rd treatment	4th treatment
Nutrient injection, mL	300	300	300	100
Inoculation, mL	200	250	200	140
Initial pore pressure, psig	500	700	750	1000
Max. pore pressure, psig	575	880	1050	1090
Incubation time, days	12	8	5	8
Oil production, mL	1	1	0	0
Gas production, mL	27	62	51	83
Effective permeability, mD	40	57	55	57

TABLE 2
Biochemical Analysis of Produced Brines from the Core

Effluent*	Glucose, mM	Acetate, mM	Butyrate, mM	Ethanol, mM	Butanol, mM	CO ₂ , mmol/L of effluent
1st treatment E1	152.6	27.0	24.0	3.2	5.3	0.52
E2	184.2	9.0	8.0	2.4	2.3	0.35
E3	114.3	0.4	1.6	ND†	ND	0.25
2nd treatment E1	19.4	29.0	29.5	7.0	9.6	3.09
E2	114.2	35.0	25.6	7.1	7.3	2.65
E3	66.3	11.4	5.2	1.3	0.9	1.35
E4	9.2	3.0	0.9	ND	ND	0.57

*1st Treatment: Liquid effluent volume was E1 = 40 mL, E2 = 43.5 mL, E3 = 50.0 mL; all effluent samples contained an oily layer and fine particulates on the liquid surface except E3. Gas volume was E1 = 9.0 mL, E2 = 7.5 mL, E3 = 11 mL.

2nd Treatment: Liquid effluent volume was E1 = 41 mL, E2 = 41 mL, E3 = 43 mL, E4 = 47 mL; all effluent samples contained fines on the surface except E4. Gas volume was E1 = 19 mL, E2 = 17 mL, E3 = 14 mL, E4 = 12 mL.

The glucose concentrations in the influent of the 1st and 2nd treatments were 166.5 and 111.0 mM, respectively.

†Concentration below detectable limit of the assay used.

increase in pressure (Fig. 2). The core pressure reached a maximum value after 20 h of incubation and again decreased by 100 psig during the next 73 h. No residual oil was recovered during this treatment, and the effective permeability did not change (57 to 55 mD). Biochemical analysis has not been completed on these samples; however, 51 mL of gas was produced during the incubation.

A continual increase in pressure was observed for 20 h when the fourth batch of nutrients was injected into the core. It is estimated that the increase in pressure that resulted from thermal expansion of the liquid should be complete within 5 h of incubation. A maximum pressure of almost 1100 psig was seen after 17 h. After 20 h of incubation, pressure decreased by almost 300 psig over the next 70 h (Fig. 3). Again no residual oil was recovered, and the effective permeability did not change. The amount of gas produced was 83 mL.

Work continues on understanding the mechanism of oil recovery using *C. acetobutylicum*.

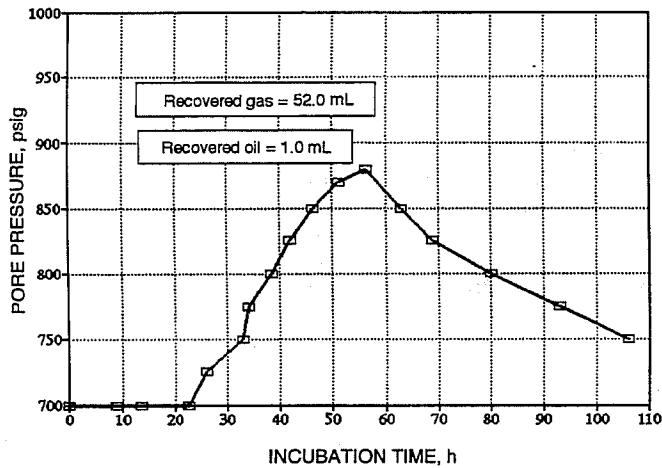


Fig. 1 Pore pressure in treatment No. 2.

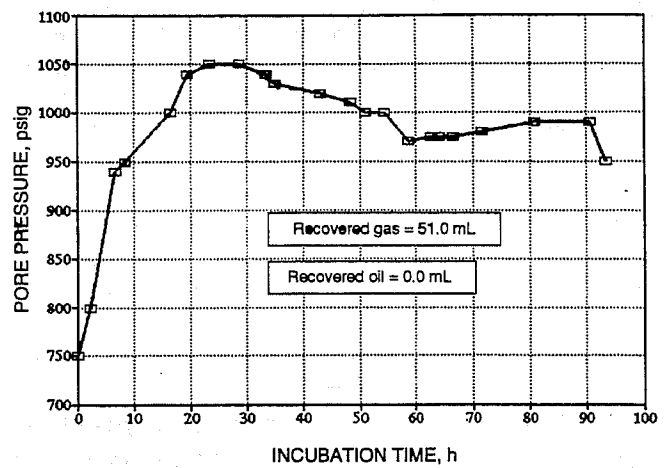


Fig. 2 Pore pressure in treatment No. 3.

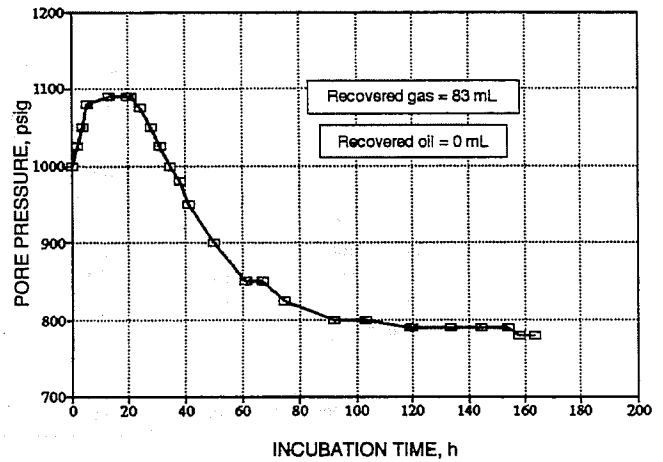


Fig. 3 Pore pressure in treatment No. 4.

EFFECTS OF SELECTED THERMOPHILIC MICROORGANISMS ON CRUDE OILS AT ELEVATED TEMPERATURES

Contract No. DE-AC02-76CH00016

**Brookhaven National Laboratory
Upton, Long Island, N.Y.**

**Contract Date: Mar. 1, 1989
Anticipated Completion: Sept. 30, 1992
Government Award: \$125,000**

Principal Investigators:

**E. T. Premuzic
M. S. Lin**

Project Manager:

**Rhonda Lindsey
Bartlesville Project Office**

Reporting Period: Oct. 1–Dec. 31, 1992

Summary of Technical Progress

Construction of Coreflooding Systems

The construction of a first-generation coreflooding system has been reported in a previous quarter.¹ The core bioreactor, which was constructed from a 304 stainless steel 1.25 x 12 in. tube with a thickness of 0.065 in. and can be operated safely up to a pressure of 2600 psi, is shown in Fig. 1. Berea sandstone (200 mD) has been cut and fitted into the stainless steel tube "bioreactors." A sample of Wilmington, Calif., crude oil was used in several experiments in which Brookhaven National Laboratory (BNL) organisms known to bioconvert this crude oil have been tried in the coreflooding experiments. Routine analyses of Wilmington, Calif., crude oil (Bartlesville Sample 71052) revealed the following data: gravity, 19.4 °API; specific gravity, 0.938; sulfur, 1.59%.²

The results of the first series of coreflooding experiments with five microorganisms from the BNL collection are given in Table 1. These results show significant additional oil recovery under the experimental conditions used. In this series of tests, different conditions and different heavy crude microorganisms systems will be examined.

Objective

The objective of this program is to determine the chemical and physical effects of thermophilic and thermoadapted organisms on crude oils and cores at elevated temperatures and pressures. Ultimately a database will be generated that will be used in technical and economic feasibility studies leading to field applications.

Duration of Biotreatment and Media Effects

Studies of trends in biochemical interactions between different microorganisms and crude oils continue.

Studies with two different crude oils that have not been previously investigated have been initiated. These include an Arkansas crude (°API = 20, S = 4.2%) and Alabama crude (°API = 19, S = 4.6%). The results of tests with the Arkansas

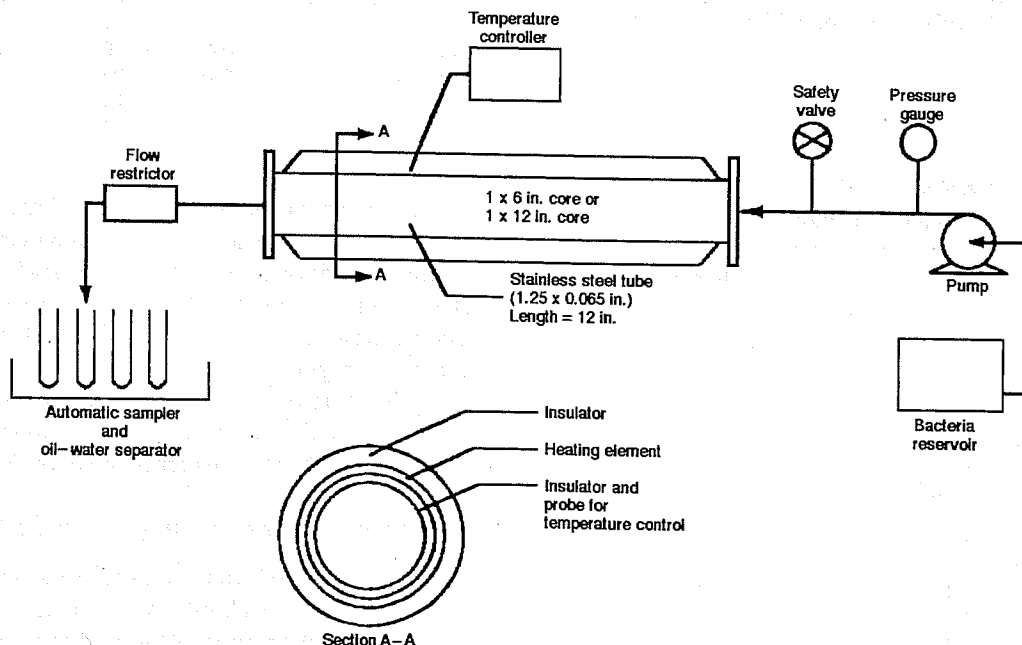


Fig. 1 Flow diagram for coreflooding bioreactor.

TABLE 1

Recovery of Wilmington Crude from Berea Sandstone Cores at 65 °C

	1	2	3	4	5
Core absorbed oil sample weight, g	16.3	16.3	16.7	16.7	16.7
Pressure, psi	44	44	44	30	30
Microorganisms	BNL-NZ-3	BNL-4-23	BNL-4-22	TAQ-2	TAQ-1
Surface tension of culture, dynes/cm	70.7	70.0	70.0	70.7	62.7
Oil recovered by brine, g	5.2	7.6	8.9	5.7	7.8
Oil recovered by growing microorganisms, g	5.7	3.7	2.8	3.2	4.1
Oil recovery by brine, %*	31	47	53	34	47
Additional oil recovery by growing microorganisms, %†	50	43	36	29	46

$$*\% \text{ Oil recovery by brine} = \frac{\text{oil recovered by brine, g}}{\text{oil sample weight, g}} \times 100$$

$$\dagger \% \text{ Additional oil recovered by growing microorganisms} = \frac{\text{oil recovered by microorganisms, g}}{\text{oil sample weight, g} - \text{oil recovered by brine, g}} \times 100$$

crude are given in Tables 2 and 3 and in Figs. 2 and 3. In the presence of tergitol, BNL-4-23 appears to be an efficient bioconverter over a period of 7 d. The controls are oil + medium + detergent (oil-C), oil + medium (control-C), and organisms + medium + tergitol (BNL-#-C). In the absence of tergitol, BNL-4-23 appears to be a weaker emulsifier and requires a longer period of time to be effective. However, gas chromatography-mass spectrometry (GC-MS) analyses and the corresponding gas chromatography analyses equipped with a flame photoemission detector (FPD) indicate little or no change as a result of the biotreatment, although there is some decrease in the overall content of organosulfur components of the crude. These results may be interpreted in the following manner. The biotreatment of Arkansas crude with BNL-4-22 and BNL-4-23 does produce emulsification and some changes in the sulfur content, which could be the result of small chemical changes causing an overall redistribution

TABLE 2

Biotreatment of Arkansas B70116 Crude in Medium 3 in the Presence of a Detergent (Tergitol)*

Microorganisms	Oil, %	Incubation, d	Klett units, OD × 500	pH
BNL-4-22	0.497	7	17.300	4.00
BNL-4-22-C	0.000	7	51.800	4.25
BNL-4-23	0.513	7	142.000	4.00
BNL-4-23-C	0.000	7	61.950	4.00
Oil-C	0.494	7	27.850	4.00
Control-C	0.000	7	10.500	4.25
BNL-4-22	0.516	20	43.000	3.50
BNL-4-22 control	0.000	20	26.000	3.50
BNL-4-23	0.518	20	61.500	3.50
BNL-4-23 control	0.000	20	15.000	3.50
Control, oil	0.510	20	15.500	3.50
Control/control	0.000	20	19.500	3.50

*From Ref. 1.

TABLE 3

Biotreatment of Arkansas B70116 Crude in Medium 3 in the Absence of a Detergent

Microorganisms	Oil, %	Incubation, d	Klett units, OD × 500	pH
BNL-4-22	0.519	7	5.000	3.50
BNL-4-23	0.588	7	0.500	3.50
Control, oil	0.500	7	0.000	3.50
BNL-4-22 control	0.000	7	5.000	3.50
BNL-4-23 control	0.000	7	0.500	3.50
Control/control	0.000	7	0.000	3.50
No Detergent Exp III				
BNL-4-22 control	0.489	20	38.750	4.25
BNL-4-23 control	0.479	20	54.595	4.25
Control, oil	0.526	20	13.625	4.25
BNL-4-22 control	0.000	20	14.595	4.25
BNL-4-23 control	0.000	20	5.365	4.00
Control/control	0.000	20	9.710	4.00

and alteration in mutual solubility of major fractions. To explore further the feasibility of such processes occurring, a sample of Arkansas crude was treated with BNL-NZ-3, an efficient bioconverter of Monterey crude, particularly A851.³ The results are presented in Table 4. Small changes do appear in the scan region of 1200 to 3000, particularly evident in the expanded scan of the 2100 to 3600 region, and even more evident in the FPD chromatograms. Analogous experiments and testing with Alabama crude are currently under way.

Microscopic Comparison of Reaction Mixtures

Results obtained from comparative studies of interaction between different crude oils and microorganisms deliberately introduced for the purpose of biotreatment continue to suggest that the biochemical process(es) may be predominantly driven by introduced and not indigenous microorganisms.

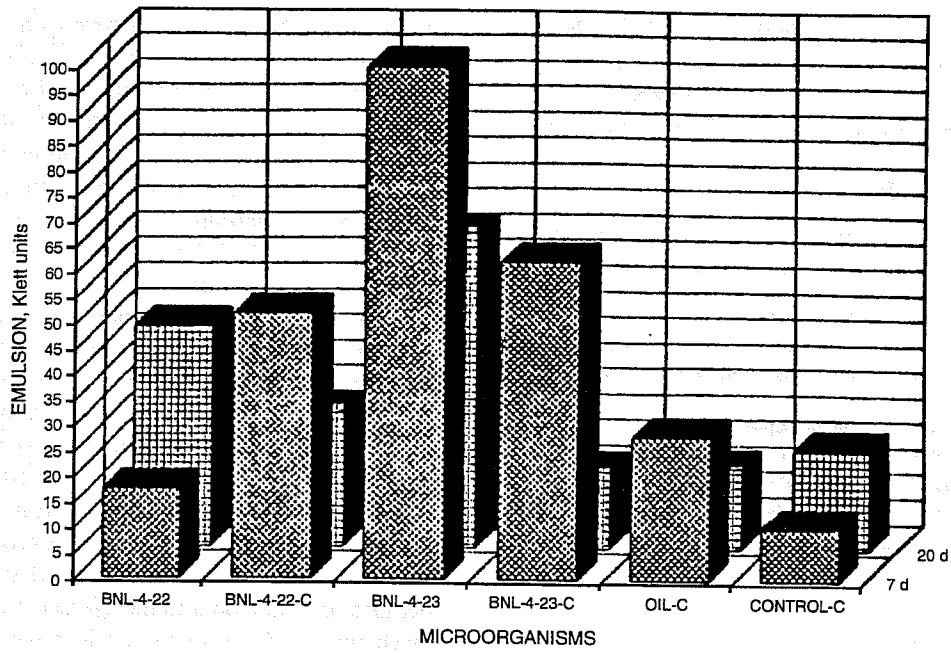


Fig. 2 Arkansas oil B70116 biotreatment, 7 vs. 20 d; media 3 + tergitol.

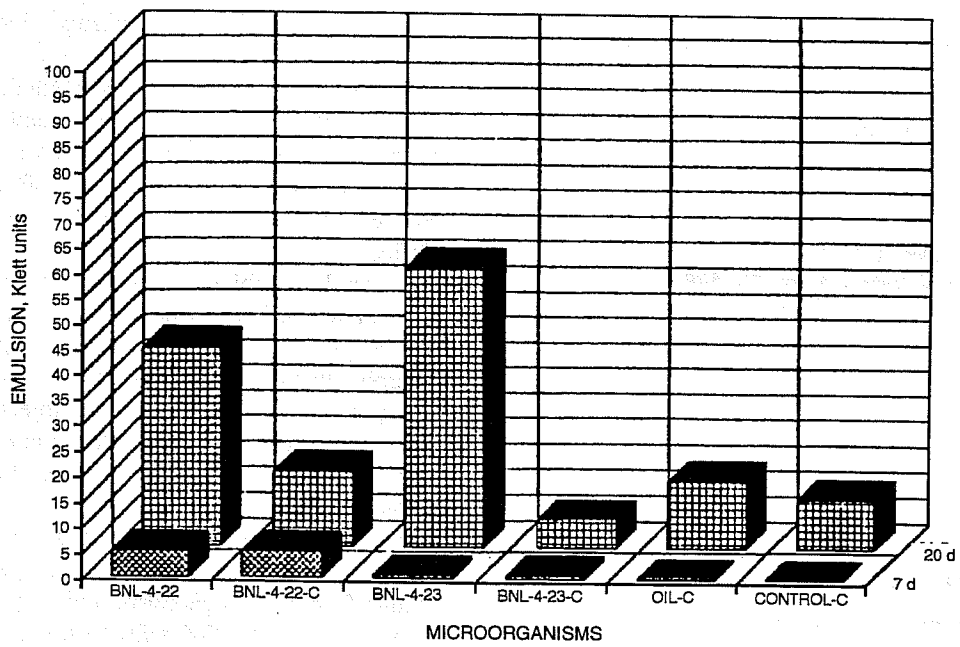


Fig. 3 Arkansas oil B70116 biotreatment, 7 vs. 20 d; media 3 - tergitol.

TABLE 4
Arkansas B70116 Crude Biotreated with BNL-NZ-3

Microorganism	Detergent	Medium	Oil, %	Incubation, d	Klett units, OD×500	pH
BNL-NZ-3	No	3	0.532	7	3.16	4.5

Microscopic comparison is continuing, and observable microscopic changes are evident for Monterey oils in the presence and the absence of tergitol. The differences between "indigenous" effects and "introduced" effects are evident.

References

1. E. T. Premuzic and M. S. Lin, Effects of Selected Thermophilic Microorganisms on Crude Oils at Elevated Temperatures and Pressures, *Quarterly Report* (July 1, 1992–Sept. 30, 1992), Report BNL 48381, September 1992.
2. K. E. Dooley, D. E. Hirsch, C. J. Thompson, J. W. Vogh, and C. C. Ward, Distillate of Wilmington, Calif., Crude Oil, *Hydrocarbon Process.*, 53(7): 141 (1974).
3. E. T. Premuzic et al., Chemical Markers of Induced Microbial Transformations in Crude Oils, in *Fourth International Conference on Microbial Enhanced Oil Recovery—Recent Advances* (E.T. Premuzic and A. Woodhead, Eds.), pp. 37-54, Elsevier, Amsterdam, 1993.

DEVELOPMENT OF IMPROVED MICROBIAL FLOODING METHODS

**Cooperative Agreement DE-FC22-83FE60149,
Project BE3**

**National Institute for Petroleum
and Energy Research
Bartlesville, Okla.**

**Contract Date: Oct. 1, 1983
Anticipated Completion: Sept. 30, 1993
Funding for FY 1993: \$320,000**

**Principal Investigator:
Rebecca S. Bryant**

**Project Manager:
Rhonda Lindsey
Bartlesville Project Office**

Reporting Period: Oct. 1–Dec. 31, 1992

Objective

The objective of this project is to develop an engineering methodology for designing and applying microbial methods to improve oil recovery.

Summary of Technical Progress

Microbial mechanisms shown by the National Institute for Petroleum and Energy Research (NIPER) to be important for oil mobilization include gas and surfactant production. It is important to determine the contribution of microbial gas and surfactant production to oil mobilization. In this regard, ex-

periments with computerized tomography/nuclear magnetic resonance (CT/NMR) imaging and an X-ray/microwave relative permeability apparatus may provide information to assist in the determination of the effect of these metabolites in porous media. To date, there are no reports in the literature where these types of experiments have been conducted with microbial formulations. The only reported relative permeability data for microbial formulations were obtained by NIPER's BE3 research program.

Work on this project has included the continuing development of a three-dimensional (3-D), three-phase, multiple-component numerical model to describe microbial transport phenomena in porous media. Initial efforts have focused on incorporating the most important phenomena for which mathematical models or correlations are available or can be available in a reasonably brief period of time.

Work for FY93 will continue to develop laboratory experiments not only to refine the model with the above parameters, but also to obtain data to incorporate microbial oil recovery mechanisms. Mechanisms considered to be important for oil recovery include changes in microscopic properties, such as interfacial tension, wettability, and adsorption, that govern oil mobilization and affect fractional flow and relative permeabilities. Other oil recovery mechanisms traditionally associated with fluid flow changes include polymer and biomass production by microorganisms.

An evaluation of the environmental, safety, and health impact of the activities, procedures, and equipment required to conduct the planned tasks for FY93 was completed. A status report was submitted on the results of these analyses to the Manager of ES&H at NIPER and to the Bartlesville Project Office.¹

Several microbial retention experiments were completed this quarter. A Berea sandstone core with a permeability of 3.5 darcys was used to determine if the same concentration of microbes that was injected could be recovered in the effluent. Five pore volumes of NIPER 6 were injected, and 42.3% of the microbes were recovered. As shown in Fig. 1, the concentration of cells recovered never reached the concentration injected. Another retention test using a 3-darcy core was conducted that showed a 60.8% recovery of cells. The core was injected with 0.5 PV of NIPER 6 to determine whether the results from very high permeability cores correlated in the same manner as the 900-mD cores. Results with the 900-mD cores showed a correlation between the amount of microorganisms injected and the amount recovered. If this 3-darcy permeability core had followed the same trend, a lower amount of cells would be recovered with the smaller slug injection than with a larger slug injection. This was not the case with this experiment. However, the core showed visible evidence of channeling, which would explain the higher recovery percentage. This experiment will be repeated in the next quarter. Another retention experiment using a ceramic core with a permeability of 766.3 mD has been initiated. Ceramic cores were chosen to determine whether retention of NIPER 6 was the result of adsorption on the rock surface.

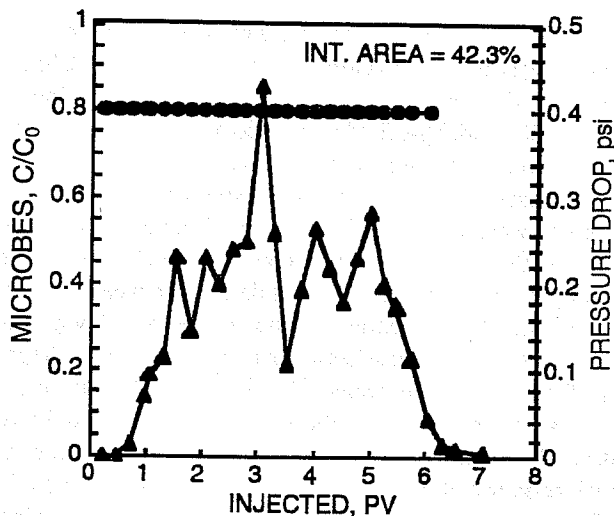


Fig. 1 Effluent from microbial retention test. —▲—, microbes. —●—, PSI.

Other experiments conducted to investigate microbial adsorption used microbial formulations and crushed Berea sandstone compared with glass beads. NIPER 6 bacterial cells were centrifuged, washed, mixed with sterile brine, and added to crushed Berea in one flask and glass beads in another flask. Both flasks were stirred 24 h. The microbial count decreased from 8.5×10^5 cells/mL to 0 in the flask containing Berea sandstone. The microbial count remained about the same (5.1×10^5 cells/mL) in the flask containing glass beads. These results indicate that there is a significant amount of adsorption occurring.

Several relative permeability experiments using NIPER 1A were conducted this quarter. The experimental protocols are being refined as a result of several problems that were encountered. The Berea sandstone core plugs initially used had problems with fines migration and clay swelling. Figure 2 shows a comparison of the relative permeability curves between brine and microbial treatment on the same core plug. The relative permeability to oil increased slightly after microbial treatment. The use of ceramic core plugs should eliminate the problems of fines and clay swelling. However, when the first ceramic core plug experiment was conducted, several pore volumes of microorganisms were injected, and plugging of the core resulted. The microbial formulation did slightly increase the relative permeability to oil before plugging occurred, and the experiment was terminated (Fig. 3). The experimental protocol is being modified to reflect solutions to the encountered problems and more results will be reported in the next quarterly.

Experiments were conducted with several species of bacteria to determine which nutrients will stimulate polymer production. Preliminary results indicate that tryptic soy broth in combination with other nutrients such as fructose may be best for polymer production. Corefloods will be conducted to compare these polymer-producing microorganisms with the surfactant and gas-producing microbial results.

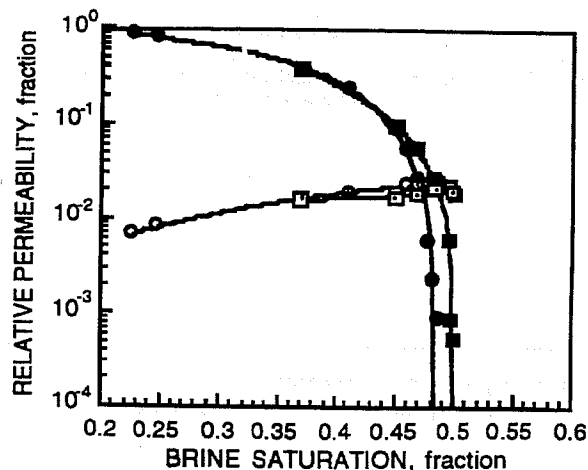


Fig. 2 Comparison of a brine and microbially treated Berea sandstone core plug. —●—, relative permeability of oil, control. —○—, relative permeability of water, control. —■—, relative permeability of oil, NIPER 1A. —□—, relative permeability of water.

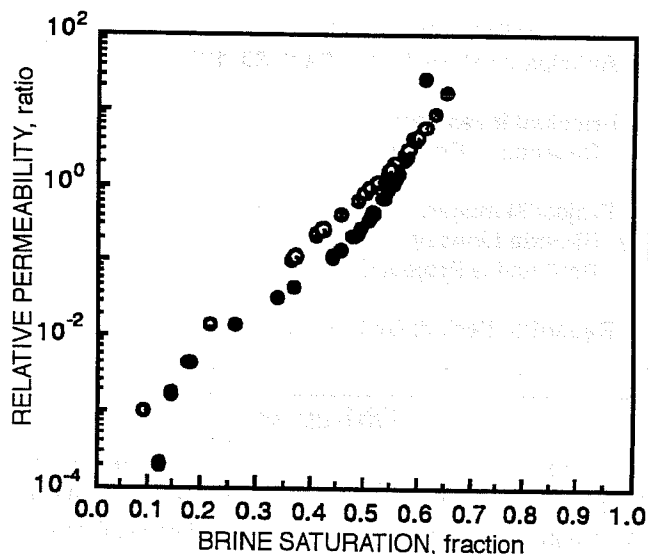


Fig. 3 Comparison of the relative permeability ratios of a brine and microbially treated ceramic core plug. —●—, relative permeability of oil/relative permeability of water, microbes. —○—, relative permeability of oil/relative permeability of water, control.

A core plug experiment using NMR has been initiated to evaluate microbial activity and metabolite production in pore throats. Results will be reported in the next quarterly.

A 4-ft core is being prepared to evaluate oil recovery using NIPER 1A and 6 microbial formulation under simulated reservoir conditions similar to those of the Phoenix Microbial Field Project (SGP13) of temperature and pressure. In accordance with the field project, continuous injection of a low concentration of nutrient will be used. Samples will be taken along the core for microorganisms and their products, and pressure taps will provide valuable data for the numerical simulator.

Reference

1. R. S. Bryant, *Environmental, Safety, and Health Assessment of FY93 Tasks for Project BE3*, DOE Report NIPER-644, December 1992.

MICROBIAL ENHANCED WATERFLOODING FIELD PROJECT

**Cooperative Agreement DE-FC22-83FE60149,
Project SGP13**

**National Institute for Petroleum
and Energy Research
Bartlesville, Okla.**

**Contract Date: Oct. 1, 1983
Anticipated Completion: Sept. 30, 1993**

**Principal Investigator:
Rebecca S. Bryant**

**Project Manager:
Rhonda Lindsey
Bartlesville Project Office**

Reporting Period: Oct. 1–Dec. 31, 1992

Objectives

The objectives of this project are to determine the feasibility of improving oil recovery in an ongoing waterflood using microorganisms and to expand the initial pilot and determine the economics of microbial enhanced waterflooding. The scope of work for FY93 of SGP13 includes continued monitoring of oil production data from the Phoenix field site.

Summary of Technical Progress

The expanded microbial enhanced oil recovery (MEOR) project site is in S8-T24N-R17E of Rogers County, Okla. This

site is part of Chelsea–Alluwe field in the Bartlesville formation and was initially developed soon after Delaware–Childers field. The site is being waterflooded and is owned by Phoenix Oil and Gas, Ltd. This field is in an isolated area with virtually no other oil-producing leases nearby.

Fluorescein was injected as a tracer on June 6, 1990. Samples were collected from all 19 injection wells at 2-h intervals the first day. Twenty-one producers were sampled 24 h after injection of tracer: first daily, then weekly, once a month, and finally, quarterly. Since the second day of sampling, the tracer response has never been higher than 0.30 ppm for all but one of the wells. The pattern of the fluorescein response seems to follow the same trend as that observed during the monitoring of the Mink Unit. There was an initial quick response of tracer from some of the nearest production wells; the response then leveled out to very low values. Fluorescein values seemed to peak at 145 d and were monitored until the end of the molasses injection (599 d).

Wellhead injection pressures and volumes continue to be monitored and have shown no signs of plugging or any other problems. Molasses injection ceased at the end of December 1991. Oil production data have been obtained through November 1992 and are presented in Fig. 1. Lower oil production rates occurred in October and November as a result of inclement weather. The incremental oil produced still shows an improvement of about 14% over the predicted hyperbolic decline. Oil production data will continue to be obtained at least through Dec. 31, 1992.

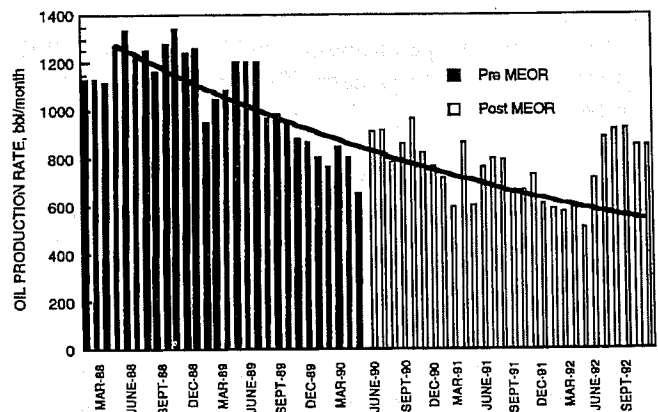


Fig. 1 Oil production from the Phoenix site through November 1992.

RESERVOIR CLASSES

GREEN RIVER FORMATION WATERFLOOD DEMONSTRATION PROJECT, UINTA BASIN, UTAH

Contract No. DE-FC22-93BC14958

**Lomax Exploration Company
Salt Lake City, Utah**

**Contract Date: Oct. 21, 1992
Anticipated Completion: Oct. 1, 1995
Government Award: \$1,304,000**

Principal Investigators:

**John D. Lomax
Dennis L. Nielson
Milind D. Deo**

Project Manager:

**Edith Allison
Bartlesville Project Office**

Reporting Period: Oct. 1–Dec. 31, 1992

Objective

The Green River Formation of the Uinta Basin, Utah, contains abundant hydrocarbons that are inefficiently produced by primary means. However, secondary recovery

projects have only been rarely implemented, largely because of complex geology and hydrocarbon chemistry. An evaluation of the successful Lomax Monument Butte Unit waterflood will be performed under this contract, and based on this information, waterfloods will be initiated in nearby Travis and Boundary units. This project will also develop new techniques to characterize reservoir heterogeneity and the response of the reservoir to waterflooding.

In 1987, Lomax Exploration Company successfully implemented a waterflood on their Monument Butte Unit which has a geologically heterogeneous low-energy reservoir with a high-paraffin crude oil. Production of about 5% of the original oil in place (OOIP) from primary methods was increased through the waterflood to an estimated recovery of 20% OOIP. The project will (1) perform a technical evaluation of the successful Monument Butte Unit; (2) on the basis of this information, extend the successful waterflood to the nearby Travis and Boundary units; (3) develop new characterization techniques; and (4) transfer the technology to operators, regulators, government agencies, and the financial community.

Summary of Technical Progress

The Monument Butte No. 10-34 was spudded on October 2, 1992, and drilled to a depth of 6400 ft. On the 38th day after the spud date, logging of No. 10-34 was started. On the basis of the results of logging, a 5½-in. casing was cemented in the hole. As of November 24, 1992, No. 10-34 has been completed. The objective was to complete "A" and the "D"

intervals in the Castle Peak, Black Shale, of the Green River Formation. All four intervals have been perforated and fractured. From November 27, 1992, through January 27, 1993, oil production has been 3393 barrels (54 barrels per day).

The Travis No. 14a-28 was spudded on October 6, 1992, and drilled to a depth of 6190 ft. On the 20th day after the spud date, logging of No. 14a-28 was started. On the basis of the results of the logging and coring, a 5½-in. casing was cemented in the hole. The Lower Douglas Creek and the "D" intervals of the Green River Formation have been completed. However, because of the fracturing of the Lower Douglas Creek, only the "D" sand interval was put on production. From January 1 through January 28 No. 14a-28 has produced 2947 barrels of oil (105 barrels per day) and 1.9 Mcf of gas (107 Mcf per day) from the "D" sand interval. Because of the success of the "D" sand, other Travis unit wells with "D" sand intervals behind pipe will be recompleted. Further study of the Lower Douglas Creek interval will be done before an attempt to put the interval on production.

A full-diameter core was taken in the upper portion of the Lower Douglas Creek in Travis No. 14a-28. This core has been logged in detail and five plugs have been analyzed using thin sections and X-ray diffraction. Horizontal and vertical permeability, porosity, oil and water saturation, and grain density have been determined on the same plugs. The sandstone units are composed of packages of planar-laminated fine-grained sandstone that exhibit varying degrees of dewatering and soft-sediment deformation. These are separated by either slightly disrupted siltstone or massive very fine-grained sandstone with abundant clasts. The planar-laminated sandstones occur in 15-ft-thick packages with an intraclast-rich base and a dewatered top and are interpreted as moderate- to low-density turbidite channels.

The strongest oil shows are in planar-laminated sandstone. The rocks are cemented largely with calcite and dolomite. Late, secondary porosity was formed through dissolution of feldspar. Most of the clay in the planar-laminated sandstone is nonswelling illite and chlorite.

The Department of Energy (DOE) program has allowed Lomax Exploration to use state-of-the-art methods to evaluate the geological processes that influence the waterflood. The Schlumberger Fullbore Formation MicroImager (FMI) and the Numar's Magnetic Resonance Imaging Log (MRIL) were used in the evaluation of the Monument Butte No. 10-34 and Travis No. 14a-28 wells.

The Schlumberger FMI was used to evaluate the stratigraphic sequences of interest to develop a better understanding of the stratigraphy and depositional environment of potential reservoir beds. This log is also valuable in locating fractures as well as determining the orientation and size of the fractures. Fractures were found in areas where they had not previously been detected. This information is critical to selecting completion intervals and designing stimulation treatments. The FMI log is also very useful for thin bed evaluation and for locating the best places to take rotary sidewall cores. In the Travis No. 14a-28 well, a large amount of fracturing

was seen using this log. The fractures normally occur in the sandstone units and are bounded by shales. A histogram of 18 fractures shows an orientation from E-W to WNW-SES, parallel to the trend of the Duchesne fault system (Fig. 1). From inspection of the core, it was found that the fractures were developed both during soft sediment deformation and dewatering and by later tectonic activity. Initial analysis of bedding orientation suggests that the turbidite sequences and slumping that are well-exposed in the core were derived from the northwest of the well.

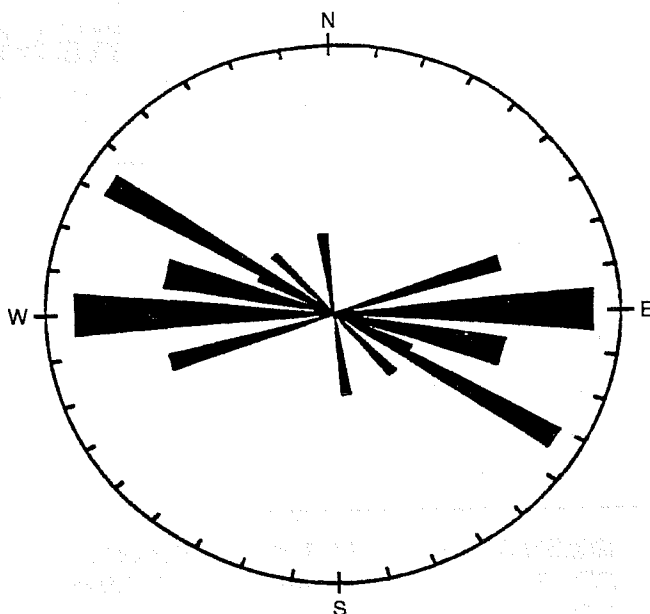


Fig. 1 Fracture orientation as determined from Fullbore Formation MicroImager (FMI) log of Travis No. 14A-28.

The second advanced research log used is Numar's MRIL. This log was used to evaluate the movable fluid content of the reservoir rock and to determine the effective permeability within the reservoir. At least one zone that by sample and core analysis appeared to be noncommercial in the Monument Butte No. 10-34 well was indicated by the MRIL to have movable hydrocarbons. Subsequent completion has established commercial production.

In the Monument Butte Unit, an average well has approximately twenty sands with production potential. Ten sands will usually be eliminated as being too discontinuous or too thin. The ten remaining sands have to be evaluated with regard to their relative permeability. The evaluation of effective permeability has been most difficult to obtain, and yet it is critical to making a commercial completion. Early indications are that prudent use of these new logs may enhance completion practices and reduce the cost of well completions.

Gas analyses have been completed on the wells sampled (Table 1). There were no significant composition differences between the two gas samples. Both gas samples consisted of approximately 50 wt % methane, 20% each of ethane and

propane, and 10% heavier hydrocarbons and nonhydrocarbons (71 mol % methane, 13 ethane, 9 propane, and 7 other).

Approximately 30 wt % of material boils above 1000 °F. The high-boiling fractions will not pass through the gas chromatograph during standard operations and are retained in the injection port and column. This accumulated material breaks down during later runs and makes it impossible to interpret the results. This problem is solved by “conditioning” the injection port and the gas chromatograph column after each test by increasing the injection port temperature to 750 °F and by keeping the oven temperature at 600 °F for 80 minutes. This drives the contaminants off and allows further tests.

The amount of high-boiling material in the samples was determined using a modification of ASTM Standard Method D2887. Running successive samples of the same crude oil,

TABLE 1

Well Gas Analyses of Monument Butte Unit Wells

Mass Fraction of Gas Components, %		
Component	Well 10-35 B and D-1 sands	Well 12-35 D-1 sands
Methane	51.44	54.85
Ethane	19.42	17.35
Propane	19.84	16.33
Isobutane	0.92	0.66
n-Butane	6.18	5.52
Isopentane	0.34	1.79
n-Pentane	0.90	2.17
Hexanes	0.97	1.31

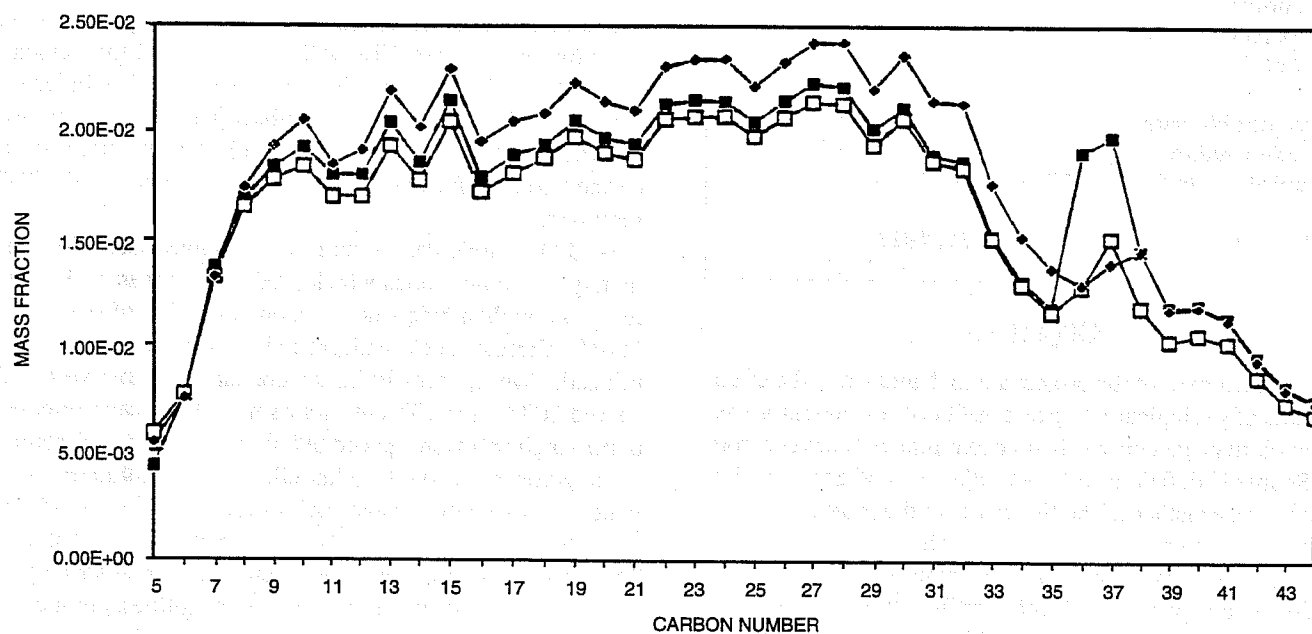


Fig. 2 Monument Butte oil composition. -■-, well 8-35. -□-, well 10-35. -◆-, well 12-35.

with a second sample mixed with a known amount of a standard material, allows the amount of high-boiling material in the sample to be calculated. The modified test method was found to be quite reproducible. See Fig. 2 for a comparison of the three crude oil compositions.

The No. 10-35 well crude has a slightly heavier material. The fact that No. 10-35 delivers oil from the B and D zones

while the No. 12-35 only delivers from the D zone suggests that the B zone has a somewhat heavier oil.

References

1. John Lomax, *Waterflood Project in the Monument Butte Field, Uinta Basin*, paper presented at the Annual Meeting of the Interstate Oil and Gas Compact Commission, Salt Lake City, Utah, December 6-8, 1992.

ADVANCED SECONDARY RECOVERY DEMONSTRATION FOR THE SOONER LIST

Contract No. DE-FC22-93BC14954

**Research & Engineering Consultants, Inc.
Palo Alto, Calif.**

Contract Date: Oct. 21, 1992

Anticipated Completion: Mar. 31, 1995

Government Award: \$281,000

(Current year)

Principal Investigators:

**Mark Sippel
James Junkin
Ronald Pritchett
Bob Hardage**

Project Manager:

**Edith Allison
Bartlesville Project Office**

Reporting Period: Oct. 1–Dec. 31, 1992

Objectives

The objectives of the project are to demonstrate the effectiveness of geologically targeted infill drilling and improved reservoir management to obtain maximum oil recovery from the Sooner Unit field using water injection and gas recycling as secondary methods. The first phase of the project involves an integrated multidisciplinary approach to identify optimum well sites and development of a reservoir operations plan.

The second phase will involve drilling three geologically targeted infill wells and establishing production/injection schedules. Reservoir simulation, transient well tests, and careful production monitoring will be used to evaluate the results.

The third phase will involve technology transfer through a series of technical papers and presentations of a short course. Emphasis will be on the economics of the project and the implemented technologies.

Summary of Technical Progress

Drill and Complete Wells

A new well was drilled and completed which confirmed and extended a reservoir compartment that was not significantly affected by pressure from water injection. The offsetting water injection well had a 6-day bottomhole shut-in pressure of 1250 psi.

The Sooner Unit 9-21 (NESE sec. 21, T. 8 N., R. 58 W.) was spudded on September 4, 1992, and drilled to a total depth of 6402 ft KB (Fig. 1). A drillstem stem test was run over the

“D” interval from 6282 to 6320 ft. The recovery was 235 ft of oil and gas cut mud. The final shut-in pressure was 533 psi and was nearly stabilized. Meaningful pressure transient analysis for permeability was not possible because of the low pressure and recovery of mostly drilling mud. The well was logged with gamma-ray, neutron-density, dual-induction, micro-log, and dipole sonic tools. Casing was run to total depth (TD) and the well was completed, pumping 12 bbl oil, 1 bbl load water, and 35 mcf gas per day after hydraulic fracture stimulation.

Seismic Data Acquisition

A vertical seismic profile (VSP) survey was run in the Sooner Unit 10-21A well on October 12, 1992. The well was surveyed from 6350 to 4350 ft at 50 ft intervals. The purpose of the survey was to identify the seismic waveform corresponding to the “D” reservoir and establish the optimum field recording parameters. The VSP data provided the velocity control needed for seismic depth conversion and an independent reflection image of the subsurface stratigraphy for transfer to the three-dimensional (3-D) data volume to define exactly which wavelet feature corresponds to the “D” reservoir.

A 3-D seismic data volume was obtained over approximately 7.7 square miles which produced images of the “D” reservoir with a frequency content extending from 10 to 100 Hz. Vibrator trucks with ground-force phase locking were utilized. Twenty receiver lines were surveyed east-west and spaced 800 ft apart. Twenty-four source lines were oriented north-south and were spaced 600 ft apart. The 200-ft source spacing used on each source line allowed four vibration points to be recorded between each pair of receiver lines. A total of 732 vibrator points were recorded to create the data volume. There were minimal deviations from the normal spacing to avoid cultural obstructions such as fences, gullies, production facilities, and agricultural crops. The 3-D stacking bins had a cross-sectional area of 100 by 100 ft. There were approximately 21,000 stacking bins in the final processed data volume.

A strong emphasis on static analysis was required because the surface topography over the Sooner Unit area has a vertical relief of 100 ft or more across rolling hills of grassland separated by erosional features. Spectral whitening was applied to the binned data to maintain the widest possible spectrum. The “D” reservoir reflections have significant energy in the range of 70 to 80 Hz and measurable energy exists at frequencies between 90 and 100 Hz.

Forward modeling was performed to infer how changes in thickness and impedance of the “D” sandstone member can affect the character of the “D” to “J” reflection and how subtle stratigraphic changes may be revealed in the seismic reflection amplitude and frequency maps. The two most important relationships are that the “D” reflection peak increases as the thickness of the “D” sandstone increases, and the frequency of the “D” reflection peak increases as the impedance of the “D”

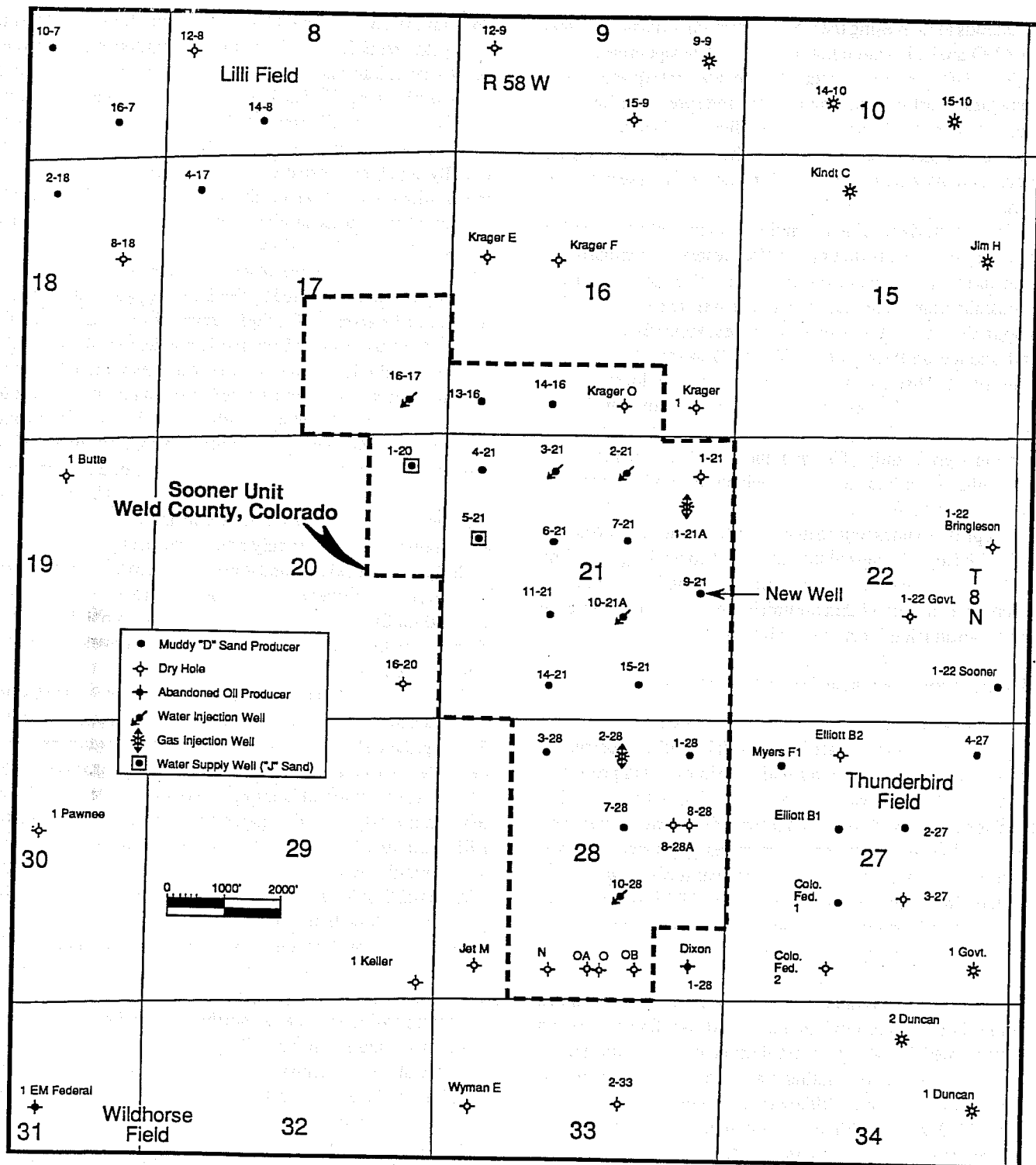


Fig. 1 Sooner Unit field area.

sandstone increases. A total of six stratigraphic units were used in the earth model to generate the synthetic reflection responses.

Modeling indicates that an Amplitude Versus Offset (AVO) analysis of the Sooner Unit 3-D seismic data would not provide definitive answers about the spatial distributions of

pore fluids within the "D" reservoir. Measurable AVO changes are created only when the gas saturation is greater than 90%, which is an unlikely condition when irreducible water saturations of 20% or greater are expected. There is also no significant change in the AVO response of the "D" reflection when the impedance increases within the "D" reservoir, which is

analogous to increasing the water saturation. This implies that an AVO analysis would not detect water-swept areas.

The 3-D processed data volume was interpreted on a GeoQuest workstation. The primary interpretation involved analysis of the "D" amplitude, time slices, and slices with the data volume flattened on the base of the "D" interval. Vertical cross sections were interpreted along and across the reservoir axis.

The "D" horizon relative amplitude map exhibits a number of strong lineaments that may reflect reservoir compartment boundaries. These major lineaments are also observed on the Huntsman amplitude map and, to a lesser degree, on the "J" amplitude map. These lineaments appear to persist in location and orientation through the "D" and Huntsman shale intervals. Faults that appear to be coincident in location and orientation with the lineaments are observed above and below the "D" horizon. Many of these faults do not offset the "D" horizon significantly. The maximum fault offset measured across the "D" is 4 ms to 5 ms which corresponds to approximately 25 to 35 ft.

Amplitude and isochron maps of the "D" horizon correlate well with isopach maps of the "D" based on well log data. The "D" amplitude and isochron maps indicate that the "D" horizon is contained mostly within the unit boundary and that there are several promising locations for infill drilling.

Geologic and Engineering Interpretation

The depositional setting descriptive of Graneros "D" member reservoir in the Sooner Unit is tidally influenced fluvial sandstones which were deposited, distributed, and preserved in an estuarine environment. Cores from five wells, one within the Sooner Unit and four from nearby fields, were examined and described for sedimentary structures, grain size, and rock types. In particular, evidence for erosional surfaces was documented. The estuarine environment of the "D" reservoir at the Sooner Unit is similar to depositional styles described by Dalrymple,¹ Dalrymple et al.,² and Thomas et al.³

The rock type is a quartz to subarkosic arenite and grain size is silt-sized (less than $\frac{1}{16}$ mm) to fine-grained (to $\frac{1}{4}$ mm). Sorting is poor (phi deviation standard trending to 1.0 and greater), which indicates distribution or redistribution of clastic material in oscillating transport energy. Grains are rounded to subangular, although sphericity tends toward a value of 1.0 (grain width in two directions is nearly the same).

A sequence stratigraphic interpretation was applied to log correlations after identification of unconformities. The core from the Sooner Unit No. 7-21 well shows a sequence of silty sandstones, interbedded shaly siltstones, and thin shale laminae. Sedimentary structures were identified in the 7-21 core that help define an estuarine environment of deposition which includes low-angle laminae, inclined heterolithic strata, clay and shale laminae (mud drapes), flaser beds, ripple-drift cross strata, and lenticular beds.

There are four subreservoirs within the "D" member which contain oil-productive sandstones. These subreservoir inter-

vals have been designated R1, R2, R3, and R4 from oldest to youngest, respectively. The spatial relationships between subreservoir intervals are shown in a diagrammatic west-east cross section (Fig. 2). The log and core data suggest that these intervals are vertically separated by less than 2 to 10 ft or more of impermeable rock types and that these intervals are not equally developed across the Sooner Unit area. In addition to the vertical separation of the four subreservoir intervals, sigmoidal mud-drape laminae within each interval may act as baffles and direct fluid flow.

Subreservoir R1 is the oldest and deepest of the reservoir sequences. It was deposited by fluvial energy above a Lowstand Surface of Erosion (LSE). Subreservoir R1 is found along the west side of the Sooner Unit and is oriented north-northwest. The areal width is less than $\frac{1}{2}$ mile with a maximum thickness of 14 ft. Well-log characteristics exhibit a fining-upward profile.

Subreservoir R2 contains sandstones exhibiting fluvial and tidal energy influences on deposition. Subreservoir R2 is the most developed sandstone across the unit area and represents the second depositional cycle of the "D." The maximum thickness is 20 ft. The sandstone consists of medium to very fine grained particles evenly graded vertically.

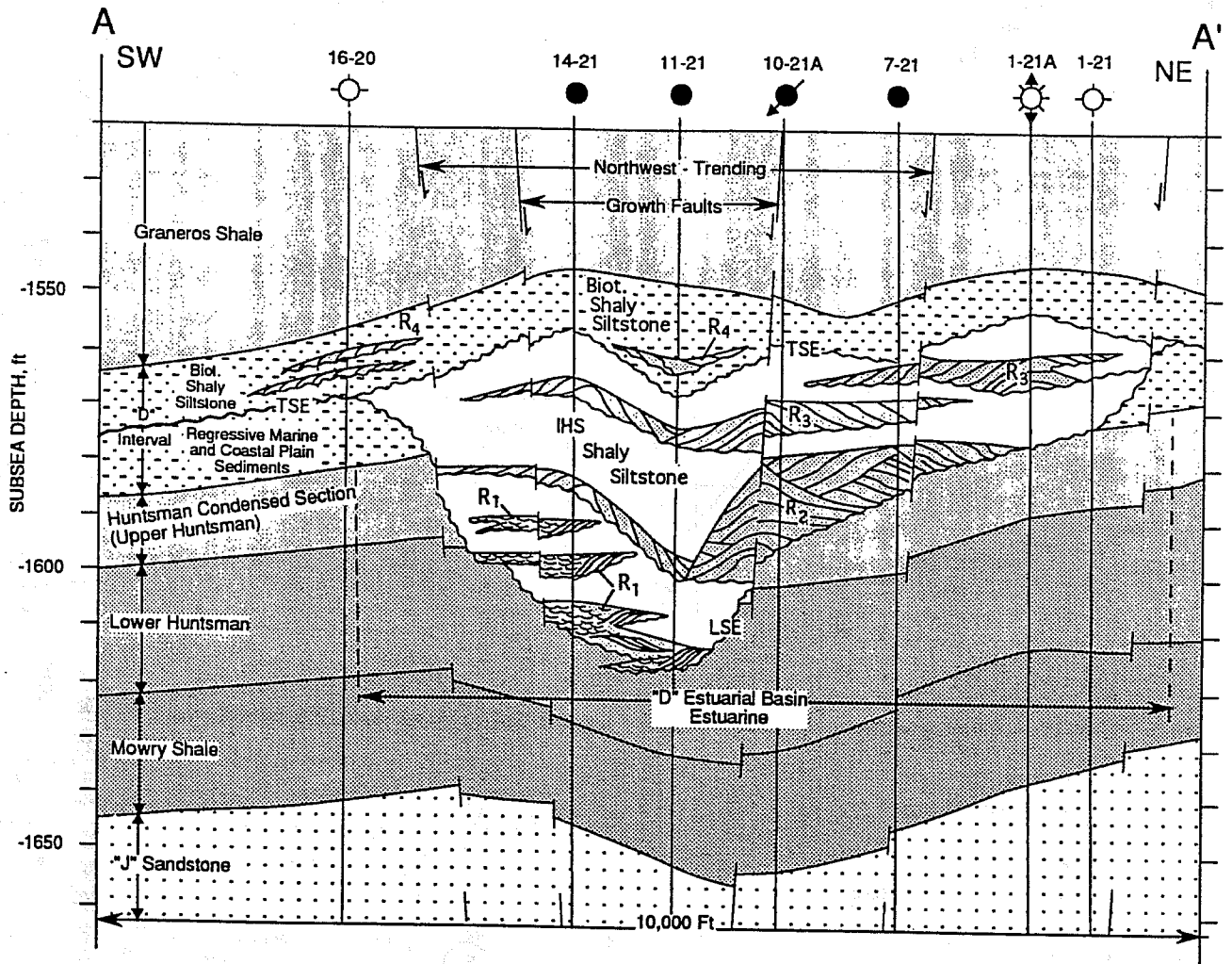
Subreservoir R3 is a sandstone interval exhibiting tidal and marine energy influences on deposition. R3 is slightly fining-upward sandstone and the interval displays a maximum productive thickness of 11 ft. This interval is developed on the north and east side of the Sooner Unit area.

Subreservoir R4 is the youngest and shallowest sandstone interval and exhibits a coarsening-upward sequence. Interval R4 migrated shoreward from the north to south and was deposited above a Transgressive Surface of Erosion (TSE). This reservoir interval is interpreted as being deposited contemporaneously with the major productive sandstone of the Lilli field, just north of the Sooner field. The interval is thin and lenticular with sandstone-thick axes semiparallel to the Lilli trend. The R4 subreservoir interval has a net productive thickness of less than 4 ft.

Seismic maps show fault displacement of events across the "D" reflectors. Disrupted amplitude events, interpreted as faults, are visible in time-section profiles from basement reflectors to the surface. A northwest-trending set of faults appears to bound thicker "D" sandstone and suggests that these faults were primary controls on deposition. Northeast trending faults are also present and appear to have occurred after deposition of the "D" reservoir.

A total of seven reservoir compartments was identified from production and pressure histories. These operational or production compartments, consisting of from one to four wells, are shown in Fig. 3. These compartments are not, in every case, absolute because there is some overlapping of boundaries.

Several previously acquired pressure buildup tests were analyzed. The permeability to oil was determined to range from 10 to 100 mD. Only one well, the Sooner Unit No. 2-28, exhibited a buildup character which indicated reservoir barrier effects. The buildup test data indicated stimulated



-  Tidal and Marine Influenced Reservoir Sandstone
-  Fluvially-Dominated Reservoir Sandstone
-  Inclined Heterolithic Strata (IHS)
-  Bioturbated Shaly Siltstone
-  Shale
-  J Sandstone

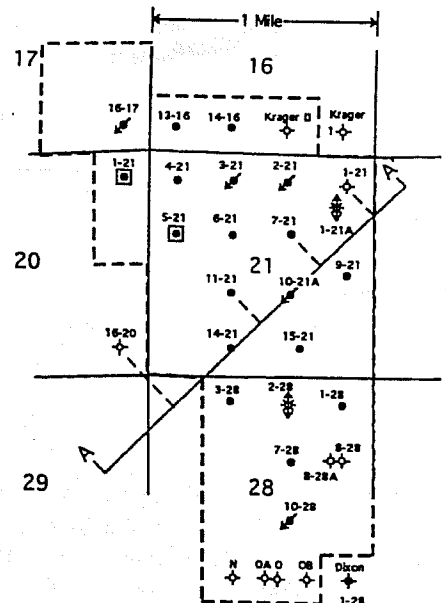


Fig. 2 Diagrammatic southwest-northeast structural section across the Sooner Unit showing spatial relationships between oil productive "D" subreservoirs R1, R2, R3, and R4.

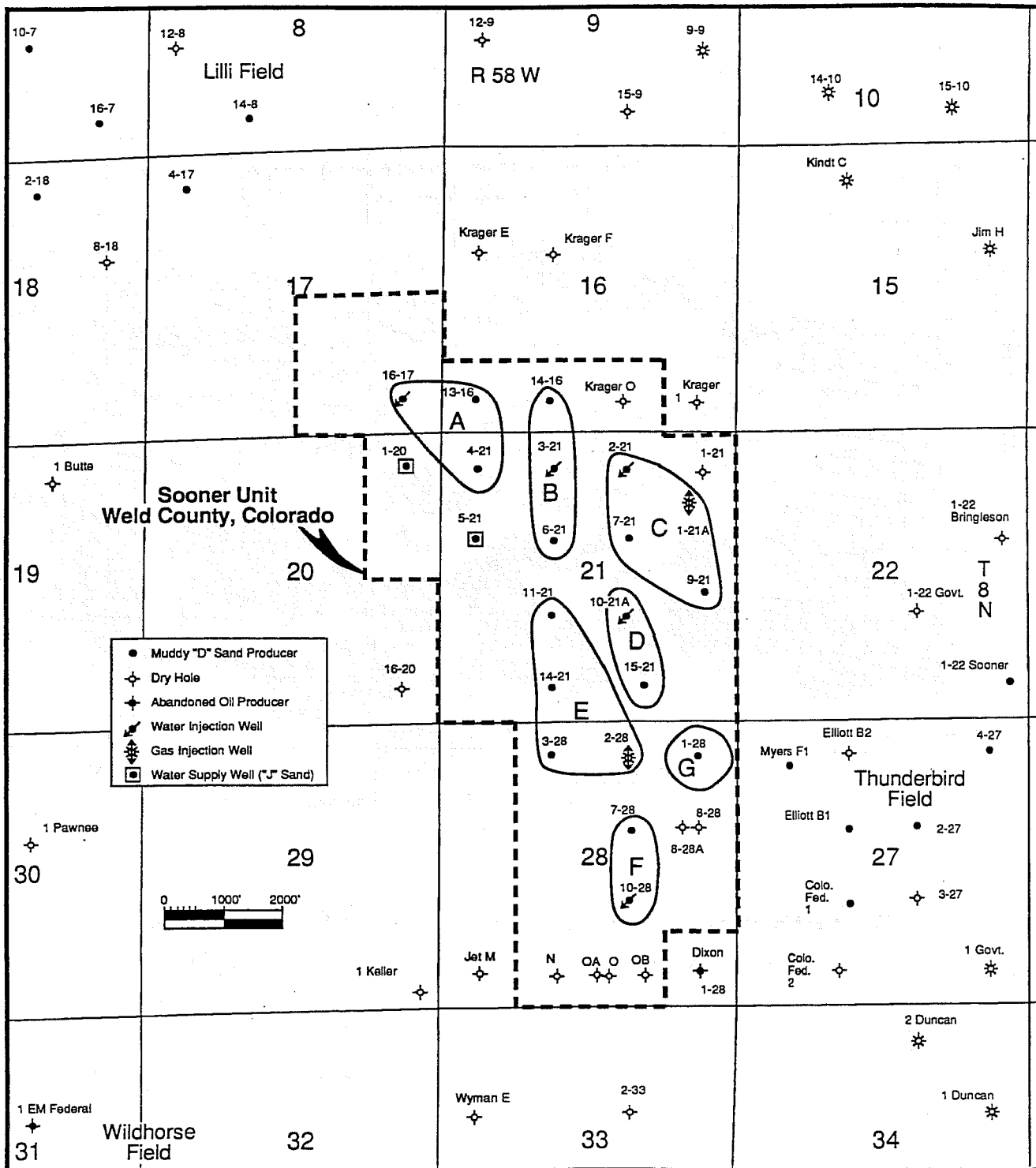


Fig. 3 Operational compartments—seven well-groups, A through G.

completions with a typical negative skin factor "S" of -3 to -4. All wells have been hydraulically fractured.

Three conventional core studies of the "D" reservoir rock were reviewed. One core was from the Sooner Unit 7-21 well and two core studies were reviewed from the Lilli field, located one mile north from the Sooner field. These core data were found to have a mean air permeability of about 10 mD

and a high Dykstra-Parsons variance factor of 0.9. Porosity and permeability data were used to develop a porosity cutoff of 8% for net pay calculations from logs. The derived permeability-porosity correlation was also used to estimate formation permeability from digitized porosity log data.

During recording of the seismic data, all wells were shut in and static pressure measurements were obtained on all wells

after 6 d. The static pressures ranged from 121 to 2399 psi. These pressure data were used to identify operational reservoir compartments and to calculate the production-voidage and injection balance in the identified reservoir compartments.

The current pressure, production, and injection data were used to determine that injection has been short of maintaining a balance with the current rate of reservoir voidage. Recommendations concerning operations, which included adjustments in injection volumes and changes of production status for several wells, were made to the operator.

The pressure-volume-temperature (PVT) analyses of the "D" reservoir fluids previously performed for the Sooner and Lilli fields were found to adequately represent the production characteristics of these fields in black-oil simulations. The Lilli field, which lies one mile north of the Sooner Unit, exhibits more homogeneous reservoir characteristics than Sooner and analyses of reservoir fluids from that field are similar to those obtained from Sooner. Successful simulation history matches of gas/oil ratio (GOR) and pressure were obtained from the Lilli Federal Rim No. 4-7 and 6-7 wells and the Sooner No. 2-28 well using rate-specified, single-layer, black-oil models. This simulation study indicates that black-oil simulations and the available PVT data adequately represent reservoir fluid properties.

Several volumetric and material balance methods were used to estimate the original oil in place (OOIP) contacted by the existing wells under primary operations. Logs from wells in the unit and adjacent areas were digitized to calculate hydrocarbon pore volumes and saturations. These log data were used to calculate an OOIP for the unit area wells. The OOIP by volumetric methods is determined to be 5.2 million stock tank barrels (STB).

The OOIP is determined to be 6.6 million STB using a method described by Calhoun.⁴ The total gas produced under primary operations for each tank battery was estimated by integrating a plot of producing GOR vs. cumulative oil produced. The static pressure data were then plotted with cumulative gas and extrapolated to atmospheric pressure to determine the total original gas in place (OGIP). Since there was originally no free gas cap, OOIP is determined by dividing the OGIP by the initial solution GOR of 502 scf/STB.

A black-oil model based on the Sooner No. 2-28 history match was used to generate a plot of primary recovery factor (N_p/N) vs. average reservoir pressure. This plot exhibits linear behavior during advanced depletion under primary production and was extrapolated to a primary recovery factor of 14% of OOIP at a final pressure of 200 psi. With this same plot, the recovery factor for each Sooner tank battery was determined by pressure surveys at the end of primary production in 1988. With the use of these recovery factors, the OOIP contacted by these wells is determined to be 6.4 million STB.

References

1. Robert W. Dalrymple, Tidal Depositional Systems, in *Facies Models—Response to Sea Level Changes*, Roger G. Walker and Noel P. James (Eds.), Geological Association of Canada, 1992.
2. Robert W. Dalrymple, Brian A. Zaitlin, and Ron Boyd, Estuarine Facies Models: Conceptual Basis and Stratigraphic Implications, *J. Sediment. Petrol.*, 62(6): 1130-1146 (November 1992).
3. R. G. Thomas, Derald G. Smith, James M. Wood, John Visser, E. Anne Calverley-Range, and Emlyn H. Koster, Inclined Heterolithic Stratification—Terminology, Description, Interpretation and Significance, *Sediment. Geol.*, 53: 123-179 (1987).
4. John C. Calhoun, Jr., *Fundamentals of Reservoir Engineering*, pp. 229-231, University of Oklahoma Press, 1947.

**REVITALIZING A MATURE OIL PLAY:
STRATEGIES FOR FINDING AND
PRODUCING UNRECOVERED OIL
IN FRIO FLUVIAL-DELTAIC
RESERVOIRS OF SOUTH TEXAS**

Contract No. DE-FC22-93BC14959

**University of Texas
Bureau of Economic Geology
Austin, Tex.**

**Contract Date: Oct. 21, 1992
Anticipated Completion: Dec. 31, 1994
Government Award: \$817,911**

**Principal Investigator:
Noel Tyler**

**Project Manager:
Edith Allison
Bartlesville Project Office**

Reporting Period: Oct. 1–Dec. 31, 1992

Objectives

Advanced reservoir characterization techniques will be applied to selected reservoirs in the Frio fluvial-deltaic sandstone (Vicksburg Fault Zone) oil play of South Texas in order to maximize the economic producibility of resources in this mature oil play. More than half of the reservoirs in this depositionally complex play have already been abandoned, and large volumes of oil may remain unproduced unless advanced characterization techniques are applied to define untapped, incompletely drained, and new pool reservoirs as suitable targets for near-term recovery methods.

Primary technical objectives of this project are to develop interwell-scale geological facies models of Frio fluvial-deltaic reservoirs and combine them with engineering assessments and geophysical evaluations in order to characterize Frio fluvial-deltaic reservoir architecture, flow unit boundaries, and the controls that these characteristics exert on the location and volume of unrecovered mobile and residual oil. These results will lead directly to the identification of specific opportunities to exploit these heterogeneous reservoirs for incremental recovery by recompletion and strategic infill drilling.

Summary of Technical Progress

Progress achieved during this initial reporting period consisted of beginning the initial task of screening fields within the play to select representative reservoirs that have a large remaining oil resource and are in danger of premature abandonment. Data are being compiled from productive Frio reservoirs distributed among fields along the entire play trend,

which extends from Starr County northeastward to Jim Wells and Nueces Counties in South Texas. The fundamental criteria for the selection of individual Frio fluvial-deltaic reservoirs appropriate for detailed characterization studies will be based on the quality of the field/reservoir data and the potential for identifying additional reserves. Those fields possessing an extensive geological, petrophysical, geophysical, and production database coupled with the greatest possibilities for infield reserve growth are the most likely candidates to be selected for further study. At the present time the Rincon Field, operated by Conoco in Starr County, is a strong candidate for selection based on the availability of an extensive database that includes abundant core data. Data from Mobil's acreage in the Tijerina–Canales–Blucher (TCB) field in Kleberg County are currently being examined, and the decision to review operator data from additional fields will take place upon completion of the screening of data from public sources. Final selection of specific fields and reservoirs that will be the subject of detailed reservoir characterization studies is scheduled for completion in the next quarter.

Introduction

This technical progress report documents work completed during the first quarter of the contract award. Work performed during the reporting period focused entirely on project start-up activities and commencement of the initial project task of screening fields in the Frio fluvial-deltaic sandstone oil play for suitable reservoirs. Productive Frio reservoirs are distributed among at least 26 fields within the play, and over 129 reservoirs (59 currently producing) have each been responsible for the production of more than 1 million barrels of oil (MMBO). Geologic, engineering, and production data from fourteen major fields in the play, from Garcia field in southern Starr County northeastward to Agua Dulce field in Jim Wells and Nueces Counties, are presently being screened in order to define fields containing reservoirs appropriate for detailed characterization studies. The field screening and reservoir selection process is scheduled to be completed in the next project quarter.

Project Description

The Bureau of Economic Geology (BEG) has entered into a 46-month cost-shared cooperative agreement with the Department of Energy that will lead to maximizing the economic producibility of oil reservoirs in the Frio fluvial-deltaic sandstone (Vicksburg Fault Zone) oil play of South Texas. This is a mature play that has already produced nearly 1 billion barrels of oil (BBO), yet still contains about 1.6 BBO of unrecovered mobile oil and nearly the same amount of residual oil resources. More than half of the reservoirs in this depositionally complex play have already been abandoned, and large volumes of oil may remain unproduced unless advanced characterization techniques can be applied to define untapped, incompletely drained, and new pool reservoirs as suitable targets for near-term recovery methods, such as well recompletion and strategic infill drilling.

The project is divided into three major phases. Phase I includes the initial tasks of (1) screening fields within the play to select representative reservoirs that have a large remaining oil resource and are in danger of premature abandonment and (2) performing initial characterization studies on these selected reservoirs to identify the potential for untapped, incompletely drained, and new pool reservoirs. Phase II will involve advanced characterization of the selected reservoirs to delineate incremental resource opportunities. This will include volumetric assessments of untapped and incompletely drained oil along with an analysis by reservoir of specific targets for recompletion and strategic infill drilling. Phase III will consist of a series of tasks associated with final project documentation, technology transfer, and the extrapolation of specific results from reservoirs in this study to other heterogeneous fluvial-deltaic reservoirs within and beyond the Frio play in South Texas.

Project Status

The selection process for representative reservoirs from the Frio fluvial-deltaic sandstone (Vicksburg Fault Zone) that will be the targets of advanced reservoir characterization is currently under way. Initial screening of fields is being accomplished with publicly available data from (1) hearing files at the Texas Railroad Commission (RRC), (2) BEG's Texas Oil Reservoir database, (3) commercially available production data from Dwight's Energydata and Petroleum Information, (4) well-log data from BEG and RRC files, (5) trade and technical literature. Some additional non-public data contributed by companies were also used. Data are presently being compiled in the form of field summaries for several of the largest fields within the Frio fluvial-deltaic sandstone play.

Criteria that will form the basis for field/reservoir selection have been established. The fundamental considerations for the selection of Frio fluvial-deltaic reservoirs suitable for detailed study focus both on the quality of the field/reservoir data and the potential for identifying additional reserves. Those fields possessing an extensive geological, petrophysical, geophysical, and production database, coupled with the best possibilities for infield reserve growth, will be the most likely

candidates for further study. Infield reserve growth is being analyzed by determining current reservoir recovery efficiency.

Project members met with Conoco geologists and engineers to review data from the Rincon field, Starr County. Conoco has an extensive, well-maintained database that includes more than 700 well logs (mostly older, 1940's vintage), and there apparently is a large amount of core available. The Conoco staff indicated that the company would be willing to make all field data available for this project. The combination of available data and operator cooperation makes the Rincon field one of the leading candidates for further study.

Future Activities

Field screening is scheduled to continue and be completed during the next project quarter. Field data from RRC hearing files and other miscellaneous data sources will be compiled, and field summaries will be prepared for many of the larger fields in the Frio fluvial-deltaic sandstone (Vicksburg Fault Zone) play. These summaries will form the basis for decisions on whether or not to pursue reviewing additional data from other operators.

Visits will be scheduled to Mobil to review data associated with their acreage in the TCB field, and a follow-up visit to Conoco for a more in-depth review of the Rincon field is likely. Decisions to schedule reviews with additional operators will be made following the completion of the initial field screening process.

Progress completed during the first quarter consisted of project start-up activities and initial screening of publicly available field data on reservoirs within the Frio fluvial-deltaic sandstone (Vicksburg Fault Zone) play. Data from RRC hearing files and other miscellaneous public data sources are being compiled in the form of field summaries that will form the basis for decisions to review additional operator data on specific fields. The Conoco-operated portion of the Rincon Field in Starr County is a strong candidate for selection for further study because of the presence of an extensive, well-maintained data set that includes core data. Other fields currently being reviewed in more detail include Mobil-operated parts of TCB field in Kleberg County.

NOVEL TECHNOLOGY

A NOVEL APPROACH TO MODELING UNSTABLE ENHANCED OIL RECOVERY DISPLACEMENTS

Contract No. DE-AC22-90BC14650

**University of Texas at Austin
Austin, Tex.**

**Contract Date: Aug. 28, 1990
Anticipated Completion: Aug. 27, 1993**

**Principal Investigator:
Ekwere J. Peters**

**Project Manager:
Jerry Ham
Metairie Site Office**

Reporting Period: Oct. 1–Dec. 31, 1992

Objective

The objective of this research is to develop a methodology for predicting the performance of unstable displacements in heterogeneous reservoirs. A performance prediction approach that combines numerical modeling with laboratory imaging experiments is being developed. Flow visualization experi-

ments are being performed on laboratory corefloods using X-ray computerized tomography (CT) and other imaging technologies to map the in situ fluid saturations in time and space. A systematic procedure is being developed to replicate the experimental image data with high-resolution numerical models of the displacements. The well-tuned models will then be used to scale the results of the laboratory coreflood experiments to heterogeneous reservoirs in order to predict the performance of unstable displacements in such reservoirs.

Summary of Technical Progress

A new procedure has been developed to simplify the analysis, numerical modeling, and scaling of laboratory coreflood experiments. The procedure consists of the following steps:

1. Image the coreflood by CT to obtain the temporal and spatial saturation profiles.
2. Transform the saturation profiles by means of a dimensionless self-similarity variable to obtain a unique, dimensionless response function that is characteristic of the coreflood.
3. History-match the characteristic response function for the coreflood with a numerical simulator.
4. After a satisfactory match, compare the experimental and computed saturation profiles and recovery curves for the coreflood.
5. Using the well-tuned numerical model, scale the results of the laboratory coreflood experiment to other systems.

Steps 1 through 4 of this procedure were demonstrated in previous quarterly reports. In the first report,¹ a dimensionless self-similarity variable (x_D/t_D) for two-phase immiscible displacement was derived and used to transform the saturation profiles of two laboratory waterfloods in sandpicks to obtain their characteristic dimensionless response functions (steps 1 and 2). In the second report,² steps 3 and 4 of the procedure were demonstrated by numerically simulating the two laboratory waterfloods. In a third report,³ heterogeneous permeable media were presented and discussed for use in implementing step 5 of the procedure. In this report, step 5 is presented by scaling one of the laboratory waterfloods in a homogeneous sandpick to predict its expected performance in heterogeneous permeable media.

Simulation of Displacements

In a previous report, an unstable waterflood experiment was successfully simulated in a water-wet sandpick and its dimensionless response curve (\bar{f}) was calculated. A two-dimensional (2-D) x-z vertical cross-sectional grid of 53×122 was used to simulate the three-dimensional (3-D) waterflood experiment. This grid was selected to coincide with the resolution of the 2-D slices of the CT images of the waterflood. The following similarity scaling groups were maintained the same in the simulation as in the experiment: viscosity ratio (μ_o/μ_w), capillary number (N_c), gravity number (N_g), and stability number (N_s). The adjustable parameters used to accomplish the history match were (1) the degree and structure of heterogeneity of the porous medium as measured by the Dykstra-Parsons (DP) coefficient and dimensionless correlation length, (2) the relative permeability curves (k_{rw} and k_{ro}), and (3) the capillary pressure curve (P_c). A DP coefficient of 0.05 and a correlation length of 0 were used to characterize the laboratory sandpick. The relative permeability curves used in the simulation were based on the following analytical models.

$$k_{rw} = k_{wr} \left(\frac{S_w - S_{wi}}{1 - S_{wi} - S_{or}} \right)^{n_w} \quad (1)$$

$$k_{ro} = k_{or} \left(\frac{S_o - S_{or}}{1 - S_{wi} - S_{or}} \right)^{n_o} \quad (2)$$

The relative permeability parameters that gave the best match of the waterflood were $k_{wr} = 0.90$, $n_w = 3.5$, $k_{or} = 0.90$, and $n_o = 0.49$. The capillary pressure curve used in the simulation was

$$P_c = 0.01 \left(1 - \frac{S_w - S_{wi}}{1 - S_{wi} - S_{or}} \right)^2 \quad (3)$$

The numerical simulation was repeated in each of 12 heterogeneous media using the preceding relative permeabil-

ity and capillary pressure curves. Table 1 lists additional parameters of the numerical simulations.

TABLE 1
Simulation Conditions

	Simulation data
Porous medium	
Length, cm	54.53
Diameter, cm	4.8
Absolute permeability, D	9.26
Average porosity, %	29.6
Initial water saturation, %	0.15
Fluids	
Density of displacing fluid, g/cm ³	1.0882
Viscosity of displacing fluid, cP	1.1276
Density of displaced fluid, g/cm ³	0.9655
Viscosity of displaced fluid, cP	103.4
Oil viscosity/water viscosity	91.7
Capillary number	4.62×10^{-4}
Gravity number	1.26×10^{-3}
Stability number	0.271×10^3

Results and Discussion

Figure 1 shows the permeability maps for the 12 heterogeneous media used in the simulations. The degree and structure of the heterogeneity are characterized by the DP coefficient and the dimensionless correlation length (L_x). The DP ranged from 0.01 for a homogeneous medium to 0.87 for a highly heterogeneous medium. The dimensionless correlation length ranged from 0 for a random permeability distribution to 2 for a highly correlated permeability distribution. It may be seen in Fig. 1 that an increase in the correlation length of the permeability field results in an increasingly layered structure. Further, high L_x and DP give rise to heterogeneous media with structures similar to those of the sedimentary rocks of petroleum reservoirs. Thus high L_x and DP permeability distributions typify petroleum reservoirs, whereas low DP and high L_x distributions typify laboratory sandpicks.

Figure 2 compares the simulated dimensionless response function for each of the twelve heterogeneous media with that of the laboratory waterflood experiment. The following observations can be made from these results. If the heterogeneous media are characterized by low variability in the permeability distributions (low DP), the waterflood response will be essentially the same as in the laboratory sandpick regardless of the structure of the heterogeneity. This is indicated by the agreement between the simulated and the experimental response functions in the first column of Fig. 2 (DP = 0.01). If the heterogeneous media are characterized by low correlation in the permeability distributions (low L_x), the waterflood response will be essentially the same as in the laboratory

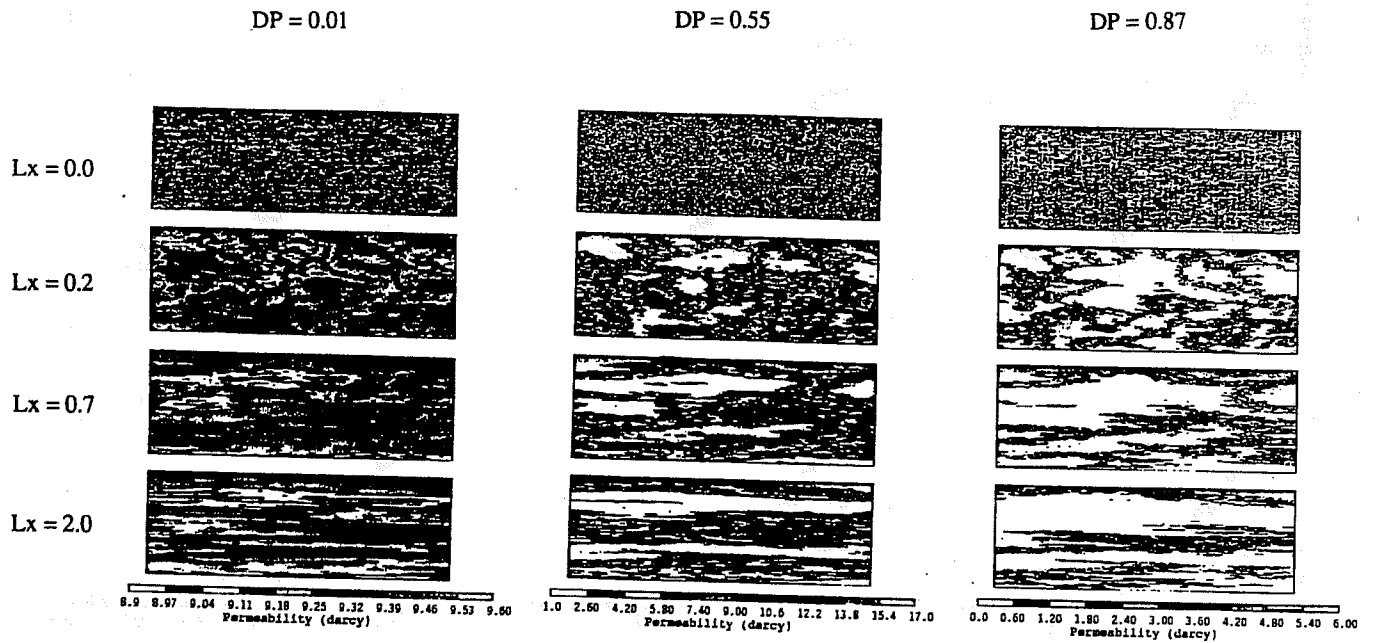


Fig. 1 Permeability maps.

sandpack regardless of the variability in the permeability distributions. This is indicated by the agreement between the simulated and the experimental response functions in the first row of Fig. 2 ($L_x = 0$). If the heterogeneous media are characterized by high variability and high correlation in the permeability distributions, the waterflood response could be significantly different from that of the laboratory sandpack. This is clearly shown by the response in the last permeability field in Fig. 2 ($L_x = 2$ and $DP = 0.87$). In this case, the waterflood response is significantly less in the heterogeneous medium than in the laboratory sandpack. These observations are confirmed by the oil recovery curves shown in Fig. 3.

The reason for the significant disparity in performance between the laboratory waterflood in a relatively homogeneous sandpack and in certain kinds of heterogeneous media has been investigated. The reason for this disparity can be seen in Figs. 4 and 5, which show the simulated water saturation maps for each of the 12 heterogeneous media at 0.10 and 0.25 pore volumes injected. It is seen that the displacement in the heterogeneous media with high DP and high L_x are dominated by channeling of the injected water as a result of the permeability stratification. This results in significant bypassing of the oil in unswept layers and consequent low oil recovery. By contrast, the displacement in the media with low DP are characterized by excellent sweep comparable with that observed in the CT images of the laboratory waterflood experiment. This results in a displacement performance that is comparable to that of the laboratory waterflood experiment in the sandpack.

Conclusions

In this report, the last step of a five-step procedure for modeling unstable displacements in heterogeneous perme-

able media is presented. An unstable laboratory waterflood experiment in a homogeneous sandpack was scaled to predict its expected performance in heterogeneous media. It was found that the performance of the displacement in heterogeneous media could be significantly lower than in the laboratory experiment, depending on the degree and structure of the heterogeneity of the media. This observation points to the need for proper scaling when using the results of laboratory coreflood experiments in relatively homogeneous media to forecast the expected performance in heterogeneous media. The five-step procedure developed and presented in this research can be used to accomplish this scaling and prevent erroneous performance forecasts.

Nomenclature

- k_{rw} = relative permeability to water
- k_{ro} = relative permeability to oil
- k_{wr} = end-point relative permeability to water
- k_{or} = end-point relative permeability to oil
- L_x = dimensionless correlation length in the x-direction
- n_o = relative permeability exponent for oil
- n_w = relative permeability exponent for water
- S = normalized water saturation
- S_o = oil saturation
- S_{or} = residual oil saturation
- S_w = water saturation
- S_{wi} = connate water saturation
- t_D = dimensionless time
- x_D = dimensionless distance in the x-direction
- μ_o = oil viscosity
- μ_w = water viscosity

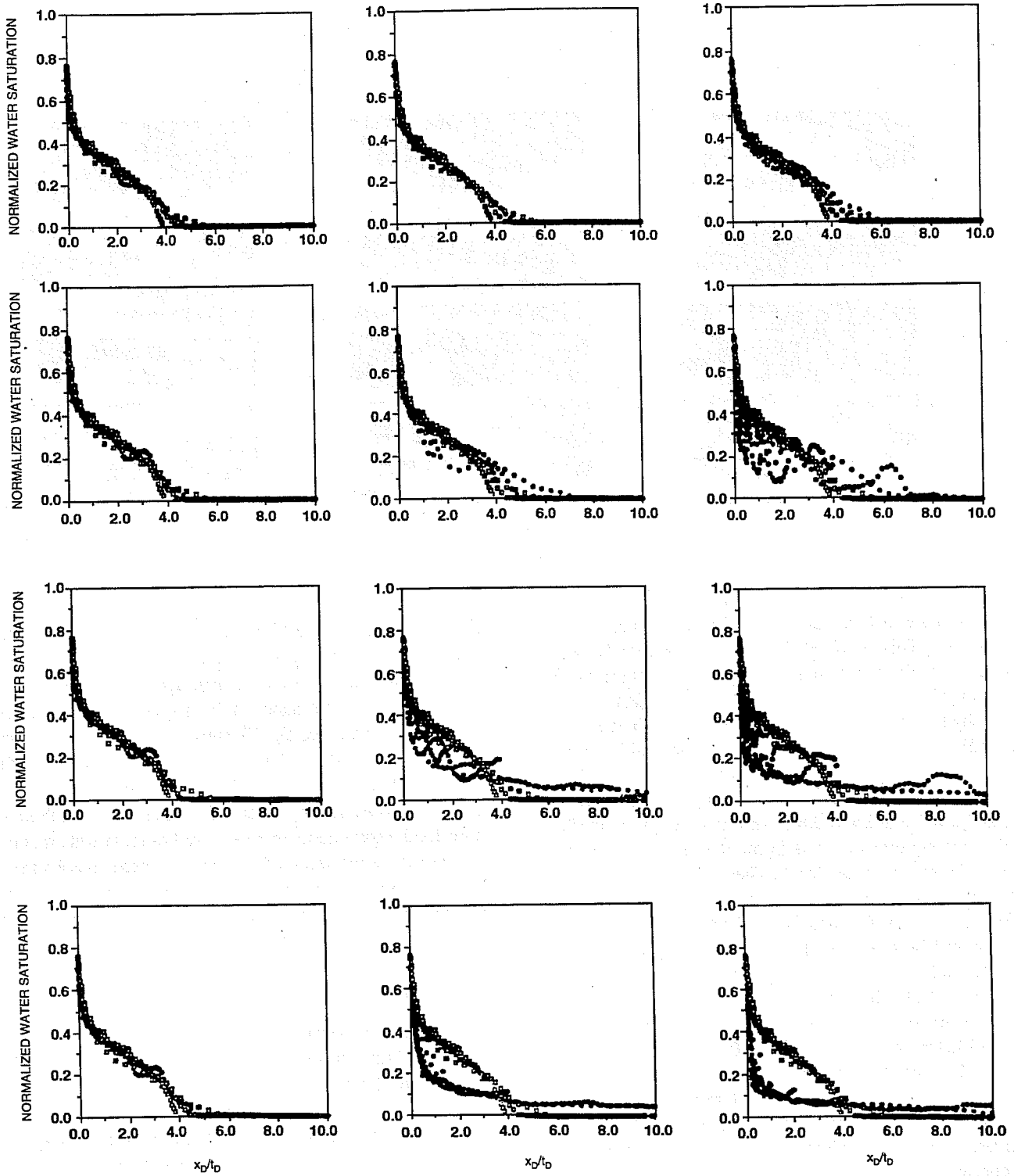


Fig. 2 A comparison of the experimental and simulated oil recovery curves. \square , experiment. \bullet , simulation.

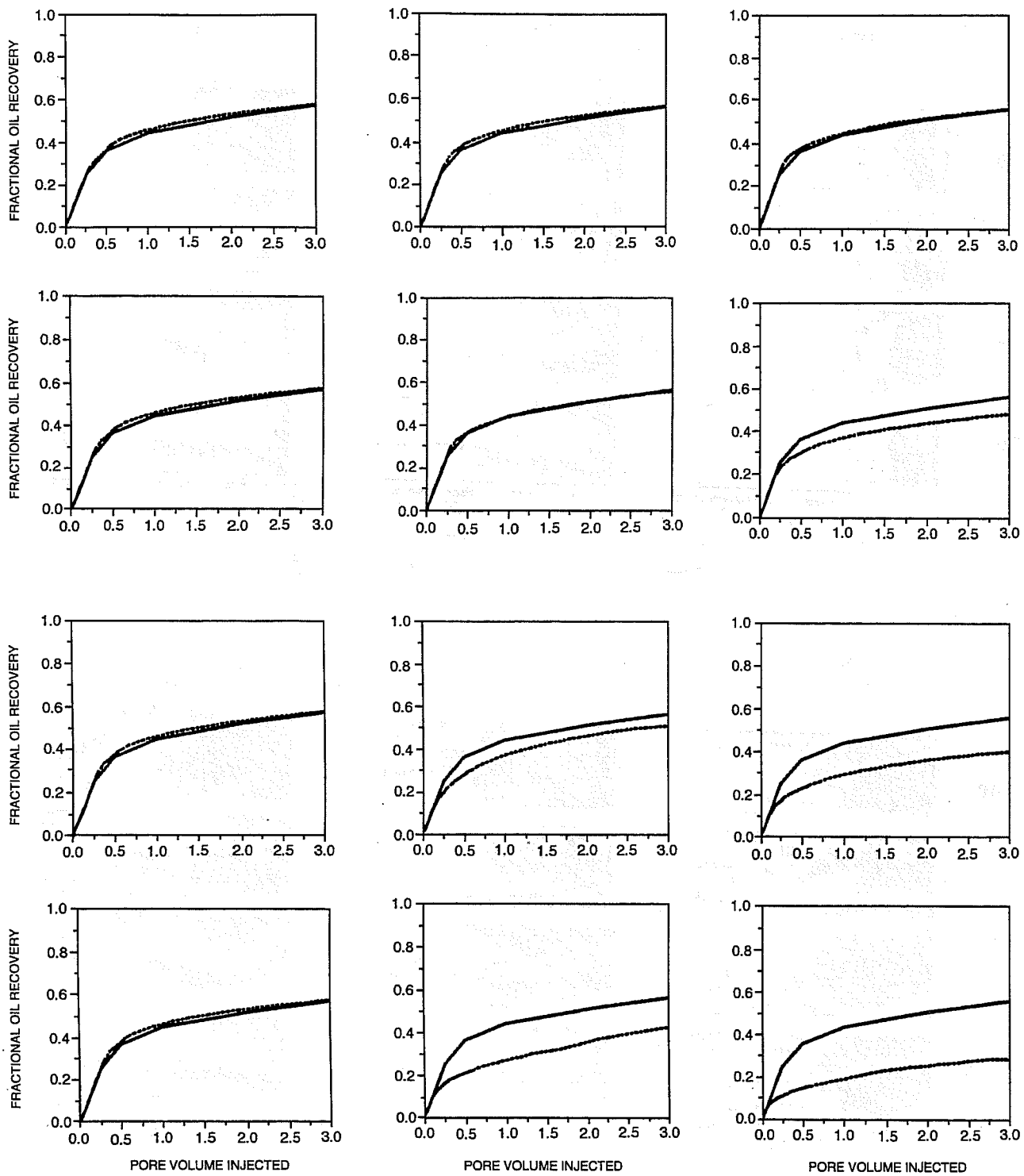


Fig. 3 A comparison of the experimental and simulated oil recovery curves. —, experiment. . . ., simulation.

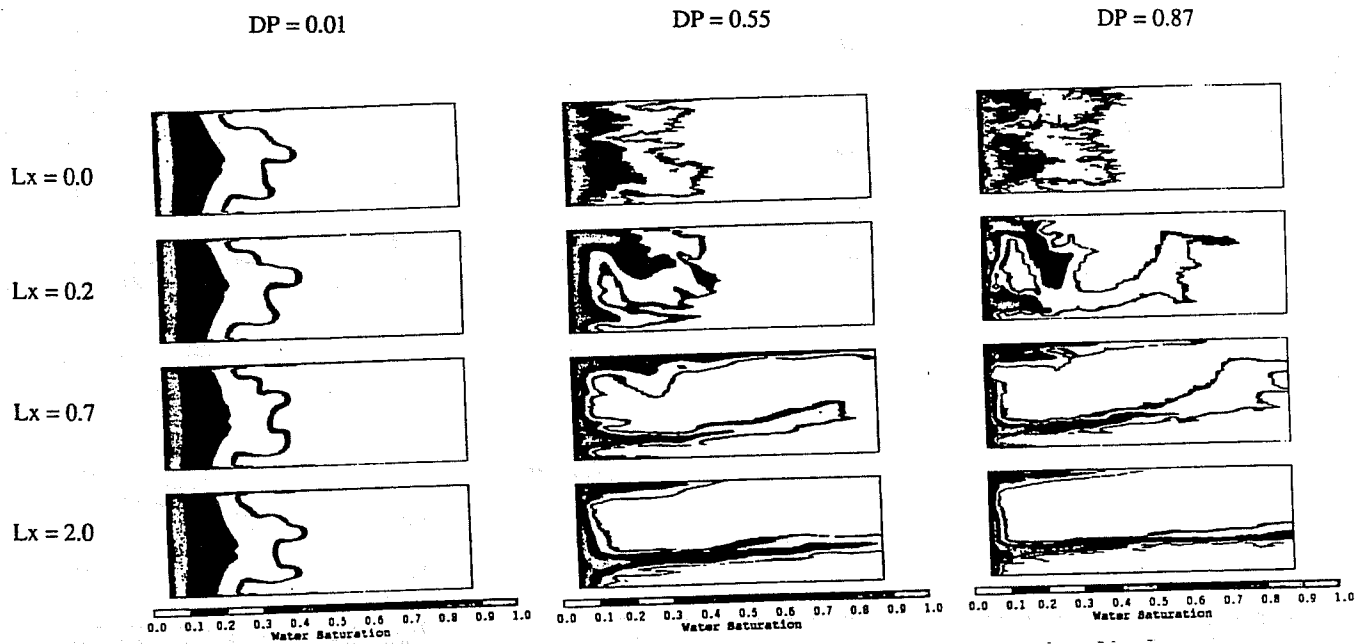


Fig. 4 Simulated water saturation maps at 0.10 pore volume injected.

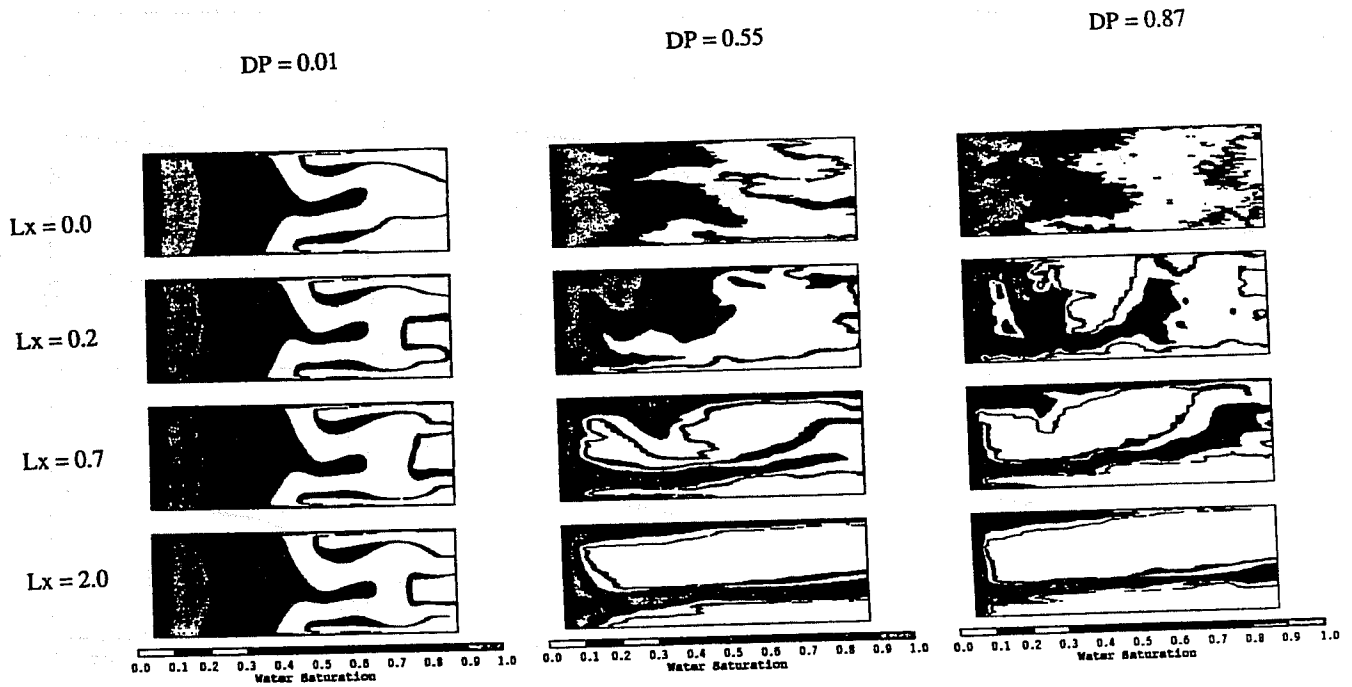


Fig. 5 Simulated water saturation maps at 0.25 pore volume injected.

References

1. E. J. Peters, A Novel Approach to Modeling Unstable EOR Displacements, *DOE Quarterly Report*, January-March 1992.
2. E. J. Peters, A Novel Approach to Modeling Unstable EOR Displacements, *DOE Quarterly Report*, April-June 1992.
3. E. J. Peters, A Novel Approach to Modeling Unstable EOR Displacements, *DOE Quarterly Report*, July-September 1992.